# Programmable Biomolecular Integration and Dynamic Behavior of DNA-based Systems for Development of Biomedical Nano-Devices

by Jaeseung Hahn
B.E. Biomedical Engineering
The City College of New York of the City University of New York, 2012

Submitted to the Harvard-MIT Program in Health Sciences and Technology
in partial fulfillment of the requirements for the degree in

DOCTOR OF PHILOSOPHY IN MEDICAL ENGINEERING AND MEDICAL PHYSICS
MASSACHUSETTS INSTITUTE OF TECHNOLOGY

~~January 2019~~ [February 2019]



Signature redacted

Signature of the author: _____
Jaeseung Hahn
Harvard-MIT Program in Health Sciences and Technology

Signature redacted

Certified by: _____
William M. Shih
Professor of Biological Chemistry and Molecular Pharmacology & Cancer Biology

Signature redacted

Received by: _____
Emery N. Brown, M.D., Ph.D.
Director, Harvard-MIT Program in Health Sciences and Technology
Professor of Computational Neuroscience & Health Sciences and Technology

# Programmable Biomolecular Integration and Dynamic Behavior of DNA-based Systems for Development of Biomedical Nano-Devices

by

Jaeseung Hahn

Submitted to the Harvard-MIT Program in Health Sciences and Technology
in partial fulfillment of the requirements for the degree in
DOCTOR OF PHILOSOPHY IN HEALTH SCIENCES AND TECHNOLOGY:
PHYSICS
MASSACHUSETTS INSTITUTE OF TECHNOLOGY

Abstract

Departing from the traditional role as a carrier of genetic information, DNA has emerged as an engineering material for construction of nano-devices. The advances in the field of DNA nanotechnology have enabled design and synthesis of DNA nanostructures of arbitrary shapes and manipulation of the nanostructures' conformations in a programmable way. DNA-based systems offer potential applications in medicine by manipulating the biological components and processes that occur at the nanometer scale. To accelerate the translation of DNA-based systems for medical applications, we identified some of the challenges that are hindering our ability to construct biomedical nano-devices and addressed these challenges through advances in both structural and dynamic DNA nanotechnology.

First, we tested the stability of DNA nanostructures in biological environments to highlight the necessity of and path towards protection strategies for prolonged integrity of biomedical nano-devices. Then, we constructed a platform for robust 3D molecular integration using DNA origami technique and implemented the platform for a nanofactory capable of production of therapeutic RNA to overcome the challenges in RNA delivery. Moreover, we established a mechanism to drive DNA devices by changing temperature with prolonged dynamic behavior that was previously challenging to accomplish without special modification of DNA and/or equipment not readily available in a typical lab setting. Together, the progress made in this thesis bring us another step closer to realization of medical applications of DNA nanotechnology by focusing on the challenges in both structural and dynamic aspects of the technology.

Thesis Supervisor: William M. Shih
Title: Professor of Biological Chemistry and Molecular Pharmacology & Cancer Biology

# Table of Contents

# Acknowledgements

First, I would like to express my sincerest respect and appreciation for my advisor William Shih. Your enthusiasm for science and solving complex problems has both amazed and inspired me throughout my PhD training. I am grateful for your support.

I would also like to thank my committee members, Daniel Anderson and Peng Yin, who have shared their time and wisdom with me. I was able to develop professionally well rounded thanks to your guidance.

I was lucky enough to work closely with many postdocs who taught me valuable lessons. Steven Perrault has provided me with a solid foundation in the field of DNA nanotechnology and related skills in molecular biology. Rasmus Sørenson taught me how to work in a group for scientific research. Leo Chou always challenged me with insightful questions that helped me grow as a researcher. I appreciate it.

Though not involved directly for a project, many other postdocs have supported me throughout my PhD training. I am especially indebted to Nandhini Ponnuswamy and Bhavik Nathwani who always cared for my well-being. Thank you.

Working at the Wyss Institute exposed me to many exciting and invigorating disciplines. However, the biggest opportunity was the chance to meet and befriend all the wonderful people at the Wyss Institute. Thank you, everyone, and go Wyss FC!

Studying at MIT and Harvard as a part of HST community was a wonderful experience. I especially thank Lee Gehrke, Julie Greenberg, Laurie Ward, Traci Anderson, Patricia Cunningham, and Joseph Stein for keeping me on track and taking care of all the administrative challenges. I also would like to thank my qualification exam committee members, Arup Chakraborty, Roger Mark, and Collin Stultz as well as ICM instructors Judith Strymish, Aasia Romano, and Courtney Dawson.

I was very fortunate to be a part of a talented and fun HST 2012 cohort. I want to give a special shout-out to the members at the HMS campus, Anik Debnath and Rida Mourtada, as well as Westgate neighbors, Britni Crocker and Daniel (Danny) Antonaccio.

I would also like to thank Yuying Gosser, Sebastian Schlücker, Jan Grimm, and Daniel Thorek who nurtured my scientific career before starting graduate school.

I am blessed to have the support of my family. I wouldn't be alive without all the care that my parents, Sangsub Hahn and Eunhee Lee, gave me. I am grateful to my siblings, Jaesik Hahn and Jaein Hahn, for always being inspirational to me. I also would like to thank my late grandparents, Dongho Hahn and Soongyu Park, for instilling me with love for nature.

I would like to acknowledge my in-laws as well. Francine (Tina) Mayas and Maria Savel have read many of my writings and provided me with valuable feedback throughout my PhD training. I also want to thank Tina for staying strong throughout the tough recovery after cancer. I am always grateful to Albert Mayas, Sr., Albert (Eddie) Mayas, Jr., and Sally Mayas as well as other members or Mayas and Chase family for welcoming me so kindly.

Of course, I must thank my wonderful wife, Susanna (Susie) Mayas, for choosing to take this wild ride with me and sticking to it all the way. I couldn't have done it without you.

There are so many wonderful people that I couldn't acknowledge. Thank you everyone so much for your positive influence in my life.

# Chapter 1: Introduction

## 1.1 Biologically inspired nanodevices for biomedical applications

To answer Richard Feynman's challenge to "make a thing very small which does what we want,"[1] nanomedicine aims specifically to construct nano-devices that detect and treat diseases at the nanometer scale for more precise and earlier intervention. Advances in biology have uncovered the molecular mechanisms of biological processes that are often at the nanometer scale. This understanding suggests the importance and necessity of detecting and treating biological abnormalities at the nanometer scale. How can we construct nano-devices that allow patients to "swallow the surgeon" for diagnosis and treatment?

Biological macromolecules often exhibit spatially organized and temporally choreographed behavior akin to engineered devices at the nanometer scale. In fact, the cell can be regarded as a self-replicating robot composed of biomolecular nano-devices. Even a simple prokaryotic cell possesses molecular machineries for complex chromosomal organization, biomolecular manufacturing, and gene regulatory networks. Therefore, biology provides both inspiration and building blocks for construction of nano-devices that, in return, can serve as a tool to interact with biological systems at the nanometer scale.

## 1.2 DNA as an engineering material

DNA is a genetic material that encodes the blueprint of life on earth. However, an ever-expanding role of DNA as an engineering material has been realized in past three decades. The field of DNA nanotechnology began with Nadrian Seeman's proposal in 1982 to program DNA for self-assembly of junctions and lattices[2]. Since then, DNA has been utilized to construct structural and dynamic systems to achieve spatial and temporal manipulation of matter at the molecular level.

### 1.2.1 Structural DNA nanotechnology

The groundwork of structural DNA nanotechnology has been established by the development and demonstration of two basic structural motifs of DNA nanostructures: DNA junctions[3,4] and DNA double-crossover (DX) molecules.[5] DNA junctions allowed the construction of DNA molecules beyond the double-helix structure such as DNA polyhedra.[6,7] However, the flexible nature of DNA junctions made it difficult to build rigid structures necessary for precise positioning. The DX molecules, which consist of two juxtaposed 4-arm junctions, were able to provide the necessary structural rigidity.

Larger structures could be constructed by tiling the DX motifs as well as other related tile motifs by introducing "sticky ends," which are short single-stranded DNA (ssDNA) regions that can be programmed to be complementary to each other for self-assembly. The tiling approach was used to construct 1D arrays and 2D lattices with repeating units[8–10] as well as finite structures.[11,12] One of the milestone achievements of this approach was the growth of 3D DNA crystals using a DNA tensegrity triangle molecule,[13] which is another structural motif with each vertex composed of a 4-arm junction. The resulting crystals were hundreds of microns in size and were able to diffract X-rays. While the tiling strategy is a powerful method for construction of DNA nanostructures, the programmable assembly of guest molecules is limited due to the small size of uniquely addressable units, both in physical dimensions and

number as well as the stringent assembly condition that requires high purity, stoichiometry control, and careful sequence design of DNA strands.

The breakthrough in building discrete nanostructures reaching the size of viral particles that can have a large number of uniquely addressable sites came with the invention of Paul Rothemund's DNA origami technique.[14] Much like the well-known art of origami, the DNA origami technique folds a long ssDNA "scaffold" strand, typically M13 phage genomic DNA (~7,000 nt), into a programmed, arbitrary shape using synthetic "staple" oligonucleotides that are complementary to different regions of the scaffold. The DNA origami folding requires thermal annealing of the circular scaffold strand in the presence of 10-100 fold excess of an appropriate set of staple strands in a one-pot reaction. Each of the staple strands can be independently modified, resulting in hundreds of uniquely addressable sites with a resolution as small as 6 nm. Moreover, the sequence, purity, and stoichiometry of staple strands are not required to be as stringently controlled compared to the tiling approach because the scaffold strand acts as a nucleation seed and can self-assemble staple strands with suboptimal sequence, self-select for full-length oligonucelotides within the excess amount of staple strands, and self-limit the number of structures that are folded in the end. Therefore, the DNA origami technique is a powerful nanofabrication method to produce highly addressable, discretely sized DNA nanostructures.

In 2009, William Shih's group achieved another milestone to produce solid 3D objects by extending the DNA origami technique to bundle DNA helices in a honeycomb lattice aided by a design platform called caDNAno.[15] The software drastically simplifies the design process and enables rapid prototyping of DNA nanostructures. The work was further developed to enable the organization of DNA helices into a square lattice[16] as well as a hexagonal lattice and hybrid lattices.[17] For more complex morphology, addition and deletion of bases in adjacent helices could introduce curvature and twists to the multi-layer structures.[18] Since then, other architectures were developed for fabrication of DNA nanostructures such as concentric rings,[19] gridiron,[20] and wireframe[21,22] using corresponding design software. Moreover, the increased size and complexity of the DNA origami technique was achieved by using longer scaffold strands[23] or hierarchical assembly of DNA origami structures,[15,18,24–26] similar to the tiling approach for small DNA tile motifs such as DX molecules.

### 1.2.2 Dynamic DNA nanotechnology

One of the basic mechanisms of dynamic DNA nanotechnology is the toehold-mediated DNA strand displacement (DSD), where hybridization of two complementary DNA strands results in displacement of one or more pre-hybridized strands.[27] The process is initiated by binding of complementary ssDNA "toehold" domains, followed by the branch migration that eventually displaces the pre-hybridized strand(s). Yurke and co-workers pioneered the use of toehold-mediated DSD for operation of DNA nanodevices.[28] The work demonstrated repeated cyclic operation of opening and closing of a DNA tweezer fueled by the addition of DNA strands. Since the initial demonstration of the mechanism, toehold-mediated DSD has been used to operate diverse and sophisticated DNA-based devices such as walkers,[29,30] logic gates,[31,32] and cascaded circuits.[33,34]

With the advances in both structural and dynamic aspects of DNA nanotechnology, the mechanical actuation of large DNA nanostructures were recently achieved. These reconfigurable structures were programmed much like the DNA tweezer by introducing ssDNA toehold regions to the DNA helices connecting structural units together. With the addition of DNA fuel strands, the structures were able to change the configurations as programmed. For instance, DNA-based molecular containers could open and close in the presence of correct DNA "keys."[35,36] Such devices can catch and release a cargo as big as a viral particle. Moreover, Carlos Castro's group designed, fabricated, and characterized DNA-based nano-devices resembling the shape and motion of macroscopic mechanical devices such as joints and sliders.[37] The programmable actuation of nano-devices demonstrates the complex molecular behaviors that are both spatially and temporally controlled.

## 1.3 Opportunities in DNA nanotechnology for biomedical applications

The original purpose of constructing DNA nanostructures by Seeman was to organize proteins for structural determination through X-ray crystallography. However, the unprecedented capability to construct and manipulate DNA-based nano-devices has inspired and resulted in applications in different disciplines such as material science and biological sciences. In particular, DNA nanotechnology has influenced nanomedicine research by providing a biocompatible material that can pattern virtually any molecules that can be modified with DNA strands.

### 1.3.1 Drug delivery vehicle

One of the goals in nanomedicine is to develop a delivery vehicle at the nanometer scale to administer drugs to target cells that exhibit pathological features. DNA nanotechnology provides a platform to program a specific number of drug molecules and targeting molecules with precise spatial organization. Moreover, DSD-driven structural reconfiguration allows exposure or release of cargo molecules. Therefore, DNA-based delivery vehicle has many features that are desirable for therapeutic applications.

Molecular organization with DNA nanostructures has been used to develop adjuvants for immunotherapy[38,39] and tumor-targeting vehicle for siRNA delivery.[40] Moreover, Shawn Douglas and co-workers developed a nanorobot capable of AND logic computation to expose antibody fragments through aptamer-mediated DSD, which was actuated by binding of cell membrane markers to DNA aptamers that are hybridized to partially complementary DNA strands to hold together a DNA nanostructure shut and hide the therapeutic molecules.[41] Such control over programmed spatial organization and dynamic behavior is impossible or very difficult to accomplish with other materials. Therefore, DNA nanotechnology can enable the development of highly sophisticated biomedical nano-devices for therapeutic applications.

### 1.3.2 Diagnostic platform

For early detection of disease markers, biosensing is a critically important function. DNA nanotechnology can allow precise organization of various sensing elements and provide means to compute and process many inputs in massively parallel manner. The resulting diagnostic nano-devices can potentially serve as a single-molecular, ultra-sensitive, and highly

multiplexing platform to detect biomarkers of interest. Therefore, DNA-based diagnostic platform has potential to enable early detection of diseases currently not possible.

A DNA nanostructure functionalized with binding motifs can serve as a molecular sensor that exhibits observable change upon the binding of specific biomarkers. DNA origami structures were programmed to bind multiple nucleic acid targets such as mRNA[42] and DNA with single nucleotide polymorphism (SNP),[43,44] and the binding could be observed under atomic force microscopy (AFM). Remarkably, the precise placement of binding motifs on the DNA nanostructure allowed discrimination of different nucleic acid species binding. Another class of biosensor changed the conformation of the DNA nanostructure upon the binding of target molecule so that the entire structure can serve as an output.[45] The conformation change could be observed under AFM or Förster resonance energy transfer (FRET) by functionalizing the structure with fluorescence dyes. The precise molecular organization and programmable behavior of DNA nanostructure make it possible to arrange multiple orthogonal sensing elements and observe conformation change upon binding to the target molecules.

Moreover, dynamic DNA nanotechnology enables molecular information processing for biosensing applications. John Picuri and co-workers demonstrated molecular translators based on toehold-mediated DSD to detect nucleic acids and adenosine.[46] The work can be extended to detect any molecules that have DNA aptamers for binding. With many circuits that can analyze molecular information and catalytic amplifiers for signal amplification, dynamic DNA nanotechnology provides tools to develop highly sophisticated molecular compilers for diagnostic applications. Further development to combine the structural and dynamic aspects of DNA nanotechnology is expected to result in a powerful diagnostic platform.

## 1.4 Challenges in DNA-based systems for development of biomedical nano-devices

The original function of DNA is storage of genetic information. Repurposed to serve alternative roles, DNA has some limitations as an engineering material. Therefore, further development of DNA nanotechnology is necessary to address challenges that are hindering it from moving towards the bedside. To accelerate translation of the advances in DNA nanotechnology for viable biomedical applications, we have identified some of the challenges that need to be overcome.

### 1.4.1 Stability of DNA-based systems in biological context

DNA is an anionic polymer due to negatively charged phosphodiester backbone. As a consequence, DNA nanostructures that are folded into compact architecture require cation in the buffer to neutralize the negative charge repulsion. Therefore, magnesium chloride ($MgCl_2$) is often added at 5-20 mM in a typical DNA origami folding reaction to supplement with divalent cation.[15] However, the concentrations of $MgCl_2$ in blood and tissue culture media are typically below 1 mM. Therefore, DNA nanostructures with compact architecture may denature in biological environments. Furthermore, the presence of a variety of nucleases in serum can degrade DNA nanostructures quickly. Therefore, a drug delivery vehicle made of DNA nanostructure could denature and get digested quickly upon intravenous injection.

DNA origami structures were previously reported to be partially resistant to nuclease digestion.[47] However, a systematic characterization of the sensitivity of various nanostructures to a low $MgCl_2$ concentration and nuclease digestion is required to assess the problem. The denaturation and digestion would lead to the loss of molecular organization and result in unreliable experimental data as well as unsuccessful therapeutic applications. Therefore, the problem needs to be addressed to obtain reliable data for the research as well as to enable development of a drug delivery vehicle using DNA nanostructures.

### 1.4.2 Robust biomolecular integration using 3D DNA nanostructures

DNA nanotechnology enabled spatial organization of molecules. In particular, 2D DNA origami has been successfully utilized for precise organization of many functional components.[48–50] The simple architecture of 2D DNA origami structures are easy to visualize and modify to meet specific needs of different applications.[42,44,51–56] However, 3D DNA origami has not been as widely adapted partially due to its design complexity. Therefore, it would be beneficial to identify key features required for varying applications and design a platform structure to meet the needs.

In addition to simple architecture for addressable sites and modular design for hierarchical assembly, 3D DNA origami structure can offer increased rigidity and compartmentalization that are not possible using 2D DNA origami. Therefore, the 3D DNA origami platform for molecular integration should include all four features. Further characterization of the platform should be carried out to determine the molecular incorporation efficiency and assess the ease of use for wide adaptation of the platform. Finally, the effect of molecular integration should be determined to verify the functional improvement based on precise organization of molecules and justify the need for such rigorous molecular integration.

### 1.4.3 Sustained dynamic behavior of DNA-based devices

Despite being a powerful method to drive DNA-based devices with complex behavior, one caveat of toehold-mediated DSD is that a set of added DNA strands brings the reaction to completion since the system is fueled by free energy change coming from DNA hybridization. Therefore, further operation requires additional DNA strands to refuel the system. The addition of DNA strands results in the accumulation of waste product as well as the dilution of molecular components that result in the deterioration of the device's function.[28]

To overcome this challenge, Toma Tomov and co-workers demonstrated a microfluidic-based apparatus for exchanging buffer to add DNA fuel strands and remove waste products.[57] Though innovative and successful, the strategy requires the DNA-based nano-devices to be tethered on the surface so that they are not washed away during the buffer exchange. Moreover, the specialized microfluidic device is not readily available in a typical lab setting. Therefore, it is difficult to implement the strategy widely.

A DNA-based diagnostic platform may require long, real-time analysis with multiple measurements of the sample to track the change over time or complex manipulation of the sample to measure multiple properties of the same molecule. To enable sustained dynamic behavior, it is necessary to develop a mechanism to drive DNA-based devices reversibly, preferably without exchanging mass to avoid need for a fluidic device and surface-tethered

nano-devices. Photons have been used to drive DSD, but this mechanism requires azobenzene-modification of DNA strands and a high-power laser apparatus to drive the system.[58-60] Therefore, the mechanism should not require any special modification to DNA or specialized equipment not readily available in a typical lab setting.

## 1.5 References


1. Feynman, R. P. *Engineering and Science*. 1960, pp. 22–36.
2. Seeman, N. C. Nucleic Acid Junctions and Lattices. *Journal of theoretical biology* **1982**, *99*, 237–47.
3. Seeman, N. C.; Kallenbach, N. R. Design of Immobile Nucleic Acid Junctions. *Biophysical journal* **1983**, *44*, 201–9.
4. Kallenbach, N. R.; Ma, R.-I.; Seeman, N. C. An Immobile Nucleic Acid Junction Constructed from Oligonucleotides. *Nature* **1983**, *305*, 829–831.
5. Fu, T. J.; Seeman, N. C. DNA Double-Crossover Molecules. *Biochemistry* **1993**, *32*, 3211–20.
6. Chen, J. H.; Seeman, N. C. Synthesis from DNA of a Molecule with the Connectivity of a Cube. *Nature* **1991**, *350*, 631–3.
7. Zhang, Y.; Seeman, N. C. Construction of a DNA-Truncated Octahedron. *Journal of the American Chemical Society* **1994**, *116*, 1661–1669.
8. Winfree, E.; Liu, F.; Wenzler, L. A.; Seeman, N. C. Design and Self-Assembly of Two-Dimensional DNA Crystals. *Nature* **1998**, *394*, 539–44.
9. Chengde Mao; Weiqiong Sun, and; Seeman*, N. C. Designed Two-Dimensional DNA Holliday Junction Arrays Visualized by Atomic Force Microscopy. **1999**.
10. Mathieu, F.; Liao, S.; Kopatsch, J.; Wang, T.; Mao, C.; Seeman, N. C. Six-Helix Bundles Designed from DNA. *Nano letters* **2005**, *5*, 661–5.
11. He, Y.; Ye, T.; Su, M.; Zhang, C.; Ribbe, A. E.; Jiang, W.; Mao, C. Hierarchical Self-Assembly of DNA into Symmetric Supramolecular Polyhedra. *Nature* **2008**, *452*, 198–201.
12. Zhang, C.; Su, M.; He, Y.; Zhao, X.; Fang, P.; Ribbe, A. E.; Jiang, W.; Mao, C. Conformational Flexibility Facilitates Self-Assembly of Complex DNA Nanostructures. *Proceedings of the National Academy of Sciences of the United States of America* **2008**, *105*, 10665–9.
13. Zheng, J.; Birktoft, J. J.; Chen, Y.; Wang, T.; Sha, R.; Constantinou, P. E.; Ginell, S. L.; Mao, C.; Seeman, N. C. From Molecular to Macroscopic via the Rational Design of a Self-Assembled 3D DNA Crystal. *Nature* **2009**, *461*, 74–7.
14. Rothemund, P. W. K. Folding DNA to Create Nanoscale Shapes and Patterns. *Nature* **2006**, *440*, 297–302.
15. Douglas, S. M.; Dietz, H.; Liedl, T.; Högberg, B.; Graf, F.; Shih, W. M. Self-Assembly of DNA into Nanoscale Three-Dimensional Shapes. *Nature* **2009**, *459*, 414–8.
16. Ke, Y.; Douglas, S. M.; Liu, M.; Sharma, J.; Cheng, A.; Leung, A.; Liu, Y.; Shih, W. M.; Yan, H. Multilayer DNA Origami Packed on a Square Lattice. *Journal of the American Chemical Society* **2009**, *131*, 15903–8.
17. Ke, Y.; Voigt, N. V.; Gothelf, K. V.; Shih, W. M. Multilayer DNA Origami Packed on Hexagonal and Hybrid Lattices. *Journal of the American Chemical Society* **2012**, *134*, 1770–1774.

18. Dietz, H.; Douglas, S. M.; Shih, W. M. Folding DNA into Twisted and Curved Nanoscale Shapes. *Science* **2009**, *325*, 725–730.
19. Han, D.; Pal, S.; Nangreave, J.; Deng, Z.; Liu, Y.; Yan, H. DNA Origami with Complex Curvatures in Three-Dimensional Space. *Science (New York, N.Y.)* **2011**, *332*, 342–6.
20. Han, D.; Pal, S.; Yang, Y.; Jiang, S.; Nangreave, J.; Liu, Y.; Yan, H. DNA Gridiron Nanostructures Based on Four-Arm Junctions. *Science* **2013**, *339*, 1412–1415.
21. Zhang, F.; Jiang, S.; Wu, S.; Li, Y.; Mao, C.; Liu, Y.; Yan, H. Complex Wireframe DNA Origami Nanostructures with Multi-Arm Junction Vertices. *Nature Nanotechnology* **2015**, *10*, 779–784.
22. Benson, E.; Mohammed, A.; Gardell, J.; Masich, S.; Czeizler, E.; Orponen, P.; Högberg, B. DNA Rendering of Polyhedral Meshes at the Nanoscale. *Nature* **2015**, *523*, 441–444.
23. Marchi, A. N.; Saaem, I.; Vogen, B. N.; Brown, S.; LaBean, T. H. Toward Larger DNA Origami. *Nano Letters* **2014**, *14*, 5740–5747.
24. Zhao, Z.; Liu, Y.; Yan, H. Organizing DNA Origami Tiles into Larger Structures Using Preformed Scaffold Frames. *Nano Letters* **2011**, *11*, 2997–3002.
25. Iinuma, R.; Ke, Y.; Jungmann, R.; Schlichthaerle, T.; Woehrstein, J. B.; Yin, P. Polyhedra Self-Assembled from DNA Tripods and Characterized with 3D DNA-PAINT. *Science* **2014**, *344*, 65–69.
26. Gerling, T.; Wagenbauer, K. F.; Neuner, A. M.; Dietz, H. Dynamic DNA Devices and Assemblies Formed by Shape-Complementary, Non-Base Pairing 3D Components. *Science* **2015**, *347*, 1446–1452.
27. Zhang, D. Y.; Seelig, G. Dynamic DNA Nanotechnology Using Strand-Displacement Reactions. *Nature Chemistry* **2011**, *3*, 103–113.
28. Yurke, B.; Turberfield, A. J.; Mills, A. P.; Simmel, F. C.; Neumann, J. L. A DNA-Fuelled Molecular Machine Made of DNA. *Nature* **2000**, *406*, 605–608.
29. Shin, J.-S.; Pierce, N. A. A Synthetic DNA Walker for Molecular Transport. *Journal of the American Chemical Society* **2004**, *126*, 10834–5.
30. Omabegho, T.; Sha, R.; Seeman, N. C. A Bipedal DNA Brownian Motor with Coordinated Legs. *Science (New York, N.Y.)* **2009**, *324*, 67–71.
31. Seelig, G.; Soloveichik, D.; Zhang, D. Y.; Winfree, E. Enzyme-Free Nucleic Acid Logic Circuits. *Science (New York, N.Y.)* **2006**, *314*, 1585–8.
32. Qian, L.; Winfree, E. Scaling Up Digital Circuit Computation with DNA Strand Displacement Cascades. *Science* **2011**, *332*, 1196–1201.
33. Zhang, D. Y.; Turberfield, A. J.; Yurke, B.; Winfree, E. Engineering Entropy-Driven Reactions and Networks Catalyzed by DNA. *Science (New York, N.Y.)* **2007**, *318*, 1121–5.
34. Yin, P.; Choi, H. M. T.; Calvert, C. R.; Pierce, N. A. Programming Biomolecular Self-Assembly Pathways. *Nature* **2008**, *451*, 318–322.
35. Andersen, E. S.; Dong, M.; Nielsen, M. M.; Jahn, K.; Subramani, R.; Mamdouh, W.; Golas, M. M.; Sander, B.; Stark, H.; Oliveira, C. L. P.; Pedersen, J. S.; Birkedal, V.; Besenbacher, F.; Gothelf, K. V; Kjems, J. Self-Assembly of a Nanoscale DNA Box with a Controllable Lid. *Nature* **2009**, *459*, 73–6.
36. Zadegan, R. M.; Jepsen, M. D. E.; Thomsen, K. E.; Okholm, A. H.; Schaffert, D. H.; Andersen, E. S.; Birkedal, V.; Kjems, J. Construction of a 4 Zeptoliters Switchable 3D

DNA Box Origami. *ACS Nano* **2012**, *6*, 10050–10053.

37. Marras, A. E.; Zhou, L.; Su, H.-J.; Castro, C. E. Programmable Motion of DNA Origami Mechanisms. *Proceedings of the National Academy of Sciences of the United States of America* **2015**, *112*, 713–8.
38. Schüller, V. J.; Heidegger, S.; Sandholzer, N.; Nickels, P. C.; Suhartha, N. a; Endres, S.; Bourquin, C.; Liedl, T. Cellular Immunostimulation by CpG-Sequence-Coated DNA Origami Structures. *ACS nano* **2011**, *5*, 9696–702.
39. Liu, X.; Xu, Y.; Yu, T.; Clifford, C.; Liu, Y.; Yan, H.; Chang, Y. A DNA Nanostructure Platform for Directed Assembly of Synthetic Vaccines. *Nano Letters* **2012**, *12*, 4254–4259.
40. Lee, H.; Lytton-Jean, A. K. R.; Chen, Y.; Love, K. T.; Park, A. I.; Karagiannis, E. D.; Sehgal, A.; Querbes, W.; Zurenko, C. S.; Jayaraman, M.; Peng, C. G.; Charisse, K.; Borodovsky, A.; Manoharan, M.; Donahoe, J. S.; Truelove, J.; Nahrendorf, M.; Langer, R.; Anderson, D. G. Molecularly Self-Assembled Nucleic Acid Nanoparticles for Targeted in Vivo SiRNA Delivery. *Nature nanotechnology* **2012**, *7*, 389–93.
41. Church, G. M.; Douglas, S. M.; Bachelet, I. A Logic-Gated Nanorobot for Targeted Transport of Molecular Payloads. *Science (80-. ).* **2012**, *335*, 831–834.
42. Ke, Y.; Lindsay, S.; Chang, Y.; Liu, Y.; Yan, H. Self-Assembled Water-Soluble Nucleic Acid Probe Tiles for Label-Free RNA Hybridization Assays. *Science* **2008**, *319*, 180–183.
43. Zhang, Z.; Zeng, D.; Ma, H.; Feng, G.; Hu, J.; He, L.; Li, C.; Fan, C. A DNA-Origami Chip Platform for Label-Free SNP Genotyping Using Toehold-Mediated Strand Displacement. *Small* **2010**, *6*, 1854–1858.
44. Subramanian, H. K. K.; Chakraborty, B.; Sha, R.; Seeman, N. C. The Label-Free Unambiguous Detection and Symbolic Display of Single Nucleotide Polymorphisms on DNA Origami. *Nano Letters* **2011**, *11*, 910–913.
45. Kuzuya, A.; Sakai, Y.; Yamazaki, T.; Xu, Y.; Komiyama, M. Nanomechanical DNA Origami "single-Molecule Beacons" Directly Imaged by Atomic Force Microscopy. *Nature Communications* **2011**, *2*, 449.
46. Picuri, J. M.; Frezza, B. M.; Ghadiri, M. R. Universal Translators for Nucleic Acid Diagnosis. *Journal of the American Chemical Society* **2009**, *131*, 9368–77.
47. Keum, J.-W.; Bermudez, H. Enhanced Resistance of DNA Nanostructures to Enzymatic Digestion. *Chemical communications (Cambridge, England)* **2009**, 7036–7038.
48. Aldaye, F. A.; Palmer, A. L.; Sleiman, H. F. Assembling Materials with DNA as the Guide. *Science (New York, N.Y.)* **2008**, *321*, 1795–9.
49. Pinheiro, A. V.; Han, D.; Shih, W. M.; Yan, H. Challenges and Opportunities for Structural DNA Nanotechnology. *Nature Nanotechnology* **2011**, *6*, 763–772.
50. Wang, P.; Meyer, T. A.; Pan, V.; Dutta, P. K.; Ke, Y. The Beauty and Utility of DNA Origami. *Chem* **2017**, *2*, 359–382.
51. Samanta, A.; Zhou, Y.; Zou, S.; Yan, H.; Liu, Y. Fluorescence Quenching of Quantum Dots by Gold Nanoparticles: A Potential Long Range Spectroscopic Ruler. *Nano Letters* **2014**, *14*, 5052–5057.
52. Hemmig, E. A.; Creatore, C.; Wünsch, B.; Hecker, L.; Mair, P.; Parker, M. A.; Emmott, S.; Tinnefeld, P.; Keyser, U. F.; Chin, A. W. Programming Light-Harvesting Efficiency Using DNA Origami. *Nano Letters* **2016**, *16*, 2369–2374.

53. Maune, H. T.; Han, S.; Barish, R. D.; Bockrath, M.; III, W. A. G.; Rothemund, P. W. K.; Winfree, E. Self-Assembly of Carbon Nanotubes into Two-Dimensional Geometries Using DNA Origami Templates. *Nature Nanotechnology* **2010**, *5*, 61–66.
54. Voigt, N. V.; Tørring, T.; Rotaru, A.; Jacobsen, M. F.; Ravnsbæk, J. B.; Subramani, R.; Mamdouh, W.; Kjems, J.; Mokhir, A.; Besenbacher, F.; Gothelf, K. V. Single-Molecule Chemical Reactions on DNA Origami. *Nature Nanotechnology* **2010**, *5*, 200–203.
55. Fu, J.; Liu, M.; Liu, Y.; Woodbury, N. W.; Yan, H. Interenzyme Substrate Diffusion for an Enzyme Cascade Organized on Spatially Addressable DNA Nanostructures. *Journal of the American Chemical Society* **2012**, *134*, 5516–5519.
56. Dai, M.; Jungmann, R.; Yin, P. Optical Imaging of Individual Biomolecules in Densely Packed Clusters. *Nature Nanotechnology* **2016**, *11*, 798–807.
57. Tomov, T. E.; Tsukanov, R.; Glick, Y.; Berger, Y.; Liber, M.; Avrahami, D.; Gerber, D.; Nir, E. DNA Bipedal Motor Achieves a Large Number of Steps Due to Operation Using Microfluidics-Based Interface. *ACS Nano* **2017**, *11*, 4002–4008.
58. Liang, X.; Nishioka, H.; Takenaka, N.; Asanuma, H. A DNA Nanomachine Powered by Light Irradiation. *ChemBioChem* **2008**, *9*, 702–705.
59. Liang, X.; Mochizuki, T.; Asanuma, H. A Supra-Photoswitch Involving Sandwiched DNA Base Pairs and Azobenzenes for Light-Driven Nanostructures and Nanodevices. *Small (Weinheim an der Bergstrasse, Germany)* **2009**, *5*, 1761–1768.
60. Kamiya, Y.; Asanuma, H. Light-Driven DNA Nanomachine with a Photoresponsive Molecular Engine. *Accounts of chemical research* **2014**.

# Chapter 2: Addressing the Instability of DNA Nanostructures in Tissue Culture

Jaeseung Hahn, Shelley F. J. Wickham, William M. Shih, Steven D. Perrault

## 2.1 Abstract

DNA nanotechnology is an advanced technique for producing molecular-scale devices that could contribute new diagnostic and therapeutic capabilities to nanomedicine. Although such devices are often developed and demonstrated using *in vitro* tissue culture models, these conditions may not be compatible with DNA nanostructure integrity and function. The purpose of this study was to characterize the sensitivity of 3D DNA nanostructures produced via the origami method to the *in vitro* tissue culture environment, and identify solutions to prevent loss of nanostructure integrity. We examined whether the physiological cation concentrations of cell culture media, and the nucleases present in fetal bovine serum (FBS) used as a media supplement, result in denaturation and digestion, respectively. DNA nanostructure denaturation due to cation depletion was design- and time-dependent, with one of four tested designs remaining intact after 24 hrs at 37ºC. Adjustment of media by addition of $MgSO_4$ prevented denaturation. Digestion of nanostructures by FBS nucleases did not appear design dependent, and became significant within 24 hrs and when media was supplemented with greater than 5% FBS. We estimated that media supplemented with 10% FBS contains greater than 256 U/L equivalent of DNAse I activity in digestion of DNA nanostructures. Heat-inactivation at 75ºC, and inclusion of actin protein in media, inactivated and inhibited nuclease activity, respectively. We examined the impact of media adjustments on cell growth, viability, and phenotype. Adjustment of $Mg^{2+}$ to 6mM did not appear to have a detrimental impact on cells. Heat-inactivation was found to be incompatible with *in vitro* tissue culture, whereas inclusion of actin had no observable effect on growth and viability. In two *in vitro* assays, immune cell activation and nanoparticle endocytosis, we show that using conditions compatible with cell phenotype and nanostructure integrity is vital to obtaining reliable experimental data. Our study thus describes considerations that are vital for researchers undertaking *in vitro* tissue culture studies with DNA nanostructures, and some potential solutions for ensuring that nanostructure integrity and functions are maintained during experiments.

## 2.2 Introduction

DNA nanotechnology[1] is a rapidly progressing field owing to the ease of producing two- and three-dimensional nanostructures through methods such as DNA origami.[2,3] DNA nanostructures can be designed with virtually any arbitrary geometry,[4,5] and to display sophisticated capabilities (e.g. mechanical,[6] logic-gating[7]) unavailable to other nano-scale materials. These can act as platforms for precise spatial organization of functional molecular features such as fluorophores,[8] biomolecules (e.g. aptamers,[9] antibodies[10]) or synthetic nanomaterials[11] (e.g. quantum dots) through coupling to an oligonucleotide that is integrated into a nanostructure's design. These unique advantages have provided ample motivation for nanomedicine researchers to develop biomedical applications for DNA nanotechnology. Recent studies have demonstrated a long circulating virus-inspired DNA nanodevice,[12] a computational molecular cascade for cell surface receptor characterization,[13] a synthetic membrane ion pore,[14] an immune activating programmable adjuvant,[15] and a logic-gated nano-robot for therapeutic delivery.[16]

*In vitro* tissue culture model systems are an obvious choice for prototyping new diagnostic and therapeutic devices, including those based on DNA nanotechnology. The

conditions used for tissue culture are typically determined by what has been empirically established as appropriate for the cells of interest. For mammalian cells this means incubation at 37°C in a defined cell culture media, e.g. RPMI or DMEM, containing amino acids, glucose and vitamins, and at a physiological pH and concentration of ions. Maintaining cell growth and phenotype often requires such media to be supplemented with 2-20% of mammalian serum (e.g. fetal bovine serum), which contributes essential but undefined factors. The compatibility of the *in vitro* tissue culture environment with DNA origami nanostructures has not been systematically tested, but is of obvious importance for biomedical applications of these materials.

The synthesis or "folding" of DNA nanostructures involves thermal annealing in the presence of a minimum concentration of cations to overcome the negative charge repulsion forces of the nucleic acid phosphodiester backbone. Compact and high density 3D nanostructures produced via DNA origami are typically produced in a buffer containing the divalent cation $Mg^{2+}$ at a concentration of ~5-20 mM,[3] ~one order of magnitude higher than its concentration in blood and tissue culture media (<1 mM). This discrepancy between the divalent cation concentration required by DNA nanostructures and that present in biological environments could cause nanostructure denaturation. Alternatively, synthesized nanostructures may have some capacity to sequester cations and may not therefore display sensitivity to low $Mg^{2+}$ environments. As well, blood and tissue culture media contain high concentrations of the monovalent cation $Na^{+}$ (~140 mM) that would likely support nanostructure integrity. Nevertheless, the sensitivity of DNA nanostructures to cation depletion when transferred into tissue culture media could impact the performance of their engineered capabilities.

A second concern is in regards to the supplementation of tissue culture media with fetal bovine serum, a blood product known to contain a variety of nucleases[17–19] that have hindered translation of nucleic acid-based biotechnologies such as gene therapy.[20,21] The digestion half-life of unprotected plasmid DNA has been measured at 20 min with freshly isolated plasma,[20] and 10 min after *in vivo* intravenous injection.[21] Nuclease digestion of DNA nanostructures[22,23] and the cross-over motifs[24] used in their architecture appears to be partially inhibited when compared to oligonucleotides or plasmid DNA. However, even partial digestion of DNA nanostructures could greatly affect their geometry and capabilities, and could cause release of attached molecular features.

In this study we present a systematic characterization of the sensitivity of various nanostructures to typical mammalian tissue culture conditions. We examined the denaturation of nanostructures due to divalent cation depletion, and their digestion by nucleases present in FBS. Based on our findings, we developed strategies to maintain nanostructure stability by making adjustments to tissue culture media. We then tested the impact of those adjustments on cell growth and viability. Finally, we carried out two typical tissue culture assays to measure the impact of nanostructure instability and media adjustments on cell phenotype and experimental outcomes.

## 2.3 Results and discussion

As test cases for this study, we synthesized three nanostructures that were designed using the DNA origami method (**Figure 1a-c, Supporting Information Fig. 1-3**). These were produced by annealing three previously described nanostructure-specific oligonucleotide "staple" sets with single-stranded, modified[25] M13 phage "scaffold" DNA of 7308 nucleotides. Owing to the sensitivity of mammalian cells to bacterial cell wall lipopolysaccharide or "endotoxin", we developed a protocol for removal of this by-product of M13 scaffold production with Triton X-114 (**Supporting Information Fig. S4**).

Using a first set of 144 staple strands, we synthesized a ~50 nm diameter wireframe DNA NanoOctahedron (DNO).[12] The DNO struts are each composed of a bundle of six DNA double-helices[26] connected by anti-parallel cross-over junctions.[27,28] An ~90° curvature is added to the struts via targeted insertions and deletions.[4,12] The scaffold and staple strands were combined in Tris-EDTA (TE) buffer with 14 mM $MgCl_2$, and the nanostructure was produced using a 15-hour thermal annealing ramp. Using the same annealing ramp and two alternative sets of staple strands, we produced NanoTubes[25] (NT) composed of a single 400 nm long six-helix bundle (168 staple strands, 20 mM $MgCl_2$), and a 16x89 nm NanoRod[29] (NR) composed of 24 inter-connected helices (178 strands, 18 mM $MgCl_2$). Correctly folded nanostructures were purified using a previously described gradient ultracentrifugation method.[29] After purification of the DNO and NR, we annealed a fluorescent Cy5-labeled oligonucleotide to single-stranded DNA "handles" present on the nanostructure to represent molecular cargo typically added to nanostructures as functional features.

We then characterized the sensitivity of these DNA nanostructures to $Mg^{2+}$ depletion in standard RPMI media (132.9 mM $Na^+$, 5.3 mM $K^+$, 0.4 mM $Mg^{2+}$, 0.4 mM $Ca^{2+}$) without FBS supplementation. To further elucidate the dependence of nanostructure integrity on $Mg^{2+}$ concentration, we included a series of adjusted RPMI media samples with $Mg^{2+}$ concentrations of 0.7 mM – 10 mM, and a control previously determined to maintain nanostructure integrity (TE buffer, 10 mM $Mg^{2+}$). Following incubation at 37°C for 24 hrs, the products were analyzed by agarose gel electrophoresis (AGE). In comparison to control samples, the DNO and NR displayed reduced electrophoretic migration after incubation in standard RPMI media, and adjusted media with $Mg^{2+}$ concentrations below ~6 mM (**Figure 1d, f**). This suggests that some degree of denaturation had occurred, which would likely increase the dimensions of the nanostructures and slow their travel through the agarose matrix. Surprisingly, NT migration did not appear dependent on $Mg^{2+}$ concentration over the tested range (**Figure 1e**), demonstrating design-dependent variability in the sensitivity of nanostructures to $Mg^{2+}$ depletion. Because the DNO and NR were labeled with fluorescent Cy5-oligonucleotides, we were able to examine *via* AGE if low divalent cation conditions may cause a loss of molecular cargo attached to the nanostructures. We imaged the gels for Cy5 fluorescence and observed a partial, $Mg^{2+}$ concentration-dependent loss of Cy5 cargo from the DNO and NR, demonstrating that denaturation *via* divalent cation depletion can cause release of attached molecular cargo (**Supporting Information Fig. S5**).

We further characterized the RPMI incubation products via negative-stain transmission electron microscopy (TEM) (**Figure 1g-l**). Imaging confirmed that the DNO and NR denature in RPMI, and that their structural integrity is maintained in media adjusted to 6 mM $Mg^{2+}$.

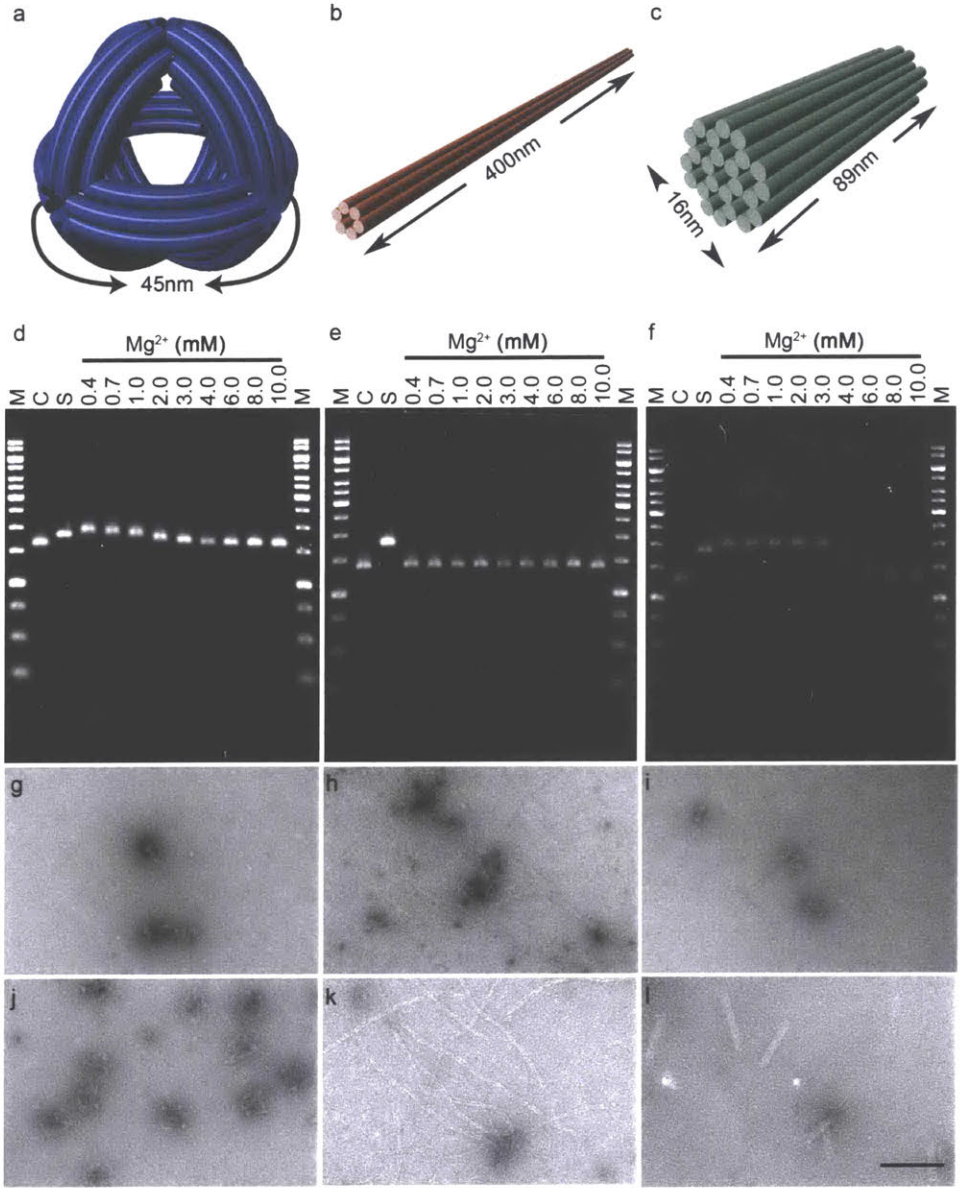


**Figure 1. DNA nanostructure sensitivity to cation depletion in tissue culture media.** The three test nanostructures, shown illustrated, are **a)** DNA NanoOctahedron (DNO), **b)** six-helix bundle NanoTube (NT), **c)** and 24-helix NanoRod (NR). **(d-f)** The three nanostructures were incubated for 24 hrs at 37ºC in unmodified RPMI tissue culture media containing 0.4 mM $Mg^{2+}$, or adjusted to 0.7 – 10 mM $Mg^{2+}$, and the products analyzed by agarose gel electrophoresis (AGE). In comparison to the control lanes of stable sample, migration of the DNO and NR is retarded after low $Mg^{2+}$ incubation, indicative of denaturation, whereas no obvious difference in migration is observed with the NT. **(g-i)** Transmission electron microscopy (TEM) Images of nanostructures incubated in unmodified media, showing varying levels of denaturation. **(j-l)** By adjusting the media to 6 mM $Mg^{2+}$, structural integrity is maintained in all three designs. M= molecular weight ladder, C = Nanostructure in TE + 10 mM $Mg^{2+}$, S = M13 scaffold. Scale bar = 100 nm.

Although we observed particles approximating the dimensions of the DNO and NR after incubation in standard RPMI (0.4 mM $Mg^{2+}$), they were amorphous and lacked recognizable features. This suggests that the low divalent and high monovalent cation concentrations in the RPMI media were unable to overcome charge repulsion of the DNA phosphodiester backbone, and that the $Mg^{2+}$ ions associated with the nanostructures from synthesis did not remain sequestered after transfer into RPMI. The impact of media on NT integrity appeared less dramatic. Intact NT were visible by TEM after incubation in 0.4 mM $Mg^{2+}$ RPMI. Relative to the control sample, there were far fewer NT present, but this may be a $Mg^{2+}$-dependent artifact of sample preparation for TEM imaging.

Based on its stability in media, DNA NT may be an excellent choice for *in vitro* tissue culture studies. To characterize a nanostructure with relevance to biomedical applications, we also examined the logic-gated DNA Nanorobot[16] for sensitivity to divalent cation depletion using the same assay as described above. After incubation at 37°C for 24 hrs, AGE analysis showed a difference in migration between controls and those incubated in standard RPMI media, and adjusted media with $Mg^{2+}$ concentrations below ~2 mM (**Supporting Information Fig. 6a**). This shift became apparent after 30 minutes of incubation (**Supporting Information Fig. 6b**). Imaging of nanostructures incubated at 2 mM $Mg^{2+}$ for 24 hrs revealed Nanorobots that were intact but which appeared stressed, in comparison to the control 10 mM $Mg^{2+}$ sample (**Supporting Information Fig. 6c, d**). We were unable to find intact nanostructures after incubation in standard media, but this might be a false negative, attributable to an artifact of TEM sample preparation. Relative to the NR and DNO, the Nanorobot appears less sensitive to low $Mg^{2+}$ concentrations. In light of the published functional data[16], it may be possible that electrostatic repulsion from divalent cation depletion causes some flexing of the Nanorobot structure, without a loss of the logic-gating molecular features and open-versus-closed conformations. Further in-depth studies would be needed to fully elucidate these details.

The variability in nanostructure sensitivity to divalent cation depletion is intriguing. The designs tested here share a common scaffold strand and GC content. The design-specific oligonucleotide sets of the DNO, NT and NR are comparable in mean (± standard deviation) length at 42.0 ± 2.5, 40.6 ± 4.6 and 41.9 ± 0.8 nucleotides, respectively, whereas the NanoRobot set is shorter (33.3 ± 7.0). The secondary structure (six-helix bundle motif) is common between the DNO and NT, although curvature included in the DNO strut design might further stress the structure in a low-$Mg^{2+}$ environment. The charge density is highest in the NR, in which 12 of the 24 double helices have three nearest-neighbors, compared to two for the double helices of the DNO, NT, and NanoRobot. Based on a lack of any clear pattern, it is possible that nanostructure sensitivity to divalent cation depletion could be dependent on a variety of design parameters. Until this is better understood, the stability of nanostructures intended for use in tissue culture experiments should be tested in appropriate conditions.

Next, the various nanostructures were incubated in RPMI supplemented with 10% FBS to assess nuclease digestion kinetics. Note that the FBS used in these experiments had been heat-treated at 56°C by the vendor for inactivation of immune factors, as is standard practice. For these experiments the RPMI media was adjusted to 6 mM $Mg^{2+}$ using $MgSO_4$ (a component of RPMI) to prevent nanostructure denaturation. After incubation of 5 nM DNO at 37°C for 0.25 – 24 hrs, samples were analyzed by AGE and compared to a control incubated in RPMI + 6 mM $Mg^{2+}$, but

lacking FBS, for 24 hrs. The results show little change in migration of the DNO (**Figure 2a**), NT and NR (**Supporting Information Fig. S7**) over the first 8 hrs. However, there is an almost complete loss of the primary product band by 24 hrs. TEM imaging of the DNO control sample showed no apparent changes (**Figure 2b**), whereas nanostructures incubated in media with serum for 2 hrs showed varying degrees of digestion (**Figure 2c**). Based on this, it appears that some amount of nuclease activity remains in the FBS typically used to supplement tissue culture media. We also observed, over numerous repetitions of these experiments, that the level of nuclease activity in different FBS lots and frozen aliquots can be quite variable, with digestion progressing faster or much slower than that presented in **Figure 2.** As well, the nuclease activity was highest after initial thawing of an FBS stock, and was lost over a time-span of weeks when prepared media was stored at 4°C. The presence of nuclease in media could have a dramatic impact on the results of tissue culture studies that utilize DNA nanostructures, and care must be taken to ensure that it is absent during experiments.

To determine the relative nuclease activity present in tissue culture media, we carried out a 12 hr, 37°C incubation of DNO in 6 mM $Mg^{2+}$ RPMI media supplemented with 1.25 - 20% FBS, or with 1 - 4096 U/L of DNase I (**Supporting Information Fig. S8**). Significant digestion was apparent at 10 and 20% FBS, and at more than 256 U/L of DNase I, suggesting that typical tissue culture conditions may contain between 256 and 1024 U/L equivalent of DNase I activity. Note that digestion was not apparent by AGE for low concentrations of FBS (1.25 – 2.5%),

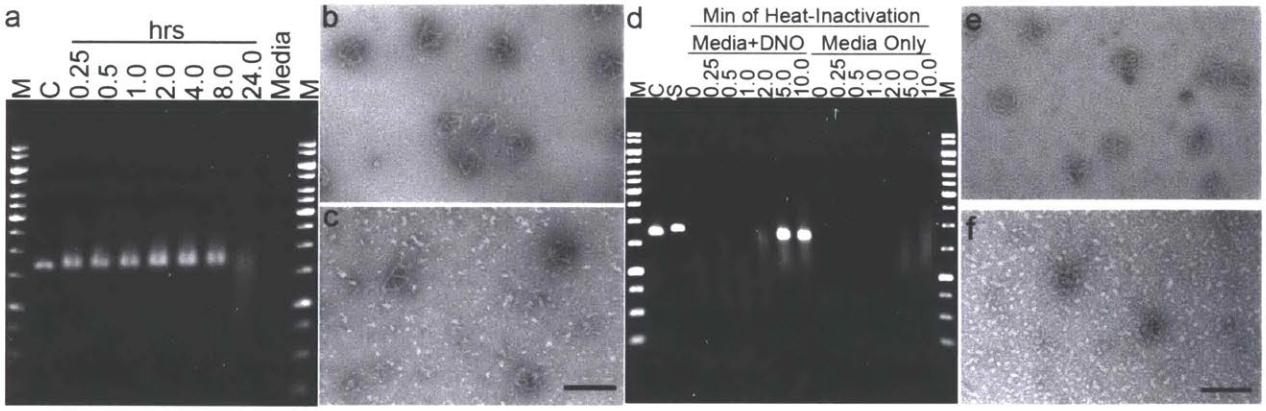


**Figure 2. Kinetics of nanostructure digestion by nucleases present in serum, and heat-inactivation. (a)** The DNO nanostructure (5 nM) was incubated at 37°C for 0.25 – 24 hrs in RPMI + 6 mM $Mg^{2+}$ + 10% FBS. Analysis by AGE shows smearing and decreased intensity of the product band as digestion progresses. **(b)** TEM image of DNO control sample showing intact nanostructures. **(c)** Partially digested DNO sample after 2hrs incubation in media + 10% FBS. Note in upper left, an example of a partially digested DNO. **(d)** Aliquots of FBS were heat-treated for 0.25 – 10.0min at 75°C prior to mediation preparation. DNO was incubated for 24 hrs at 37°C and analyzed by AGE. Media without nanostructures was analyzed on the right half of the gel, showing a change in appearance from 5 and 10 min heat treatment. **(e)** TEM of a control and **(f)** DNO incubated in RPMI media prepared with FBS heat-inactivated for 5 min. M = molecular weight ladder, C = Nanostructure in TE + 10 mM $Mg^{2+}$, S = M13 scaffold. Scale bars = 100 nm.

suggesting one potential solution for circumventing media nuclease activity when short incubations times and low serum concentrations are compatible with the assay and cells of interest.

Heat treatment of FBS is a potentially easy and scalable method for inactivation of nuclease activity. In order to determine the minimum heat treatment required, FBS was incubated at 75°C for 0 – 10 min. This was carried out in 1 mL aliquots to allow for efficient heat transfer. We used this to prepare RPMI + 6 mM $Mg^{2+}$ + 10% FBS, to which the DNO nanostructure was added at 5 nM and incubated at 37°C for 24 hrs. Analysis of the incubation products by AGE showed that a minimum treatment of 5 min was required to prevent altered migration of the nanostructure (**Figure 2d**). TEM imaging confirmed that DNO (**Figure 2e, f**) incubated in FBS treated thusly remained intact, with no obvious difference in appearance compared to a control. Heat inactivation of FBS could therefore address the problem of nuclease activity in tissue culture experiments. However, the altered appearance of the 5 and 10 min treated FBS in our AGE analysis (**Figure 2d**) suggests it has a more general effect on serum proteins, which could also impact cell growth and phenotype.

An alternative to heat inactivation of FBS is inclusion of a nuclease inhibitor, such as actin protein,[30] in tissue culture media. Actin inhibition occurs via competitive binding to nuclease, and should therefore be concentration dependent. To test this and determine an appropriate relative concentration of actin, we incubated 5 nM DNO in RPMI + 6 mM $Mg^{2+}$ + 10% FBS, and 0 – 2048 nM actin. After 24 hrs at 37°C we observed by AGE that a 10-fold or greater molar excess of actin appears sufficient to inhibit digestion of nanostructures (**Supplementary Information Fig. 9**). The corresponding TEM image of intact DNO is comparable to a control, and both the NT and NR (**Supporting Information Fig. 10**) were similarly protected, providing a potential alternative to heat inactivation.

Next we aimed to determine the effect of our various media adjustments on the growth of three different cell lines: mouse embryonic fibroblast cells (3T3), human embryonic cells (HEK-293) and human adenocarcinoma cells (H441). These were first established in standard media + 10% FBS for a minimum of 32 population doublings. They were then seeded at low density in media modified by 1) adjustment to 6 mM $Mg^{2+}$, 2) use of 75ºC heat-inactivated FBS, 3) inclusion of 200 nM actin, or 4) a combination of $Mg^{2+}$ adjustment and heat- inactivated FBS or 5) actin. In cases where the $Mg^{2+}$ concentration of the media was adjusted, osmolarity was maintained by an equivalent dilution (~5%). Cell content was measured on days 0, 1, 3 and 5 and 7 after seeding using the CyQuant cell proliferation assay, which measures fluorescence of a cell nucleus stain (**Figure 3a-c**), and the change over time was normalized to Day 0. Heat treatment of FBS produced a consistent, detrimental impact on growth, with all three cell lines showing significantly reduced fluorescent signal on day 7 relative to standard media ($p<0.05$). Adjustment of media to 6 mM $Mg^{2+}$ had a cell line-dependent impact on growth. The 3T3 cells produced a significantly lower signal by day 7 ($p<0.01$), whereas HEK293 and H441 fluorescence were similar to control media ($p>0.05$). The combination of $Mg^{2+}$ adjustment and FBS heat inactivation resulted in slower cell growth with only the 3T3 cells ($p<0.01$). Inclusion of 200 nM actin with and without $Mg^{2+}$ adjustment produced no significant differences in signal by Day 7 for all three lines ($p>0.05$). Taken together, our data suggests that *in vitro* mammalian cell growth may not be sensitive to adjustment of media $Mg^{2+}$ up to a concentration of at least 6 mM,

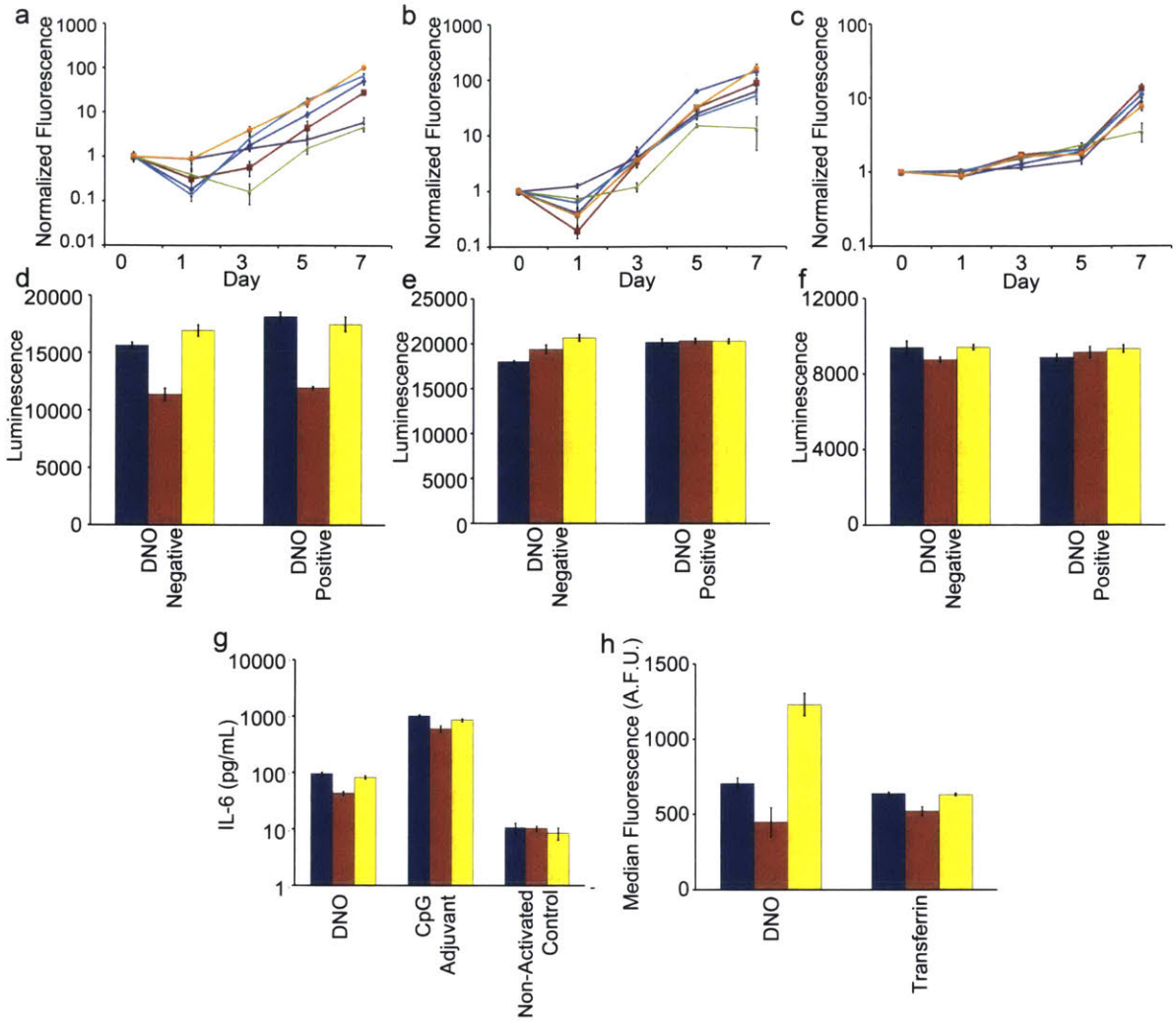


**Figure 3. Measuring the impact of media modifications on cell growth, viability and phenotype. (a)** Mouse 3T3 fibroblasts, **(b)** human HEK-293 embryonic kidney, and **(c)** human H441 adenocarcinoma cell lines were seeded into standard media (—), $Mg^{2+}$-adjusted (—), heat-inactivated FBS (—), $Mg^{2+}$ + heat-inactivated FBS (—), 200 nM actin (—), or combination $Mg^{2+}$ + 200 nM actin media (—). Change in cell number was estimated by fluorescence of CyQuant stain over time, and was normalized to signal on Day 0. **(d)** Cell viability and metabolism of 3T3, **(e)** HEK-293, and **(f)** H441 cells were profiled after 24 hrs incubation with and without 5 nM DNO. **(g)** Primary mouse immune cells were isolated from spleens and incubated with 1 nM DNO, an equivalent mass of CpG phosphorothioate oligonucleotide adjuvant, or media only, and the concentration of IL-6 cytokine released into the supernatant was determined by ELISA. **(h)** 3T3 fibroblast cells were incubated for 16 hrs with 1 nM fluorescently-labeled DNO or transferrin and endocytosis of the two agents was measured by Flow cytometry after extensive washing to remove surface-bound particles. (**d – h**) Culture conditions are standard media (■), media + 6 mM $Mg^{2+}$ + heat-inactivated FBS (■), or media + 6 mM $Mg^{2+}$ + FBS + 200 nM actin (■). (**a - h**) Error bars represent standard error of the mean of n = 5 replicates.

and to the presence of actin at 200 nM. This tolerance to a $Mg^{2+}$ concentration higher than that found in blood (<1 mM) is surprising, but some established media such as EGM-2 used for human umbilical vein endothelial cell (HUVEC) tissue culture contains non-physiological concentrations of $Mg^{2+}$ (10 mM). Heat-inactivation of FBS for nuclease removal does not appear to be compatible with normal cell growth. It likely causes denaturation of a substantial fraction of serum proteins, leading to a state of serum-starved quiescence or cell death. The impact of this would be greatest when cells are seeded at a low density, as they were in this experiment to avoid them reaching confluence before day 7. Primary cells such as 3T3 fibroblasts may also be more sensitive to a low nutrient environment than cancer cell lines (e.g. H441), which are generally more robust owing to autocrine signaling and previous selective pressure for nutrient-deprived survival.

To cross-validate our cell growth data, we used the CellTiter-Glo Luminescence Assay to quantitate ATP concentrations in media following a 16 hr incubation of the three cell lines (**Figure 3d-f**). The media concentration of ATP and corresponding luminescent signal correlates linearly with the number of metabolically active, viable cells in culture. Measurements were taken after incubation in standard media, or in the two adjusted conditions that we have identified as supportive of nanostructure integrity: 6 mM $Mg^{2+}$ + 10% heat-inactivated FBS, or 6mM $Mg^{2+}$ + 10% FBS + 200 nM actin. For each condition, we included DNO-positive (5 nM) and -negative treatments to investigate whether the presence of DNA nanostructures may be toxic to these cell lines. Consistent with the cell growth CyQuant data, the 3T3 line displayed sensitivity to heat-inactivation of FBS, with DNO-positive and –negative treatments reduced to ~75% of the luminescent signal observed for control DNO-negative standard media ($p<0.01$). No difference was observed with the actin media for the 3T3 cells. Neither the H441 nor HEK293 cells showed reduced luminescence in the two adjusted media conditions, suggesting that these combinations of media and cells could be used for short assays without impacting cell metabolism and viability. As well, the presence of 5 nM DNO did not independently reduce luminescence in any of the media conditions, suggesting that this combination of nanostructure and assay conditions may not be toxic to these specific cell lines.

We next aimed to measure the impact of media adjustments on cell phenotype using two assays relevant to nanomedicine. In a first assay, we examined how media adjustment and nanostructure integrity impact results of immune cell activation by DNA nanostructures (**Figure 3g**). Immune cells have previously been shown to elicit an inflammatory cytokine response to DNA origami nanostructures, including release of the cytokine interleukin-6 (IL-6)[15]. Primary immune cells isolated from mouse spleens were washed extensively to remove inherent tissue nucleases, and we verified that nuclease-free media incubated with splenocytes for 24 hrs does not regain nuclease activity capable of nanostructure digestion (**Supporting Information Fig. 11**). We then incubated splenocytes for 16 hrs with 1 nM DNO in standard media or the two adjusted media conditions that support nanostructure integrity, and measured the concentration of IL-6 released into the tissue culture supernatant *via* an ELISA assay. As positive and negative controls, we measured response to a nuclease-resistant DNA adjuvant (CpG 1826) or no activating agent, respectively, in the same panel of media conditions. These controls showed that the cells were phenotypically normal for IL-6 response in all three media conditions. IL-6 was produced at high levels in response to the CpG adjuvant, and

negative control cells were not activated in the presence of actin or heat-inactivated FBS. The level of IL-6 produced in response to DNO (37.7 ± 3.7 pg/mL) and CpG (743.9 ± 85.8) was significantly reduced in adjusted media with heat-inactivated FBS, in comparison to standard media (94.8 ± 6.5 pg/mL for DNO and 1013.4 ± 50.2 pg/mL for CpG, $p<0.01$). No significant differences were observed for either agent in adjusted media with actin (81.9 ± 5.4 pg/mL for DNO and 862.7 ± 49.5 pg/mL for CpG, $p>0.05$), suggesting that this media environment should produce reliable IL-6 response data. Yet having demonstrated that our DNO is not stable in standard media, we might expect a meaningful difference in immune cell response when nanostructures are intact (*i.e.* in adjusted media with actin) compared to standard media where we expect nanostructure instability. Other work from our laboratory has found that the response of splenocytes to DNA nanostructures is dependent on the total mass of DNA present, and not on their design or integrity (data not shown). Therefore, the results from this assay demonstrate that adjusted media with actin may be a good choice for maintaining normal cell phenotype and nanostructure integrity. Perhaps more importantly, this assay shows that a seemingly normal cell phenotype and expected experimental outcomes are poor indicators of nanostructure integrity and may lead to an incorrect interpretation of results.

In a second assay and final experiment, we determined how adjusted media and nanostructure integrity can impact the results of particle endocytosis (**Figure 3h**). We incubated 3T3 fibroblast cells with 1 nM DNO fluorescently labeled by Cy5-coupled oligonucleotides. A16 hr incubation was carried out in standard media or the two adjusted media conditions that support nanostructure integrity, and uptake was measured *via* Flow cytometry. Similar to the immune response assay, we verified that media enriched through incubation with 3T3 cells does not display nuclease activity capable of digesting the DNO (data not shown). As a positive control we used fluorescently-labeled transferrin. In comparison to standard culture media (637.8 ± 10.4 A.F.U.), uptake of transferrin was similar in media + 6 mM $Mg^{2+}$ + actin (631.6 ± 6.8 A.F.U., $p>0.05$) but lower in media + 6 mM $Mg^{2+}$ + heat-inactivated FBS (520.2 ± 29.7 A.F.U., $p<0.01$). This was unsurprising based on our earlier observation that 3T3 growth and metabolism are decreased in media with heat-inactivated FBS. After incubation with the DNO we observed that 3T3 fluorescence was lowest in media + 6mM $Mg^{2+}$ + heat-inactivated FBS (446.6 ± 96.5 A.F.U.), but the difference relative to standard media was not meaningful (704.8 ± 38.3 A.F.U., $p>0.05$). More remarkably, fluorescence of cells in media + 6 mM $Mg^{2+}$ + actin (1230.2 ± 73.8 A.F.U.) was 75% higher than in standard media ($p<0.01$). Based on our earlier analysis we would expect the growth and metabolism of 3T3 cells to be similar in standard media and adjusted media with actin. This increase in uptake might therefore be due to a difference in DNO integrity between the two conditions, and would suggest that uptake of intact nanostructures may be higher than Cy5-labeled debris that would result from denaturation and digestion of DNO in standard media. Therefore, this endocytosis assay shows a drastic difference in experimental outcome when media is supportive of normal cell phenotype and nanostructure integrity, unlike what was observed from immune activation.

DNA nanotechnology offers unique and exciting advantages that may contribute to important advances in nanomedicine. However, this *in vitro* study and our earlier *in vivo*[12] study have shown that DNA nanostructures produced *via* the origami method are susceptible to denaturation and degradation in biological environments. Previous studies have probed the

stability of DNA nanostructures exposed to cell lysate[31] and after injection into the lumen of *C. elegans*[32]. DNA origami nanostructures exposed to cell lysate were found to remain largely intact, which is in contrast to our findings in cell culture media. The intracellular compartment has high total $Mg^{2+}$ content of 5 – 20 mM[33]. Much of this is associated with proteins and so should be unavailable, but the cell lysate was generated using sodium dodecyl sulfate, which may have denatured proteins (including nucleases) and released ionic $Mg^{2+}$ into solution. The nanostructures tested in *C. elegans* were smaller and so are not directly comparable to origami particles, but may be less susceptible to $Mg^{2+}$ depletion and denaturation. Significant nuclease activity was not observed in either case. This perhaps suggests that not all biomedical applications of DNA nanotechnology will face the same challenges to nanostructure integrity, and that systemic injection of origami-based particles into mammalian systems may be one of the most difficult.

## 2.4 Conclusions

Researchers designing nano-devices for biomedical applications should consider what degree of protection strategies, such as compartmentalization in a lipid membrane,[12] are required to maintain integrity within the biological environment of interest. Even without protection strategies, *in vitro* tissue culture studies are highly useful for development and prototyping of DNA nano-devices and their functions, such as in the case of the Nanorobot[16]. Based on this rationale, we have identified and characterized the sources of DNA nanostructure instability within the tissue culture environment, and demonstrated methods to overcome them. Our data shows that DNA nanostructures can be sensitive to depletion of $Mg^{2+}$ in tissue culture media, causing denaturation in a design-dependent manner, and that they are digested by nucleases present in FBS used as a media supplement.

Avoidance of FBS nuclease activity is perhaps the easier challenge to overcome. Our experience has been that the level of nuclease activity present in tissue culture FBS is variable and disappears over days to weeks when prepared media is stored at 4ºC. High levels of nuclease activity may therefore only be a concern for a short period following preparation of media from freshly thawed FBS. We found that media supplemented with low volumes of FBS (1 – 2.5%) had little capacity to digest a 5 nM concentration of DNA nanostructure over 24 hrs, suggesting that assays requiring short incubations could make use of low serum concentrations to avoid significant nuclease activity. This may slow, but not drastically alter cell metabolism and phenotype. Various serum-free media are also available from vendors for specific cell types. In any case where FBS nuclease activity is a concern, our data supports the use of actin as an inhibitor. We did not observe any difference in cell growth, viability, or phenotype when actin was included in media at 200 nM. In contrast, heat inactivation of nuclease activity using a 5 min, 75ºC treatment of FBS had a consistently detrimental impact on cells and on results of murine immune cell activation and 3T3 fibroblast endocytosis assays. Heat inactivation using these conditions does not therefore appear to be a viable option.

The denaturation of DNA origami nanostructures due to depletion of divalent cations is a major challenge to *in vitro* and *in vivo* applications. We observed that the sensitivity of nanostructures to cation depletion is design-, and time-dependent. Of the four designs that we tested, only one (DNA NanoTube) appeared stable in physiological cation concentrations.

Adjustment of media $Mg^{2+}$ concentration to ~one order of magnitude higher than physiological was able to prevent denaturation of the DNO, NR and DNA Nanorobot. Surprisingly, we observed little impact of $Mg^{2+}$ adjustment on the growth and viability of mouse 3T3 fibroblast cells, and human H441 adenocarcinoma and HEK293 embryonic kidney cells. Similarly, the phenotype of primary mouse splenocyte immune cells and 3T3 fibroblast cells was not sensitive to higher $Mg^{2+}$ concentrations during immune activation and uptake assays, respectively. This, and the fact that other examples of high $Mg^{2+}$ standard media are well established (e.g. EGM-2 for HUVECs), suggests that many mammalian cell types may not be sensitive to higher than physiological extracellular $Mg^{2+}$ concentrations. Addition of $MgSO_4$ to tissue culture media, and an equivalent dilution to prevent osmotic shock, thus appears to be a potentially viable and perhaps generalizable approach for maintaining DNA nanostructure integrity during *in vitro* experiments.

In any case of tissue culture media modification, it is strongly recommended that extensive testing and appropriate controls with standard media are used to ensure that the cell property being investigated is not sensitive to the adjustments. Similarly, the data presented in this study reinforces the need for more rigorous testing and verification of nanostructure integrity in applications involving biological environments.

The media adjustments tested here will suffice for some *in vitro* prototyping studies and applications of DNA nanotechnology. But ultimately, many DNA nanotechnology-based diagnostic and therapeutic devices will be developed towards *in vivo* use, or in biological conditions (e.g. blood, urine) that may not be easily modified. Future studies could therefore aim to develop DNA nanostructure protection strategies that obviate the need to alter their environment.

## 2.5 Materials and Methods

### Chemicals and Supplies

Endotoxin test cartridges (0.05 – 5.0 EU/mL) were purchased from Charles River. Accugene 10X TBE buffer, PCR tubes and 96-well PCR plates (Axygen) were purchased from VWR. SYBR Safe stain and CyQUANT Direct Cell Proliferation assay were purchased from Life Technologies Corporation. Agarose was purchased from Lonza. Glycerol, Tris base, EDTA, Triton x-114, Tween20, magnesium chloride, magnesium sulfate, and sodium chloride were purchased from Sigma-Aldrich. Actin was purchased from Cytoskeleton Inc. RPMI, DMEM, PBS, FBS and penicillin-streptomycin were purchased from Gibco. Carbon formvar grids and uranyl formate were purchased from Electron Microscopy Sciences. Amicon Ultra filtration devices and Seton ultracentrifugation tubes were purchased from Fisher Scientific. DNA gel extraction spin column was purchased from BIO-RAD.

### M13 Scaffold Prep, Endotoxin Removal, Nanostructure Synthesis and Purification

The four sets of design-specific staples strands were purchased reverse-phase purified from Bioneer or Life Technologies Corporation. The fluorescent Cy5-coupled oligonucleotide feature (5′-GTGAGTTGTGGTAGATAATTT-3′) was synthesized by IDT Technologies. The p7308 scaffold strand was produced from M13 phage replication in E. coli, as described previously[25].

The scaffold strand was endotoxin purified using Triton x-114. In brief, surfactant was added to scaffold stock to a final concentration of 2% (V/V). This was incubated at 4°C on an inversion mixer for 30 min to solubilize endotoxin. The solution was mixed at 37°C for 5 min to cause phase separation, and then centrifuged at 37°C for 30 min at maximum speed. The upper aqueous fraction was transferred to a new tube. This was repeated four times to reduce endotoxin in the scaffold stock solution to acceptable levels of less than 5 EU/mL, quantified using the Endosafe-PTS system and test cartridges (Charles River).

Nanostructure synthesis was carried out by mixing 50 nM M13 scaffold with a 5x excess of staples in TE + 14 mM (DNO), 20 mM (NT), 18 mM (NR), or 8 mM (NanoRobot) $MgCl_2$. The solutions were subjected to a thermal annealing ramp on a Tetrad 2 Peltier Thermal Cycler (Bio-Rad) according to the following schedule:

80°C for 5 minutes
Decrease to 65°C at 5 min/°C
Incubate at 65°C for 20 min
Decrease to 25°C at 20 min/°C

Solutions of folded DNA nanostructures were concentrated using a 30K MWCO Amicon Ultra centrifugal filter device (Millipore) and then purified by glycerol gradient ultracentrifugation[29]. Following purification, the stock solution was diluted appropriately for TEM imaging to verify quality. The stock concentration was determined by UV-absorbance at 260 nm on a Nanodrop spectrophotometer (Thermo Scientific) using disposable cuvettes (Sarstedt). Stock solutions were stored at 4°C until use.

**Agarose gel analysis**

DNA nanostructures were analyzed by gel (1.5% agarose, 0.5x TBE 10 mM $MgCl_2$, 1x SYBR Safe) electrophoresis with Thermo Scientific Owl B2 EasyCast Mini Gel System apparatus. The samples were loaded into the agarose gel and allowed to migrate for 4 hr (running buffer: 0.5x TBE, 10 mM $MgCl_2$; 4.3V/cm). The gel was imaged with Typhoon FLA 9000 (GE Healthcare Life Sciences). To recover nanostructures, the bands were visualized with UV light and cut out from the gel. Extracted bands were crushed and placed into DNA gel extraction spin column (BIO-RAD). Then, the nanostructure solution was recovered by centrifugation of the loaded column for 3 min at 4000 x *g*.

**Negative-Stain Transmission Electron Microscopy**

TEM imaging was carried out by dropping 3.5uL of product onto a plasma-treated carbon-formvar grid (Electron Microscopy Sciences). This was incubated for 1 min. The solution was wicked away onto filter paper, and 3.5 uL of 2% uranyl formate (in $H_2O$, W/V) was immediately added. This was incubated for 0.5 min, and then wicked away by filter paper. Imaging was carried out on a JEOL 1400 transmission electron microscope.

**Cation Depletion Assay**

RPMI media (Gibco) was modified to 0.7, 1.0, 2.0, 3.0, 4.0, 6.0, 8.0, and 10 mM $Mg^{2+}$ by addition of $MgSO_4$ from a 500 mM stock solution. Each nanostructure was adjusted to 150 ug/mL and then mixed with unmodified RPMI media (0.4 mM $Mg^{2+}$) or modified RPMI media at a 1:10 ratio. The samples were incubated at 37°C for 24 hrs on a Tetrad 2 Peltier Thermal Cycler (Bio-Rad) and analyzed using agarose gel electrophoresis (AGE) and TEM imaging.

**Nuclease Digestion Kinetics Assay**

RPMI media (Gibco) was adjusted to 6 mM $Mg^{2+}$ by addition of $MgSO_4$ and supplemented with 10% freshly thawed FBS (Gibco; heat-inactivated at 56°C by the vendor). Each nanostructure was adjusted to 150 ug/mL and mixed with modified RPMI at a 1:10 ratio. The samples were incubated at 37°C for 0.25, 0.5, 1, 2, 4, 8, and 24 hr on a Tetrad 2 Peltier Thermal Cycler (Bio-Rad) and crushed into ice to stop nuclease digestion. The nanostructures were immediately analyzed using AGE. Then, the bands were extracted to recover nanostructures, and the nanostructures were imaged under TEM.

**Nuclease Digestion Quantitation Assay**

RPMI media (Gibco) was adjusted to 6 mM $Mg^{2+}$ by addition of $MgSO_4$ and supplemented with either 1.25 – 20% freshly thawed FBS (Gibco; heat-inactivated at 56°C by the vendor) or 1 – 4096 U/L of DNase I (New England Biolabs). The DNO was adjusted to 150 ug/mL and mixed with each media condition 1:10 ratio. These were incubated for 12 hrs at 37°C, and the products were analyzed by AGE.

**Serum Heat-Inactvation Assay**

Freshly thawed FBS (Gibco) was heat-treated at 75°C for 0.25, 0.5. 1, 2, 5, and 10 min in 1 mL aliquots on an Eppendorf Thermoshaker with rapid shaking. RPMI media (Gibco) was adjusted to 6 mM $Mg^{2+}$ by addition of $MgSO_4$ and supplemented with 10% freshly thawed FBS or heat-treated FBS. Each nanostructure was adjusted to 150 ug/mL and mixed with modified RPMI at a 1:10 ratio. The samples were incubated at 37°C for 24 hr on a Tetrad 2 Peltier Thermal Cycler (Bio-Rad) and crushed into ice to stop nuclease digestion. The nanostructures were analyzed using AGE. Then, the bands were extracted to recover nanostructures, and the nanostructures were imaged under TEM.

**Actin Nuclease Inhihbition Assay**

RPMI media (Gibco) was adjusted to 6 mM $Mg^{2+}$ by addition of $MgSO_4$ and supplemented with 10% freshly thawed FBS (Gibco; heat-inactivated at 56°C by the vendor). A dilution series of actin protein was prepared and added to the media. A 150 ug/mL solution of each nanostructure was prepared and mixed with modified RPMI + actin at a 1:10 ratio. The samples were incubated at 37°C for 24 hrs on a Tetrad 2 Peltier Thermal Cycler (Bio-Rad) and crushed into ice to stop nuclease digestion. The nanostructures were analyzed using AGE. Then, the bands were extracted to recover nanostructures, and the nanostructures were imaged under TEM.

**Cell Proliferation Assay**

To prepare media with 6 mM $Mg^{2+}$, equiosmolar $MgSO_4$ solution was prepared and added to RPMI and DMEM media (149 and 175 mOsM, respectively). Heat-inactivated FBS was prepared by incubation at 75°C for 5 min in 1 mL aliquots. 3T3 and HEK-293 cells were grown in DMEM media, and H441 cells were grown in RPMI media. Cells were grown to confluency in appropriate media supplemented with 10% freshly thawed FBS (Gibco). 3T3 ($2.5x10^3$ cells/mL), HEK293 ($1x10^4$ cells/mL), and H441 ($1.5x10^4$ cells/mL) cells were seeded by adding 200 uL of cell suspension into the wells (n=5) of a 96-well plate for each time point (0, 1, 3, 5, or 7 days after seeding), in modified media prepared as following:

Media + 10% FBS
Media + 10% FBS + 6 mM $Mg^{2+}$
Media + 10% heat-inactivated FBS
Media + 10% heat-inactivated FBS + 6 mM $Mg^{2+}$
Media + 10% FBS + 200 nM actin
Media + 10% FBS + 200 nM actin + 6 mM $Mg^{2+}$

At each time point, cell proliferation was measured by CyQUANT Direct Cell Proliferation Assay (Life Technologies) following the vendor protocol exactly. Fluorescence was measured on a BioTek NEO HTS plate reader with excitation at 480 nm and emission at 530 nm.

**Cell Viability Assay**

The same methods from cell proliferation assay were used to modify media. Each cell line was seeded by adding 100 uL of $10^5$ cells/mL cell suspension into wells (n=5) of a 96-well plate for control or experimental groups in the following media conditions:

Media + 10% FBS
Media + 10% heat-inactivated FBS + 6 mM $Mg^{2+}$
Media + 10% FBS + 200 nM actin + 6 mM $Mg^{2+}$

5 uL of 100 ng/uL DNO was added to experimental group after overnight incubation to allow cell attachment. 24 hrs following addition of the nanostructure, cell viability was measured by CellTiter-Glo® Luminescent Cell Viability Assay (Promega) following the vendor protocol exactly. Luminescent signal was measured on a BioTek NEO HTS plate reader.

**Splenocyte Activation Assay**

Standard and adjusted media was prepared as described above. Spleens were obtained from female 8 week old C57Bl/6 mice (Charles River). Two spleens were processed for this experiment. They were transferred into 70 μm cell strainers (BD Falcon) and were dissociated using a sterile syringe plunger. The single cell suspension was washed with 25 mL of PBS (Gibco) into a petri dish. The suspension was transferred to a 50 mL Falcon tube, centrifuged at 500x g for 5 min, and the supernatant discarded. A total of 3x washes were used to remove nuclease activity carried over from the tissue. 2 mL of ACK Lysing Buffer (Lonza) was added and the cells were gently resuspended and incubated for 7 min. Following this, 20 mL of PBS

and 20 mL of RPMI media were added, and the suspension was centrifuged as above. Cell concentration was determined and $1x10^6$ live cells were transferred in 450 uL of the various media to 5x wells of a 48-well plate, for each agent to be assayed (DNO, CpG adjuvant, non-activated control). 50 μL 10 nM DNO, or 50 μg/mL CpG oligonucleotide 1826 (InvivoGen) was transferred into the wells (n=5). These were incubated for 16 hrs in a $CO_2$ incubator at 37°C. Supernatants were removed and centrifuged for 10 min at 500x g, transferred to new tubes and assayed for IL-6 concentration immediately by ELISA (R&D Systems).

**Endocytosis Assay**

3T3 fibroblast cells were first grown in standard culture media to establish normal growth. The cells were then trypsinized, collected and washed 3x *via* centrifugation at 500x g for 5 min with PBS to remove any nuclease present in the culture media. $1x10^4$ cells were then transferred into the various media conditions and seeded into wells of a 96-well plate. After 24 hrs to allow cell attachment, 1 nM of Cy5-labeled DNO or FITC-labeled transferrin (Life Technologies) was added. This was incubated for 16 hrs. Cells were then washed 2x with ice-cold PBS, then incubated with glycine-HCL (50 mM) in PBS (pH 2.8) for 10 minutes at room temperature to dissociated surface-bound particles. The cells were resuspended in standard PBS and analyzed by Flow cytometry on a LSRFortessa (BD), measuring 10,000 events/sample (n=5). Gating was performed on the cells by gating upon the forward scatter and side scatter plot. Identical gates were applied to all samples. After gating, a negative population was defined using the histogram obtained for media-only negative control samples. Samples that showed a rightward peak shift were determined as positive, and median values of each sample population were reported.

**Statistics**

ANOVA with post-hoc Dunnet's or Tukey's tests were performed using an excel plug-in, inerSTAT-a v1.3 by Mario H. Vargas (Instituto Nacional de Enfermeda Respiratorias, Mexico).

## 2.6 Author contributions

The manuscript was written through contributions of all authors. All authors were given an opportunity for approval of the final version of the manuscript.

## 2.7 Acknowledgement

This work was supported by an NIH grant to William Shih, and by the Wyss Institute at Harvard. This material is based upon work supported by the National Science Foundation Graduate Research Fellowship (Jaeseung Hahn) under Grant No. 1122374. We thank the Wyss Institute for support of this project.

## 2.8 References

1. Seeman, N. C. Nanomaterials Based on DNA. *Annu. Rev. Biochem.* **2010**, *79*, 65–87.
2. Rothemund, P. W. K. Folding DNA to Create Nanoscale Shapes and Patterns. *Nature* **2006**, *440*, 297–302.

3. Douglas, S. M.; Dietz, H.; Liedl, T.; Högberg, B.; Graf, F.; Shih, W. M. Self-Assembly of DNA into Nanoscale Three-Dimensional Shapes. *Nature* **2009**, *459*, 414–418.
4. Dietz, H.; Douglas, S. M.; Shih, W. M. Folding DNA into Twisted and Curved Nanoscale Shapes. *Science* **2009**, *325*, 725–730.
5. Liedl, T.; Högberg, B.; Tytell, J.; Ingber, D. E.; Shih, W. M. Self-Assembly of Three-Dimensional Prestressed Tensegrity Structures from DNA. *Nat. Nanotechnol.* **2010**, *5*, 520–524.
6. Mao, C.; Sun, W.; Shen, Z.; Seeman, N. C. A Nanomechanical Device Based on the B-Z Transition of DNA. *membranes* **1999**, *18*, 2531–2537.
7. Seelig, G.; Soloveichik, D.; Zhang, D. Y.; Winfree, E. Enzyme-Free Nucleic Acid Logic Circuits. *Science* **2006**, *314*, 1585–1588.
8. Dutta, P. K.; Varghese, R.; Nangreave, J.; Lin, S.; Yan, H.; Liu, Y. DNA-Directed Artificial Light-Harvesting Antenna. *J. Am. Chem. Soc.* **2011**, *133*, 11985–11993.
9. Liu, Y.; Lin, C.; Li, H.; Yan, H. Aptamer-Directed Self-Assembly of Protein Arrays on a DNA Nanostructure. *Angew. Chem.* **2005**, *117*, 4407–4412.
10. He, Y.; Tian, Y.; Ribbe, A. E.; Mao, C. Antibody Nanoarrays with a Pitch of 20 Nanometers. *J Am Chem Soc* **2006**, *128*, 12664–12665.
11. Schreiber, R.; Do, J.; Roller, E.-M.; Zhang, T.; Schüller, V. J.; Nickels, P. C.; Feldmann, J.; Liedl, T. Hierarchical Assembly of Metal Nanoparticles, Quantum Dots and Organic Dyes Using DNA Origami Scaffolds. *Nat. Nanotechnol.* **2013**, *advance online publication.*
12. Perrault, S. D.; Shih, W. M. Virus-Inspired Membrane Encapsulation of DNA Nanostructures To Achieve In Vivo Stability. *ACS Nano* **2014**.
13. Rudchenko, M.; Taylor, S.; Pallavi, P.; Dechkovskaia, A.; Khan, S.; Butler Jr, V. P.; Rudchenko, S.; Stojanovic, M. N. Autonomous Molecular Cascades for Evaluation of Cell Surfaces. *Nat. Nanotechnol.* **2013**, *8*, 580–586.
14. Langecker, M.; Arnaut, V.; Martin, T. G.; List, J.; Renner, S.; Mayer, M.; Dietz, H.; Simmel, F. C. Synthetic Lipid Membrane Channels Formed by Designed DNA Nanostructures. *Science* **2012**, *338*, 932–936.
15. Schüller, V. J.; Heidegger, S.; Sandholzer, N.; Nickels, P. C.; Suhartha, N. A.; Endres, S.; Bourquin, C.; Liedl, T. Cellular Immunostimulation by CpG-Sequence-Coated DNA Origami Structures. *ACS Nano* **2011**, *5*, 9696–9702.
16. Church, G. M.; Douglas, S. M.; Bachelet, I. A Logic-Gated Nanorobot for Targeted Transport of Molecular Payloads. *Science*, 2012, *335*, 831–834.
17. Miyauchi, K.; Ogawa, M.; Shibata, T.; Matsuda, K.; Mori, T.; Ito, K.; Minamiura, N.; Yamamoto, T. Development of a Radioimmunoassay for Human Deoxyribonuclease I. *Clin. Chim. Acta* **1986**, *154*, 115–123.
18. Koizumi, T. Tissue Distribution of Deoxyribonuclease I (DNase I) Activity Level in Mice and Its Sexual Dimorphism. *Exp. Anim. Jpn. Assoc. Lab. Anim. Sci.* **1995**, *44*, 181–185.
19. Koizumi, T. Deoxyribonuclease II (DNase II) Activity in Mouse Tissues and Body Fluids. *Exp. Anim. Jpn. Assoc. Lab. Anim. Sci.* **1995**, *44*, 169–171.
20. Houk, B.; Hochhaus, G.; Hughes, J. Kinetic Modeling of Plasmid DNA Degradation in Rat Plasma. *AAPS J.* **1999**, *1*, 15–20.

21. Kawabata, K.; Takakura, Y.; Hashida, M. The Fate of Plasmid DNA After Intravenous Injection in Mice: Involvement of Scavenger Receptors in Its Hepatic Uptake. *Pharm. Res.* **1995**, *12*, 825–830.
22. Castro, C. E.; Kilchherr, F.; Kim, D.-N.; Shiao, E. L.; Wauer, T.; Wortmann, P.; Bathe, M.; Dietz, H. A Primer to Scaffolded DNA Origami. *Nat. Methods* **2011**, *8*, 221–229.
23. Keum, J.-W.; Bermudez, H. Enhanced Resistance of DNA Nanostructures to Enzymatic Digestion. *Chem. Commun. Camb. Engl.* **2009**, 7036–7038.
24. Lu, M.; Guo, Q.; Seeman, N. C.; Kallenbach, N. R. DNase I Cleavage of Branched DNA Molecules. *J. Biol. Chem.* **1989**, *264*, 20851.
25. Douglas, S. M.; Chou, J. J.; Shih, W. M. DNA-Nanotube-Induced Alignment of Membrane Proteins for NMR Structure Determination. *Proc. Natl. Acad. Sci.* **2007**, *104*, 6644–6648.
26. Mathieu, F.; Liao, S.; Kopatsch, J.; Wang, T.; Mao, C.; Seeman, N. C. Six-Helix Bundles Designed from DNA. *Nano Lett.* **2005**, *5*, 661–665.
27. Fu, T. J.; Seeman, N. C. DNA Double-Crossover Molecules. *Biochemistry (Mosc.)* **1993**, *32*, 3211–3220.
28. Li, X.; Yang, X.; Qi, J.; Seeman, N. C. Antiparallel DNA Double Crossover Molecules as Components for Nanoconstruction. *J Am Chem Soc* **1996**, *118*, 6131–6140.
29. Lin, C.; Perrault, S. D.; Kwak, M.; Graf, F.; Shih, W. M. Purification of DNA-Origami Nanostructures by Rate-Zonal Centrifugation. *Nucleic Acids Res.* **2013**, *41*, e40.
30. Lazarides, E.; Lindberg, U. Actin Is the Naturally Occurring Inhibitor of Deoxyribonuclease I. *Proc. Natl. Acad. Sci. U. S. A.* **1974**, *71*, 4742–4746.
31. Mei, Q.; Wei, X.; Su, F.; Liu, Y.; Youngbull, C.; Johnson, R.; Lindsay, S.; Yan, H.; Meldrum, D. Stability of DNA Origami Nanoarrays in Cell Lysate. *Nano Lett.* **2011**, *11*, 1477–1482.
32. Surana, S.; Bhatia, D.; Krishnan, Y. A Method to Study in Vivo Stability of DNA Nanostructures. *Methods* **2013**, *64*, 94–100.
33. Jahnen-Dechent, W.; Ketteler, M. Magnesium Basics. *Clin. Kidney J.* **2012**, *5*, i3–i14.

## 2.9 Supporting information

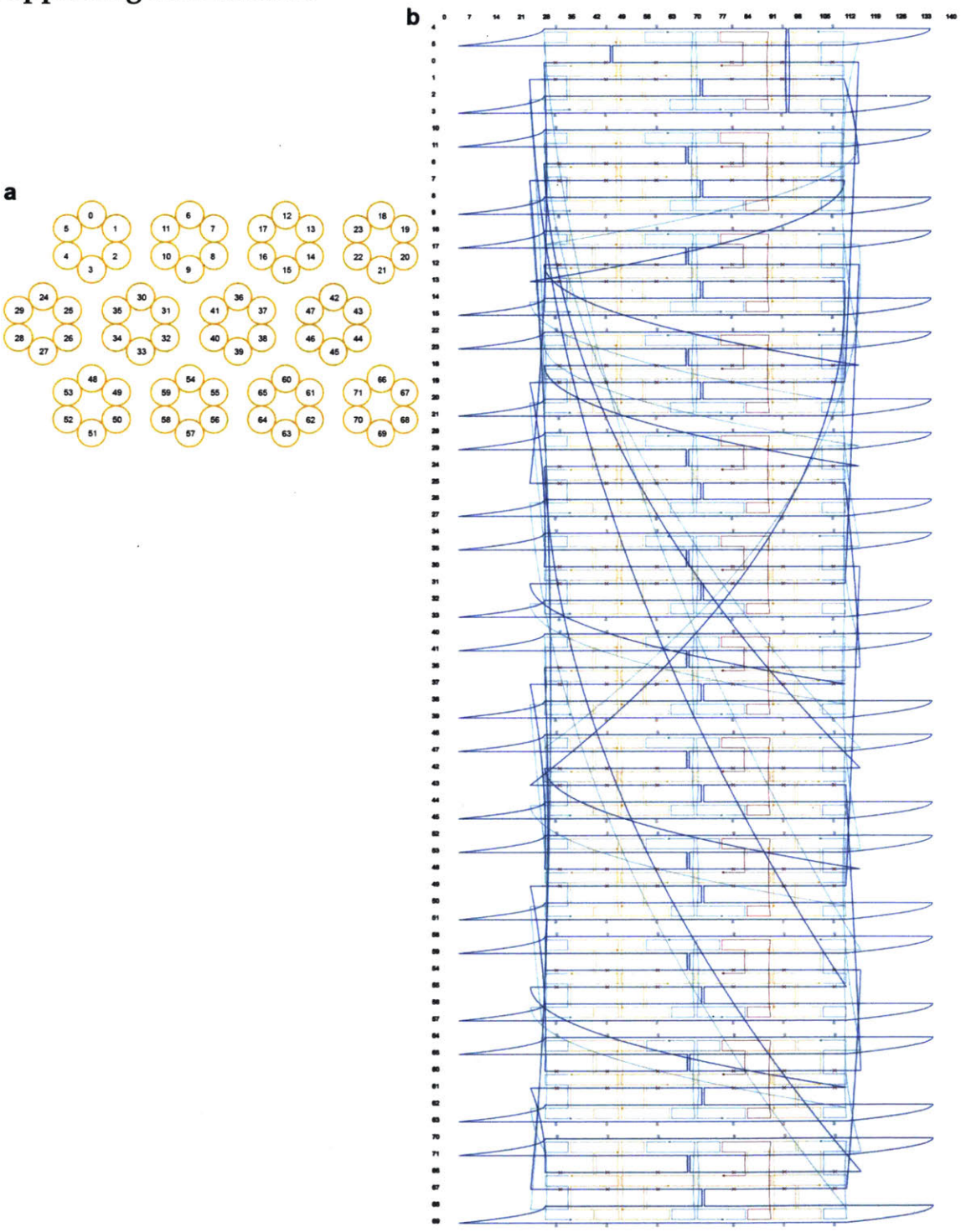


**Supporting Information Fig. 1. Schematic of the DNO design and scaffold routing. (a)** Organization of helices into six-helix bundles for the 12 struts. **(b)** Scaffold and staple strand organization.

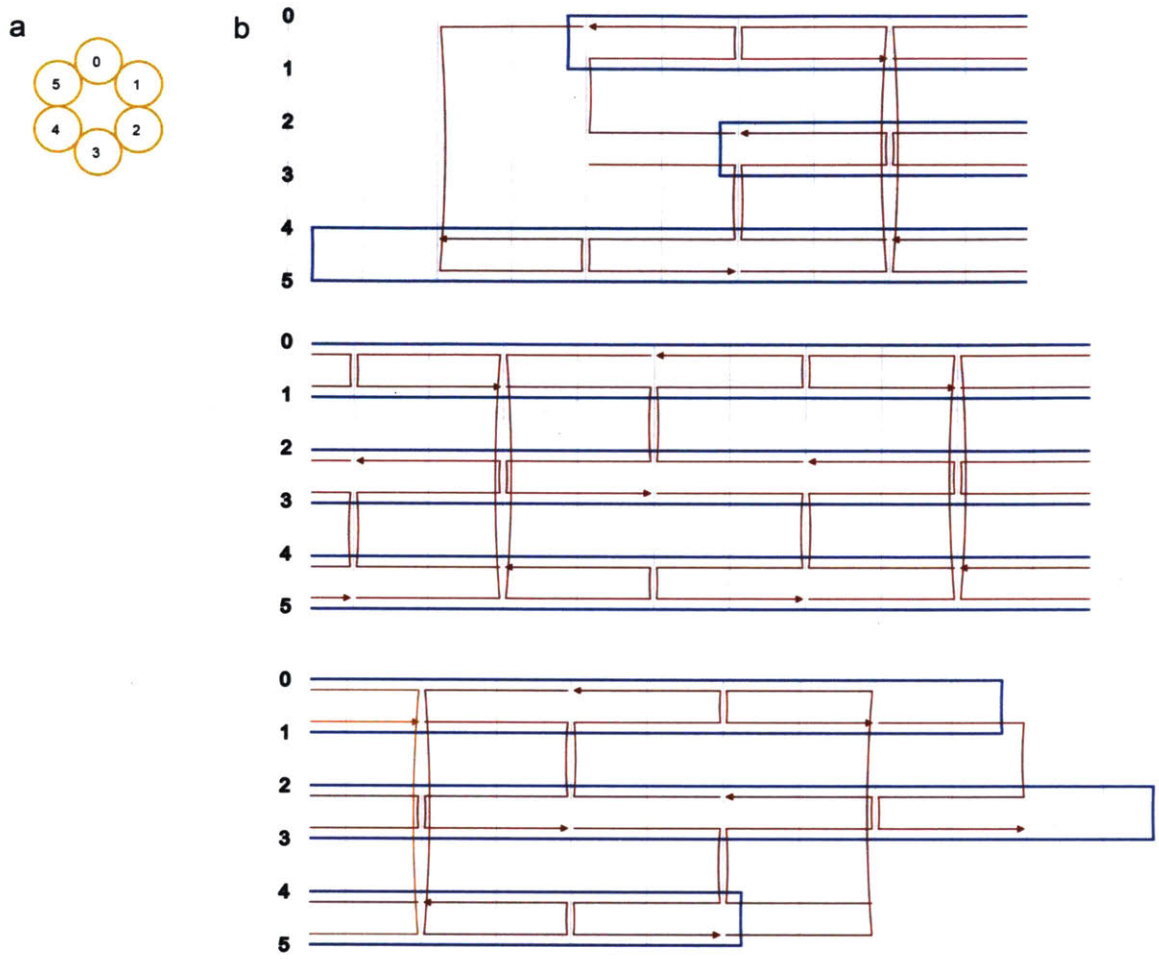


**Supporting Information Fig. 2. Schematic of the NT design and scaffold routing. (a)** Organization of helices into the six-helix bundle. **(b)** Representative scaffold and staple strand organization at the left (top), center (middle) and right (bottom) of the nanostructure. Note that the staple organization is repeated across the entire nanostructure length.

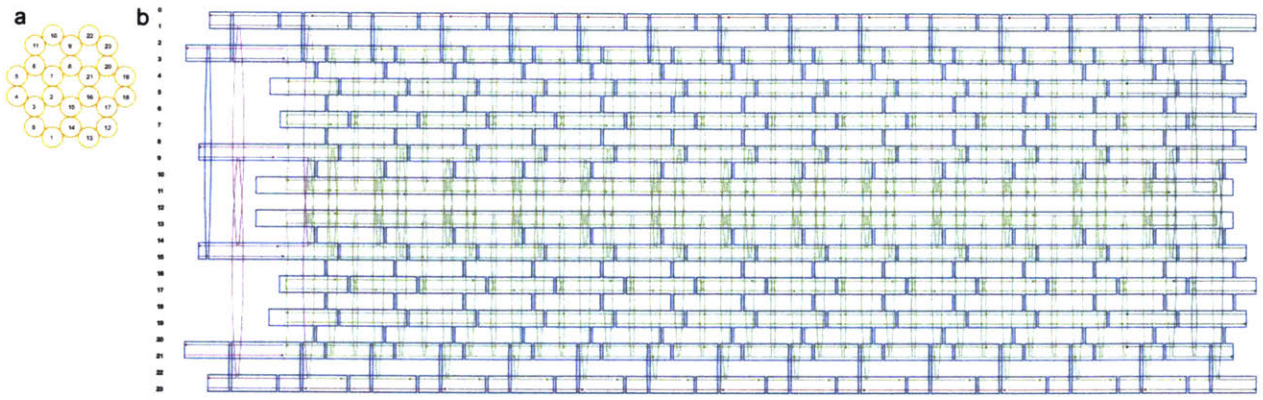


**Supporting Information Fig. 3. Schematic of the NR design and scaffold routing. (a)** Scaffold and staple strand organization. **(b)** Organization of helices into the 24-helix architecture.

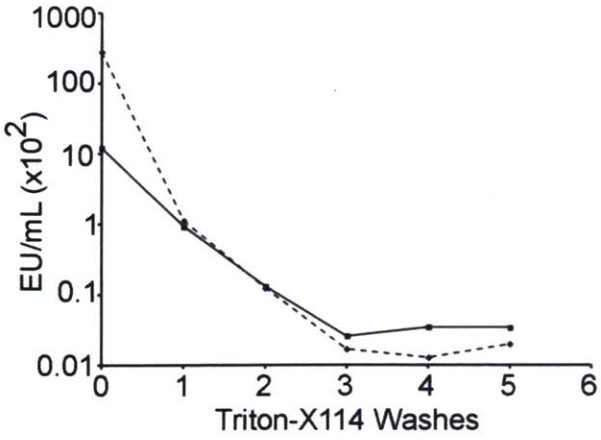


**Supporting Information Fig. S4. Removal of endotoxin from M13 scaffold stock and DNO nanostructure.** Endotoxin was removed from a 500 nM M13 single-stranded DNA stock (—), and a 10 nM DNO sample (- - -) using 5x sequentially scrubs with Triton X-114. Endotoxin levels were reduced to a maximum of 5 EU/mL in scaffold stocks prior to synthesis and purification of nanostructures.

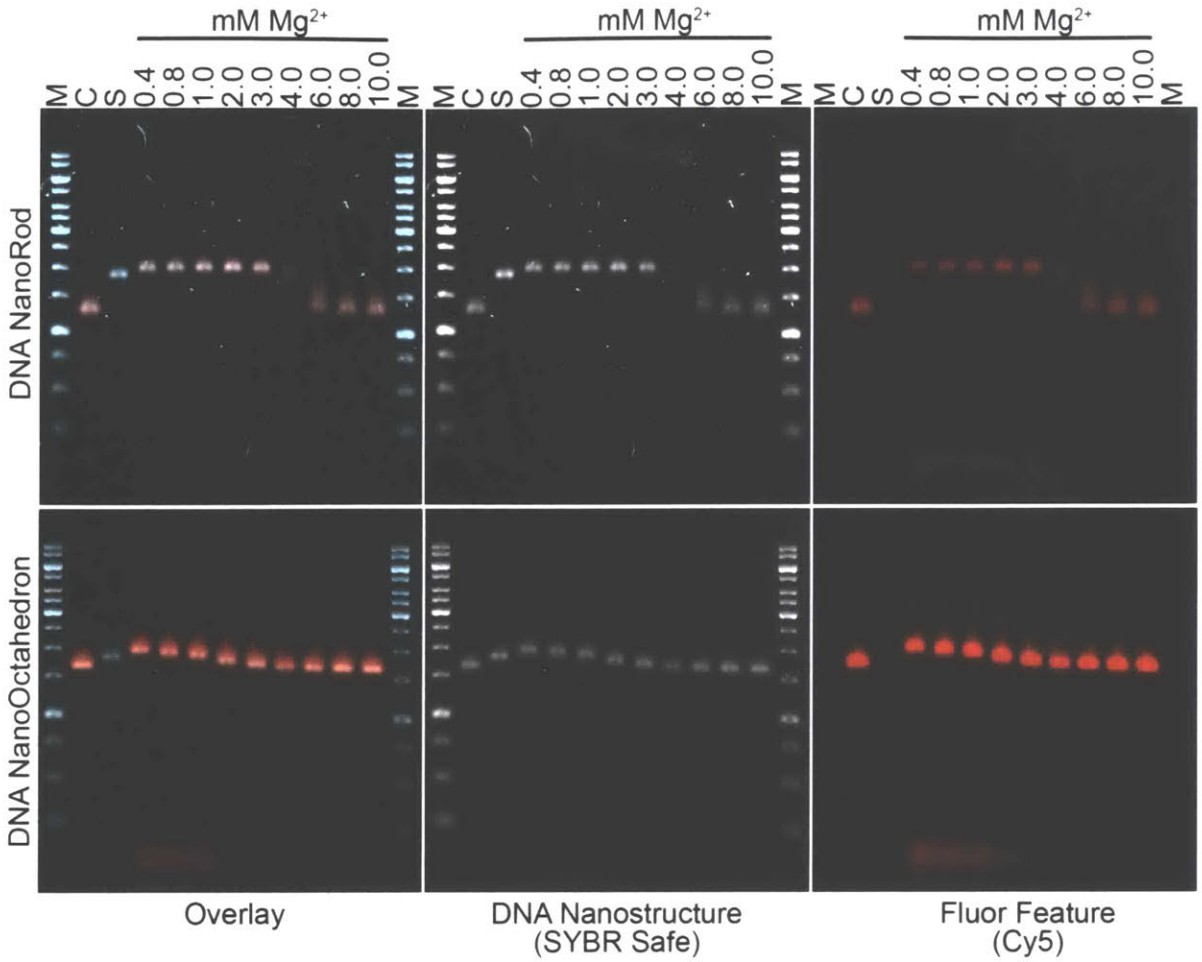


**Supporting Information Fig. 5. Nanostructure loss of molecular cargo during denautration in RPMI media.** A fluorescent Cy5-oligonucleotide feature (5′-GTGAGTTGTGGTAGATAATTT-3′) was annealed to the DNO and NR and the products purified. These were then incubated in standard or $Mg^{2+}$-adjusted RPMI media at 37ºC for 24 hrs, and the products analyzed by AGE. Imaging of the gel in SYBR Safe and Cy5-fluoresence channels show a partial loss of the Cy5-labeled feature after incubation at $Mg^{2+}$ concentrations below ~6 mM.

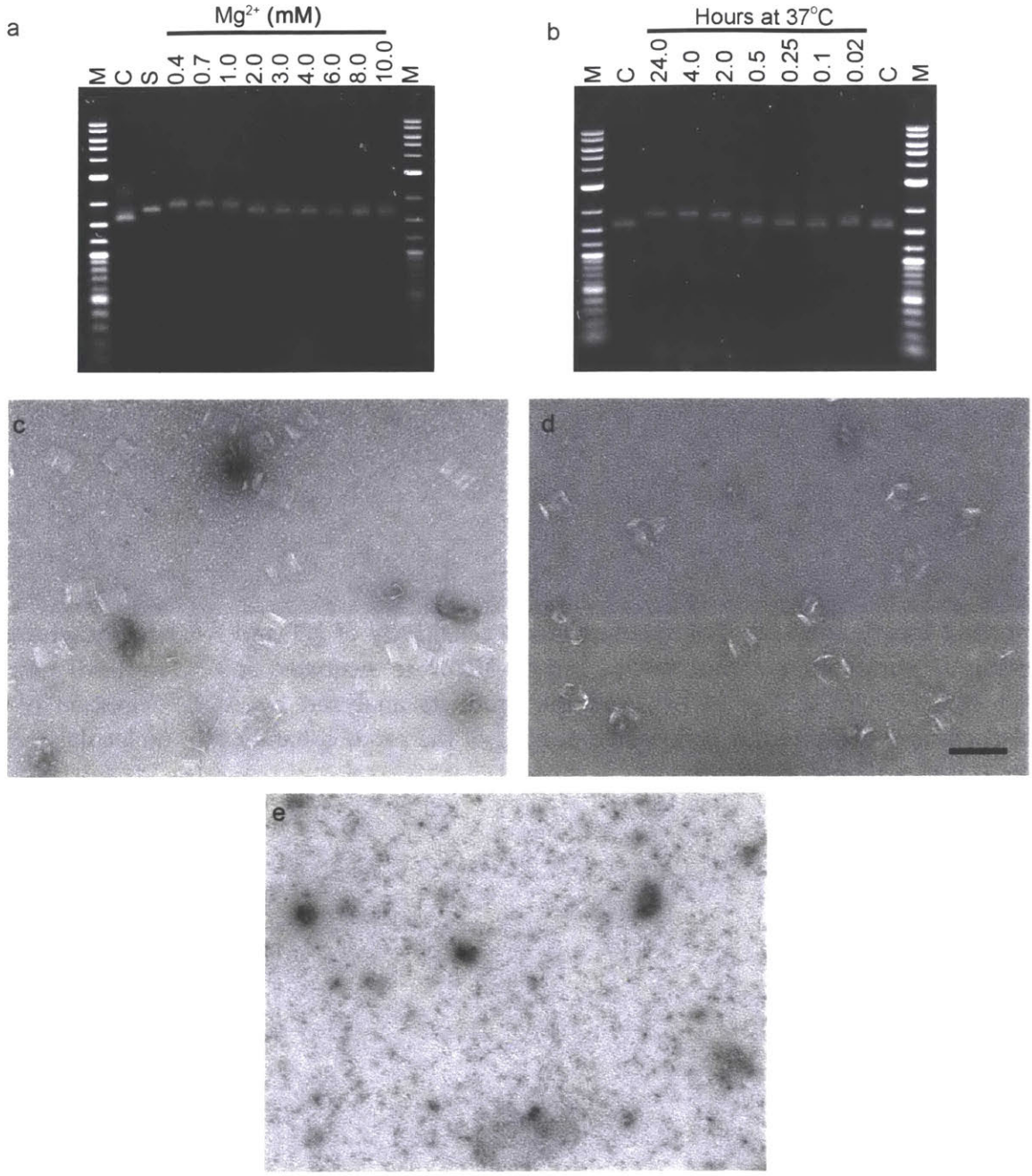


**Supporting Information Fig. 6. Sensitivity of the DNA NanoRobot to denaturation in RPMI media. (a)** AGE analysis of the NanoRobot after incubation in RPMI media and a range of $Mg^{2+}$ concentrations for 24 hrs at 37°C. Relative to the controls, there is a shift in migration below ~2 mM $Mg^{2+}$. **(b)** This shift was apparent after 0.5 hrs of incubation at 37°C in RPMI media (0.4 mM $Mg^{2+}$). M = molecular weight ladder, C = RPMI + 6 mM $Mg^{2+}$. **(c)** TEM imaging of the NanoRobot after incubation in 10 mM, and **(d)** 2 mM $Mg^{2+}$. In comparison to the 10 mM $Mg^{2+}$ sample, those incubated at 2 mM have a stressed morphology, but were largely intact. **(e)** After incubation in standard RPMI with 0.4 mM $Mg^{2+}$, no intact nanostructures were visible. Scale bar = 100 nm.

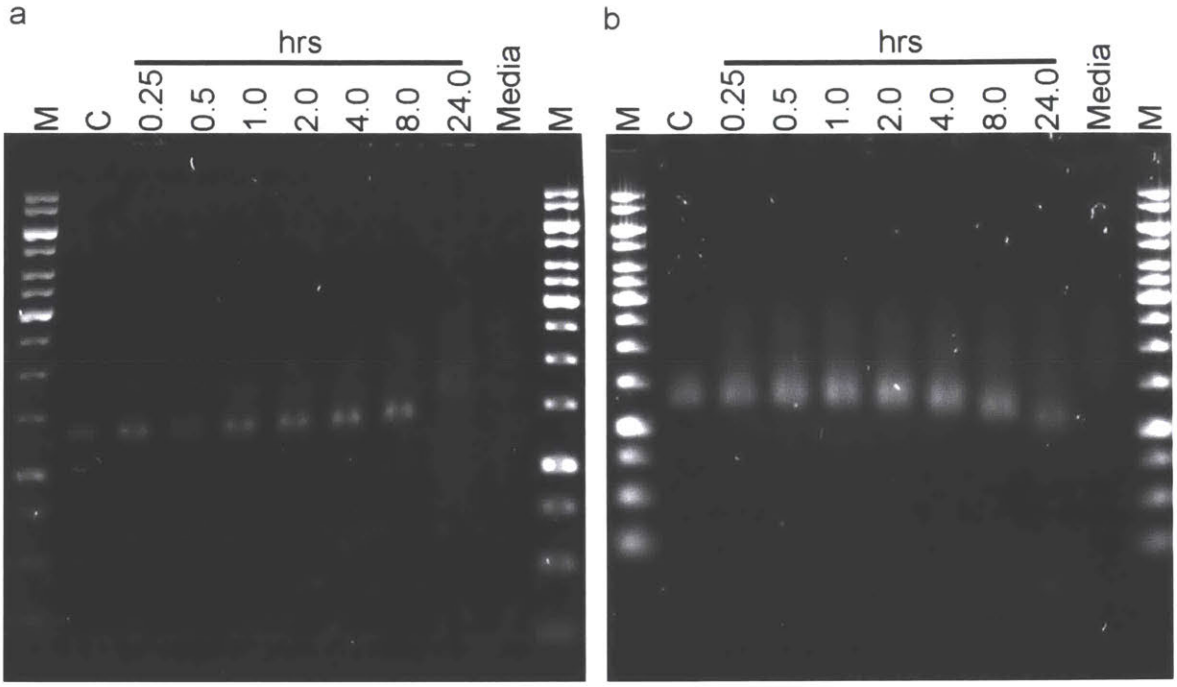


**Supporting Information Fig. 7. Time-dependent sensitivity of NT and NR nanostructures to digestion by nucleases in serum. (a)** NT and **(b)** NR were incubated at 37°C in RPMI + 6 mM $Mg^{2+}$ + 10% FBS for 0.25 – 24 hrs, and the products analyzed by AGE. Digestion of the nanostructures is indicated by increased smearing of the product bands. M = molecular weight ladder, C = TE + 10 mM $Mg^{2+}$.

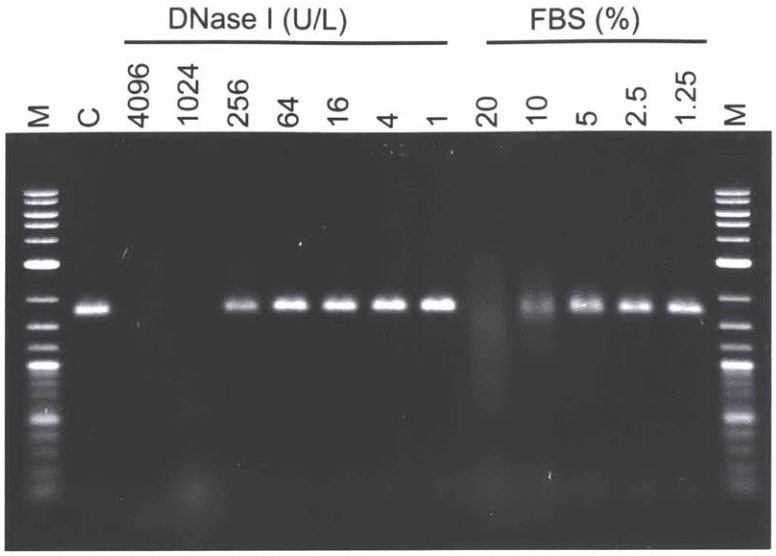


**Supporting Information Fig. 8. Digestion of the DNO nanostructure by DNase I *vs* RPMI + 6mM $Mg^{2+}$ + FBS.** 5 nM DNO was incubated at 37°C for 12 hrs in 6mM $Mg^{2+}$ RPMI with a range of added DNase I, or FBS, and the products were analyzed by AGE. In comparision to the control DNO lane, DNase I concentrations greater than 256 U/L resulted in complete loss of the product band, and FBS concentrations of 10 and 20% resulted in smearing, indicative of partially digested product. M = molecular weight marker, C = DNO in RPMI + 6 mM $Mg^{2+}$.

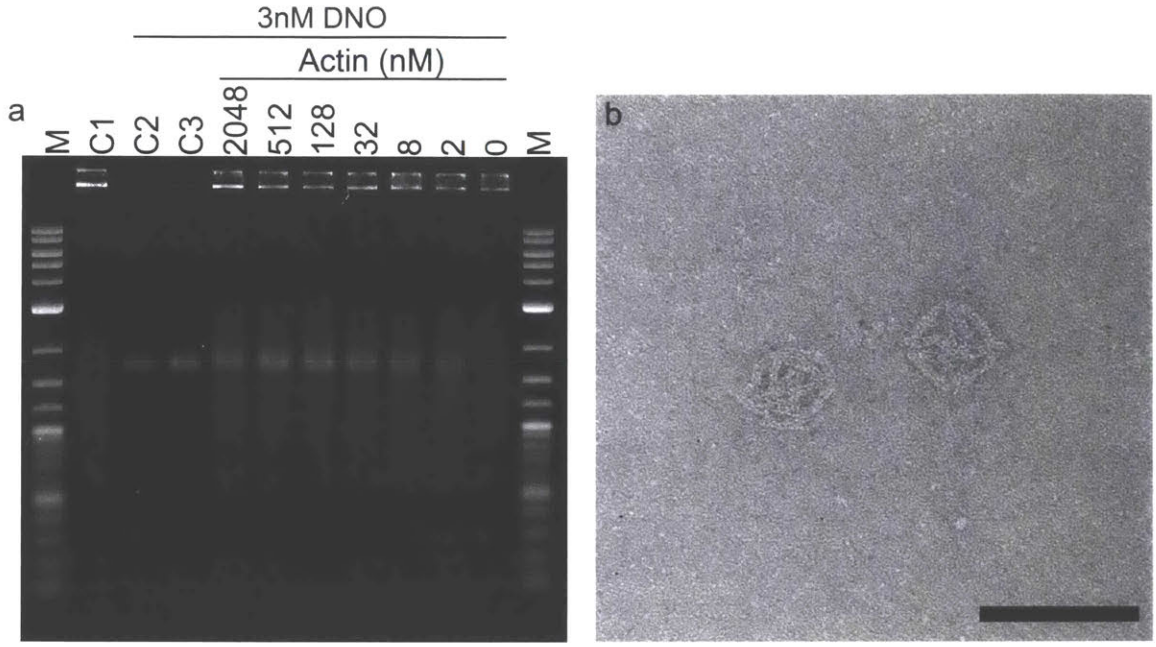


**Supporting Information Fig. 9. Concentration-dependent actin inhibition of DNO nuclease digestion. (a)** RPMI + 6 mM $Mg^{2+}$ + 10% FBS was prepared, and 0 – 2048 nM actin was added with 15 nM DNO. Following incubation for 24 hrs at 37°C, the products were analyzed by AGE to assess inhibition of DNO nuclease digestion. M = molecular weight marker, C1 = RPMI + 6mM $Mg^{2+}$ + 10% FBS + 1000 nM actin, C2 = RPMI + 6 mM $Mg^{2+}$ + DNO, C3 = RPMI + 6 mM $Mg^{2+}$ + DNO + 1000 nM actin. **(b)** TEM imaging showing intact DNO incubated in 250 nM actin. Scale bars = 100 nm.

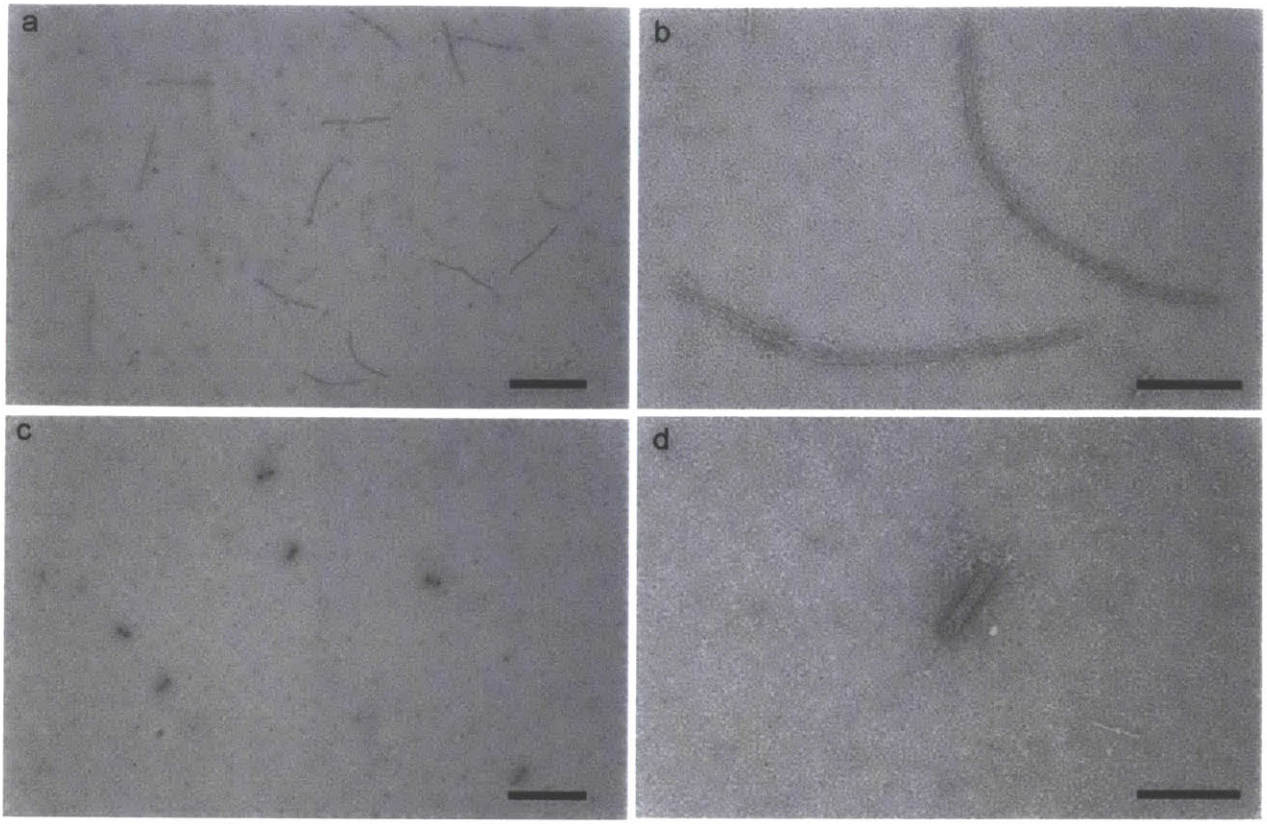


**Supporting Information Fig. 10.** TEM imaging of the **(a,b)** NT and **(c,d)** NR after incubation in RPMI + 6 mM $Mg^{2+}$ + 10% FBS + 200 mM actin at 37°C for 24 hrs. Scale bars = 500 nm (a,c) and 100 nm (b,d).

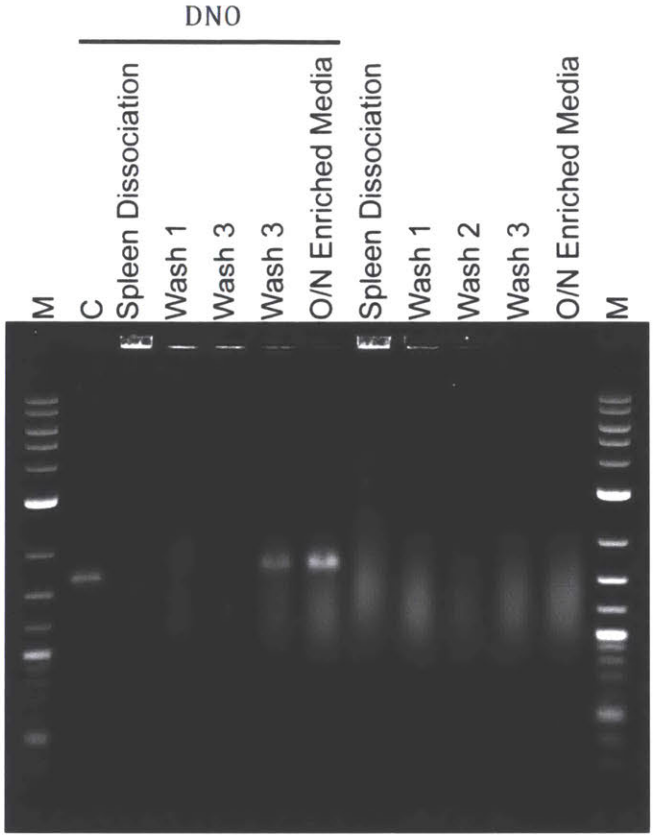


**Supporting Information Fig. 11. Analysis of nanostructure digestion by nucleases present in splenic tissue.** Immune cells were obtained from spleen dissociation. The cells were washed three times with large volumes of nuclease-free media to remove inherent nuclease activity by dilution. The cells were then incubated with media (RPMI + 10% heat-inactivated FBS) for 24 hrs. Aliquots of the dissociation supernatant, washes, and cell-enriched media were then incubated with 5 nM DNO for 24 hrs at 37°C, and the products were analyzed by AGE. The nanostructure remains intact after 3 washes, and nuclease activity is not regained by splenocyte enrichment. A slight shift in DNO migration is observed compared to the control, which may be due to an interaction with factors present in the media. The right side of the gel shows DNO-negative samples and smearing from heat-inactivation of the FBS. M = molecular weight marker, C = control DNO in TE + 10 mM $Mg^{2+}$.

**Supporting Table 1. Staple list for the DNO.**

| Number | Sequence | Length |
|---|---|---|
| 1 | CCAGCGAGTTACTTAGCCGACTAAAGACACTCATCAGCGCTAA | 43 |
| 2 | TTCTTAACAGGGAGTTAAATAGAAAGGAGCTTTCGATCATCAT | 43 |
| 3 | GAAAACACCTTGCTTCTGTCATCGGGAGTGAAACATTTTCCCA | 43 |
| 4 | CCTGCCTCGGCAAAATCCCTTATAAATCAAACAGTTGGTAATA | 43 |
| 5 | ACCGAACATATTGAATAACTTTTCTCAGAGCCGGAACCCGTAACAAA | 47 |
| 6 | CTCAGTGCCAGCAGAATGGTTTTAGCTACACTTAAATCCGCCACCCT | 47 |
| 7 | GTAGATATTTTGTTTTCACTTTTACAGACAACCAGTACATCAGATAT | 47 |
| 8 | GGAAACGCATCGGGTAAAATTTTAACCGATGCCGACAAATTATCATT | 47 |
| 9 | GGCTTTTTCATTGAATCCCTAGGAATACACCAAAATTTGACGA | 43 |
| 10 | AAACTTTAATAAGAATAAATAGTGAATTACAAAGAGATTAGAG | 43 |
| 11 | TTTAGTAAATCACCGAAAGTTTTGTATTGGAATCGGCCTCGAGCCAG | 47 |
| 12 | TATCAGATTTTTAAGAAAATTAACGTCAGTAATTGTTTGACCC | 43 |
| 13 | AATTCATTAAAGGTGAATTTTAAGACTCTCACAATACAAAGGC | 43 |
| 14 | CATATAAACATACTTTTTATTTTGTAATAATTACATTGGGTGGCATC | 47 |
| 15 | ACCCATGATCTAAAGTTTTCGGAATAGGGCAAGCCTTTAGCGA | 43 |
| 16 | AGTACCTTTTTAAATATGCAGCAAAGCGAGGTCAGACGCGAGA | 43 |
| 17 | TTAGAGCTCATAATCACCATTTTTGTACCAAATAAAGCATATTACCG | 47 |
| 18 | TCCAGACATCCCATCCTAAAACAGTAGGGGTAAAGTCCAGTCG | 43 |
| 19 | GGCTGTAATTCGAGCATAATTTTCCTTTGACCAAGCTTGAATTATTC | 47 |
| 20 | AAATATGAAACGGAAAATATTTTAATAGCATTAAGCCCCAACCTAAA | 47 |
| 21 | GCCCTGTATGCGACGCCAATTTTATCACCCGGGCGAAATAAAGAACG | 47 |
| 22 | GGAAACCTCACCAGTGAGATTATCCGCTCCCGCTTTAATTCTG | 43 |
| 23 | ACCTCCCACGCTAACGAGCTCATCGAGAGAGGCGTCAATAGGA | 43 |
| 24 | TATCAGGTTGATAATCAGAAAGATTCAAGAGATCTCAATAGAA | 43 |
| 25 | CGTTTGCCCCTCAGAGCCAACGTCACCATAGCCCCAAACACCA | 43 |
| 26 | AATAAAGGCGGACCGCCACTTTTTTGTGTCTACAACGGCGGGAGAAT | 47 |
| 27 | AATCCTCACCGCGCGGGCCTTTGCTGAATGGTCATTTTAACTATAT | 47 |
| 28 | TCTGTACCTTATAGGAATCTTTTTAGATAAAGCTAATGGAGTGAGCT | 47 |
| 29 | CAGAGCCCAACTACAAGAATTTTAAGAGAAAACATGAATTCCAGTAA | 47 |
| 30 | TTTTAGTCCATCACTATCGTTTTAGGGATTTCAGAGCGACACTATCA | 47 |
| 31 | GTCACGAGACCGTATACGCCATTCAGGCGCCAGGGAACATCAA | 43 |
| 32 | GAACTACAAAATCAGTAGCTTTTAAGGTAAAAAAGGGCGCTGATAAA | 47 |
| 33 | ACCGAGAGGTTTTGAATACTTTTCTGAATATCAATATATCCAAAAGG | 47 |
| 34 | GCACGTAGAATCCTGAGAAAGAAAGCGATGGTTGCTAGCGAGA | 43 |
| 35 | GATTTAAGTTGCGTTGTTCTTTTTCCAATAGGGTAATACCCGCCGCG | 47 |
| 36 | GAACGAGTACCAGTCAGGACGCATAGGCTGACGAGCTTATTAG | 43 |
| 37 | CCGTGGGGGGACGACGACATTGTTAAATAACCCGTATGAAAAA | 43 |
| 38 | AGTTTTAAGGTGCCGTAAACTTGATATTAGTGTACTAATGCCC | 43 |
| 39 | AAAGAGAACAACCCAAAAGTTTTTTATGCGTTTAATTTGTCAGACTG | 47 |
| 40 | ATTCCTGATATCAAAATTAACAAACAATCGGAATTAGGTGAAT | 43 |
| 41 | AGCTTTTTTGAAGCAGAAGTTTTACATAAATCATTTGAAAAGGGGGA | 47 |
| 42 | GCGAAACAATAGGAACGTTTTTTGCAAATCTATCAAACTAGCCAGCT | 47 |
| 43 | GAATGATTGACGTGTAGCGTTTTTACCGACTCATCTTCGAGCTTCAA | 47 |
| 44 | TTAGAGATTGTACATCAAATTTTACTAGCAAAACAAGAAAAGAAACG | 47 |

| | | |
|---|---|---|
| 45 | AGACAATTGATTCTATATTTTTTATCGTAAATGGGATATATTAACAC | 47 |
| 46 | TTGACGCAGATAGAACCCTTAGTAATAAGGAAATAATCATACA | 43 |
| 47 | TCTAAAGAAGGTTATCTAATAAAACATCGCAGCAACGGATTCT | 43 |
| 48 | GGCAAGGACTTTTGCGGGATTAGATACACCAATAACCTACATT | 43 |
| 49 | ACCGCCACATCTTTGAATAAGGCTTGCCCTGGCTGAGGTGTA | 42 |
| 50 | TATTCATATGGTTTGGTAGCTATTTTTGAAAGGGTGAGTAAT | 42 |
| 51 | CTGTAATCAAAGAAAGGAAAAACGCTCATCATCACTCAATAC | 42 |
| 52 | GTTTGAGAACAAACCCACGCTGAGAGCCAGCCATTAGCGAAC | 42 |
| 53 | TAAATATGCAAAAGACAGGGCGCGTACTAAAGGAGCCGAGAA | 42 |
| 54 | TGAATAAAAATTAAATTAAGTTGGGTAACTGCGCAACAAAGC | 42 |
| 55 | GCTCCATTTATACCGAACAAAGTCAGAGGAAAATGAGAAACG | 42 |
| 56 | TTTCTTTTGTCGTGAAAGTACCGACAAAAGCTTAATATAAAG | 42 |
| 57 | ACCTACCATTATCATCGGTTTATCAGCTTACAACTATCAGCG | 42 |
| 58 | GGGGTCGACGGGGTTAACAGTGCCCGTATAAAAGAATTGCCC | 42 |
| 59 | CGTAACGTACCGTAGTATTCTAAGAACGCACAAGCAAACCAA | 42 |
| 60 | CAACATGTTAATTGAAATCCAATCGCAAGTATCAAAGCTGAG | 42 |
| 61 | CAGAGCTTTAGTATAAGTGCCGTCGATTGCCACCTGAAT | 39 |
| 62 | TGTGCTGATCGGTTTCTGGTGCCGGAAATTTTATGTGAG | 39 |
| 63 | ATTAAATCCAATATCTTTAGGAGCACTTGTTAAATTTTTTA | 41 |
| 64 | GAAGGGCGCAAGGCGTTACATTTAACAATTTCAATATCCCTTAG | 44 |
| 65 | CAAGAGTCATTCAGTTCATAATCAAAATCACCGCCACCCACCAC | 44 |
| 66 | GCCATTCTAAAATCGTCGCTATTAATTAACCAGGCTGTTGG | 41 |
| 67 | TACCTTTGCATGGCTAGTACCCGTATATATACAGAACGGAT | 41 |
| 68 | CTCATTATAGTAAACGGCATTTTCGGTCAATGAAACTTAGCA | 42 |
| 69 | ATTTTTTGGGAACGAGGCGCAGACGGTCAAATAAAAATAGC | 41 |
| 70 | TAAATCCAACAAAGAGATACCGATAGTTGCATATTCGCTCAGCA | 44 |
| 71 | TTCTTTGCAGAAGCCTTTATTTCAACGGTTGTAGTGCCTGA | 41 |
| 72 | AGGCCGGGGCGTTGGGAAGAAAAATCTATTACCACATCGAT | 41 |
| 73 | CAGACCAAACCACCCTCAGAGCCGCCAGATGAACCCTTCAT | 41 |
| 74 | GTTTGACATTCTGACCTGAAAGCGTAAACGAGTAAATGGTC | 41 |
| 75 | GTAGAAGATTGCAACTTAGCAAAATTAAGCAAAACATTAAAAAT | 44 |
| 76 | ACCAATAAACATTAATTGCTGAACCTCAAAAACAGTTTAATAGA | 44 |
| 77 | CCAACAGTCAATCGTAGTAGCATTAACATTTTCGCAGATTTA | 42 |
| 78 | TGATAGCTTGTATCGGCCTCAGGAAGATTAATGCAAAATAC | 41 |
| 79 | CGAACGACAACAGTGGGCGGATTGACCGTACCGTGCATCCAGCC | 44 |
| 80 | AATTCTTGTTTAGCCCAATTCTGCGAGAATACATTCTGG | 39 |
| 81 | CCAGCCAACTCAAACGCAAATTAACCCAAGGATATGACC | 39 |
| 82 | ATTGAGGCATCACCATGTGAGCGAGTAACCAGCTCAATTCGC | 42 |
| 83 | TTGCGGTTTGCCCATAATACATTTGAGTCACCGTCGCTG | 39 |
| 84 | CGCCTGACCACCATGGCTATTAGTCTTCGCACTCTGCCA | 39 |
| 85 | TTCATCGGAACGCAACGTTAATATTTAACAACGAAAGGA | 39 |
| 86 | AATAACCACTAATAGTCTGAAATGGATTATAAGGGACGTGGCAC | 44 |
| 87 | AGCAGCAGTTTTCATTTGGGCTTGAGATGGATTTTAAATAAAAC | 44 |
| 88 | AGTATAGACGTCTTTCCAGAGCCTAATGAGGGTTCCGTACT | 41 |
| 89 | GTACCGCCCGTCGTCTTTCCAGACGTTGGTATTAAGCCGTT | 41 |
| 90 | TAGCGCCCGTAATCACCAGTAGCACCACGTTAGAACTGG | 39 |

| | | |
|---|---|---|
| 91 | TTTATTTCTTATCCGACACTGAGTTTCGTCGCCCTCATGAATTT | 44 |
| 92 | CTTACCAGACTTGCTCATTTTCAGGGATATGTATCAGATATA | 42 |
| 93 | AGAAGGTCATCGTCATTCCAAGAACGAGTAAATAGTTAG | 39 |
| 94 | TTAATGCAGTCAATATTTTAAATGCAAGCCATCGGAAAT | 39 |
| 95 | ACCCCGGTCATTGCAATAAGTTTATTTTGCTTATTAAAAGAA | 42 |
| 96 | AACTCAAGCCGGATAATCATGGTCATCCAATCACAAGAA | 39 |
| 97 | TCGCCTGATTACCTGAAACGACGGCCAGTGTAGCGAGCCCGGGT | 44 |
| 98 | ACATACGCATTAATTATAAACAACATGTTCGTCCTGAAATAATC | 44 |
| 99 | CCGGAGACCGGAGAGACCAGCGCCAAAGACATATTGATTGGGAA | 44 |
| 100 | GTGAAATTCTTTACGAGCATGTAGAAAAGCTGTTCCACACA | 41 |
| 101 | CCAACGCTGCGGGCAACAGCTGATTGCTACCAGTTGAGAAT | 41 |
| 102 | GTGTAGGGAATCACCGTCACCGACTTGATGCCTGAGAAAGG | 41 |
| 103 | CGCCATAGAGAATATCCAGCTGCATTAATGGCGCCAGCCGCCTG | 44 |
| 104 | AAATAATGACGACAGCGTTGCGCTCACTGCACAATTTCCTGT | 42 |
| 105 | TAATAATTTAACATTATACAAATTCTCCTTCAGGTGGTT | 39 |
| 106 | CTGGCATTAAAAGCCCCAAAAACAGGAATACCCACGCAGTA | 41 |
| 107 | TGTTAGCCACCACGGCTGAGAGTCTGGAGCTGTCAATTATAAGC | 44 |
| 108 | AGCGAAAGGAAGCAAAATCAGGTCTTTAGAAATAAATAA | 39 |
| 109 | CGCTAGCCGTTGTAAGCAAAAGAAGATGAAAACAATTAACAG | 42 |
| 110 | GATTAAGCCAGACCGATATTTTAGTTAATTCGTGTGAAAGCCTG | 44 |
| 111 | CAAAGAAAACGTACAATAATAACGGAAGATTGCATATGT | 39 |
| 112 | ATAGTCAAACACCGGAATCATAATTACTACCCTGTCAAAAA | 41 |
| 113 | AAGAGTCGAAACTAAAGTACGGTGTCTTTAAGACATCATAG | 41 |
| 114 | TAACTGACAGAGAATTTATCCCAATCCAATCAGCGACCT | 39 |
| 115 | GTCTGAGGCTGATGCCTCCTTTTGATAAGAATAATGCTTCATTC | 44 |
| 116 | GGCGTTATTCAAATGAAGCAAACTCCAACGATTGCAACTATT | 42 |
| 117 | GTAAATAGACTACGCGATAGCTTAGAGGAAGTTGTAGCT | 39 |
| 118 | GAAGCCCGAGATAAAGAATACACTAAAACTTTTTCAACAGAG | 42 |
| 119 | AGCCTTTAACACCCTAAGCGCGAAACAAAGGAAATCCTAAGGGA | 44 |
| 120 | TAACCCCATAACGATTATTACAGGTAAGGCCAGGAACGG | 39 |
| 121 | CAGGAGGCACCACCCGGGAGGTTTTGAAGCATTTTATGTTACAA | 44 |
| 122 | GCAGATATCGTTTACCTTTCCTCGTTAGAATTAGACACCGAGTA | 44 |
| 123 | TTAGACTAAGGCCGCTTTTGCGGGATCGGATTTACTCGTAT | 41 |
| 124 | GTTGAGAGAGTGTTTTTATAATCAGTGGAAAGATAACTAAT | 41 |
| 125 | AGGAAGGTTCCTCAAATGCTTTAAACAAACGTGGGGGCGCT | 41 |
| 126 | GAGTGAGTTTTTGCACGTAAAACAGAAAACAGTTAAGGAAT | 41 |
| 127 | AGGGCGCGCGCCGCTAAGTTTTGCCAGAGGCTGCGGAAAAACGA | 44 |
| 128 | TACGCCATAACGTGCAGACGACGATAAAACACATTCTCATCA | 42 |
| 129 | CTTAATTGGCAAGGGGAAAGCCGGCGGTTCAGATCGTCA | 39 |
| 130 | TGCGAATTAATTGTAGATGATGGCAATTCAATGGAAGAAATTGC | 44 |
| 131 | AGGCTTGACAGCTTAACCACCAGAAGGAGTCGACAAGAAGTA | 42 |
| 132 | GCGTCATAAAGCCATTGACAGGAGGTGGGCGGGATTATT | 39 |
| 133 | AGCCTTAATAATTCTAAACAACTTTCATAAAGGGTTAGA | 39 |
| 134 | TCCTCATTACATGGCAACCTATTATTCTGAGGATTAGGGTTTTG | 44 |
| 135 | GTTTCCAGAGGCAAACCCACAAGAATTGAGATAGCTAACCAGAA | 44 |
| 136 | ACGATTGCGAAAATCCTGTTTGATGGTTGAGGCAAAATAAA | 41 |

| | | |
|---|---|---|
| 137 | CAGCAGGGCGCACTAAATCGGAACCCTCGCTGGTTAGCCCG | 41 |
| 138 | ACGAAATTAAACGGAACGAGGGTAGCAAAGTTTCTTACC | 39 |
| 139 | AGATAGGCCCTTGAGCAGTGCAACGTCAAAAAATCAAAGCCCCC | 44 |
| 140 | CCGAAATATTTCGGTTTTGATGATACAGGCACAAACGGTCAG | 42 |
| 141 | TGGACTGTTGAGTAGCAAGCGGTCCAAAAGGGGTTTTTT | 39 |
| 142 | ATTTCAATTGCTTAACGTCAGATGAAAGGATCGCAAGTC | 39 |
| 143 | GCTTTGAGTGTAAGCAGATAGCCGAACAACGGCTTGAGGAA | 41 |
| 144 | GCTGCTAATCTTGTTGAAAGAGGACACCAGAACCTCAGA | 39 |

**Supporting Table 2. Staple list for the 6-helix bundle NT.**

| Number | Sequence | Length |
|---|---|---|
| 1 | AGTAATAAAAGGGACTGTTTCCTGTGTGCCTTTGATAGCGAG | 42 |
| 2 | AAATGGATTATTTAAACATACGAGCCGGACGGCCAGTGCCAA | 42 |
| 3 | AACGCTCATGGAAATAATGAGTGAGCTATGGGTAACGCCAGG | 42 |
| 4 | AATATCCAGAACAACCCGCTTTCCAGTCCGCCAGCTGGCGAA | 42 |
| 5 | ACTTGCCTGAGTAGTGAATCGGCCAACGAACTGTTGGGAAGG | 42 |
| 6 | ATTAACCGTTGTAGCGCCAGGGTGGTTTGCCGGAAACCAGGC | 42 |
| 7 | ATCAGTGAGGCCACCTGATTGCCCTTCAGGAAGATCGCACTC | 42 |
| 8 | AGACAGGAACGGTAGCGGTCCACGCTGGTGCATCTGCCAGTT | 42 |
| 9 | ATCAGAGCGGGAGCGATGGTGGTTCCGAATGGGATAGGTCAC | 42 |
| 10 | GGTTGCTTTGACGAGAATAGCCCGAGATCCCGTCGGATTCTC | 42 |
| 11 | ACACCCGCCGCGCTAAGAGTCCACTATTTGTAGCCAGCTTTC | 42 |
| 12 | AGGGCGCTGGCAAGCGAAAAACCGTCTACCAATAGGAACGCC | 42 |
| 13 | GTGGCGAGAAAGGATCACCCAAATCAAGAAAATTCGCATTAA | 42 |
| 14 | GGGAGCCCCCGATTCTAAATCGGAACCCTGTATAAGCAAATA | 42 |
| 15 | AAGAACTGGCTCATCGGAACAACATTATTACCCCGGTTGATA | 42 |
| 16 | TAATTTCAACTTTATTTAGGAATACCACATCGATGAACGGTA | 42 |
| 17 | GAGAAACACCAGAAAAAGGAATTACGAGGGCTATCAGGTCAT | 42 |
| 18 | CGTAACAAAGCTGCCTCGTTTACCAGACATTAATGCCGGAGA | 42 |
| 19 | GAGTAATCTTGACATTTTGCAAAAGAAGCAAATCACCATCAA | 42 |
| 20 | CGGTGTACAGACCATTTAGACTGGATAGTGTAGGTAAAGATT | 42 |
| 21 | TAAGGGAACCGAACATTCATTGAATCCCTTTAGAACCCTCAT | 42 |
| 22 | CTCCATGTTACTTACGAGAATGACCATATTTTGCGGGAGAAG | 42 |
| 23 | TTGTATCATCGCCTATTATAGTCAGAAGAGCTAAATCGGTTG | 42 |
| 24 | CCCAGCGATTATACAGGAAGCCCGAAAGCAAAGAATTAGCAA | 42 |
| 25 | CGAAAGAGGCAAAATTCAAAGCGAACCAAATAGTAGTAGCAT | 42 |
| 26 | GGGTAAAATACGTAATTAGAGAGTACCTTTCATTTGGGGCGC | 42 |
| 27 | TTGAGGACTAAAGATTTTGCGGATGGCTAGATACATTTCGCA | 42 |
| 28 | AAAGACAGCATCGGTAGCTCAACATGTTTGATTCCCAATTCT | 42 |
| 29 | TTACCAGCGCCAAATTAGTTTGACCATTTAGAGCTTAATTGC | 42 |
| 30 | AATAAGTTTATTTTTGTTTAGCTATATTTTAATTGCTCCTTT | 42 |
| 31 | ATAAAGGTGGCAACGCATCAATTCTACTGACCGGAAGCAAAC | 42 |
| 32 | TCCTTATTACGCAGTCATACAGGCAAGGACTTCAAATATCGC | 42 |
| 33 | CAATAATAACGGAAGCCTCAGAGCATAACAAAGCGGATTGCA | 42 |
| 34 | CAGATAGCCGAACATGACCCTGTAATACAATCAAAAATCAGG | 42 |
| 35 | AGCAATAGCTATCTCAAGGATAAAAATTCCTCAAATGCTTTA | 42 |
| 36 | AATTGAGTTAAGCCATGCCTGAGTAATGCGTCCAATACTGCG | 42 |
| 37 | AGAGGGTAATTGAGAGGCCGGAGACAGTTTTTGCCAGAGGGG | 42 |
| 38 | CGCATTAGACGGGAGTTCTAGCTGATAAGACGATAAAAACCA | 42 |
| 39 | AATAGCAGCCTTTAGAGAGATCTACAAAGCATAGTAAGAGCA | 42 |

| | | |
|---|---|---|
| 40 | ATCCAAATAAGAAAGAGCAAACAAGAGAATTCAACTAATGCA | 42 |
| 41 | AATTTGCCAGTTACATGTCAATCATATGTACAGGTAGAAAGA | 42 |
| 42 | TCCTGAATCTTACCAAAAACAGGAAGATTAAAATCTACGTTA | 42 |
| 43 | AAATCAAGATTAGTGTTAATATTTTGTTTTTTTTGGGGTCGA | 42 |
| 44 | GTTTTAGCGAACCTAGCTCATTTTTTAATCAGGGCGATGGCC | 42 |
| 45 | TCAGATATAGAAGGGCGTCTGGCCTTCCAAAGAACGTGGACT | 42 |
| 46 | TTTTCATCGTAGGATGAGCGAGTAACAAAGGGTTGAGTGTTG | 42 |
| 47 | AACCAAGTACCGCAGCGGATTGACCGTAAATCGGCAAAATCC | 42 |
| 48 | ATAATCGGCTGTCTGCGCATCGTAACCGTTTGCCCCAGCAGG | 42 |
| 49 | ATAATATCCCATCCCAGTATCGGCCTCACCGCCTGGCCCTGA | 42 |
| 50 | CGCGCCTGTTTATCGCACCGCTTCTGGTTTCTTTTCACCAGT | 42 |
| 51 | TCCAGACGACGACACATTCAGGCTGCGCCGCGGGGAGAGGCG | 42 |
| 52 | ATAAGAGAATATAACCTCTTCGCTATTAGGGAAACCTGTCGT | 42 |
| 53 | ACGCCAACATGTAACAAGGCGATTAAGTACTCACATTAATTG | 42 |
| 54 | CGCTCAACAGTAGGGACGTTGTAAAACGAAGCATAAAGTGTA | 42 |
| 55 | GTATCATATGCGTTAGGTCGACTCTAGAAAATTGTTATCCGC | 42 |
| 56 | GAATAAACACCGGAGACCGTATACGCATGAGCTCGAATTCGT | 42 |
| 57 | AAACTTTTTCAAATCCTGAAAGCGTAAGGAGATAGAACCCTT | 42 |
| 58 | AAATGCTGATGCAATGGCTATTAGTCTTCCAGTCACACGACC | 42 |
| 59 | CTTTTTAACCTCCGTCGCCATTAAAAATCGCTCAATCGTCTG | 42 |
| 60 | GTCAATAGTGAATTACAGAGGTGAGGCGATTGCAACAGGAAA | 42 |
| 61 | CTTGAAAACATAGCCCACGCTGAGAGCCTCGGCCTTGCTGGT | 42 |
| 62 | CTTCTGTAAATCGTCCTTGCTGAACCTCTTAGTAATAACATC | 42 |
| 63 | GGAAACAGTACATATCAGTTGGCAAATCTGTCCATCACGCAA | 42 |
| 64 | TTAATTACATTTAATCTAAAATATCTTTGAAGTGTTTTTATA | 42 |
| 65 | TGAGCAAAAGAAGACCGTCAATAGATAAATTAAAGGGATTTT | 42 |
| 66 | GTTACAAAATCGCGTTTACAAACAATTCCTTTCCTCGTTAGA | 42 |
| 67 | GGAGAAACAATAACACGTTATTAATTTTAGGGCGCGTACTAT | 42 |
| 68 | TTAACGTCAGATGAGGAACAAAGAAACCTGCGCGTAACCACC | 42 |
| 69 | GCACGTAAAACAGATCCTGATTATCAGAAAGGAGCGGGCGCT | 42 |
| 70 | TGAATAATGGAAGGTTGTTTGGATTATAGAAAGCCGGCGAAC | 42 |
| 71 | AGTAACAGTGCCCGGAAAGTATTAAGAGCGTTGGGAAGAAAA | 42 |
| 72 | AGGAGTGTACTGGTATTAGCGGGGTTTTCCTTATGCGATTTT | 42 |
| 73 | TTTACCGTTCCAGTGAGAGGGTTGATATGGCTTGAGATGGTT | 42 |
| 74 | TAAATCCTCATTAAGTACTCAGGAGGTTAGGCTTGCCCTGAC | 42 |
| 75 | TTGAGGCAGGTCAGCTCAGAACCGCCACATTACCCAAATCAA | 42 |
| 76 | ACCAGAACCACCACGATAGCAAGCCCAACTGACCTTCATCAA | 42 |
| 77 | CTCAGAACCGCCACTTCGTCACCAGTACAGAGGACAGATGAA | 42 |
| 78 | ACCAGAGCCACCACACAGCCCTCATAGTCAGACGGTCAATCA | 42 |
| 79 | CTTATTAGCGTTTGTTTCCAGACGTTAGAAATCCGCGACCTG | 42 |
| 80 | AGACTGTAGCGCGTTAAACAACTTTCAAAGTACAACGGAGAT | 42 |

| | | |
|---|---|---|
| 81 | ACCGTAATCAGTAGAACAACTAAAGGAAACTCATCTTTGACC | 42 |
| 82 | AGCAAGGCCGGAAAAATCTCCAAAAAAAGCACCAACCTAAAA | 42 |
| 83 | GGAATTAGAGCCAGCGGTTTATCAGCTTAGTTTCCATTAAAC | 42 |
| 84 | CATTAAAGGTGAATTGATACCGATAGTTCGGCTACAGAGGCT | 42 |
| 85 | TGAATATAATGCTGAACGAGGGTAGCAAGCGCCGACAATGAC | 42 |
| 86 | TGATAAGAGGTCATCTTTTTCATGAGGAGCTTTCGAGGTGAA | 42 |
| 87 | TCCAACAGGTCAGGATGCCACTACGAAGAGGCTCCAAAAGGA | 42 |
| 88 | GTTTTAATTCGAGCGAATACACTAAAACTTGCGAATAATAAT | 42 |
| 89 | TCAAAAAGATTAAGCAAGCGCGAAACAACAGTTTCAGCGGAG | 42 |
| 90 | TCTTTACCCTGACTGATAAATTGTGTCGTAAATGAATTTTCT | 42 |
| 91 | AACAGTTCAGAAAAGCCGGAACGAGGCGTAGCGTAACGATCT | 42 |
| 92 | GAATCGTCATAAATTGACCAACTTTGAAAAACTACAACGCCT | 42 |
| 93 | GTAATAGTAAAATGGGCGCATAGGCTGGTAGGAACCCATGTA | 42 |
| 94 | AAATAGCGAGAGGCAGAACCGGATATTCCCTCAGAGCCACCA | 42 |
| 95 | ACACTATCATAACCTCATTCAGTGAATATAGTACCGCCACCC | 42 |
| 96 | GATACATAACGCCACGAGTAGTAAATTGAAGTATAGCCCGGA | 42 |
| 97 | TTCATCAGTTGAGAATCATTGTGAATTAGCTCAGTACCAGGC | 42 |
| 98 | ATAAAACGAACTAATATACCAGTCAGGAGCTGAGACTCCTCA | 42 |
| 99 | GGTGCCGTAAAGCATAGAGCTTGACGGGCTTTTCGGAACCTA | 42 |
| 100 | CACTACGTGAACCAAGGGAAGAAAGCGATGATGGCAATTCAT | 42 |
| 101 | CCAACGTCAAAGGGTGTAGCGGTCACGCACCAGAAGGAGCGG | 42 |
| 102 | TTCCAGTTTGGAACTAATGCGCCGCTACAAAAGTTTGAGTAA | 42 |
| 103 | CTTATAAATCAAAAGCACGTATAACGTGGACAACTCGTATTA | 42 |
| 104 | CGAAAATCCTGTTTTAAACAGGAGGCCGTACATTTGAGGATT | 42 |
| 105 | GAGAGTTGCAGCAACGCCAGAATCCTGAAGGAGCACTAACAA | 42 |
| 106 | GAGACGGGCAACAGCGAGTAAAAGAGTCAACAGTTGAAAGGA | 42 |
| 107 | GTTTGCGTATTGGGCAATACTTCTTTGAAAATATCAAACCCT | 42 |
| 108 | GCCAGCTGCATTAAAAGAACTCAAACTAAGCAGCAAATGAAA | 42 |
| 109 | CGTTGCGCTCACTGTATTACCGCCAGCCGTCAGTATTAACAC | 42 |
| 110 | AAGCCTGGGGTGCCTACCTACATTTTGAACCGAACGAACCAC | 42 |
| 111 | TCACAATTCCACACCATTGGCAGATTCATAATGCGCGAACTG | 42 |
| 112 | AATCATGGTCATAGCATTCTGGCCAACAAATACGTGGCACAG | 42 |
| 113 | GCAAGTCCGCTAGCATCATAATTACTAGCAAAGAACGCGAGA | 42 |
| 114 | GCTTGCATGCCTGCATACAAATTCTTACATATAACTATATGT | 42 |
| 115 | GTTTTCCCAGTCACGCTTAATTGAGAATGTCTGAGAGACTAC | 42 |
| 116 | AGGGGGATGTGCTGTTTAGGCAGAGGCAAGACGCTGAGAAGA | 42 |
| 117 | GCGATCGGTGCGGGAGTACCGACAAAAGTTTCCCTTAGAATC | 42 |
| 118 | AAAGCGCCATTCGCATAAACAACATGTTAGTGAATAACCTTG | 42 |
| 119 | CAGCCAGCTTTCCGAACAATAGATAAGTTTACCTTTTTTAAT | 42 |
| 120 | TGAGGGGACGACGATAATTTACGAGCATTCAAGAAAACAAAA | 42 |
| 121 | GTTGGTGTAGATGGTTCCTTATCATTCCTCATTTCAATTACC | 42 |

| | | |
|---|---|---|
| 122 | CGTGGGAACAAACGCTCATCGAGAACAAGCTTTGAATACCAA | 42 |
| 123 | ATCAACATTAAATGATCATTACCGCGCCTACCTTTTACATCG | 42 |
| 124 | ATCAAAAATAATTCCTTATCCGGTATTCGTAGATTTTCAGGT | 42 |
| 125 | ATTTTTGTTAAATCCCCGACTTGCGGGATATCAAAATTATTT | 42 |
| 126 | TTTAAATTGTAAACTGCTATTTTGCACCGCCCCCTGCCTATC | 42 |
| 127 | ATCAGAAAAGCCCCAACGCTAACGAGCGGGGTCAGTGCCTTG | 42 |
| 128 | ATCGTAAAACTAGCAAAATAAACAGCCAGCTTTTGATGATAC | 42 |
| 129 | TGCCTGAGAGTCTGCGATTTTTTGTTTAGCGCAGTCTCTGAA | 42 |
| 130 | GGGTAGCTATTTTTCAGAGAGAATAACATATTCACAAACAAA | 42 |
| 131 | TATGATATTCAACCGAATTAACTGAACAGCATTGACAGGAGG | 42 |
| 132 | CAAAAGGGTGAGAACGCTAATATCAGAGCCCTCAGAGCCGCC | 42 |
| 133 | ATATTTTAAATGCACAATAATAAGAGCATCAGAGCCGCCACC | 42 |
| 134 | CCTTTATTTCAACGTACCGAAGCCCTTTTCAAAATCACCGGA | 42 |
| 135 | TACCAAAAACATTAAAGTTACCAGAAGGTCGGTCATAGCCCC | 42 |
| 136 | AATTAAGCAATAAATACCCAAAAGAACTTTGCCTTTAGCGTC | 42 |
| 137 | TAACATCCAATAAATATGTTAGCAAACGCCATCGATAGCAGC | 42 |
| 138 | GAGCTGAAAAGGTGATATAAAAGAAACGGCACCATTACCATT | 42 |
| 139 | AATGGTCAATAACCGTCACAATCAATAGACTTGAGCCATTTG | 42 |
| 140 | GCGAACGAGTAGATGACAAAAGGGCGACTGACGGAAATTATT | 42 |
| 141 | AACAACCATCGCCCGGGAAGGTAAATATATTCAACCGATTGA | 42 |
| 142 | TTTCTTAAACAGCTTATCACCGTCACCGAAAATTCATATGGT | 42 |
| 143 | GCCTTTAATTGTATCAAAATCACCAGTACAAAGACACCACGG | 42 |
| 144 | TTTTTCACGTTGAACGTCACCAATGAAATAGAAAATACATAC | 42 |
| 145 | TGAGAATAGAAAGGCGACAGAATCAAGTGGCATGATTAAGAC | 42 |
| 146 | GTATGGGATTTTGCTTTCATCGGCATTTAAACCGAGGAAACG | 42 |
| 147 | AAAGTTTTGTCGTCCCATCTTTTCATAATTAAGAAAAGTAAG | 42 |
| 148 | GTAGCATTCCACAGCGGAACCGCCTCCCAGAAACAATGAAAT | 42 |
| 149 | CCGTAACACTGAGTCCTCAGAGCCACCAAGATAACCCACAAG | 42 |
| 150 | CCCTCATTTTCAGGCAGAGCCGCCGCCACCCTGAACAAAGTC | 42 |
| 151 | TCAGAACCGCCACCACGATTGGCCTTGATAAAAACAGGGAAG | 42 |
| 152 | ATAGGTGTATCACCAGCCAGAATGGAAAACGTCAAAAATGAA | 42 |
| 153 | GGATAAGTGCCGTCAAGCGTCATACATGTATTATTTATCCCA | 42 |
| 154 | AGAGAAGGATTAGGAATAAGTTTTAACGTCTTTCCAGAGCCT | 42 |
| 155 | TTATTCTGAAACATTATAAACAGTTAATCAGCTACAATTTTA | 42 |
| 156 | CAATATAATCCTGAGTTAGAACCTACCAGGTTTTGAAGCCTT | 42 |
| 157 | AATTATCATCATATAATAAAGAAATTGCTAAGAACGCGAGGC | 42 |
| 158 | CATTATCATTTTGCATATACAGTAACAGCAATAGCAAGCAAA | 42 |
| 159 | AATCCTTTGCCCGAGGATTCGCCTGATTGCAAGCCGTTTTTA | 42 |
| 160 | TAGAAGTATTAGACCAGAGGCGAATTATAAGAACGGGTATTA | 42 |
| 161 | CTAATAGATTAGAGTGATGAAACAAACAGTAGAAACCAATCA | 42 |
| 162 | ATTGAGGAAGGTTACAATTTCATTTGAACCTGAACAAGAAAA | 42 |

| | | |
|---|---|---|
| 163 | CAATCAATATCTGGAATCAATATATGTGCAGCTAATGCAGAA | 42 |
| 164 | AATCTAAAGCATCACGCTATTAATTAATGTAAAGTAATTCTG | 42 |
| 165 | CGCCTGCAACAGTGGATAGCTTAGATTATTTTCGAGCCAGTA | 42 |
| 166 | CAGCAGAAGATAAATATCAAAATCATAGCGCCATATTTAACA | 42 |
| 167 | ATAGCCCTAAAACAGCTTAGGTTGGGTTCAGTATAAAGCCAA | 42 |
| 168 | ACAATATTTTTGAAATCCAATCGCAAGAAAAAAGCCTGTTTA | 42 |
| 169 | GGATGTAAATGCTGTTCCATATAACAGTTTAAATATGCAACT | 42 |
| 170 | TTATATAACTATGAACGCATAACCGATACACCCTCAGCAGCG | 42 |
| 171 | AAAGTACGGTGTACTTTTGCGGGATCGTTATTCGGTCGCTGA | 42 |
| 172 | AGGATCCCCGGGTACCGGCTAGTACCCGTATA | 32 |
| 173 | ATATTTTAGTTAATTTCATCTTCTGACCTAAATTTAATGG | 40 |
| 174 | TTTGAAATACCGACCGTGTGATAAATAAGGCGTTAAATAA | 40 |

**Supporting Table 3. Staple list for the 24-helix bundle NR.**

| Number | Sequence | Length |
|---|---|---|
| 1 | CGCCTGTAGCATAACAGCTCGGTTTATCAGCTTCACTACGGG | 42 |
| 2 | TAAAGAACTTTTGGGAATTAGAGGAATTATCGCCTGGCCCTG | 42 |
| 3 | AACATTATGACCAACAAGAAAGGCTATCAGGTCTCATCAAAA | 42 |
| 4 | AAGCCCGAAAGATTGACCAGTTGATTCCCAATTAGCCTTTAA | 42 |
| 5 | ACCTTATGCGATTTTGCCAAAACCAAAATAGCGTCGAGCTGG | 42 |
| 6 | AAGTTTCCATTAGAACGGTGGAACCGAACTGACCCAGTCATT | 42 |
| 7 | TAAGAAAACATGTAAATGCTGATTCCGGCTCAGTAGGGCTTA | 42 |
| 8 | ATTTCTTACGTAGAAACCAATCAATAATATGATTAGTTGCTA | 42 |
| 9 | AACCACCACCAGTGCCGTCATTAGCGGGGTTTTTAGCGTAAA | 42 |
| 10 | TTTGCGGGACCCTGAACAAAGTCCGCATTATACGCAGTATGT | 42 |
| 11 | ATAAATACCGTCAGTATTAACACCAGCAGAATTAGACTTTAC | 42 |
| 12 | AATAGATAAATTTGCACGTAAAAAAGGGTTTTTCATTTGAAT | 42 |
| 13 | CATTAATGAATCGGTGGTTTTTCTTTTCAC | 30 |
| 14 | CAGAATGTTGATATTCACAAAGAGGTTGAG | 30 |
| 15 | AGCCCGAGATAGCATTAAAGC | 21 |
| 16 | GTTCCAGTTTCATTGACAGCAAATAAATCCTGGTTGAGTGTT | 42 |
| 17 | GCGGGGAGAGGGAAACCTGTC | 21 |
| 18 | TGAATTTACCGTTCCAGTAAGCGTCATACA | 30 |
| 19 | CAAAATCCCTTATAAATCAAAAGAAT | 26 |
| 20 | GGTCAGACGATTGGCCGAAAGCGCAGTCTC | 30 |
| 21 | CGTTTGCCATCTTTTCATAATCACCAGCTG | 30 |
| 22 | GTGAAATCACCGGAACCAGAGCCACC | 26 |
| 23 | GCTTTCCAGTCGGCGGTTTGCGTCAACAGCTGCTCACTGCCC | 42 |
| 24 | AGAGACGGGATTGGGCGCCAGGGCCAACGC | 30 |
| 25 | AAATATTCCAATGAAACCAGGGCGACCACGCAATACACCACC | 42 |
| 26 | AGTAGATAAAACCGGAGACAGTCATAGGTAAAGGGATTTAGA | 42 |
| 27 | TCAACAACCGCACTCATCGACATGTTTTTAGTATCCAGGCTT | 42 |
| 28 | GCGTACATTTTGATATTTAAATTGGCCCCAAGCAGAGGTGAG | 42 |
| 29 | CATCGCCCATCACCTTGCTTAGTCTTCTTGCAACAAATAAAC | 42 |
| 30 | TCATAGGTTAGTTAATTTCCGCTGAGCTAGAAGATCAATGAC | 42 |
| 31 | CGTTTTAGACAGATCGTAACCGTGGGGATAGAAACGCTCAAT | 42 |
| 32 | TATGACGGGAGATAGAAAGGAACACAACTTTCAAAGACTCCT | 42 |
| 33 | TACAGAGAAGCCCAATAATTTGTTTATCGCGTTTTGCACCCT | 42 |
| 34 | CACCACCGTCACTAAACAGTTAATGGGTCAGCGATTGCCCTT | 42 |
| 35 | ACAAATGAGTAGCTACCTTTTTAACCGCAATATTGAAACAAA | 42 |
| 36 | CATCACCTTAATCTTCTGAATAATGGCAGAATAATTAGAGCC | 42 |
| 37 | CCAGGCATGATTCCCTCAGAGCCACCCTCAGTACGACTTGAG | 42 |
| 38 | GATTGTTCAGTAACAGTACTATCAGAAAAACTAATAAATAAA | 42 |
| 39 | GTCAAACAATTTACCGAACGAACCACCGCCCCCAAAAACGCT | 42 |

| | | |
|---|---|---|
| 40 | CAATTGAAAATAGGTAATTGAGCGCTTACCAGAACGTAGAAA | 42 |
| 41 | ATTTAGAACGCGTCGGCTGTCTTTCCTCCGGTAACCCAGCTA | 42 |
| 42 | AAACAGTGAATTATCCAATCGCAAGATAATTACAATCGCCAT | 42 |
| 43 | TCGTACATCAATAATAAAGAAATTGCTCATTTCTTTTAATGG | 42 |
| 44 | TTCACCTGATAGTGCAACAGTGCCACAAATATCTTCGACAAC | 42 |
| 45 | CAGTGAGAGTAGTATTCATTAAAGGTCCAGGGGAACGGAATA | 42 |
| 46 | CTGGTTTGCCCCATTTGCACCATTACCATTAGCCGATTACAT | 42 |
| 47 | AAAGGTGGCAACAAGTAATATCAGAGAGATAACAAATTTATC | 42 |
| 48 | CTGAATCTTACCCTTATTATCATTCCAAGAACGTGCAACAAC | 42 |
| 49 | GCCAACATGTAAATCACAAAGAACGCGAGAAAAAATAGTACA | 42 |
| 50 | TAAATCAATATATTATGTAGATTTTCAGGTTTAAATTTTAAA | 42 |
| 51 | TCCTTTGCCCGATCTAGCTGAGAGCCAGCAGCACGAACAGTC | 42 |
| 52 | ATACATGAGGGACAAAATCACCAGTATCGGTCATTGCAGCAA | 42 |
| 53 | CGGAAACAAAACCGTCAAGTTTGCCTTTAGCGTAAACGTCAA | 42 |
| 54 | AGAATTGCCCAAATCTTACCGAAGCCCTTTTTAATTACGTGA | 42 |
| 55 | TAAACCAAATCGGAGAATCATTACCGCGCCCAATAGCCGTAA | 42 |
| 56 | CGACTTTGCTTCCCTGAACAAGAAAAATAACCTATGCGTTAT | 42 |
| 57 | AGATGAAAAAGGAGCTGATTGCTTTGAATACCACCAAGGGAA | 42 |
| 58 | AAAATCTCTGCGCGGGTCAGTTGGCAAATCAACAGGTGTAGC | 42 |
| 59 | CCCAAGCAAAGGTAAAAACAGGGAAGAGAGGCACGAACCTCC | 42 |
| 60 | GTTTTCAGACGGAACGGCCCCCTGCCTATTTCGGCATAAGGT | 42 |
| 61 | GATAGTTAGAATAAAAACTAAAGGAATTGCGAATCAGGCCTT | 42 |
| 62 | AGATATATAGATAAGATCGCCTGATAAATTGTGTTATGTTTA | 42 |
| 63 | ATAAATTTCTGAGAAACAGATACATAACGCCAATTGACAAAA | 42 |
| 64 | CGCAGTATGGATTACTGCTGAATATAATGCTGTGAAGATCCT | 42 |
| 65 | TGAGGAGATTAAAATGAATCACCATCAATATGAAAGGTAAAA | 42 |
| 66 | GGGGTGCTGTGCCTTGAGTAACAGTGCCAAAGTGTAACATGA | 42 |
| 67 | TCTCCACCGATAAGCCTGTGTGAAATTGAGTGCAGGGAGTTA | 42 |
| 68 | TTGTCAATCGTCTTAATAGTACCGAACCTATTATTCCGGAAT | 42 |
| 69 | ACAAATTACGAAAGCGTATTCGGTAATAATTTTTTATGACAA | 42 |
| 70 | AAAGTAAAATCTACAGCCGGATATCGAAATCCGCGGCTGACC | 42 |
| 71 | ATTAAAACGGAAGCCCATAAATAAAGGAATTACGAAGACTGG | 42 |
| 72 | GCGGATGAAAAATTGCGCGAGCTAGCTCAACATGTAATAACC | 42 |
| 73 | GACCTCTGTAACAATTTAATCAGTATTCAACCGTTAACTAGC | 42 |
| 74 | AACTATTGGGGCAACTGCAGGTCGACTCGGATCAATTCTACT | 42 |
| 75 | ATTAACGGTTGAAATCACGACGTTGTAAAGAAACAGGAAGAT | 42 |
| 76 | CGTTAAAATTCGCACCCGTCGGATTCGGGGTAGAACCCTTCT | 42 |
| 77 | GTTTACCAGCGCAATCTATCAGGGCGATCGATTCAACAAGGC | 42 |
| 78 | CAATCCAAATAAATCAAGTTTTTTGGGGCGACGTCAACCACA | 42 |
| 79 | TGTCCAGACGACAGACCCTAAAGGGAGCCACAGCTAAGGTAT | 42 |
| 80 | CATAGCGATAGCACCGGCGAACGTGGCGACAAGAGTCCTTTT | 42 |

| | | |
|---|---|---|
| 81 | TCAAATAGGAAAGCCGACCGTGTGATAAATAAGAATTAGAGC | 42 |
| 82 | AGACAATATTTTCTTAACCACCACACCCTTTAATGCGAATGA | 42 |
| 83 | AGGGCGAGTCATCGGCAGCAGGCGAAAAGACTCCACAAGAGT | 42 |
| 84 | ACCATCAAGCCGAACAATATAAAAGAAAGGCCCACTCATATG | 42 |
| 85 | AGCACTAAGTAGAAGGAACGCTAACGAGTCGAGGTTTTATCC | 42 |
| 86 | TTGACGGTACACCGGATTTAGGCAGAGGCCCCGATGTAATTC | 42 |
| 87 | GAAAGCGTAAGGCGAATGTGAGTGAATAAGAAAGGTTGAAAA | 42 |
| 88 | TATAAAATTAATCAGAAAACGAGATTGAATCACTTATATAAC | 42 |
| 89 | CAAAGAACCTACTAGAGCTTAATTTTTGATATTTACATTTAA | 42 |
| 90 | CAACCCATCCTAAGATTTGTATCATTATACCTTGCCTTAAAT | 42 |
| 91 | TTCCACAGCCAACAGTTTCAGCGGAGTGTTATCCGTTGAAAA | 42 |
| 92 | GGTCATACTAAGCGCGAAACAAAGTACAGAATTCGGCTCCAT | 42 |
| 93 | CGTATAACTCAGTTGAGATTTAGGAATAGCATGGCTAGTAAG | 42 |
| 94 | CGAGGCAAGAGAGGTCATTTTTGCGGATTAGACCTAATATGC | 42 |
| 95 | CCAAGCTGTAGATTCAAAAGGGTGAGAAAACGACGCTGATAA | 42 |
| 96 | GAGGACATAAAAAAAAAGGCTCCAAATTCTCCGTAACACTGA | 42 |
| 97 | ATTGCGTCTAATGACCCTCAGAACCGTGGTAATGAAAAGCCT | 42 |
| 98 | CAGAACCCAACATAGGAACCCATGTAGTATGGGCGCTCACAA | 42 |
| 99 | AAGGCCGGCTGTTTGGTAGCAACGGCATCTTTGCTTAATCAT | 42 |
| 100 | AAAGCTGGGATCCCGTAAATTGGGCTCATTATTCATAGTACC | 42 |
| 101 | TTTAAACAGTCCGCGACTATTATAGTGTACCTTTATTGATAG | 42 |
| 102 | AATAGTATGCATGCAATTAAGCAATACAATGCCAGGCCAGTG | 42 |
| 103 | TGTATAATTCCCAGATTTTTGTTAAACGGCGGATCGTAACGC | 42 |
| 104 | TTAACACCCTGCCGGAGAGGGTAGCTAATGAAGCCTCAGAGC | 42 |
| 105 | ATAAATCATAAGTACGGTGTCTGGAAGAGACAGAAGCAAAGC | 42 |
| 106 | GGGTAAAATATTAGCAAGTTTATTTTCATCAGGACAGATAAC | 42 |
| 107 | ACCGGAACCGCCAAATCCCCCTTATTAGGTTTGATGGTGGGC | 42 |
| 108 | CTCATTTTCAGGTACAAAACCGAGGAAAAAGACACCACGGCA | 42 |
| 109 | CAGCAGCGAAAGGCGTTAAGAACGCGAGTTTCCAGAGCCTTC | 42 |
| 110 | GCCCTGACGAGAGAGAAAAAAGCCTGTTTTCGAGCCAGTAGA | 42 |
| 111 | CATAAATCAAAATCTATACCTGAGCAAATGCTTCTGTAAACG | 42 |
| 112 | TCATACAGGCAATGATAGGAGCACTAACAAGTTTGAGTAAAT | 42 |
| 113 | GTTAATATTTTGTAAAACCGCCAGCCATGGCCAACAGAGACC | 42 |
| 114 | TTTCCCTCAGAGCCTGGCTTTTGATGAAGCTTCCGAAATCGG | 42 |
| 115 | GCGATAGCAAGCCCTCCAGACGTTAGGCAGAATAAGTTTATT | 42 |
| 116 | CAACAGCATCGGAAAGGCAAAAGAATCAAAAATTTGCCAGTT | 42 |
| 117 | TAAACACCAGAACGGTTAATAAAACGAAAAATAAGAGAATAT | 42 |
| 118 | GCATCAGGTCTTTAAAACTCCAACAGCAATTCGTCGCTATTA | 42 |
| 119 | AAGGCAAAGAATTATTTAGAACCCTCTAGACATTATCATTTT | 42 |
| 120 | CAAATATCGATAGTTACAACAATAACGGATAGATTTAGTCTT | 42 |
| 121 | CCTTCCTGTATCAAACTATTAGTAATAACATCGCCATTCTGG | 42 |

| | | |
|---|---|---|
| 122 | AAGTAGGAGGTTTACGAGCCGGAAGCATCGAACCGCCACCCT | 42 |
| 123 | TAATACTTTCCAGTTGAACCCTCAATCAATTCTGGAGCACTG | 42 |
| 124 | GTTACACAAGAATACGGGTACCGAGCTCACAATCAACGTAAC | 42 |
| 125 | AGCAAAATCGTCCTTAGCGACCGTATACCCCCCCTCAAATGC | 42 |
| 126 | CTTTGAAAGGTGACAATAACCGACAAAAGGCTCATTATACAA | 42 |
| 127 | GGCTTTTGCATTTAGATTTTTTCCCTTAGACGTTTTAATAGA | 42 |
| 128 | GTTTCCTCATTAAGAGGCTGAGACTCGTACCCACCCTCAGAG | 42 |
| 129 | ACCAACCTAATCGTATTGATACCGATAGTTTAACTACACGAT | 42 |
| 130 | ATTTCCTTGTTAGCCGGAACGAGGCGACTCTACAGAGGCTTT | 42 |
| 131 | GGATTGCGGCACTATCATAACCCTCGACAATGAGATGGTTTA | 42 |
| 132 | TTCGAGGTGCTGAAACGAATAAACAGCCATACGTAATGCGCT | 42 |
| 133 | GCGAACCAGGTCATAAGAGGGGGTAATAGTAACTGAAGGACG | 42 |
| 134 | GCCTGAGAGATTGAATGGGAAAGCGTAAGAAGCCAGCTTATT | 42 |
| 135 | CAGAGCCGCCAGGAGTCTCAAGAGAAGGATCACCGTAGTCAC | 42 |
| 136 | CAGTACAAAATGAATTAGGAGCCTTTAATTGCCCACGCTAAA | 42 |
| 137 | GACTTTTTCCTAAAACCAGACGGTCAATCAGAGTAATAACTT | 42 |
| 138 | TAATCATTGTAACGGATTTACCAGACGACGCAATACTGCATC | 42 |
| 139 | AAAAAGATTAGGATTAGTTTCATTCCATATTATATTTGCTAA | 42 |
| 140 | ATCGGTTGTTATTTTAATTTTTGAGAGATCCATATGTCAATA | 42 |
| 141 | CGAACGAGTTCATATTCCACAAAGAAACCATGCGGGAGACTG | 42 |
| 142 | ACAGACAGCAAAGAAAAGAAATAGCAATAGAATTTCTTATCC | 42 |
| 143 | CTAAAGTTTTATTAGGGAGAGGGTTGATATATACACCAGGCA | 42 |
| 144 | AGGTGTGAATCGATAGCAGCACCGTATAGTATAGCCTAAGTT | 42 |
| 145 | TTGGGAAGACAATAAGGTACAGACCAGGCGACAATGAAAGGC | 42 |
| 146 | CAACCAATTAAGAGCAAGAAACAATGTAGCCGACACAATTTT | 42 |
| 147 | AACGCAAGGAGCAACATTAGATACATTTCGGTCAAGATCAAA | 42 |
| 148 | AATGTGAGCAATTACAGAATCGATGAACGGATAACCAATTTC | 42 |
| 149 | CAGTACCAGAGCAAAGACACAATCAATAGACCTCATAGTGCT | 42 |
| 150 | ATAGCACGAATCTTCTGACCTAAATTATAATGTTTGGACAGG | 42 |
| 151 | TTCATAACAAGAACAAGCAAGCCGTTCATAGGCTGACACCCC | 42 |
| 152 | CGCCGCCAGGGCAGACTGATCAGTAGCGACGCGGATAAGAGC | 42 |
| 153 | ATGTCGAATGAACCTCAAATATCAAAAGATCGTAACTTGAGT | 42 |
| 154 | TGTTTATATCTTTTACATCGGGAGAAAAAATGGTCTTTAATT | 42 |
| 155 | CATCAGTATAAATTCAGTGAATAATTACCCAGGATTTACGAG | 42 |
| 156 | ATTTACATTTGACATTAACATCCAAGGTGGCCTCATATCAAA | 42 |
| 157 | ACAGGTTTTGAATGCGGGATCGTCTGAGGCTAAATTAACTGA | 42 |
| 158 | CAATAGGTTGGGATTCAACTAATGGATTCATCAGCCAACGCT | 42 |
| 159 | GGTCACGAAAAGGTTAACGTTATTAATTCTGGCAAAAGGAGC | 42 |
| 160 | GCCGCTACGGGTAATAATAAAAGGGACAGCCGCGCGTGGCAC | 42 |
| 161 | GGAATTATCATCGCCGGGCGCTAGGGCGTTTGATGGCACGTC | 42 |
| 162 | AAGAACTGGTAGCGTTAATAATGGTTTGAAAAAAGAAGTTTT | 42 |

| | | |
|---|---|---|
| 163 | TGCTGCAGCGAACGGTACGCC | 21 |
| 164 | TTTCCTCTTTATAATCAGTGAGAACAATATTGGCAGA | 37 |
| 165 | GTATAACGTCTGTCCATCACAGGGCGTTGCCTGAGTAGAAGAACTACTTAATGC | 54 |
| 166 | CATGGTTACATTCAGGAGGCCGATTATGTTGTT | 33 |
| 167 | TTGCTCAGGAGCTAATCATCTGCCAGTTTGAGGGATG | 37 |
| 168 | CAGGGTTGCGTCACGTTGGTGTAGATGGAAGTTGGGGCCTCAGGAAGGCTGGCG | 54 |
| 169 | ACACGACCAGTATCCAGGCCACCGAGTAAAAGAGTGC | 37 |
| 170 | TTGATAGCAATACTTCTTTGATCGCGATCGTATTGAC | 37 |
| 171 | AGAATCAGAGCGAATTAACCGTTGCGAGCAC | 31 |
| 172 | AGAATCCTGAGAAGAAGGGATCTGAAATGGATT | 33 |
| 173 | AAAGGGGGGACGACGACAGGTGCGGGCCTCT | 31 |
| 174 | GCCAATCGCACTCCAGCCAGCCAAATCAGCTCATTTT | 37 |
| 175 | GGAACGCCAGTGGGAATTTCCGGCACCGCTCTATTAC | 37 |
| 176 | TCGTCTGGCAACTGTTGGGAATCCTCAACATTA | 33 |
| 177 | GCAAAGCGCCATTCGGTTGCT | 21 |
| 178 | ATAATTCGCGTCAGGCTGCGTGCCGGAAACCAG | 33 |

**Supporting Table 4. Staple list for the Nanorobot.**

| Number | Sequence | Length |
|---|---|---|
| 1 | TTTAGTTAATTTCAATTAATTTTCCCTTTGAGTGA | 35 |
| 2 | AGAAAACTTTTTCATTGAAAACATAGCG | 29 |
| 3 | AATCGCAAGACAAAAGATTAAGACGCTG | 28 |
| 4 | GTTATATTCATAGGTCTGAGACATCAAGAAAACAAATTTCAA | 43 |
| 5 | TGAATTTTACATTTAACAATTTCGCGCA | 29 |
| 6 | ATAACCTCCTTTTACATCGGGTTTCAGGTTTAACGAAAAGTT | 42 |
| 7 | ACAATATATGAGAATCCAATATAT | 24 |
| 8 | ATTCGCCAAATAAAGAAATTGATTTTGC | 28 |
| 9 | TGCATGGAAAATAGCTTGAACGCG | 24 |
| 10 | AAATCATTTGAGAAGAGCAAATCC | 25 |
| 11 | GAGGCGAGGTTAGAACCTACCATCATAT | 28 |
| 12 | TTACCTGTATACTTCTGAATATGATGGC | 28 |
| 13 | TGAGTAAACTCGTATTAAATCCAGAGATACATCGCCATTA | 40 |
| 14 | GGAACAAGACTTTACAAACAACTGAAAGGCGCGAAAGATAAA | 42 |
| 15 | GGAGCGGTTTGAGGATTTAGAGCACAGACAATAATCTCAATC | 42 |
| 16 | TCCTGATGAGCCGTCAATAGACAGTTGGATCAAACAACAGTG | 42 |
| 17 | AATTCATGCACTAACAACTAAAAAGGAATCACCTTAGCAGCA | 42 |
| 18 | TAAAGCATTGAGGATGCAACAGGAAAAATTGC | 32 |
| 19 | AAAATACCGAACGAACCACCAGTGAGAATTAACCGTTGTAATTC | 44 |
| 20 | AGACTGATAGCCCTAAAAGAACCCAGTCACA | 31 |
| 21 | ACAGAGGCCTGAGATTCTTTGATTAGTAATGG | 32 |
| 22 | GCGTATTAGTCTTTAATCGTAAGAATTTACA | 31 |
| 23 | TTAACACACAGGAACACTTGCCTGAGTATTTG | 32 |
| 24 | CCACGCTGGCCGATTCAAACTATCGGCCCGCT | 32 |
| 25 | GCCGCTGAACCTCAAATCAAATCAGGAAATA | 31 |
| 26 | AATGAAACAGAGCGTAATATC | 22 |
| 27 | CGACCAGTCACGCAGCCACCGCTGGCAAAGCGAAAGAAC | 39 |
| 28 | ACCTTCTGACTTCGACACATTATCCGTAGATAGAA | 35 |
| 29 | TTGGCAGGCAATACAGTGTTTCTGCGCGGGCG | 32 |
| 30 | ATTATACGTGAGTATTAAGAAACCAAAACAGTGAT | 35 |
| 31 | GTCTGAAATAACATCGGTACGGCCGCGCACGG | 32 |
| 32 | ACGATCTGGTTAATACAAATTATCATATCAATACA | 35 |
| 33 | CCTACATGAAGAACTAAAGGGCAGGGCGGAGCCCCGGGC | 39 |
| 34 | CATACAGTTGTAGATTATATCAGAATGGAAGATTA | 35 |
| 35 | TGGGGAGCTATTTGACGACTAAATACCATCAGTTT | 35 |
| 36 | GGAAGAAGTGTAGCGGTCACGTTATAATCAGC | 32 |
| 37 | AGAGAACGTGAATCAAATGCGTATTTCCAGTCCCC | 35 |
| 38 | CGAACGTTAACCACCACACCCCCAGAATTGAG | 32 |
| 39 | GGAAGGGCGAAAATCGGGTTTTTCGCGTTGCTCGT | 35 |
| 40 | GAGCTTGTTAATGCGCCGCTAATTTTAGCGCCTGCCCTCAAT | 42 |

| | | |
|---|---|---|
| 41 | CTAAAGGCGTACTATGGTTGCAACAGGAGAGA | 32 |
| 42 | 42 core GCCGTAAAGCAGCACGTATAA | 29 |
| 43 | AAGTAGGGTTAACGCGCTGCCAGCGGCTAGTAGTCCGC | 39 |
| 44 | GATTCCTGTTACGGGCAGTGAGCTTTTCCTGAACGACG | 38 |
| 45 | GCCTTCACCGAAAGCCTCCGCTCATTCCCAG | 31 |
| 46 | GTCCACGCTGCCCAAATCAAG | 21 |
| 47 | GGCGGTTAGAATAGCCCGAGAAGTCCACTATTAAAAAGGAAG | 42 |
| 48 | CAGGGTGCAAAATCCCTTATAGACTCCAACGTCAAAAGCCGG | 42 |
| 49 | CAGTGAGTGATGGTGGTTCCGAAAACCGTCTATCACGATTTA | 42 |
| 50 | ATTGCCCCCAGCAGGCGAAAAGGCCCACTACGTGACGGAACC | 42 |
| 51 | AAATGCCAGTTTGAGGGGGATTGAGTGAGCGAATAGGA | 38 |
| 52 | GGGTAGACCTTTGATAGATTAAATCCGTAAT | 31 |
| 53 | CTCGAATGCTCACTACAGTAT | 21 |
| 54 | AATTGCATGCCTGCAGGACCCGTCGGATTTCAAATCAG | 38 |
| 55 | GCTCATGGTCATAGCTGAACTCACTCGCACT | 31 |
| 56 | TAATGTGAAATTGTTATGGGGTGCGGCACCG | 31 |
| 57 | TCACGACTGTGCTGGCGCAAC | 22 |
| 58 | AACGCCAGGGTTCAATTCCACACAACATACG | 31 |
| 59 | GGGATAGGTGCATCCCTGTCGGGGGAGA | 28 |
| 60 | AAACGGCGACGACGGCCCGCTTGGGCGC | 28 |
| 61 | CGGGCCTAGGAAGAATTAATTTTTTCAC | 28 |
| 62 | TGTTGGGGCTTTCCCTAATGAACAGCTG | 28 |
| 63 | TCGCCATTGCCGGAAAAGTGTCCTGGCC | 28 |
| 64 | CGTAACCGTCACGTCAGCTTTAATTCGC | 28 |
| 65 | CCAGCCAAAGGGCGTGGCGAAAATTCGC | 28 |
| 66 | CTTCTGGTCAGGCTCAAGGCGTAAACGT | 28 |
| 67 | AATCATCAACCGAGGCAACCCGTATAAGGATCGGG | 35 |
| 68 | ACGCCATGAACGGTAATCGTAGAGATCTACAAAGGTAAAAAT | 42 |
| 69 | CTCATTTCATGTCAATCATATGGAGAGGGTAGCTATATATTT | 42 |
| 70 | ATTAAATGGTTGATAATCAGATCTAGCTGATAAATGAGTAAT | 42 |
| 71 | TAATATTCAAAAACAGGAAGAATCAATATGATATTTCAAAAG | 42 |
| 72 | ATATTTAAATTGATTAAGTTGGGT | 25 |
| 73 | ACAAGAGGTCATTGCCTGAGAGCCTTTATTTCAACAATACTT | 43 |
| 74 | TGAAAACTAGTTTAACCAGTAACATCGACTCTACCGAG | 38 |
| 75 | GCCGTACCCCTTTTGTTGCTATTACCAA | 28 |
| 76 | TTTTAGACCAAAAACATTATGCAATAAC | 28 |
| 77 | TAAATGCCATAAAGCTAAATCTTTCATTTGGGGCG | 35 |
| 78 | GGTGAGACAAGGCAAAGAATT | 21 |
| 79 | AGCAAAATAAAGATCAACCGTAAAGCCCTTGTTAAAGGGGGAGTTG | 46 |
| 80 | ATTTCGCAAATGGTACCCTGTGCAAGGACTATCAGAATCGATCAAA | 46 |
| 81 | 81 core CTGTTTAGCTATATGGTTGTAACCCTCATTTT | 40 |

| | | |
|---|---|---|
| 82 | CGAGCTGCTCAGAGAATGCCTTAAT | 25 |
| 83 | TAGATTTAGTTTGAAACCAGAGCGTTTTAGGG | 32 |
| 84 | CCATATATACCTTTCATCAAACTGCGGACCCT | 32 |
| 85 | TTTTAAATGGCTTAGGTCTTTCTTTAAACAAA | 32 |
| 86 | AGGGCCCGAATAGACTGTAAAAACAAATCTATCAT | 35 |
| 87 | TAGAGAGACAGTTGATTCCCAATTCTGCCAAC | 33 |
| 88 | CCTTTTGCTGGAAGTTTCATT | 21 |
| 89 | TCAAAAATCAGAGCTTAATTG | 21 |
| 90 | GGTGCTTTTGCAGTCAGGATTTTAACAG | 28 |
| 91 | AAATGTTAGACTTCAAATATCCCGGAAGCAAACTCGAACGAG | 42 |
| 92 | TGAGTAAGAGCAGGTAGGAGTAGTCAAGAACAATC | 35 |
| 93 | ACGACGAGATAGCGTCCAATAAAGATTAAGAGGAATCAGGAT | 42 |
| 94 | CGTACTAACGATGGTTTCTTCATCTACTTAGGAGG | 36 |
| 95 | ATCATAAATCGTCATAAATATAGCAAAGCGGATTGAATTGCT | 42 |
| 96 | AGGCATAATCCCCCTCAAATGACCCTGACTATTATGTCATTT | 42 |
| 97 | AGGTGAGATTCCTGACGCCAAATCTCGCCTGCGAT | 35 |
| 98 | TACATAACGCCAGTTCAGAAA | 21 |
| 99 | CTTATGCGACGTTGGGAAGAACAAAATAGCGAGAGAATAGTA | 42 |
| 100 | TGTCAGGCGCAGACGGTAGGCACCTGAGGAC | 31 |
| 101 | ACTTTAACGTTAATAAAACGATTACCAG | 28 |
| 102 | GCTTGAGGAACAACATTATTACAACACT | 28 |
| 103 | CCAGAACAAAGATTCATCAGTAATTACG | 28 |
| 104 | GGCTTGCTAGGAATACCA | 18 |
| 105 | ATGCCGAACTAAATACGTGAGGAA | 24 |
| 106 | CGCACACTCAAAGACAGCATCGGAATATGACAACAACC | 38 |
| 107 | AACGAAACCGGAACTTTTTCACGTTGAAGGGA | 32 |
| 108 | CAATAGCAACGGCTACATTTCCAGTGCTAAA | 31 |
| 109 | CACTAAAGACCTGCAAAAAAAAAGGCTCCGTTGCGCC | 37 |
| 110 | CCCCCAGATAAATTGCCTTTAATTGTATTTAA | 32 |
| 111 | TATGATCGTCACCCTCAACGCATAGCTTGATACCGATAAAAA | 42 |
| 112 | TCATAATGCCACTACGACAATCATAAAGGAATTGCGAACAAC | 42 |
| 113 | TAAAGACACGATCTTTCAGCGGAGTGAG | 28 |
| 114 | GGCCGCTTCGCTGATCGAGGTGAATTTCCGGTTTATGTATCAAACGTAA | 49 |
| 115 | AGTAAAGTTTTCACCAGTACAAACGGATAAG | 31 |
| 116 | CAACTTTTAATAATGAGGCGC | 21 |
| 117 | GACATTTCTGTATAATCTCCTCCATGT | 27 |
| 118 | ACAACCGATACCACCCTCATTTTCGGAGGTT | 31 |
| 119 | AAAGGAACAACTAAGGGAAAACGGTGTACAGACGAATTAC | 40 |
| 120 | GGAGTGTCGACGGATATTCATTACAGAAACA | 32 |
| 121 | CATTAAATGAACGAGGGAAGAATA | 24 |
| 122 | GAACCGCCACCCTCTCAGAAC | 22 |

| | | |
|---|---|---|
| 123 | TGCCGTCAGAGGCTGAGACTCCCAGAATGGAAAGCGGTTGAG | 42 |
| 124 | GGGAGTTTCGTGTCGTCGAGGCTTAACCTAA | 31 |
| 125 | AAGTATATTCTGAAACATGAACTGAATTTACCGTTCCGCCGCCAG | 45 |
| 126 | TATCACCTGCCTATTTCGGAAGCGTCATACATGGCCCACCAG | 42 |
| 127 | TCAAGGGATAATCGCCCGCAGCGATCTTTGA | 32 |
| 128 | TAGTACCGTATAAACAGTTAAGATACAGGAGTGTAGAGCCAC | 43 |
| 129 | CCCAGAGCCATATTCGGTTTGCGGACCAAGC | 31 |
| 130 | AAGCTCAAGAACCAGGCTACAACGTAGCGTATTTT | 35 |
| 131 | GCAGGTCAACCGATTTGGGAAACCATTA | 28 |
| 132 | AACCACCCAATAATCAAAATCTATAAAA | 28 |
| 133 | CACCCTCCCAGAGCCCCTTATGACAGAA | 28 |
| 134 | AACCGCCCCTCCCTTCGGCATAGCGTCA | 28 |
| 135 | ATTACCAGAGCCAGTAACCTATTAGCCCGGAAACC | 35 |
| 136 | GCAAGGCGAAACAATAGCCGAACAAAGTTATT | 32 |
| 137 | AACCCGACTTGAGCCATTGAGGGATCACAAT | 31 |
| 138 | ATGAAACTAAGCCCAGGAAACCGAGGAAAAAGACAAATT | 39 |
| 139 | GATAAAGGTGAATTATCTGACGGACCACGGA | 31 |
| 140 | CCGTAATGATAACCAATAACGGAATACCGGCA | 32 |
| 141 | TCAAGTTATTGAGCACTGGCATGATTAAAGAA | 33 |
| 142 | TTTTTTCGGTCATAGCCCACCACCACATACATAAAGGTCAAAAGAGCTA | 49 |
| 143 | CAATAGAAAGCAGATGAAATAAAACGATAGTT | 33 |
| 144 | TTGGGGAAGGGACAGGAGCAGTCTAGTATTAGAGA | 36 |
| 145 | ATAAGTTTACCAGAAATAATACAAAAATCTTT | 32 |
| 146 | GAAACGCACGCAATCACAAGATTACAGACTTACCATTCTAAGCATT | 46 |
| 147 | ACAACCGGAAAGAGCCGTTTTGATTGCCCCCGTAC | 36 |
| 148 | AATGGAACCGACCCTCACTGGTAAAGTGCCCGCCA | 35 |
| 149 | CAAACGTGACTCCTAAAGTCAGGAGAATATTA | 32 |
| 150 | GAAAAGTAAATTCAGACATTCAGACGATATTA | 32 |
| 151 | ATAAACAGGGAGCTACATAGCGAATAATCGGATAGATA | 38 |
| 152 | AAATAAGGCAATAGCACCATTTTAGAGCCAGCAAAAAAGGGCTATGGTT | 49 |
| 153 | ACAGCCCAATGAACAAGCTGTCCACCAGTAACCGACCG | 38 |
| 154 | ATTTGCCTTTTTGTTTAACGTAGAGCAACGGA | 32 |
| 155 | CCAATATAGAACCAAGTACAACATTTAGGCACGTTAAA | 38 |
| 156 | CGAGCGTGAAAATAGCAGCCTATTGAGTCATC | 32 |
| 157 | CCTGAATGAGAATAACATAAATCAGAGACAGTAGCTAGCGTT | 42 |
| 158 | TGCACCCAAGCGCATTAGACGGAGGGTATGCC | 32 |
| 159 | GTTGGAGGTTGAGCATGAAAATAA | 24 |
| 160 | ATCATTACCGCAAATAAACAGC | 22 |
| 161 | TCATCGAAGCAAGCAAATCAGGAGCCTA | 28 |
| 162 | GTATTAAAGGCTTATCCGGTAACGCTAA | 28 |
| 163 | CCAGAACGCGTTAACAAGGAATCA | 24 |

| | | |
|---|---|---|
| 164 | TCCTTATAACGCGAGGCGTTTATTTTAT | 28 |
| 165 | CAATCAACCTCCCGACTTGCGGCTATTT | 28 |
| 166 | AAGGTAAAGTAATTCAAGCCG | 21 |
| 167 | TTTCGAGGACGACGACAATAAACCGCAC | 28 |
| 168 | ATGTAATGTTCAGCTAATGCAAGAACGG | 29 |
| 169 | GCCATATCCTGTTTATCAACACTGTCTT | 28 |
| 170 | AGTAGGGAGTCCTGAACAAGATAGAAAC | 28 |
| 171 | GGTTTGAAATATAAGAGAATAT | 22 |
| 172 | TGTGATAAATAAGGGAGGCAT | 22 |
| 173 | TAAGAATAAACACCCGCCAAC | 21 |
| 174 | TAATTACTAGAAAAGAGAATC | 21 |
| 175 | TTCAATTAATATCAAAAAACTATA | 24 |
| 176 | TTAGTATCATATGCGCTCAAC | 21 |
| 177 | CTAAAGTACGGTGTATAAGAGAGTCAGATCAT | 32 |
| 178 | GTGTAGGTTAAGCAATAAAGCAAAAGGTGGCATCA | 35 |
| 179 | CAGTACATAAATCAATAACGGTTGTGCTACTCCAGTTC | 39 |
| 180 | AATTACCTTTTTTATTTGAATTTGTGCTACTCCAGTTC | 38 |
| 181 | CATTTTTGAATGGCGTCAGTATTGTGCTACTCCAGTTC | 38 |
| 182 | GCCAGTGCGCCAGCATCGGTGTTGTGCTACTCCAGTTC | 38 |
| 183 | CGGCCTCCTCTCCGTGGGAACTTGTGCTACTCCAGTTC | 38 |
| 184 | ATAGGCTGGCTGACAATTTCATTGTGCTACTCCAGTTC | 38 |
| 185 | AAGAGTAATCTTGAAAATTGGTTGTGCTACTCCAGTTC | 38 |
| 186 | GCAAGCCCAATAGGATAGGTGTTGTGCTACTCCAGTTC | 38 |
| 187 | CATTTAAATATACCGTCAGTCACCATTGTGCTACTCCAGTTC | 42 |
| 188 | TGCCATCTTTTCTTAGCAGCATTGTGCTACTCCAGTTC | 38 |
| 189 | ACCAAGTAATTATTTGCACGTACCAGAATTGTGCTACTCCAGTTC | 45 |
| 190 | TTTACGTTAGGTACCGTAACACTGTTGATATTTGTGCTACTCCAGTTC | 48 |
| 191 | CTTAATTAGCCTGTTGTAAATGCTGATGTCAATAGCATCATGG | 43 |
| 192 | TTGCGGATATGCAAATTCTACTAATAGTGCTGACGT | 36 |
| 193 | TACTCAGCCCATTGGGACCACAAT ATTTTTTTTTTTTTTTTTTT TTAATGCTGTAGCTCAACATG | 67 |
| 194 | TACTCAGCCCATTGGGACCACAAT ATTTTTTTTTTTTTTTTTTT TTAACCTCCGGCTTAGGTTGG | 67 |
| 195 | CCAACGTTATACAAATTCTTATAACAGGGTCGCCCATCGGTTCGAATCAG ACGGTTTAAGGCAGT | 65 |
| 196 | AGTAGCATTAACATCCAATTACTCAGGGCACTGCAAGCAATTGTGGTCCC AATGGGCTGAGTA | 63 |
| 197 | CTTAATTAGCCTGTTGTAAATGCTGATGTCAATAGCATCATGG | 43 |
| 198 | TTGCGGATATGCAAATTCTACTAATAGTGCTGACGT | 36 |

# Chapter 3: DNA origami capsule for 3D molecular integration

Jaeseung Hahn, Leo Y. T. Chou, William M. Shih

## 3.1 Introduction

DNA nanotechnology, particularly DNA origami, has been widely adapted for applications requiring precise spatial organization of small molecules, proteins, aptamers, nanoparticles, and other functional components.[1–3] This success can be attributed to the architecture of 2D DNA origami structures such as a DNA origami rectangle with regularly spaced addressable sites that allow easy modification to meet the specific needs of a wide array of applications.[4–11] Moreover, DNA origami can be designed modularly to allow for hierarchical assembly, which can potentially scale up the complexity.[12] 3D DNA origami has not been applied as ubiquitously due to its design complexity, which makes it difficult to design a suitable structure for different applications.

In general, DNA origami architectures are divided into two categories: wireframe and space-filling architectures. In 2D DNA origami,[13] the space-filling architecture is the assembly of DNA duplexes in parallel to its helical axis through the formation of parallel multi-crossovers based on DNA double-crossover motif[14], thereby forming an array of DNA duplexes. In 3D DNA origami, on the other hand, there are three major space-filling architectures: square,[15] honeycomb,[16] and hexagonal[17] lattice. 3D DNA origami structure can be achieved by packing a DNA duplex in different lattices through the formation of appropriately angled multi-crossovers. In addition, a hollow 3D structure can be constructed by another architecture that uses concentric rings to define the surface feature of the 3D object.[18] For the wireframe architecture, each edge is usually a DNA duplex or DNA double-crossover molecules, and the edges are connected to each other at a vertex by formation of DNA junctions with or without ssDNA region between the edges.[19–22] Wireframe DNA origami is constructed by placing edges and vertices on either 2D or 3D space that imposes constraint. However, the construction of wireframe DNA origami with a 3D network of edges and vertices is challenging both to design and implement due to its complexity, and most 3D wireframe structures are produced by placing vertices and edges on the surface of the target 3D object (i.e. skeletal polyhedra). The vast design space of 3D DNA origami can be sometimes daunting and challenging to identify and implement a structure suitable for different applications. On the other hand, there is a huge opportunity enabled by the freedom and flexibility afforded to construction of 3D DNA origami.

3D DNA origami offers unique features that cannot be achieved by 2D DNA origami beyond the realization of structural components in 3D. DNA origami structures are flexible as DNA itself is a soft material.[23] Therefore, a single layer of DNA array or network has large degrees of freedom in solution. 3D DNA origami with closely packed architecture[15–17] or sophisticated design features such as tensegrity[24] can increase the rigidity of the structures. In the context of molecular integration, flexible structure can be disadvantageous as programmed spatial organization of molecules of interest can be compromised due to flexible structural components that do not keep the intended distance or orientation. Another major feature that distinguishes 3D from 2D architecture is the compartmentalization[25,26] that separates different volumes by limiting accessibility of molecules. A 3D enveloping surface can separate the content inside from other molecules outside in the environment as well as enable substrate channeling between compartments. In fact, these features are found in biology such as cytoskeletons that increase structural integrity and phospholipid membrane that sets the

boundaries of an individual cell. Therefore, 3D DNA origami can achieve reliable and complex molecular integration that may be impossible with 2D DNA origami alone.

In this work, we designed and constructed DNA origami capsule with design features reflecting the success of 2D DNA origami while incorporating unique properties afforded by 3D DNA origami. We focused on the ease of modification for molecular integration in 3D, the modular design for hierarchical assembly, the structural rigidity for reliable spatial organization, and the structural architecture for potential substrate channeling and compartmentalization. We designed a DNA origami barrel that makes up the body of the capsule for molecular integration and a DNA origami cap that compartmentalizes the lumen of the capsule. We then verified the assembly of individual components and their complexes. The DNA origami capsule possesses a simple architecture for addressable sites both inside and outside, a stackable cylindrical barrel at its stem for modular assembly, a multilayer wall for rigidity, and a form-fitting cap for compartmentalization.

## 3.2 Results and Discussion

### 3.2.1 DNA origami barrel

The DNA origami barrel was designed as previously described using the caDNAno software[16] (Figure S1). The wall of the barrel has three layers of DNA duplex to increase the rigidity of the structure. The structure's inner and outer diameters are 46 and 58 nm, respectively, and its height is 24 nm (Figure 1a). We incorporated regularly spaced addressable sites both inside and outside of the barrel structure to facilitate design and implementation of 3D molecular organization. The addressable sites are DNA nick points that can be extended at the 5'-or 3'-end of the staple strand to have to form molecular "pixels". With careful sequence design, the structure can integrate virtually any molecules that can be modified with complementary sequence of DNA oligonucleotide at any of the pixels. There are 48 pixels (4

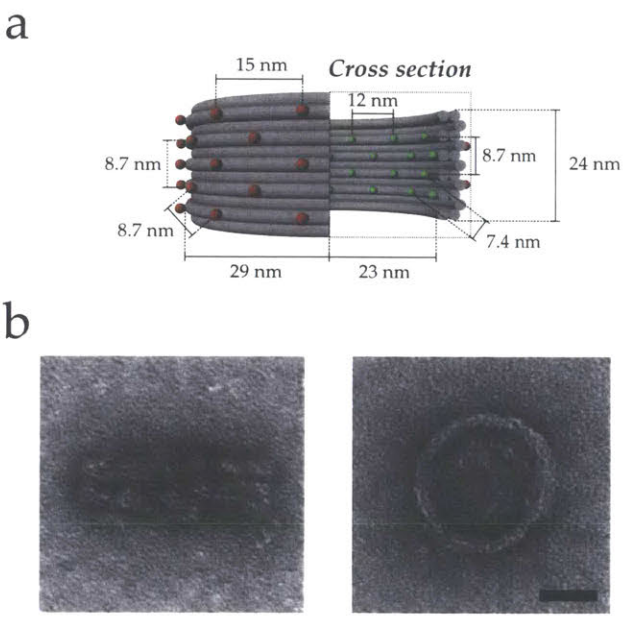


**Figure 1. DNA origami barrel.**
(a) Illustration of DNA origami barrel design. Cylinders represent double-stranded DNA (dsDNA), and the addressable sites via ssDNA overhang are shown as green (inside) or red (outside) spheres. Designed dimensions of the barrel as well as distance between addressable sites are labeled. (b) TEM images of DNA origami barrel. Depending on the way the particle deposits on the grid, the barrel appears rectangular (left) or circular (right). Scale bar = 20 nm.

inner layer DNA helix x 12 pixels per helix) and 60 pixels (5 outer layer DNA helix x 12 pixels per helix) inside and outside of the barrel, respectively. The pixels are organized in a rhombic-like lattice along the inner or outer surface of the barrel at the distance of 7-9 nm to the closest neighbors. Each pixel can be selectively modified to arbitrarily integrate target molecules. The transmission electron microscopy (TEM) image in Figure 2b confirms the correct formation of the DNA origami barrel as intended (also see Figure S2, bottom, for additional TEM images). The drying process during the deposition and negative-stain of the sample on TEM grid resulted in flattening of the barrel when it was placed sideways (Figure 2b, left) due to the large cavity. The analysis of agarose gel electrophoresis (AGE) estimated the folding yield of 87% (Figure S2, top). The unintended aggregation that resulted mostly in dimer formation was the source of error.

### 3.2.2 Modular assembly of DNA origami barrels

We designed two distinct interfaces between the barrels for hierarchical assembly by stacking. For the facile formation of the symmetric DNA capsule with the plane of symmetry placed at the interface between two barrels in the middle, we designed a barrel structure to form homodimer of the structure via DNA hybridization (Figure 2a and S3). This way, we can form a capsule with half the number of unique origami components. If one needs asymmetric spatial organization, simply changing the DNA sequence at the interface can allow the formation of heterodimer instead. The successful formation of homodimer structure was confirmed under TEM (Figure 2b and S4, bottom), and the homodimerization efficiency was estimated to be 75% using AGE (Figure S4, top). While a small amount of monomer did not associate to form the intended homodimer, but the more significant source of error was from unintended aggregation. We have observed some aggregation resulting from monomer folding (Figure S2, top), and it is possible that the larger size of homodimer increases the degree of aggregation since there is a larger surface area to interact with each other, which may contribute to slightly lower yield for the homodimer.

For modular assembly of barrels to increase the size and available pixels for molecular integration of the capsule, we designed the interface between two barrels so the programmed barrels can stack on top of one another in the presence of connecting strands (Figure 2c and S5). Implementing the interface between the homodimer barrel and another barrel allowed the barrel monomer stacking on each available side of the homodimer barrel in the presence of a set of stacking strands, and the assembly was confirmed using TEM (Figure 2d and S6, bottom). The analysis of AGE estimated 48% yield of assembly (Figure S6, top). However, we were able to purify the tetramer using rate-zonal centrifugation[27] (Figure S7), which would allow downstream applications with the pure structure. Potentially any number of barrels can be stacked in any order by tweaking the DNA sequence at the interface to increase the complexity of molecular integration that allow different permutation of assembly as long as sequence design is stringent. This feature could be particularly useful to design and optimize nanofabrication of molecular devices by programming a distinct functional unit in each barrel and testing different organization through modular assembly.

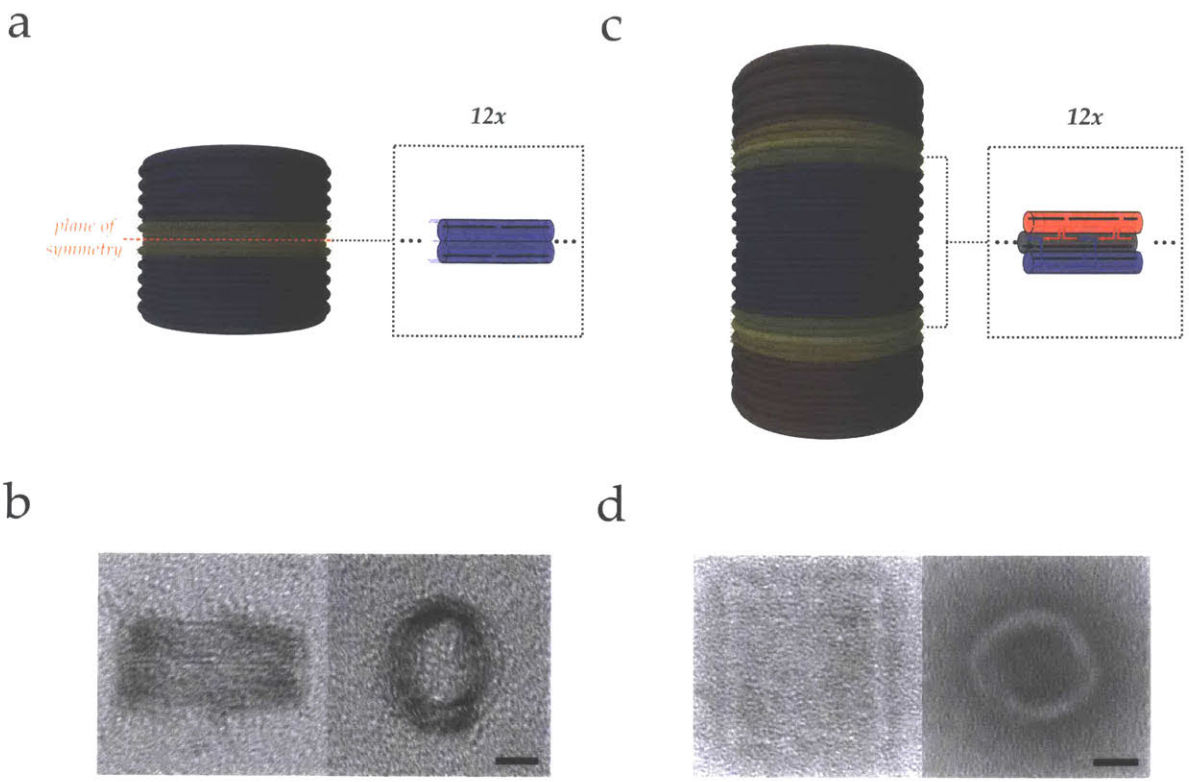


**Figure 2. Modular assembly of DNA origami barrels.** (a) Illustration of homodimer interface between a pair of identical DNA origami barrels. The homodimer is assembled by the formation of double crossover between inner-layer DNA helices at the bottom of two identical DNA origami barrels. (b) TEM images of homodimerized DNA origami barrel. The assembled barrel is twice as tall as monomer. (c) Illustration of stacking interface between homodimer (blue) and two identical barrels (red) to be assembled. Two barrels with ssDNA overhangs at the top (blue; inset) and bottom (red; inset) can stack on top of one another by binding to twelve connecting strands (black; inset) with complementary sequence to the overhangs from both barrels and forming a connecting helix (gray) between the barrels. Because homodimer (blue) is identical at either side, two identical barrels (red) can stack on both sides. (d) TEM images of tetramerized DNA origami barrel. The assembled barrel is about four times taller than monomer. Cylinders in the illustration represent dsDNA, and line and arrowhead represent ssDNA and 3'-end, respectively. Scale bar = 20 nm.

### 3.2.3 DNA origami cap

The cap structure was designed to bring three distinct domains together (Figure 3a and S8). A ring domain has the same architecture as DNA origami barrel for seamless assembly between barrel and cap structures. A square domain was designed by modifying the previously described DNA origami architecture[28] with the largest dimension of 62 nm to fit on top of the ring domain and form a closure with the largest gap dimension of 5 nm at the center. Finally, a

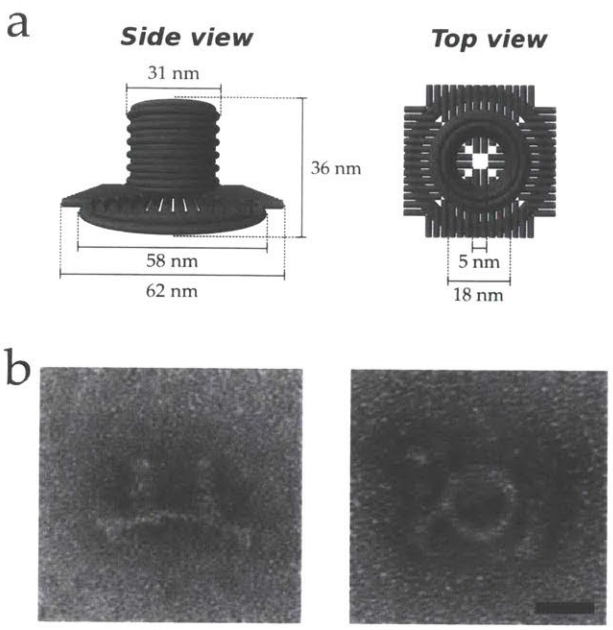


**Figure 3. DNA origami cap.**
(a) Illustration of the DNA origami cap design. The DNA origami cap consists of three distinct domains: ring, square, and mini-barrel. The three domains folded on the same scaffold DNA assemble with one another to from the final conformation of the cap. The dimensions of the structure are labeled. (b) TEM images of the DNA origami cap. Two different orientations of the cap can be observed depending on the way the structure is deposited on the grid. Cylinders in the illustration represent dsDNA. Scale bar = 20 nm.

mini-barrel domain with inner and outer diameters of 31 and 18 nm, respectively, was designed to fit on top of the square domain centering the largest gap to provide more structural rigidity to the square domain that is composed of a single layer of DNA duplexes and also to serve as a visual guide since the other two domains are relatively flat structures. The total height of the assembled structure is designed to be 36 nm. The TEM images confirm the correct folding of each domain as well as assembly of different domains in correct conformation (Figure 3b and S9, bottom). The analysis of AGE estimated 97% yield of folding reaction (Figure S9, top).

### 3.2.4 Assembly of DNA origami capsule

The interface between a barrel and a cap was designed so that addition of each component possessing the interface can self-assemble through DNA hybridization. In particular, we introduced single-stranded DNA (ssDNA) plugs at the interface of the cap by extending the staple strands and complementary sockets at the interface of the barrel by receding the staple strands (Figure 4, left, and S10). In the presence of an excess concentration of DNA origami cap, the tetramer of the DNA origami barrel was completely converted to a DNA origami capsule when observed using AGE, though it also resulted in some aggregation (Figure S11). The TEM images confirm that the formation of a DNA origami capsule (Figure 4, right, and S12). The resulting DNA origami capsule possesses 192 pixels and 240 pixels for molecular integration inside and outside of the lumen. The compartment formed inside the DNA origami capsule could potentially limit the access of molecules larger than 5 nm, which is the largest gap dimension on the structure.

## 3.3 Conclusion

Despite the additional functions enabled by 3D DNA origami technique, the progress towards more robust and complex molecular integration has been hampered due to challenges

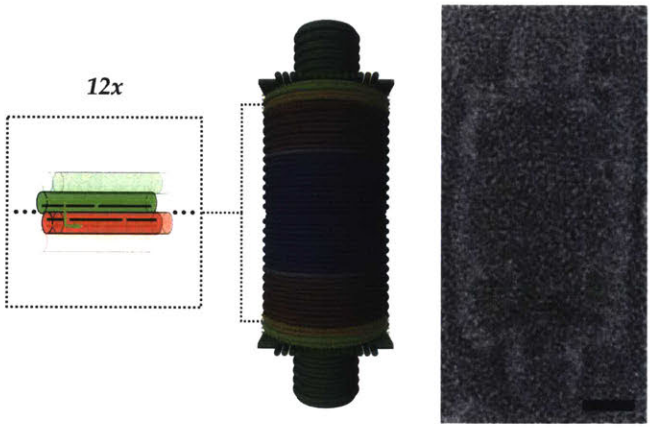


**Figure 4. DNA origami capsule.** The assembly between DNA origami barrels and DNA origami caps results in the DNA origami capsule with compartmentalized cavity. Left: Illustration of DNA origami capsule interface between DNA origami barrel and DNA origami cap. DNA origami cap (green) binds on top of DNA origami barrel (red) by hybridization between ssDNA overhang "plug" from the cap (green; inset) and "socket" (black; inset) that is left single-stranded by receding staple strand of the barrel (red; inset). Right: TEM image of DNA origami capsule. The DNA origami capsule compartmentalizes inner cavity of cylindrical shape with the diameter and height of estimated 46 and 109 nm, respectively. Cylinders in the illustration represent dsDNA, and line and arrowhead represent ssDNA and 3'-end, respectively. Scale bar = 20 nm.

in design and implementation of suitable architecture for varying applications. We identified features attributing to the success of 2D DNA origami as well as advantageous features relevant to the molecular integration only possible through 3D DNA origami and produced a potential platform that can serve as a 3D molecular breadboard. The rhombic-like lattice pattern of addressable sites inside and outside of the capsule provide a 3D canvas that can be easily visualized to design and implement complex molecular integration. The modular design allows complex nanofabrication through hierarchical assembly that increases size of the breadboard in both the physical dimension and the number of addressable sites. The multi-layer and multi-domain designs increase the rigidity of the structure to keep the intended distance between the molecules placed on the DNA origami capsule. Finally, the compartmentalization can potentially allow the study of the effect of confinement or substrate channeling for development of functional nanodevices. Further study is required to quantitatively analyze the molecular integration and verify the effectiveness of compartmentalization in this platform. Moreover, additional architecture inside the capsule that allows the formation of network of addressable sites that fills the cavity would increase the complexity of possible molecular integration even further. Nonetheless, the developed platform for 3D molecular integration creates opportunities for facile design and implementation of nanodevices with complex behavior unachievable using 2D DNA origami structures.

## 3.4 Acknowledgement

Leo Chou acknowledges support from Banting Fellowship and NSERC. This material is based upon work supported by the National Science Foundation Graduate Research Fellowship (Jaeseung Hahn) under Grant No. 1122374. We thank the Wyss Institute for support of this project.

## 3.5 References

1. Aldaye, F. A.; Palmer, A. L.; Sleiman, H. F. Assembling Materials with DNA as the Guide. *Science (New York, N.Y.)* **2008**, *321*, 1795–9.
2. Pinheiro, A. V.; Han, D.; Shih, W. M.; Yan, H. Challenges and Opportunities for Structural DNA Nanotechnology. *Nature Nanotechnology* **2011**, *6*, 763–772.
3. Wang, P.; Meyer, T. A.; Pan, V.; Dutta, P. K.; Ke, Y. The Beauty and Utility of DNA Origami. *Chem* **2017**, *2*, 359–382.
4. Samanta, A.; Zhou, Y.; Zou, S.; Yan, H.; Liu, Y. Fluorescence Quenching of Quantum Dots by Gold Nanoparticles: A Potential Long Range Spectroscopic Ruler. *Nano Letters* **2014**, *14*, 5052–5057.
5. Hemmig, E. A.; Creatore, C.; Wünsch, B.; Hecker, L.; Mair, P.; Parker, M. A.; Emmott, S.; Tinnefeld, P.; Keyser, U. F.; Chin, A. W. Programming Light-Harvesting Efficiency Using DNA Origami. *Nano Letters* **2016**, *16*, 2369–2374.
6. Maune, H. T.; Han, S.; Barish, R. D.; Bockrath, M.; III, W. A. G.; Rothemund, P. W. K.; Winfree, E. Self-Assembly of Carbon Nanotubes into Two-Dimensional Geometries Using DNA Origami Templates. *Nature Nanotechnology* **2010**, *5*, 61–66.
7. Voigt, N. V.; Tørring, T.; Rotaru, A.; Jacobsen, M. F.; Ravnsbæk, J. B.; Subramani, R.; Mamdouh, W.; Kjems, J.; Mokhir, A.; Besenbacher, F.; Gothelf, K. V. Single-Molecule Chemical Reactions on DNA Origami. *Nature Nanotechnology* **2010**, *5*, 200–203.
8. Fu, J.; Liu, M.; Liu, Y.; Woodbury, N. W.; Yan, H. Interenzyme Substrate Diffusion for an Enzyme Cascade Organized on Spatially Addressable DNA Nanostructures. *Journal of the American Chemical Society* **2012**, *134*, 5516–5519.
9. Dai, M.; Jungmann, R.; Yin, P. Optical Imaging of Individual Biomolecules in Densely Packed Clusters. *Nature Nanotechnology* **2016**, *11*, 798–807.
10. Ke, Y.; Lindsay, S.; Chang, Y.; Liu, Y.; Yan, H. Self-Assembled Water-Soluble Nucleic Acid Probe Tiles for Label-Free RNA Hybridization Assays. *Science* **2008**, *319*, 180–183.
11. Subramanian, H. K. K.; Chakraborty, B.; Sha, R.; Seeman, N. C. The Label-Free Unambiguous Detection and Symbolic Display of Single Nucleotide Polymorphisms on DNA Origami. *Nano Letters* **2011**, *11*, 910–913.
12. Li, Z.; Liu, M.; Wang, L.; Nangreave, J.; Yan, H.; Liu, Y. Molecular Behavior of DNA Origami in Higher-Order Self-Assembly. *Journal of the American Chemical Society* **2010**, *132*, 13545–52.
13. Rothemund, P. W. K. Folding DNA to Create Nanoscale Shapes and Patterns. *Nature* **2006**, *440*, 297–302.
14. Fu, T. J.; Seeman, N. C. DNA Double-Crossover Molecules. *Biochemistry* **1993**, *32*, 3211–20.
15. Ke, Y.; Douglas, S. M.; Liu, M.; Sharma, J.; Cheng, A.; Leung, A.; Liu, Y.; Shih, W. M.; Yan,

H. Multilayer DNA Origami Packed on a Square Lattice. *Journal of the American Chemical Society* **2009**, *131*, 15903–8.

16. Douglas, S. M.; Dietz, H.; Liedl, T.; Högberg, B.; Graf, F.; Shih, W. M. Self-Assembly of DNA into Nanoscale Three-Dimensional Shapes. *Nature* **2009**, *459*, 414–8.
17. Ke, Y.; Voigt, N. V.; Gothelf, K. V.; Shih, W. M. Multilayer DNA Origami Packed on Hexagonal and Hybrid Lattices. *Journal of the American Chemical Society* **2012**, *134*, 1770–1774.
18. Han, D.; Pal, S.; Nangreave, J.; Deng, Z.; Liu, Y.; Yan, H. DNA Origami with Complex Curvatures in Three-Dimensional Space. *Science* **2011**, *332*, 342–346.
19. Han, D.; Pal, S.; Yang, Y.; Jiang, S.; Nangreave, J.; Liu, Y.; Yan, H. DNA Gridiron Nanostructures Based on Four-Arm Junctions. *Science* **2013**, *339*, 1412–1415.
20. Zhang, F.; Jiang, S.; Wu, S.; Li, Y.; Mao, C.; Liu, Y.; Yan, H. Complex Wireframe DNA Origami Nanostructures with Multi-Arm Junction Vertices. *Nature Nanotechnology* **2015**, *10*, 779–784.
21. Veneziano, R.; Ratanalert, S.; Zhang, K.; Zhang, F.; Yan, H.; Chiu, W.; Bathe, M. Designer Nanoscale DNA Assemblies Programmed from the Top Down. *Science* **2016**, *352*, 1534–1534.
22. Benson, E.; Mohammed, A.; Gardell, J.; Masich, S.; Czeizler, E.; Orponen, P.; Högberg, B. DNA Rendering of Polyhedral Meshes at the Nanoscale. *Nature* **2015**, *523*, 441–444.
23. Kim, D.-N.; Kilchherr, F.; Dietz, H.; Bathe, M. Quantitative Prediction of 3D Solution Shape and Flexibility of Nucleic Acid Nanostructures. *Nucleic Acids Research* **2012**, *40*, 2862–2868.
24. Liedl, T.; Högberg, B.; Tytell, J.; Ingber, D. E.; Shih, W. M. Self-Assembly of Three-Dimensional Prestressed Tensegrity Structures from DNA. *Nature nanotechnology* **2010**, *5*, 520–4.
25. Andersen, E. S.; Dong, M.; Nielsen, M. M.; Jahn, K.; Subramani, R.; Mamdouh, W.; Golas, M. M.; Sander, B.; Stark, H.; Oliveira, C. L. P.; Pedersen, J. S.; Birkedal, V.; Besenbacher, F.; Gothelf, K. V; Kjems, J. Self-Assembly of a Nanoscale DNA Box with a Controllable Lid. *Nature* **2009**, *459*, 73–76.
26. Zhao, Z.; Fu, J.; Dhakal, S.; Johnson-Buck, A.; Liu, M.; Zhang, T.; Woodbury, N. W.; Liu, Y.; Walter, N. G.; Yan, H. Nanocaged Enzymes with Enhanced Catalytic Activity and Increased Stability against Protease Digestion. *Nature Communications* **2016**, *7*, 10619.
27. Lin, C.; Perrault, S. D.; Kwak, M.; Graf, F.; Shih, W. M. Purification of DNA-Origami Nanostructures by Rate-Zonal Centrifugation. *Nucleic Acids Research* **2013**, *41*, e40–e40.
28. Tikhomirov, G.; Petersen, P.; Qian, L. Programmable Disorder in Random DNA Tilings. *Nature Nanotechnology* **2017**, *12*, 251–259.

## 3.6 Supplementary information

### SI1. Detailed design and characterization of DNA origami structures

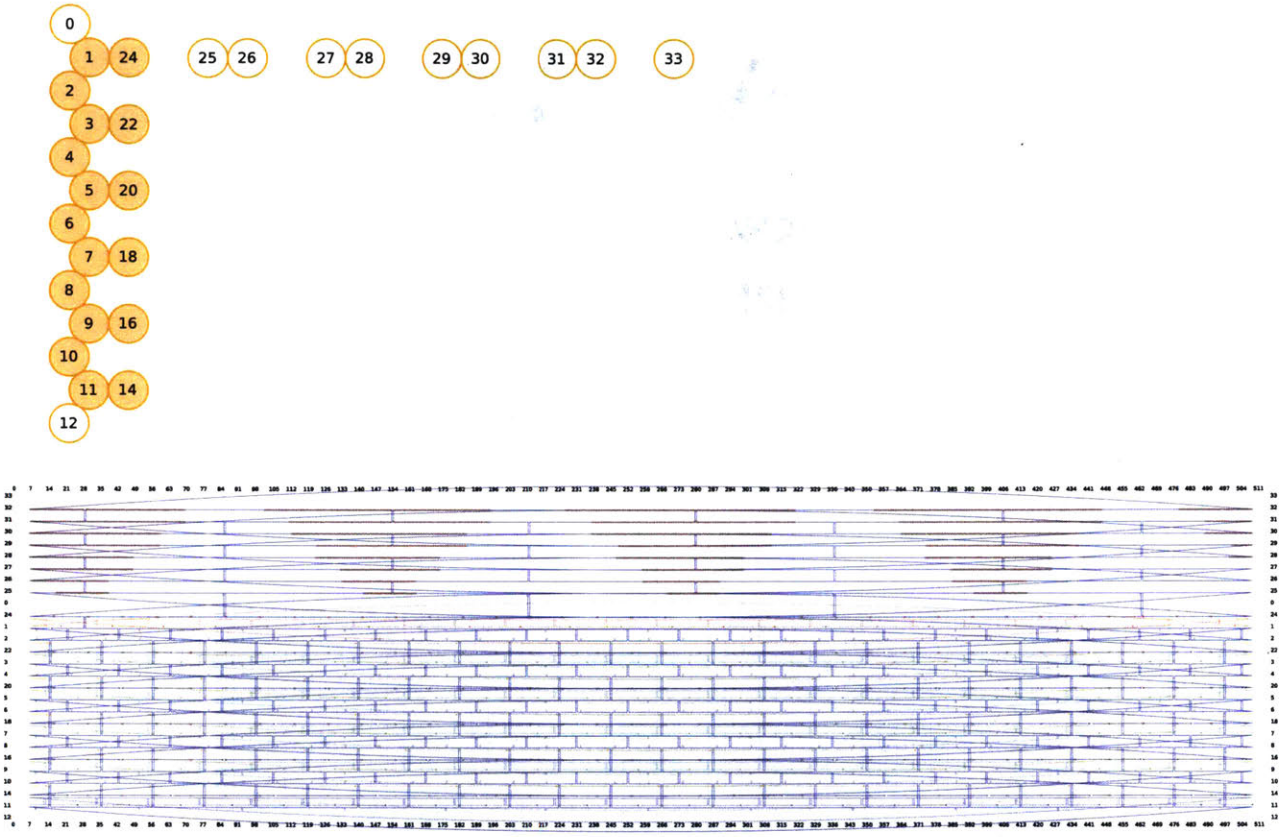


**Figure S1. caDNAno design of DNA origami barrel.** Top: Organization of helices into three-layer architecture of the barrel. Only the filled-in helices have double-stranded DNA (dsDNA). Blank helices either have no scaffold or left single-stranded. Bottom: Scaffold and staple strand organization. Addition (loop) and deletion (x) of DNA bases result in bending of structure that form a shape of cylindrical barrel.

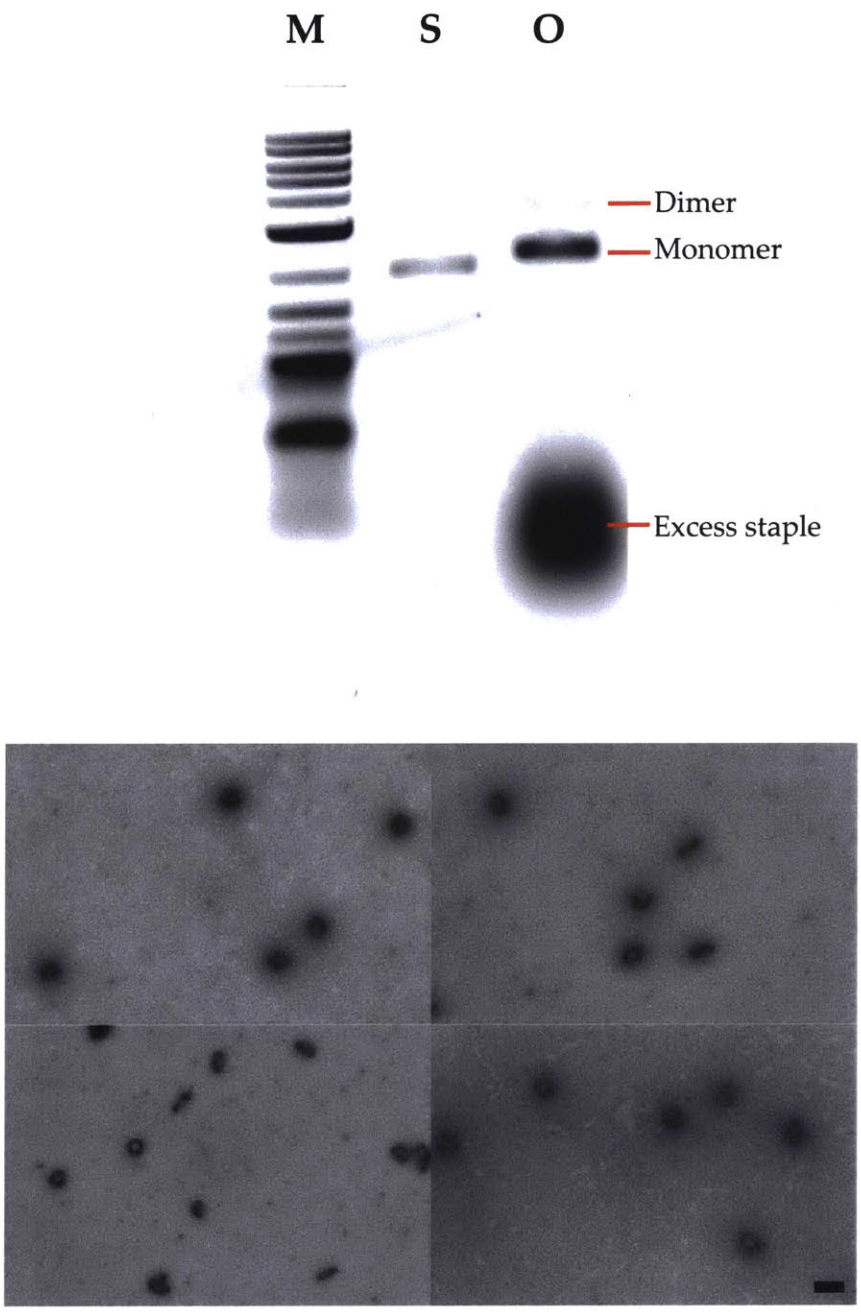


**Figure S2. Characterization of DNA origami barrel.** Top: Agarose gel electrophoresis (AGE) of DNA origami barrel. M = 2-log ladder, S = p8634 scaffold, O = crude folding reaction of DNA origami barrel. Bottom: TEM images of DNA origami barrel. Scale bar = 100 nm.

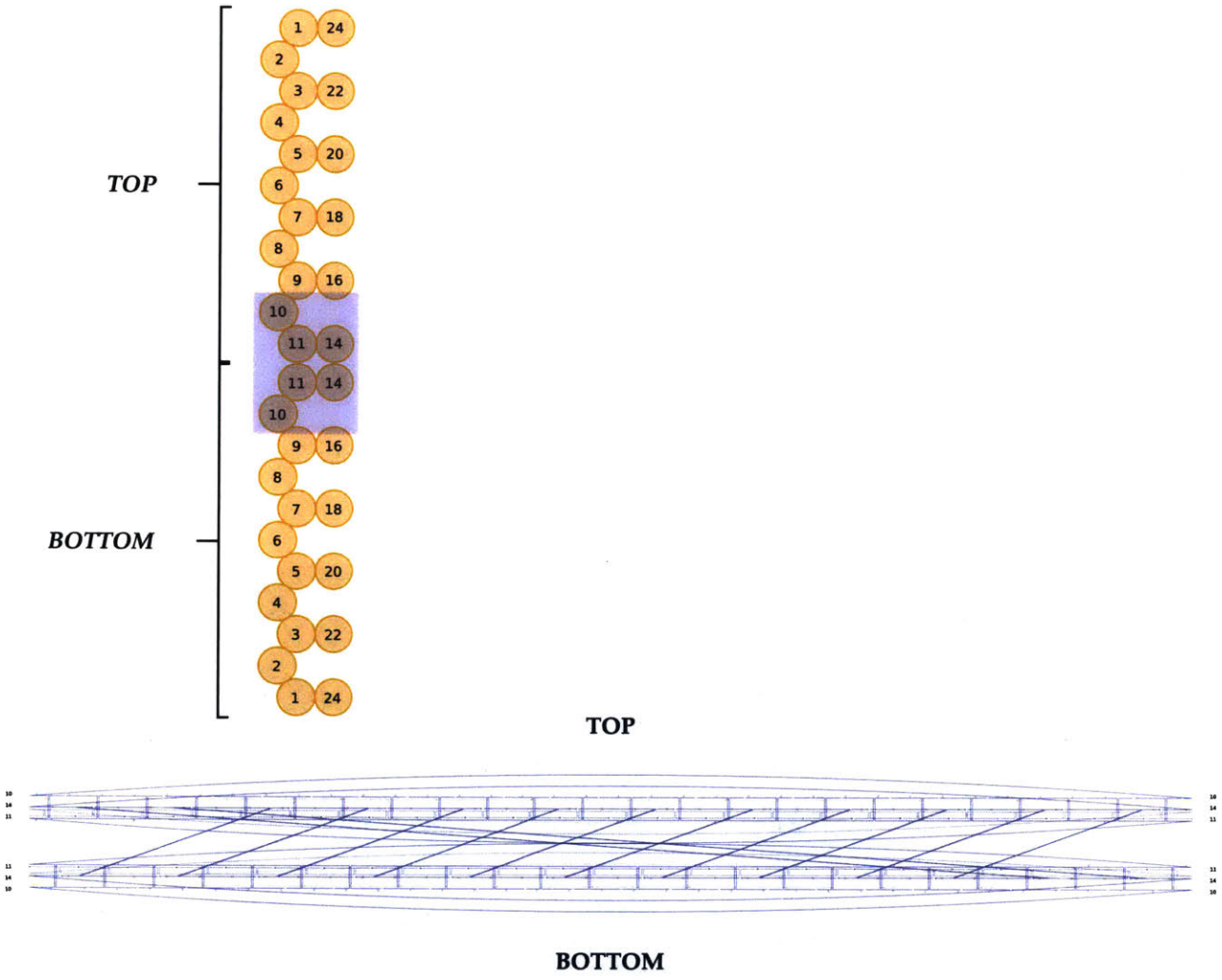


**Figure S3. caDNAno design of homodimer interface between identical DNA origami barrel.** Top: Organization of helices symmetric with respect to the interface between two identical DNA origami barrels. Two sets of three helices closest to the interface are highlighted to note that these helices are shown below. Bottom: Scaffold and staple strand organization at the interface of homodimer. A pair of inner-layer helices (helices 14) exchange staple strands and form double crossover to homodimerize the barrels.

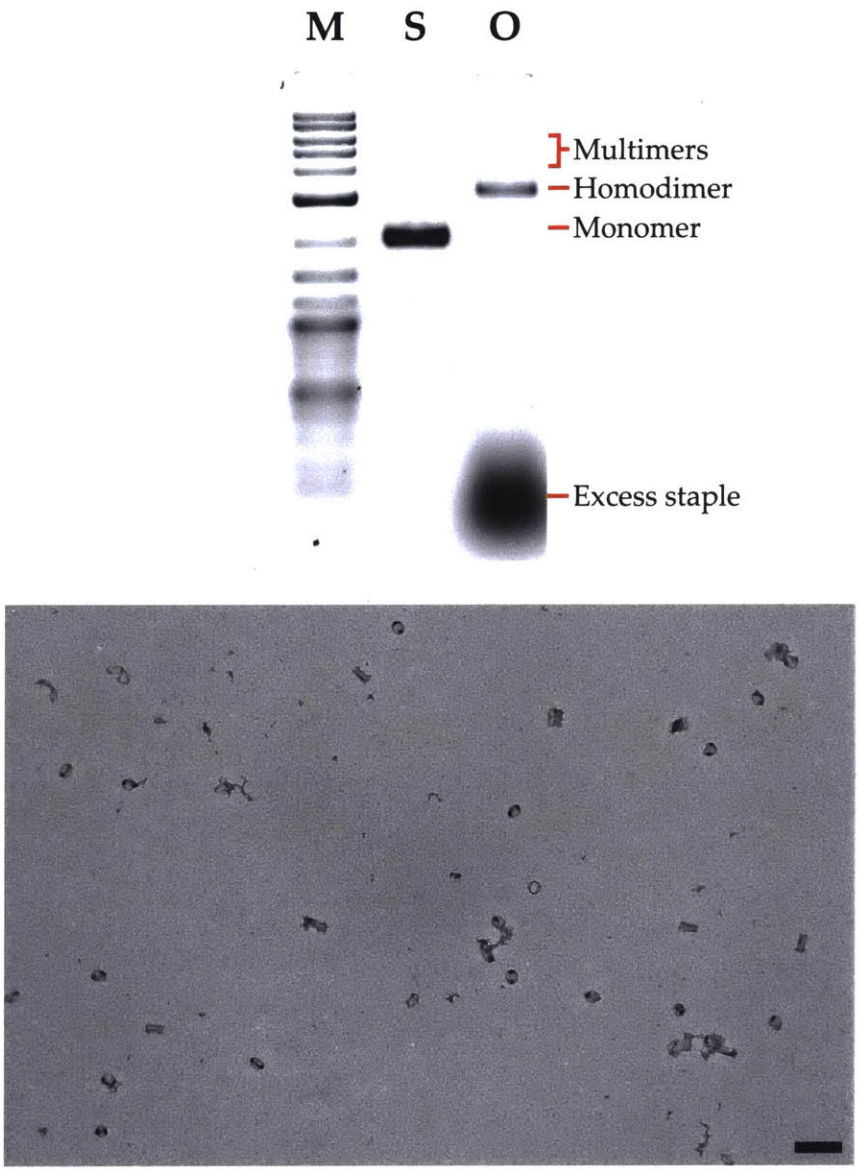


**Figure S4. Characterization of homodimerization of DNA origami barrels.** Top: AGE of the homodimer of the barrels. M = 2-log ladder, S = p8634 scaffold, O = crude folding reaction of homodimerized DNA origami barrels. Bottom: TEM image of the homedimerized barrels. Malformed homodimer (top-left corner) can be spotted sometimes, but most structures are homodimerizaed as intended. Scale bar = 200 nm.

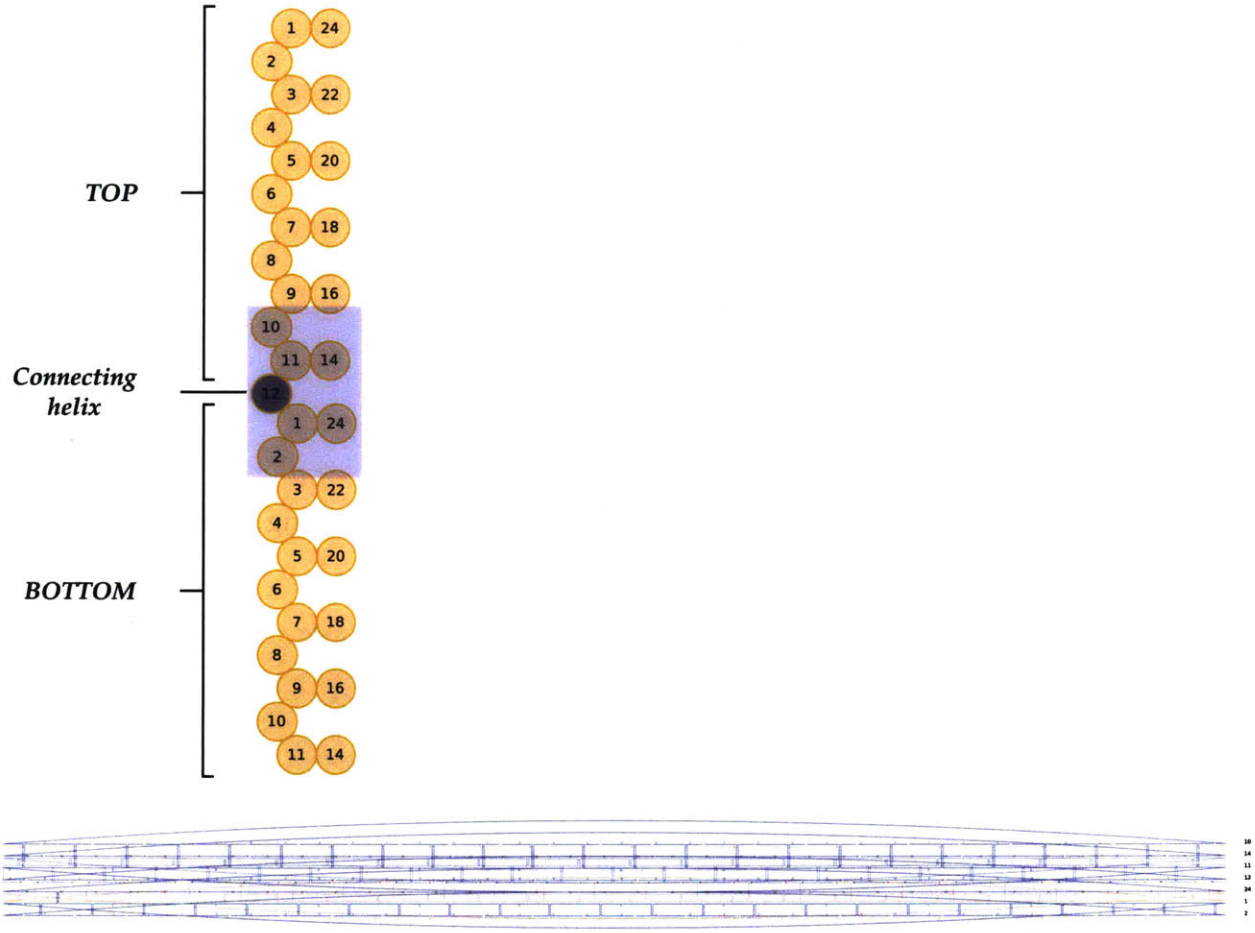


**Figure S5. caDNAno design of stacking interface between two DNA origami barrels.** Top: Organization of helices for two DNA origami barrels (TOP and BOTTOM) and their interface. Two sets of three helices closest to the interface and the connecting helix are highlighted to note that these helices are shown below. Bottom: Scaffold and staple strand organization at the stacking interface between the barrels. A pair of middle-layer helices (helices 11 from TOP barrel and 1 from BOTTOM barrel) has ssDNA overhangs that are complementary to 12 connecting strands, and the resulting hybridization form connecting helix (helix 12; gray) to stack the barrels on top of one another.

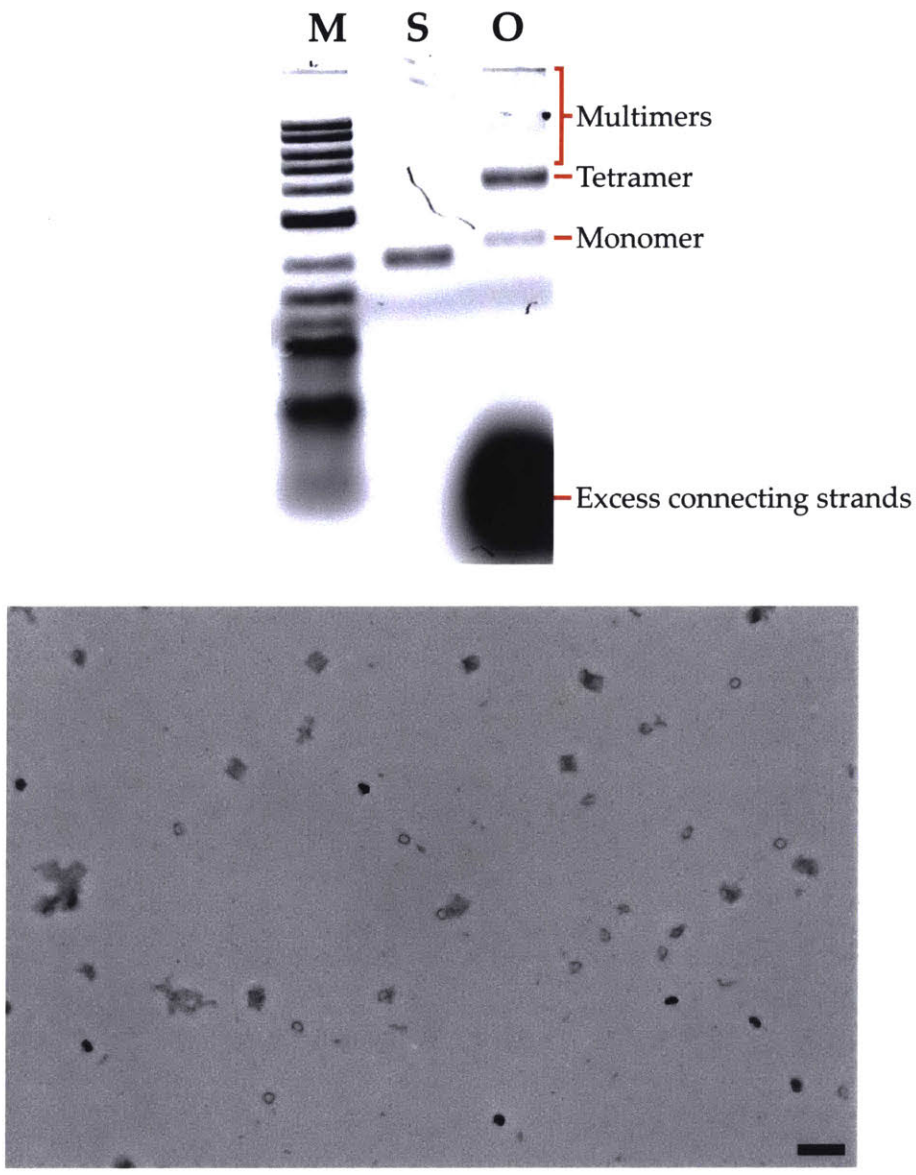


**Figure S6. Characterization of stacking interface of DNA origami barrels.** Top: AGE of the tetramer of the barrels formed by stacking two identical barrels on each end of the homodimerized barrels. M = 2-log ladder, S = p8634 scaffold, O = crude assembly reaction between homodimerized DNA origami barrels and stacking barrels in the presence of excess connecting strands. Bottom: TEM image of the tetramerized barrels. Scale bar = 200 nm.

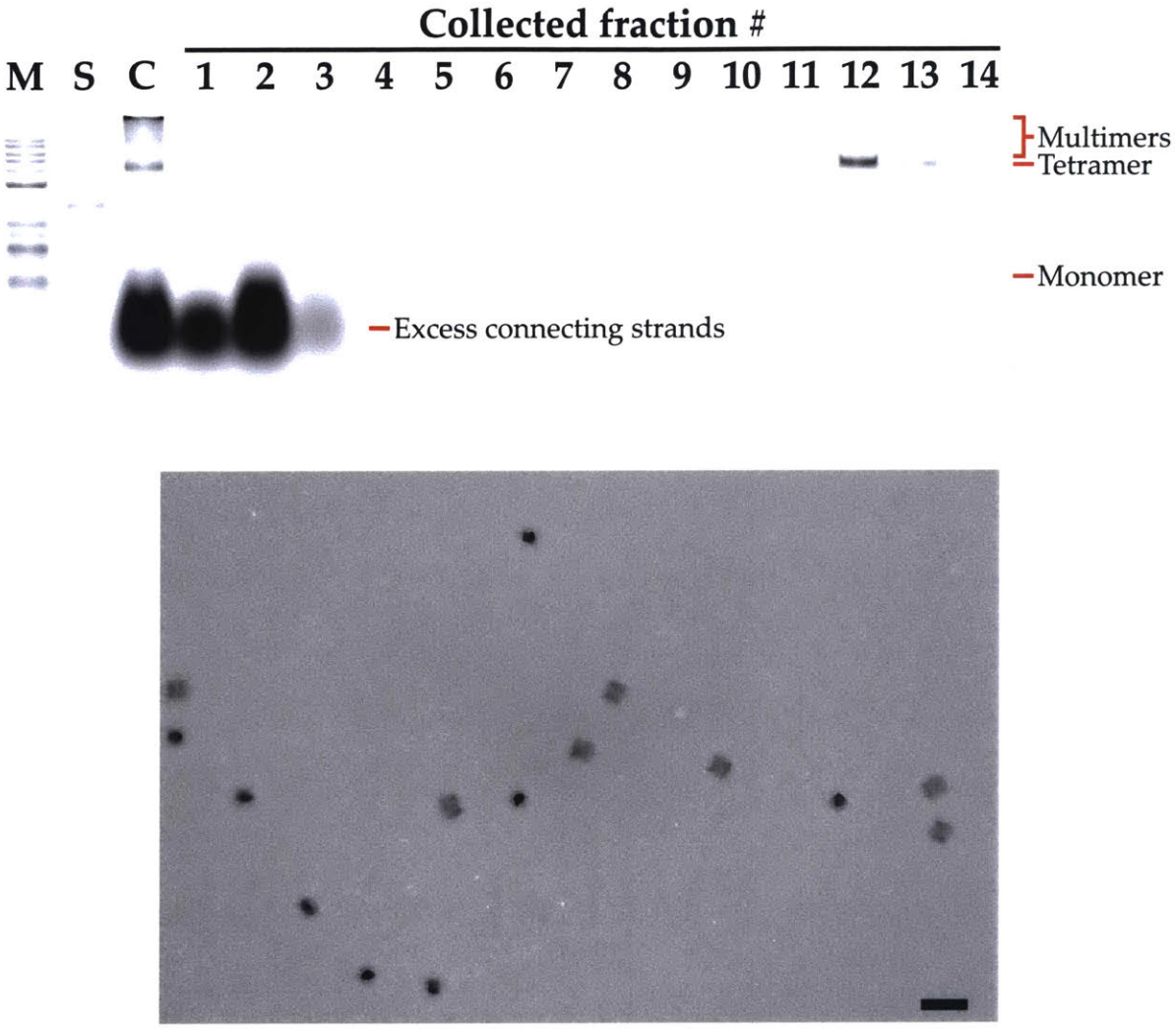


**Figure S7. Purification of tetramerized DNA origami barrels.** Top: AGE of the fractions of glycerol gradient after centrifugation. Fraction 12 is enriched with tetramerized DNA origami barrels. M = 2-log ladder, S = p8634 scaffold, C = crude assembly reaction between homodimerized DNA origami barrels and stacking barrels in the presence of excess connecting strands. Bottom: TEM image of the purified tetramers of DNA origami barrels. Scale bar = 200 nm.

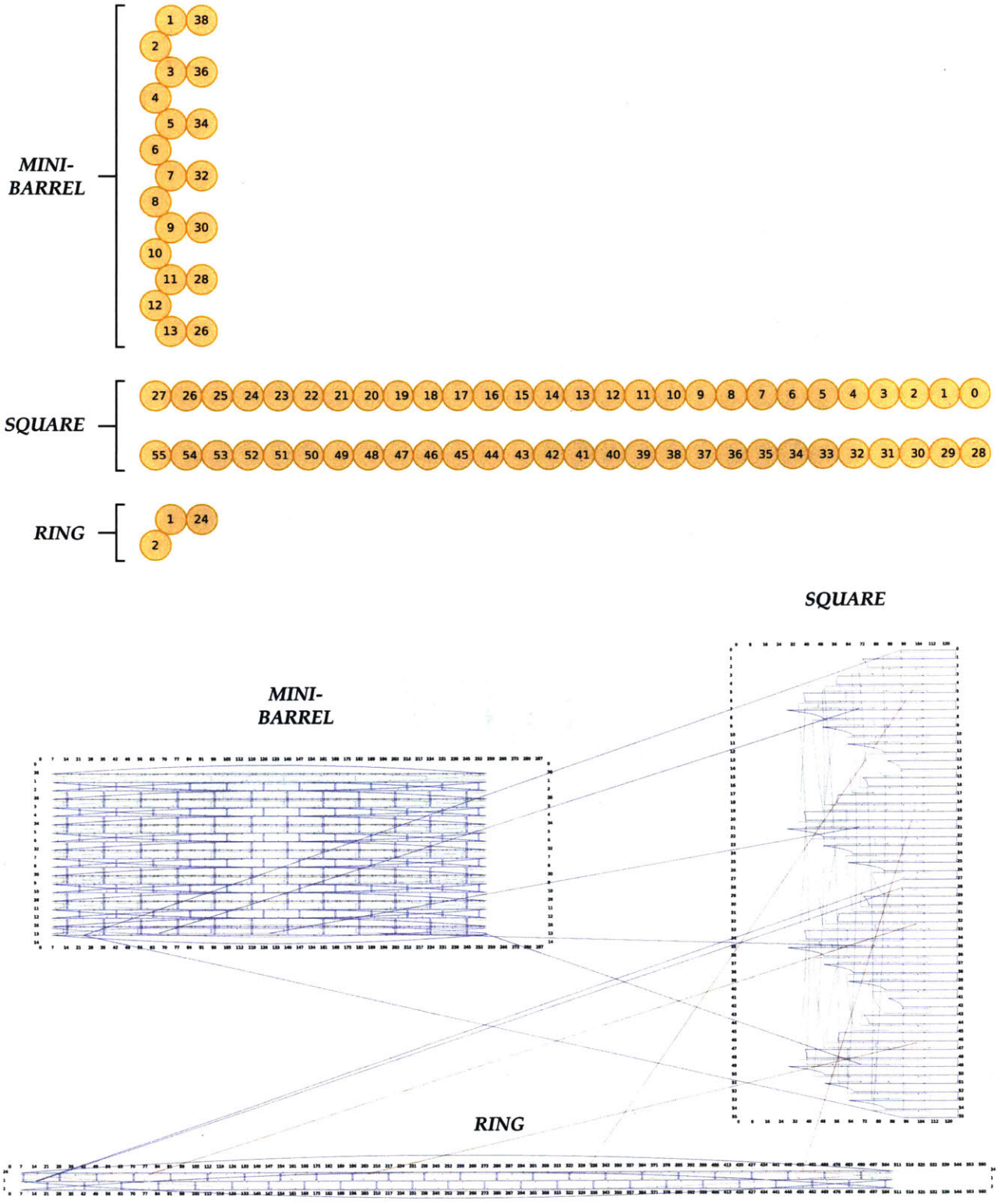


**Figure S8. caDNAno design of DNA origami cap.** Top: Organization of helices of DNA origami cap. Bottom: Scaffold and staple strand organization of the cap.

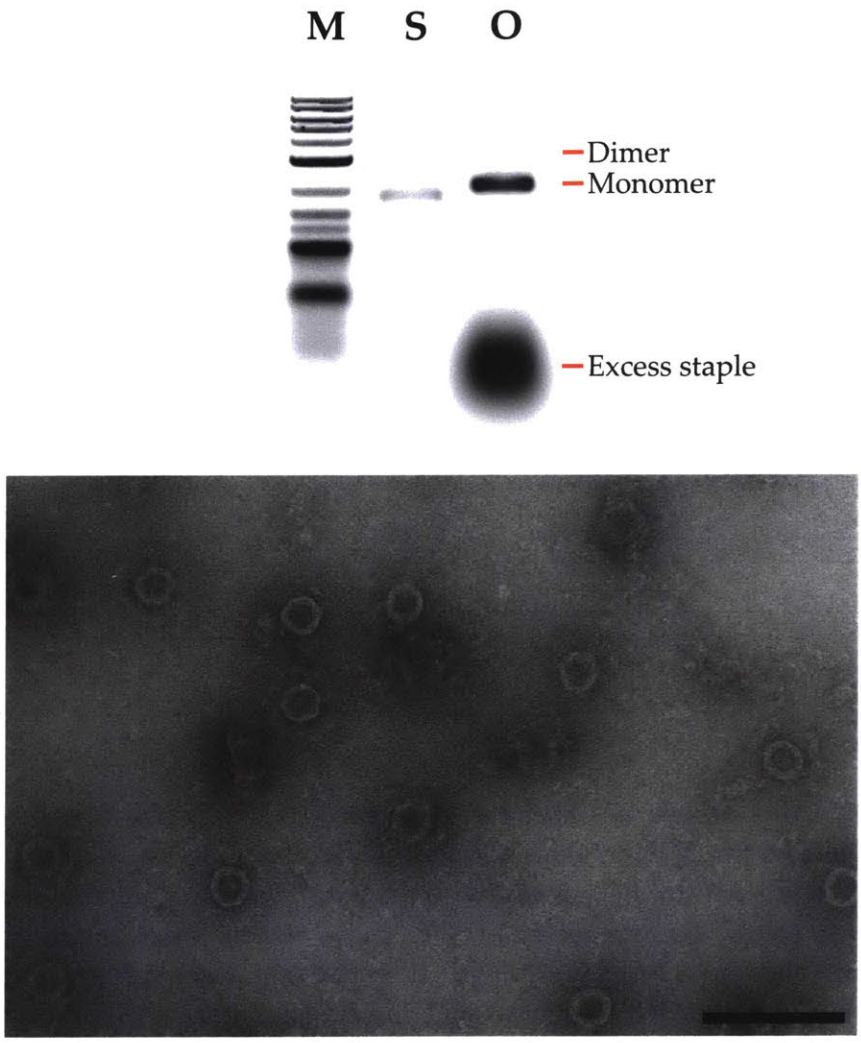


**Figure S9. Characterization of DNA origami cap.** Top: Agarose gel electrophoresis (AGE) of DNA origami cap. M = 2-log ladder, S = p8634 scaffold, O = crude folding reaction of DNA origami cap. Bottom: TEM image of DNA origami cap. Scale bar = 100 nm.

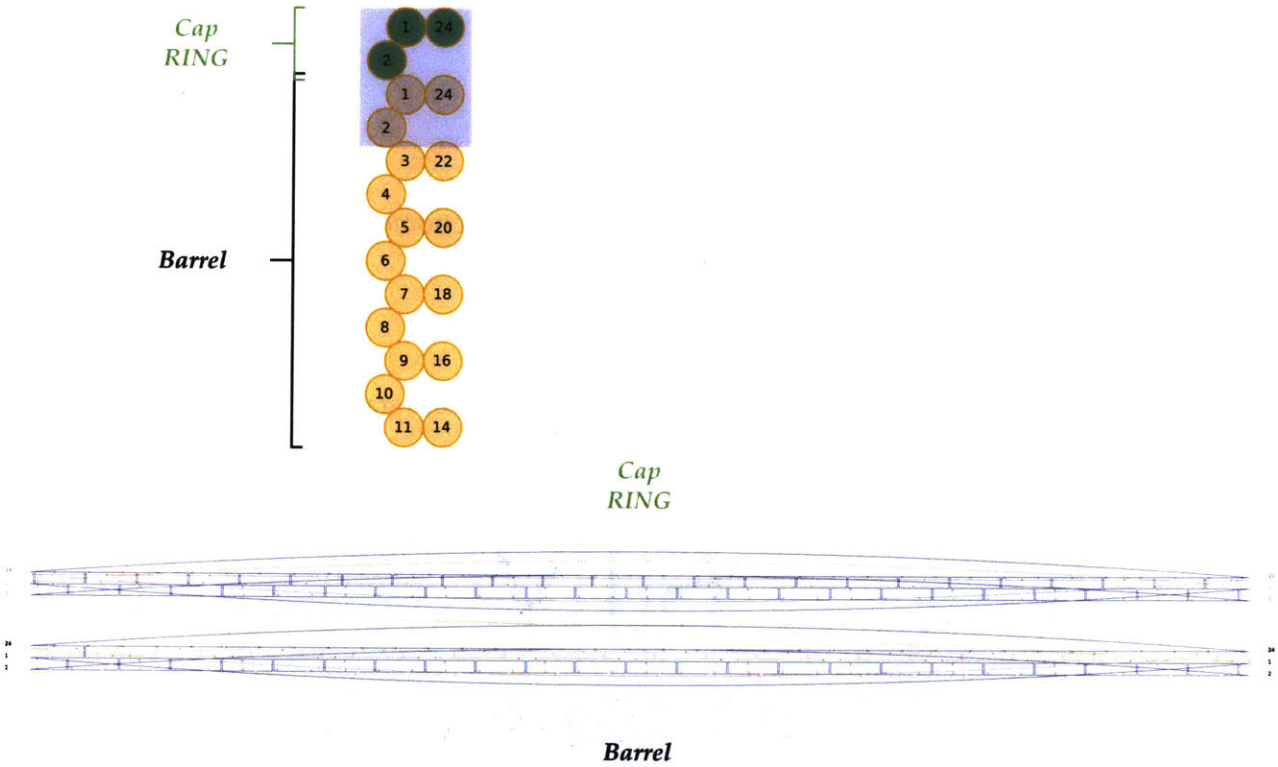


**Figure S10. caDNAno design of interface between DNA origami barrel and cap.** Top: Organization of helices for DNA origami barrels and cap (only the ring domain is shown) and their interface. Two sets of three helices closest to the interface are highlighted to note that these helices are shown below. Bottom: Scaffold and staple strand organization at the interface between the barrel and cap. 12 ssDNA "plugs" from the ring domain (helix 2; green) of DNA origami cap binds to the 12 ssDNA "sockets" on DNA origami barrel (helix 2; orange).

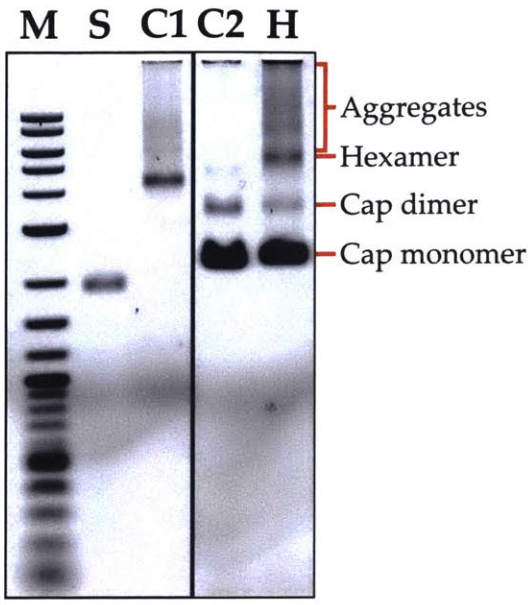


**Figure S11. AGE of DNA origami capsule assembly.** Different lanes from the same gel were cropped and put together to omit irrelevant lanes. M = 2-log ladder, S = p8634 scaffold, C1 = purified tetramer of DNA origami barrels using rate-zonal centrifugation, C2 = purified DNA origami cap using polyethylene glycol (PEG) precipitation, H = crude assembly reaction between tetramerized DNA origami barrels in the presence of excess DNA origami cap. Hexamer band is the assembled DNA origami capsule.

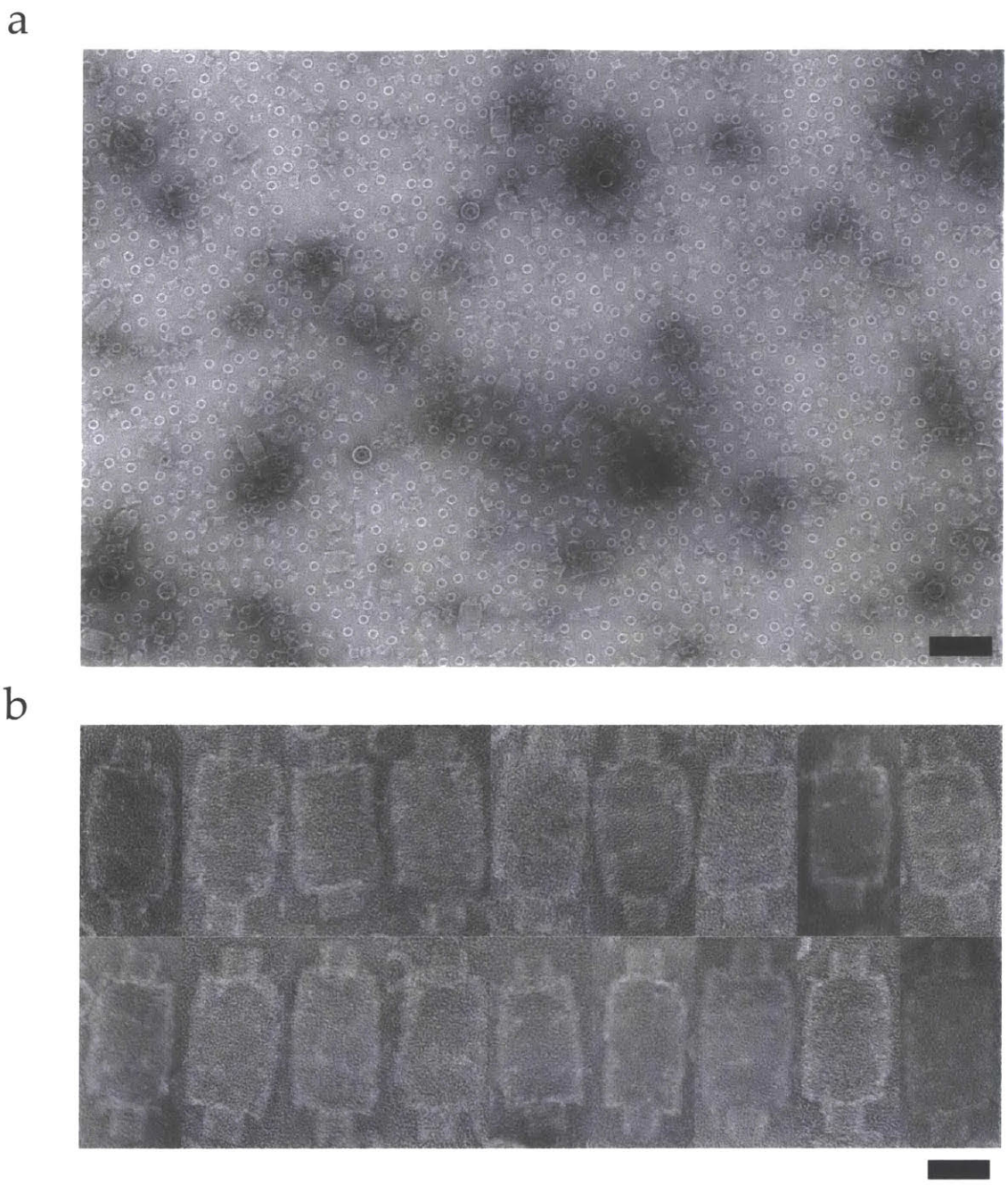


**Figure S12. TEM of DNA origami capsule assembly.** (a) Low-magnification image showing DNA origami capsule structures distributed among excess DNA origami cap structures. Scale bar = 200 nm. (b) Collage of high-magnification images of DNA origami capsule. Scale bar = 50 nm.

## SI2. Materials and methods

### SI2.1. Chemicals and supplies

10x TBE buffer was purchased from National Diagnostics. PCR tubes were purchased from USA Scientific. SYBR Safe was purchased from Life Technologies Corporation. UltraPure™ Agarose was purchased from Thermo Fisher Scientific. Glycerol, PEG 8000, Tris base, EDTA, Tween20, magnesium chloride, and sodium chloride were purchased from Sigma-Aldrich. Sera-Mag™ Magnetic SpeedBeads™ (carboxylated, 1 μm, 3 EDAC/PA5) was purchased from GE Healthcare Life Sciences. Carbon formvar grids and uranyl formate were purchased from Electron Microscopy Sciences. Amicon Ultra filtration devices were purchased from Fisher Scientific. DNA gel extraction spin column was purchased from BIO-RAD.

### SI2.2. Scaffold prep

The p8634 scaffold strand was produced from M13 phage replication in E. coli, as described previously[SI-R1].

### SI2.3. Staple strand

The sequences were generated using the caDNAno software by applying p8634 scaffold to each design of DNA origami structures (see Tables below). All DNA strands were purchased from Integrated DNA Technologies (IDT) with standard desalting option. The DNA strands were shipped dry and suspended at 100 nM in Millipore purified water and stored at -20°C.

**SI Table 1. Staple list for DNA origami barrel**

| Subpool | # | Sequence |
|---|---|---|
| IM | 1 | ACGTGGACGGCCCGAGTCAGAGGGCAGTCGAACAGCTAAAGA |
| IM | 2 | TGAGGCCGACCGGTACTACGGAAGCGTCGCGTAACATCAG |
| IM | 3 | ATTTTCGGACGGCAACCACACCTTTCGCACCATTAAATCGGC |
| IM | 4 | TTAAAGCGACGAAAGGTGAACACGCATCACCGGAACCTCA |
| IM | 5 | ACCAGGCGCTCGCCACGGAACTGCTAGGCAATACATGTCAGT |
| IM | 6 | TCATAGTCGCGGAGACCGCCAAGGTGGATGTATCAAGCCC |
| IM | 7 | TGATACCGGTGCGGGAGAGCTATACGATTATGAATTTCAGCT |
| IM | 8 | CAACCTACGAACAGGTCGCTGAACCCATTATATTCGGCAC |
| IM | 9 | TGGCTGACGTGACGTGTGCCTAGCTCGCAACCAGCGATAGGC |
| IM | 10 | TAAAACGCCAGGAGGAACACTACCCGCTATCAACGGTTAA |
| IM | 11 | ACTGCGGATACTGCAAGTCTCGCCCGACAAGATTTAGCCAAT |
| IM | 12 | GTACCTTGCAAACGTAGCGGCCCATCATTCAGAAAAGAGA |
| IM | 13 | GAAAAGGTTAACCGTCTCGGGCGTGTGATACTTAATTGAGCT |
| IM | 14 | GTAAAGAGCCGGGAGCCGGCGCGATCGGTACAGGCTGTAG |
| IM | 15 | ATTGTATAAGAAGGCAGGCATACGTACGTTTGATATTGGAAG |
| IM | 16 | GGGCGCATGGGCCACTGACTGCAGGTAGTTAAATTTAGAT |
| IM | 17 | CCCAGTCACGCGCACCCAATTGGCGAAATCCCTCAGGGTTTT |
| IM | 18 | CTGGTCGCAGTCTACCGTTCACAGTGCGCACCCTCGACGC |
| IM | 19 | GAGAACGACGGGCGCCCATGGCCCTAACTTTATCAGTACCAG |
| IM | 20 | GGCAGTTTGAGTGGGCACCTCATTGAGGGCAAAATTCTGC |

| IM | 21 | ATCGGGTTGGCGTGAGCGTGCTAGTGCAAATATTACGCAAAC |
|---|---|---|
| IM | 22 | GGTTTATCGGCCGCGGCTCCATCCCAGATAGCTGAATGAA |
| IM | 23 | TGGATCCCGCCAGGCTGCTATGTAAATGAACTGATACGAGAA |
| IM | 24 | CGGTTTGCCTTTCACAGACGATACATCGTGTGAAAAGAGG |
| IM | 25 | CAGTTTGGCACGAGCGGTCCGCGTCGCATCTTCACCGTGTTC |
| IM | 26 | AGAATCCGAGACGCAATACTCACGATAACCCGCCGACGCC |
| IM | 27 | AGCGTCAGGGATGTTCGCCGCTCCTCGGTGATCACCGCCTTT |
| IM | 28 | CTTGATAACGCACGATGCTCCGACGTACCACCACCTTGGC |
| IM | 29 | AGGATTAGACACGTCAGCTGGGTCAAGGTTTGATACAAGAGA |
| IM | 30 | CAACGCCCTCAATGCTCCGGTGGCGAGACAGGAGGAACTA |
| IM | 31 | TTGCTTTCTCGGCGCATCGATGGGCTGTTGGGATTTTTCAGC |
| IM | 32 | TAAAATACTGACTGATAGCACGCGTGGAGAGGCTTACGGG |
| IM | 33 | ATGAACGGCTGATGCGCGCACCAACGGTCGAGCGCGAGACAG |
| IM | 34 | AGGACGTACTCGTGCTTCCCGGGCAGTGGCTGCTCCAGTC |
| IM | 35 | GTAAAATGTGTCCGGTAGAAATCAATGCTGCATTCAATAATA |
| IM | 36 | AGCAAACGGGTCTTTACGCCGCTGTCTTTGACCATCCGGA |
| IM | 37 | TTAGCTATGTCTTCATCGTGCCGCTTTCTCTAATGCTCCTGT |
| IM | 38 | TTTAAATAGGGCCGATTCGAGGGCCGATAGAATTATATAT |
| IM | 39 | GATAATCATCATGCCGCCCATGAGTCCGGCCTAGCTGCGGTT |
| IM | 40 | GTAATGGGGACGTCACTGAGGTGCCTGAAATCAGCTGACC |
| IM | 41 | GGCGATTAGAGCGCTGACCGCCTAGACTGAACTCCAGTGCAA |
| IM | 42 | GTGGCGAACGTCGGATAACAGTTACCAGTTAACCATGAGT |
| IM | 43 | AACCAGCAACCACCGGCAGCCGCGGTACTCAGGTTCGAAAGA |
| IM | 44 | CTGCACTGTCGTGGATGACGGGTTGGATCAACGAGAAGCA |
| IM | 45 | TGTAGTGTTTCATTGAGCTCGTCTAACGGGGGTCAATGAGTC |
| IM | 46 | ATAGAGTCCGCCCTGAAAAGAGGCCCCATACATTGTAGAT |
| IM | 47 | TGATAAATGTGCTTAGTTTGTCCGCAGCCGATTATTAGGAGA |
| IM | 48 | TAATGAAATGGCCCGCATCTCGATGAGCCCGCTCATGCAT |
| IM | 49 | AATAGCCCATACCGGGACAAGATAGCTGAATGAGAGAAAAAG |
| IM | 50 | AAAGGGAAGGAAAGCAGTCGCCGCCCGATGCGCCGCGATT |
| IM | 51 | ATCAGTAGCGGCCGAGCTGGTCCGAGACTTTTGAGCCCCGTA |
| IM | 52 | AGGAGGTCGCCGGCGCACATCTCCACCGCCTCCCTTTGAC |
| IM | 53 | AGTATTAAGCGAAACCGATGCTACACTTTGCTGGTAAATGAA |
| IM | 54 | ACACTGACGCGGCTGTCGTTGTCGTAGACCGCCACCCGTA |
| IM | 55 | AGGAGCCTCTTCTCACGCAACGATCAACGTACTTTCACCAAA |
| IM | 56 | TTTTCATGGATTGCCGAGGGTAGACGTTGTTAAAGAGACT |
| IM | 57 | ACCGAACTGGATCTCGAACTAGGCTGTCGAACAACGGAGGGA |
| IM | 58 | ATTTTAAGGGTCCTGTGACGCGGCTCGAGAATAAGATGCG |
| IM | 59 | GCAAAAGAAGGGCCTTGGCGAAACTCACGAGATACATCTTTT |
| IM | 60 | ATTCGAGCGGTGGCCGACGTGCAAACAGAAATCAGTTTTA |
| IM | 61 | GATACATTTGGACGTCTAGACATGCGACCTACATGTTCATTA |
| IM | 62 | GGATAAAGGCAAAGTTAGAAGGCTTGTCTAAGCAACGCAA |
| IM | 63 | ACTAGCATGCCGGCTTCACCACAGCAGAAAATGCCGGGTAAA |
| IM | 64 | TCTCCGTTTGAGGCCCTGCAAGGCGAGTTTAACCACGGAT |
| IM | 65 | GCCAGCTGCTGCTGGTGCAATCGTCGCTGGCCGGCACATTAC |
| IM | 66 | GGCTATATCACTACACGCCCACTAGGGCAGGGATTCACCA |

| IM | 67 | GTGCTGGACCGAGGTCCGCGGTAAAATGTCGAAATTACGATT |
|---|---|---|
| IM | 68 | CATCCTGCCTCACAGCCGGTGCAGCGACAGTATTATTCGC |
| IM | 69 | TCGCGTCGGAGCACACGCACTCTCAAAGGGGATGCAGGAATT |
| IM | 70 | AAGGTGTTGCTACACAACGGAACGCTTCTTTATAATCACG |
| IM | 71 | CTCGCTACCGTGCACCGCGTTAACGGGCTTACGGTGGCTGAA |
| IM | 72 | AGTCGGGCACTGTGGCTTTAGCCGACGGACACAACTTTCC |
| IM | 73 | AAATCGGCAGATAGAACGTGGCCCGCTATTAAGCGGTTTCCG |
| IM | 74 | CAGAGCGGTCCTGCCCTCCCGCTGGTAAGCGCGTAAGAAT |
| IM | 75 | ACCAATGAGACACTCGACGCCCAACGCAGGATTAGAGACGTC |
| IM | 76 | CCACCACAAGTCTCCCACTGACCGCCAAGCCACCCCAGAA |
| IM | 77 | ATTTCGGACTTGTTACGCACATCGCAGCCAAACGGGGTGCCT |
| IM | 78 | GCAAGCCCGAGCTTCCTGAAAGCGCAACACCGCCAGGATA |
| IM | 79 | GTTGAAAAAGGCCGGTCCCCGCCGCTTACAAGCGGAGTTCAC |
| IM | 80 | GGCTACAACGTCTTAAGCGTTTCCCATCTTGCGGGGCAAC |
| IM | 81 | AACGAGGCTAACCTGCCGCAGCACTGCGGAATCATCGGCCGG |
| IM | 82 | ACTTTAAGACGCCCTTGGCCGAGCTTGCCTGACGATTTCA |
| IM | 83 | CGATAAAAGTGGCCCGATCTCAGCACAATCAAGGAATGACGA |
| IM | 84 | GCCCGAAGGGAGCGCGTCCATTACGTACCCCTGACAGGAA |
| IM | 85 | TGCGAACGTCTCGGAGTGCTTGAAGCCAAGGCAACTAAATTC |
| IM | 86 | TTGCGGGGCGGCGTGTCGAGTAGTCGAGTCAGAGCTACTT |
| IM | 87 | ACAAGAGAAACGCCGTTAAACACCTCGGAGGCTATTTAGCAA |
| IM | 88 | AAATGTGTCGTGACCAGTTGGCCTCAATCGCCATCACATT |
| IM | 89 | GGCGATCGGAGGCTCTCCCTCCCGCTGAAGGTGCCGGGGAAG |
| IM | 90 | GCAATAACTCGGCACTCGTGATCGTAGTGATGGCAACACA |
| IM | 91 | CTTTTCCATAGCTACGCCGCGGGTTCAGAAGCACTGCCAGAC |
| IM | 92 | AAGACGGCGAGCGGCCAGATACGGAGTGGTTATCTCCGTG |
| IM | 93 | AAAAGATACTAGAGTCTCGGCTCTTGAGAACTGCATATTTGT |
| IM | 94 | CGGTGTCAGCTCGCGCCCGCCCTACCACTCAATGAAGATC |
| IM | 95 | TCGCACTCATCTCTGGCGGCTACTCTCCTTCTTGCCCAATCC |
| IM | 96 | AATTGCGCCCTCGCACGCATTAAGCAGCCCGGAAGACATT |
| IM H1/24 - overhang | 1 | TCGTCCATCGTAAAGAAGACGCAAATTAACCGTCAAGCGG |
| IM H1/24 - overhang | 2 | GGGCGTTTGCCATCTATTCAACCGATTGAGGGAGGTATTGAC |
| IM H1/24 - overhang | 3 | ATTCTCTGAATTTACCAAAGACAAAAGGGCGACTTTCATA |
| IM H1/24 - overhang | 4 | AGGGGTTGATATAAGAGCTACAATTTTTACCAGCGCCGTTCC |
| IM H1/24 - overhang | 5 | CGGTTTTGTCGTCTTAGTTGCTATTTTGCACCCTATAGCC |
| IM H1/24 - overhang | 6 | CGGACAACAACCATCTTGAAGCCTTAAATCAAGATTTCCAGA |
| IM H1/24 - overhang | 7 | CAGAATACACTAAATCCCGACTTGCGGGAGGTTGCCCACG |
| IM H1/24 - overhang | 8 | TCTTGACAAGAACCGGCGAGGCGTTTTAGCGAACCACACTCA |

| | | |
|---|---|---|
| IM H1/24 - overhang | 9 | ATTATTACAGGTAGTATCCGGTATTCTAAGAACGATATTC |
| IM H1/24 - overhang | 10 | CATTGAATCCCCCTCTCAAATATATATAGAAGGCTAAAGATT |
| IM H1/24 - overhang | 11 | TTAAGAGGTCATTTAGAACGCGAGAAAACTTTTAAATGCT |
| IM H1/24 - overhang | 12 | TGTAGTAGTAGCATTCAAATCCAATCGCAAGACAATTGCGGA |
| IM H1/24 - overhang | 13 | AAGGCCGGAGACAGCTATATGTAAATGCTGATGAACATCC |
| IM H1/24 - overhang | 14 | ACTAAACGTTAATATGCTTAGGTTGGGTTATATAATCAAATC |
| IM H1/24 - overhang | 15 | AACCAGTTTGAGGGACTACCTTTTTAACCTCCGTTTGTTA |
| IM H1/24 - overhang | 16 | ACGGCCAGTGCCAAGTCATTTTGCGGGTCTGAGAGGACGACG |
| IM H1/24 - overhang | 17 | ATTGTGCAAGTTGCAAAAGTTTGAGTAACATTACTTTATT |
| IM H1/24 - overhang | 18 | ATTAGGGAAACTGCGGCCCGAACGTTATTAATTTTCAGGAGG |
| IM H1/24 - overhang | 19 | CTTAGTAACTATCGAACTCGTATTAAATCCTTTTGTTGAG |
| IM H1/24 - overhang | 20 | TATTCTTTACATAAAGACTTTACAAACAATTCGACACATCAT |
| IM H1/24 - overhang | 21 | GAATCCCCATTCTGTGAGGATTTAGAAGTATTACATTGCT |
| IM H1/24 - overhang | 22 | CGTTCGTAATCATGGCTGAGTAGAAATAATACATTCAATGTG |
| IM H1/24 - overhang | 23 | TGTGGTTTTTCTTTTAGTAATAACATCACTTGCTCATAGC |
| IM H1/24 - overhang | 24 | TGAAAAACCGTCTATTGTAGCAATACTTCTTTGATTCACCAG |
| IM H11/14 - overhang | 1 | AGGCGAAATCGGTTCATGCGTGCAGGCCAAGTTTGCCCCAGC |
| IM H11/14 - overhang | 2 | CACGTATTACCTCGCGTTCGAGCTAGATTGCTTTGACGAG |
| IM H11/14 - overhang | 3 | ACCATTACCCTCTCACCTCCCGACGGAGAAATCACCAGTAGC |
| IM H11/14 - overhang | 4 | AGCCACCATGGCGTACGTCGACTCTGCACGCCACCCTCAG |
| IM H11/14 - overhang | 5 | GCCCGTATCTGCTTGGGCCAGGACAGTGACTTGAGTAACAGT |
| IM H11/14 - overhang | 6 | CAGAGCCATGACCTCCCGCCATTTGGAAAACCGCCACCCT |
| IM H11/14 - overhang | 7 | TAAAGGAACGATGACTGACGTCTGTCCCACGAAAGGAACAAC |

| | | |
|---|---|---|
| IM H11/14 - overhang | 8 | AAAGACAGGACTGCCCAGTTCCGCCGTTCCCTCAGCAGCG |
| IM H11/14 - overhang | 9 | TCCGCGACACATCGGGCTCGGTTGCGGAGCATTGTGTCGAAA |
| IM H11/14 - overhang | 10 | TAAATTGACCTTCACTTCCCTCTCTACTCAGAACGAGTAG |
| IM H11/14 - overhang | 11 | ACACTATCCCGTGGTGCCGTCGTCATCTGGATAGTAAGAGCA |
| IM H11/14 - overhang | 12 | GCGGATTGATTGGTCGTCCGCCCGTAATGTCAGAAGCAAA |
| IM H11/14 - overhang | 13 | TCATTCCAGAGTGGAGCACCGAAGGAGGGCTGTCTGGAAGTT |
| IM H11/14 - overhang | 14 | ACCAAAAAATCTTTTGTCCGATCCCGTATAAATCGGTTGT |
| IM H11/14 - overhang | 15 | ATCAGGTCTGCATTGTCCGGCGTGCACGACTCTACAAAGGCT |
| IM H11/14 - overhang | 16 | CCTTCCTCCGTGGCACTGCGTGGCGAATATTCGCGTCTGG |
| IM H11/14 - overhang | 17 | CGCCATTCCGTTGCGAGAGCGAGACCTAGTCAAAGCGCCATT |
| IM H11/14 - overhang | 18 | CAGAAATAAGGTGGGTCTCTCACCTGAGTTGATTCAGCAT |
| IM H11/14 - overhang | 19 | ATGCATGATGGCCGCAGCCTGTTTGGTCAGGCAGAGCAGGCA |
| IM H11/14 - overhang | 20 | TGCTAAACATTGCGCGAGCTTATCGCCGGAGTAAGCGTAT |
| IM H11/14 - overhang | 21 | CGCATCAAAGCACGGCCCGCTTACACTTCTGACGCTGGCATT |
| IM H11/14 - overhang | 22 | GATTGGGGCCCTAGGCCCTTTACCGGAGTCTGAGCAAAAA |
| IM H11/14 - overhang | 23 | ATGATTAAGGACCAATCCACGTACAGCCCGCAAAACATATAG |
| IM H11/14 - overhang | 24 | GGTGCCTGAGTGTGTGGGTGTGTGTGACTGTAAAGCCTGG |
| Outside Pixel | 1 | ACGTCAAAGGGCGAGACGGGCTATTGGGCGCCAGGGTTTCCTGGG |
| Outside Pixel | 2 | AGCCCCCTTATTAAAATTATTCGAGTAAAAGAGTCTACGCTGCCA |
| Outside Pixel | 3 | AGTGCCGTCGAGATAAGCGTCGAATGGAAAGCGCAGCAAAATCAT |
| Outside Pixel | 4 | TTGCGCCGACAATTTAGTAAAGCGTAACGATCTAAAGAATAGGTA |
| Outside Pixel | 5 | ATCAAGAGTAATCTTTGACCCACGAAAGAGGCAAAATAACCGAAG |
| Outside Pixel | 6 | TCATAAATATTCATCAGTTGACTAACGGAACAACATTACCCAATC |
| Outside Pixel | 7 | TCAATTCTACTAAGCTTAGAGATTGCTCCTTTTGATAAACAGTCG |
| Outside Pixel | 8 | AATATTTAAATTGCATCAATACAAAAGGGTGAGAAATAAATCACA |
| Outside Pixel | 9 | GTTGTAAAACGACAGTATCGGGTAACCGTGCATCTGATTCGCACA |
| Outside Pixel | 10 | ATTGCGCTAACAGCTGGAACTCAGGGTTGTCGGACTTCGCATTAC |
| Outside Pixel | 11 | ATTATCTTACTGTCGCATCGCTCGAACAAGACCCGTTGAAACAAT |
| Outside Pixel | 12 | TACCGAGCTCGAAAGAAATGAGTCTAATGAAGACAATACCGTTGT |

| | | |
|---|---|---|
| Outside Pixel | 13 | AAGTGTTTTTATACACCACACAAGAGTCCACTATTGATTGCCCGG |
| Outside Pixel | 14 | CAAACAAATAAATCCAGAGCTGTAGCGCGTTTTCAGGTGAATTAG |
| Outside Pixel | 15 | GCATTCCACAGACCCGTACTTTAGCGGGGTTTTGCGCTTTTGACA |
| Outside Pixel | 16 | ATGCCACTACGAAGGTCGCTGGTGAATTTCTTAAATCTGTATGTA |
| Outside Pixel | 17 | AAGAAAAATCTACTAACAAATACAGACCAGGCGCATTATACCATA |
| Outside Pixel | 18 | ACAGGTCAGGATTACGAGAATAGACTGGATAGCGTGAATACCAGG |
| Outside Pixel | 19 | TGCCTGAGTAATGAAGGCAATTTCATTTGGGGCGCGCTGAATACA |
| Outside Pixel | 20 | GGTCACGTTGGTGTTTGTTAAAAGCCCCAAAAACACAACCGTTAA |
| Outside Pixel | 21 | ATAGATGAACGAAATGCGTATTGGGTAACGCCAGGAAGATCGCTA |
| Outside Pixel | 22 | ACCTGGAAGAGTTCAAAACTACATCAAACGCCGCGAAACAGAGCG |
| Outside Pixel | 23 | ATACAAATATTCCAACGACAGATGATGACCGTACTGGGTTGGATG |
| Outside Pixel | 24 | CCAACGCGCGGGGTTGTTATACTTCCGAGTCACAGCGTGCAAAGC |
| Outside Pixel | 25 | TAGGGTTGAGTGTCCTGGCCCACCTGTCGTGCCAGCCAATTCCCG |
| Outside Pixel | 26 | AGAATCAAGTTTGTCACCGACTTAGACAGGAACGGTCGCTTAAGA |
| Outside Pixel | 27 | CTGAGACTCCTCAGGAGTGTAAGGCAGGTCAGACGAGGAACCGAC |
| Outside Pixel | 28 | TTGTATCGGTTTAGCTAAACATTCGTCACCAGTACATTTAGTAGG |
| Outside Pixel | 29 | AACTTTGAAAGAGAACAAAGTGGAAGTTTCCATTAAGCAGGGAAA |
| Outside Pixel | 30 | TTGCCAGAGGGGGCTAATGCAACTGGCTCATTATACATTCAGTCC |
| Outside Pixel | 31 | AAATGGTCAATAAGTAGCTCATCAAAGCGAACCAGAAAATCAATT |
| Outside Pixel | 32 | ATCATATGTACCCATAAATTATTTTTAGAACCCTCAGCAAAATGC |
| Outside Pixel | 33 | AAGGGGGATGTGCCCAGCTTTGAACAAACGGCGGATTCATTTTCA |
| Outside Pixel | 34 | CTGGATGAACGGGAAGTGAGCTGCCACTCATTGTTGACAGTTCGA |
| Outside Pixel | 35 | CACAGCGATGCCAGGGTTCAGAAGACTCCTGTTATCCAGCGTGTG |
| Outside Pixel | 36 | GGTTTTGTTTTATTCACGAGTATGTAGATGAAGGTACAAGGAGTT |
| Outside Pixel | 37 | CTAAACAGGAGGCCTACAGGAATCCCTTATAAATCGTTGCAGCGC |
| Outside Pixel | 38 | GCCGCCGCCAGCACAGAGCCCCATCGATAGCAGCAATTTGGGAAG |
| Outside Pixel | 39 | AGGAACCCATGTACCTCAGACTATTATTCTGAAACTAAGTTTTGA |
| Outside Pixel | 40 | CTTTGAGGACTAAGCCGCTTTCCAAAAAAAAGGCTACAGTTTCAT |
| Outside Pixel | 41 | TGTGAATTACCTTGCTTGCCAGACGGTCAATCATAAGATTTGTGG |
| Outside Pixel | 42 | TTCAAATATCGCGGTCTTTACAAAATAGCGAGAGGAACGCCAAAT |
| Outside Pixel | 43 | GCCTTTATTTCAATAAAGCCTAGATTTAGTTTGACTTAAATATAC |
| Outside Pixel | 44 | AGTAACAACCCGTATAGGAACGATGAACGGTAATCAGAGGGTAAA |
| Outside Pixel | 45 | GCGCCGCCTGAACAATGAAAGCGGGCCTCTTCGCTCGCTTCTGCG |
| Outside Pixel | 46 | CAGTTTCTTGTTGCGAAGGTAATTGGTAACACCATACTCTCAGAT |
| Outside Pixel | 47 | CTCCATGCAGACAATGAGTAGCTTGTGAAAATGCTGTGAGTATAC |
| Outside Pixel | 48 | GCTCACTGCCCGCATACGAGGGGGATTTATTTTATAAACGATAGT |
| Outside Pixel | 49 | TGTTTGATGGTGGCCACGCTGTGAGTGAGCTAACTCCATAAAGCC |
| Outside Pixel | 50 | AGCAAGGCCGGAACCAGCAAACGTGCTTTCCTCGTTCTATGGTCC |
| Outside Pixel | 51 | AGTTAATGCCCCCTCAGTGCCCCTCAGAGCCGCCACTCAGAACTT |
| Outside Pixel | 52 | GAATAATAATTTTTGAGAATACACCCTCATTTTCAGCCCTCAGAC |
| Outside Pixel | 53 | TCCATGTTACTTACCTGATAAATCGGAACGAGGGTAATCGTCAGC |
| Outside Pixel | 54 | CCCTCGTTTACCATACGAGGCCTTGAGATGGTTTAAGAAACACGC |
| Outside Pixel | 55 | ACAGTTGATTCCCAAGTACGGATCAAAAAGATTAAGTATTATAAA |
| Outside Pixel | 56 | CCTGAGAGTCTGGTTGAGAGAATTATGACCCTGTAAATAAAGCTA |
| Outside Pixel | 57 | TGCGCAACTGTTGAAACCAGGAGCCAGCTTTCATCAAAAAATATG |
| Outside Pixel | 58 | TGGGGATTTGACGGTGAAGCGAAGAATTACAGCGCAGACATCAGC |

| Outside Pixel | 59 | GAGTGAGATCGGTTGATGTCTGGAAAGCAACGAAGTCGGATGGAC |
|---|---|---|
| Outside Pixel | 60 | AATATTACATAACTCTCTGTATTATCAATGTTGTGCGTTAGAGGA |
| Inside Pixel | 1 | AGTACCGGTCGCGAAAGGTGTGGTTGCCGTTGCGTGTTC |
| Inside Pixel | 2 | ACCTTTCGTCCCTAGCAGTTCCGTGGCGAGCACCTTGGC |
| Inside Pixel | 3 | GGTCTCCGCGATCGTATAGCTCTCCCGCACGGGTTCAGC |
| Inside Pixel | 4 | GACCTGTTCGGCGAGCTAGGCACACGTCACCGGGTAGTG |
| Inside Pixel | 5 | TTCCTCCTGGGTCGGGCGAGACTTGCAGTAGATGGGCCG |
| Inside Pixel | 6 | CTACGTTTGCTCACACGCCCGAGACGGTTAGATCGCGCC |
| Inside Pixel | 7 | GGCTCCCGGCCGTACGTATGCCTGCCTTCTACCTGCAGT |
| Inside Pixel | 8 | CAGTGGCCCATTTCGCCAATTGGGTGCGCGCACTGTGAA |
| Inside Pixel | 9 | CGGTAGACTGGTTAGGGCCATGGGCGCCCGTCAATGAGG |
| Inside Pixel | 10 | TGCCCACTCATGCACTAGCACGCTCACGCCTGGGATGGA |
| Inside Pixel | 11 | GCCGCGGCCGCATTTACATAGCAGCCTGGCATGTATCGT |
| Inside Pixel | 12 | CTGTGAAAGGACTGCCCTCTGACTCGGGCCCGCTTCCGT |
| Inside Pixel | 13 | GCGAACATCCACGTCGGAGCATCGTGCGTCCTTGACCCA |
| Inside Pixel | 14 | GCTGACGTGTTCGCCACCGGAGCATTGAGACAGCCCATC |
| Inside Pixel | 15 | GATGCGCCGACACGCGTGCTATCAGTCAGACCGTTGGTG |
| Inside Pixel | 16 | CGCGCATCAGCTGCCCGGGAAGCACGAGTGCATTGATTT |
| Inside Pixel | 17 | CTACCGGACAGACAGCGGCGTAAAGACCCGAAAGCGGCA |
| Inside Pixel | 18 | CGATGAAGACCGGCCCTCGAATCGGCCCTCGGACTCATG |
| Inside Pixel | 19 | GGCGGCATGAAGGCACCTCAGTGACGTCCAGTCTAGGCG |
| Inside Pixel | 20 | GTCAGCGCTCGGTAACTGTTATCCGACGTGTACCGCGGC |
| Inside Pixel | 21 | TGCCGGTGGTCCAACCCGTCATCCACGACCGTTAGACGA |
| Inside Pixel | 22 | GCTCAATGAAGGGCCTCTTTTCAGGGCGGGCTGCGGACA |
| Inside Pixel | 23 | AACTAAGCACTCATCGAGATGCGGGCCATTGCGACGCGG |
| Inside Pixel | 24 | ACCGCTCGTGATCGTGAGTATTGCGTCTCCCGAGGAGCG |
| Inside Pixel | 25 | CTGCTTTCCTGTCTCGGACCAGCTCGGCCGGTGGAGATG |
| Inside Pixel | 26 | TGCGCCGGCGAAGTGTAGCATCGGTTTCGCTACGACAAC |
| Inside Pixel | 27 | GACAGCCGCGGTTGATCGTTGCGTGAGAAGCGTCTACCC |
| Inside Pixel | 28 | TCGGCAATCCGACAGCCTAGTTCGAGATCCGAGCCGCGT |
| Inside Pixel | 29 | CACAGGACCCGTGAGTTTCGCCAAGGCCCTGTTTGCACG |
| Inside Pixel | 30 | TCGGCCACCGGTCGCATGTCTAGACGTCCACAAGCCTTC |
| Inside Pixel | 31 | TAACTTTGCCTCTGCTGTGGTGAAGCCGGCTCGCCTTGC |
| Inside Pixel | 32 | AGGGCCTCAAAGCGACGATTGCACCAGCAGCCTAGTGGG |
| Inside Pixel | 33 | CGTGTAGTGACATTTTACCGCGGACCTCGGCGCTGCACC |
| Inside Pixel | 34 | GGCTGTGAGGCTTTGAGAGTGCGTGTGCTCAGCGTTCCG |
| Inside Pixel | 35 | TTGTGTAGCAGCCCGTTAACGCGGTGCACGGTCGGCTAA |
| Inside Pixel | 36 | AGCCACAGTGCAGCTATCTTGTCCCGGTATGGGCGGCGA |
| Inside Pixel | 37 | GTCGAGTGTCGGCGGTCAGTGGGAGACTTGCTGCGATGT |
| Inside Pixel | 38 | GCGTAACAAGTGCGCTTTCAGGAAGCTCGTAAGCGGCGG |
| Inside Pixel | 39 | GGACCGGCCTTGGGAAACGCTTAAGACGTCGCAGTGCTG |
| Inside Pixel | 40 | CGGCAGGTTAAAGCTCGGCCAAGGGCGTCTTGTGCTGAG |
| Inside Pixel | 41 | ATCGGGCCACACGTAATGGACGCGCTCCCTGGCTTCAAG |
| Inside Pixel | 42 | CACTCCGAGACGACTACTCGACACGCCGCCCGAGGTGTT |
| Inside Pixel | 43 | TAACGGCGTTTGAGGCCAACTGGTCACGATCAGCGGGAG |
| Inside Pixel | 44 | GGAGAGCCTCTACGATCACGAGTGCCGAGCTGAACCCGC |

| | | |
|---|---|---|
| Inside Pixel | 45 | GGCGTAGCTACTCCGTATCTGGCCGCTCGCTCAAGAGCC |
| Inside Pixel | 46 | GAGACTCTAGGGTAGGGCGGGCGCGAGCTGGAGAGTAGC |
| Inside Pixel | 47 | CGCCAGAGATTGCTTAATGCGTGCGAGGGTAGCGGGCCA |
| Inside Pixel | 48 | CGTTCTATCTACCAGCGGGAGGGCAGGACTGCGTTGGGC |
| IP H14 - homodimer | 1 | ACGCGAGGTACTCCGTCGGGAGGTGAGAGGCAGAGTCGA |
| IP H14 - homodimer | 2 | CGTACGCCATCACTGTCCTGGCCCAAGCAGCCAAATGGC |
| IP H14 - homodimer | 3 | GGGAGGTCATGGGACAGACGTCAGTCATCGCGGCGGAAC |
| IP H14 - homodimer | 4 | TGGGCAGTCCTCCGCAACCGAGCCCGATGTTAGAGAGGG |
| IP H14 - homodimer | 5 | AAGTGAAGGTAGATGACGACGGCACCACGGTACGGGCGG |
| IP H14 - homodimer | 6 | ACGACCAATCCCTCCTTCGGTGCTCCACTCCGGGATCGG |
| IP H14 - homodimer | 7 | ACAAAAGATTCGTGCACGCCGGACAATGCATCGCCACGC |
| IP H14 - homodimer | 8 | AGTGCCACGGTAGGTCTCGCTCTCGCAACGCAGGTGAGA |
| IP H14 - homodimer | 9 | GACCCACCTTGACCAAACAGGCTGCGGCCAGCGATAAGC |
| IP H14 - homodimer | 10 | TCGCGCAATGAAGTGTAAGCGGGCCGTGCTCCGGTAAAG |
| IP H14 - homodimer | 11 | GGCCTAGGGCGGCTGTACGTGGATTGGTCCCACACACAC |
| IP H14 - homodimer | 12 | CCACACACTCGGCCTGCACGCATGAACCGACTAGCTCGA |

**SI Table 2. Staple list for homodimerization of DNA origami barrels (replace "Subpool IP H14 -homodimer")**

| Subpool | # | Sequence |
|---|---|---|
| IP H14 +homodimer | 1 | CTCCGTCGGGAGGTGAGAGGCAGAGTCGACGTCGAGGTA |
| IP H14 +homodimer | 2 | CACTGTCCTGGCCCAAGCAGCCAAATGGCGGGCACACTC |
| IP H14 +homodimer | 3 | GGGACAGACGTCAGTCATCGCGGCGGAACTGGCTAGGGC |
| IP H14 +homodimer | 4 | TCCGCAACCGAGCCCGATGTTAGAGAGGGAAGCGCAATG |
| IP H14 +homodimer | 5 | AGATGACGACGGCACCACGGTACGGGCGGACGCCACCTT |
| IP H14 +homodimer | 6 | CCTCCTTCGGTGCTCCACTCCGGGATCGGACAGCCACGG |
| IP H14 +homodimer | 7 | CGTGCACGCCGGACAATGCATCGCCACGCAGTAAAGATT |
| IP H14 +homodimer | 8 | TAGGTCTCGCTCTCGCAACGCAGGTGAGAGACACCAATC |
| IP H14 +homodimer | 9 | GACCAAACAGGCTGCGGCCAGCGATAAGCTCGTGAAGGT |
| IP H14 +homodimer | 10 | AAGTGTAAGCGGGCCGTGCTCCGGTAAAGGGCGCAGTCC |
| IP H14 +homodimer | 11 | GGCTGTACGTGGATTGGTCCCACACACACCCAAGGTCAT |
| IP H14 +homodimer | 12 | GGCCTGCACGCATGAACCGACTAGCTCGAACGACGCCAT |

**SI Table 3. Staple list for stacking interface between DNA origami barrels (replace subpools "IM H1/24 -overhang" and "IM H11/14 -overhang")**

| Subpool | # | Sequence |
|---|---|---|
| IM H1/24 +overhang | 1 | TCGTCCATCGTAAAGAAGACGCAAATTAACCGTCAAGCGGTTCGGTT |
| IM H1/24 +overhang | 2 | GGGCGTTTGCCATCTATTCAACCGATTGAGGGAGGTATTGACTGCTTCCT |
| IM H1/24 +overhang | 3 | ATTCTCTGAATTTACCAAAGACAAAAGGGCGACTTTCATATCAAGAC |
| IM H1/24 +overhang | 4 | AGGGGTTGATATAAGAGCTACAATTTTTACCAGCGCCGTTCCAAAGCTTC |
| IM H1/24 +overhang | 5 | CGGTTTTGTCGTCTTAGTTGCTATTTTGCACCCTATAGCCGGCAATC |
| IM H1/24 +overhang | 6 | CGGACAACAACCATCTTGAAGCCTTAAATCAAGATTTCCAGAGCTCTACA |
| IM H1/24 +overhang | 7 | CAGAATACACTAAATCCCGACTTGCGGGAGGTTGCCCACGCGTCCAA |
| IM H1/24 +overhang | 8 | TCTTGACAAGAACCGGCGAGGCGTTTTAGCGAACCACACTCAACGTGTAA |
| IM H1/24 +overhang | 9 | ATTATTACAGGTAGTATCCGGTATTCTAAGAACGATATTCAGACACA |
| IM H1/24 +overhang | 10 | CATTGAATCCCCCTCTCAAATATATATAGAAGGCTAAAGATTCCACCTCT |
| IM H1/24 +overhang | 11 | TTAAGAGGTCATTTAGAACGCGAGAAAACTTTTAAATGCTTTCCCCT |
| IM H1/24 +overhang | 12 | TGTAGTAGTAGCATTCAAATCCAATCGCAAGACAATTGCGGAACAGCTGT |
| IM H1/24 +overhang | 13 | AAGGCCGGAGACAGCTATATGTAAATGCTGATGAACATCCCCATCAC |
| IM H1/24 +overhang | 14 | ACTAAACGTTAATATGCTTAGGTTGGGTTATATAATCAAATCCTGCGTAA |
| IM H1/24 +overhang | 15 | AACCAGTTTGAGGGACTACCTTTTTAACCTCCGTTTGTTACTTTACC |
| IM H1/24 +overhang | 16 | ACGGCCAGTGCCAAGTCATTTTGCGGGTCTGAGAGGACGACGGCCATCAA |
| IM H1/24 +overhang | 17 | ATTGTGCAAGTTGCAAAAGTTTGAGTAACATTACTTTATTATGTCCC |
| IM H1/24 +overhang | 18 | ATTAGGGAAACTGCGGCCCGAACGTTATTAATTTTCAGGAGGTATCCTTG |
| IM H1/24 +overhang | 19 | CTTAGTAACTATCGAACTCGTATTAAATCCTTTTGTTGAGTCTCGAA |
| IM H1/24 +overhang | 20 | TATTCTTTACATAAAGACTTTACAAACAATTCGACACATCATCCTGTCAA |
| IM H1/24 +overhang | 21 | GAATCCCCATTCTGTGAGGATTTAGAAGTATTACATTGCTCACACGA |
| IM H1/24 +overhang | 22 | CGTTCGTAATCATGGCTGAGTAGAAATAATACATTCAATGTGTAACCATG |
| IM H1/24 +overhang | 23 | TGTGGTTTTTCTTTTAGTAATAACATCACTTGCTCATAGCTTGCCTT |
| IM H1/24 +overhang | 24 | TGAAAAACCGTCTATTGTAGCAATACTTCTTTGATTCACCAGTCGACTAG |

| | | |
|---|---|---|
| IM H11/14 +overhang | 1 | GAAGCACAAGGCGAAATCGGTTCATGCGTGCAGGCCAAGTTTGCC CCAGCCACTGTC |
| IM H11/14 +overhang | 2 | CTTTCCCCACGTATTACCTCGCGTTCGAGCTAGATTGCTTTGACGAG TGCGATCA |
| IM H11/14 +overhang | 3 | TGTCACCAACCATTACCCTCTCACCTCCCGACGGAGAAATCACCAG TAGCAATACCG |
| IM H11/14 +overhang | 4 | ACACCTAAGCCACCATGGCGTACGTCGACTCTGCACGCCACCCTC AGGCTTGACA |
| IM H11/14 +overhang | 5 | ATCGGTTAGCCCGTATCTGCTTGGGCCAGGACAGTGACTTGAGTAA CAGTAATGCAC |
| IM H11/14 +overhang | 6 | CATTACTCAGAGCCATGACCTCCCGCCATTTGGAAAACCGCCACCC TCCTCATTC |
| IM H11/14 +overhang | 7 | CCCCAATCTAAAGGAACGATGACTGACGTCTGTCCCACGAAAGGA ACAACTCTCAAA |
| IM H11/14 +overhang | 8 | CCTTACCAAAGACAGGACTGCCCAGTTCCGCCGTTCCCTCAGCAGC GTACATGGC |
| IM H11/14 +overhang | 9 | CATACCCATCCGCGACACATCGGGCTCGGTTGCGGAGCATTGTGTC GAAAGTTTACC |
| IM H11/14 +overhang | 10 | CCACAATTAAATTGACCTTCACTTCCCTCTCTACTCAGAACGAGTA GTCTGTTTC |
| IM H11/14 +overhang | 11 | CTCTCTCCACACTATCCCGTGGTGCCGTCGTCATCTGGATAGTAAG AGCACCCTTTC |
| IM H11/14 +overhang | 12 | TGAGTCTGCGGATTGATTGGTCGTCCGCCCGTAATGTCAGAAGCAA ATGGTCCAT |
| IM H11/14 +overhang | 13 | CTTCGATCTCATTCCAGAGTGGAGCACCGAAGGAGGGCTGTCTGG AAGTTTGACAAC |
| IM H11/14 +overhang | 14 | ATCGTTCACCAAAAAATCTTTTGTCCGATCCCGTATAAATCGGTTGT TGTCACTT |
| IM H11/14 +overhang | 15 | CCGCAATAATCAGGTCTGCATTGTCCGGCGTGCACGACTCTACAAA GGCTCAGCAAG |
| IM H11/14 +overhang | 16 | AGTTCGACCTTCCTCCGTGGCACTGCGTGGCGAATATTCGCGTCTG GTCCTTCAG |
| IM H11/14 +overhang | 17 | TCTACTCCCGCCATTCCGTTGCGAGAGCGAGACCTAGTCAAAGCGC CATTACCTACC |
| IM H11/14 +overhang | 18 | AAGCTTCCAGAAATAAGGTGGGTCTCTCACCTGAGTTGATTCAGCA TTCCAGACC |
| IM H11/14 +overhang | 19 | CTTACACCATGCATGATGGCCGCAGCCTGTTTGGTCAGGCAGAGCA GGCACCAATCC |
| IM H11/14 +overhang | 20 | TGGAACCTGCTAAACATTGCGCGAGCTTATCGCCGGAGTAAGCGT ATGCTTCAAG |
| IM H11/14 +overhang | 21 | CTACTGCCCGCATCAAAGCACGGCCCGCTTACACTTCTGACGCTGG CATTTAAAACG |
| IM H11/14 +overhang | 22 | TACCTTCGATTGGGGCCCTAGGCCCTTTACCGGAGTCTGAGCAAAA ATACTAGGG |
| IM H11/14 +overhang | 23 | CTGGACCTATGATTAAGGACCAATCCACGTACAGCCCGCAAAACA TATAGCCTCAAC |

| | | |
|---|---|---|
| IM H11/14 +overhang | 24 | CCTCTGAGGTGCCTGAGTGTGTGGGTGTGTGTGACTGTAAAGCCTG GTGCTACTC |
| Connecting strand | 1 | CGAATGATCGCAGGGAAAGAGGAAGCACGGTATTTGGTGACAGTC |
| Connecting strand | 2 | TTGATGTCAAGCTAGGTGTGAAGCTTTGTGCATTTAACCGATGAT |
| Connecting strand | 3 | TGCCGAATGAGGAGTAATGTGTAGAGCTTTGAGAGATTGGGGTTG |
| Connecting strand | 4 | GACGGCCATGTAGGTAAGGTTACACGTGGTAAACTGGGTATGTGT |
| Connecting strand | 5 | GTCTGAAACAGAATTGTGGAGAGGTGGGAAAGGGGGAGAGAGAG G |
| Connecting strand | 6 | GGAAATGGACCAAGACTCAACAGCTGTGTTGTCAGATCGAAGGTG |
| Connecting strand | 7 | ATGGAAGTGACAGAACGATTTACGCAGCTTGCTGTATTGCGGGGT |
| Connecting strand | 8 | AAAGCTGAAGGATCGAACTTTGATGGCGGTAGGTGGAGTAGAGGG |
| Connecting strand | 9 | ACATGGTCTGGAGAAGCTTCAAGGATAGGATTGGGGTGTAAGTTC |
| Connecting strand | 10 | GAGACTTGAAGCGGTTCCATTGACAGGCGTTTTAGGCAGTAGTCG |
| Connecting strand | 11 | TGTGCCCTAGTAGAAGGTACATGGTTAGTTGAGGAGGTCCAGAAG |
| Connecting strand | 12 | GCAAGAGTAGCATCAGAGGCTAGTCGAGACAGTGTGTGCTTCAAC |

**SI Table 4. Staple list for DNA origami cap**

| **Subpool** | # | **Sequence** |
|---|---|---|
| Ring | 1 | CGCTATTCAATGAATGCCTTTAGCGTCAGACTGTGTTTGCCATCTT |
| Ring | 2 | AAGGTAAATACTTGAGCCATTTGGGAATTCGGAAACGTCACAATTAATT |
| Ring | 3 | CGTAAGACCGAACACCCAAAAGAACTGGCATGATATACATAAAGGT |
| Ring | 4 | GGTAATTGAAATAATAAGAGCAAGAAACAGTAAGCAGATAGATACGTGG |
| Ring | 5 | AAAACGACAAGATTCAACGCTAACGAGCGTCTTTTATCCCAATCCA |
| Ring | 6 | TTTCATCGTGGCTTATCCGGTATTCTAAGGAAGCCTTAAATACTAACGG |
| Ring | 7 | CTGTATGTAAGAGAGACAATAAACAACATGTTCAAACAAGAAAAAT |
| Ring | 8 | TAGTATCATGTAGGGCTTAATTGAGAATCTCGAGCCAGTAAGGATTTTG |
| Ring | 9 | TTCATAAAGAGCCGCCACCCTCAGAACAAAGCCTGTTTTCGAATTAGGAAT ACCGTGTCC |
| Ring | 10 | GGCAACAACAATCAATAGAAAATTCATTGAGGGAGGGTTCGAATTAGGAA TACCGTGTCC |
| Ring | 11 | AATAAGACAGAGAGAATAACATAAAAAAAAGTCAGAGTTCGAATTAGGA ATACCGTGTCC |
| Ring | 12 | AATATCCTCTTTCCTTATCATTCCAAGCCGTTTTTATTTCGAATTAGGAATAC CGTGTCC |
| Ring | 13 | AATCATAATTTTCTTACCAGTATAAAGCCAACGGCCAACATGTAA CGTTCGT |
| Ring | 14 | ATAGCCCCCTACCAGAGCCACCACCGGAACCGCAATAAACACCGG TGAAAAA |
| Ring | 15 | ATTACCATTACACCGTAATCAGTAGCGACAGAAGCATTTTCGGTC GGGCGTT |
| Ring | 16 | GGCGACATTCTTCATTAAAGGTGAATTATCACCACCAGTAGCACC AGGGGTT |
| Ring | 17 | GCAAACGTAGAAAGACACCACGGAATAAGTTTACAAAGACAAAAG CGGACAA |
| Ring | 18 | AGCCCTTTTTAAACCGAGGAAACGCAATAATAACGCAGTATGTTA TCTTGAC |

| | | |
|---|---|---|
| Ring | 19 | AACTGAACACGAGATAACCCACAAGAATTGAGTCTATCTTACCGA CATTGAA |
| Ring | 20 | TAAACAGCCATAACGTCAAAAATGAAAATAGCAGACGGGAGAATT TGTAGTA |
| Ring | 21 | GACTTGCGGGACCCAGCTACAATTTTATCCTGACCAGTTACAAAA ACTAAAC |
| Ring | 22 | CATCGAGAACCGCCCAATAGCAAGCAAATCAGAAGCGAACCTCCC ACGGCCA |
| Ring | 23 | ACAATAGATAAGCATGTAGAAACCAATCAATAAAAGTACCGCACT ATTAGGG |
| Ring | 24 | TTTAGGCAGACAAAAGGTAAAGTAATTCTGTCCGCCTGTTTATCA TATTCTT |
| Ring | 25 | ACTCACTCA CACCGGATATTAGCAGCGCGTTTTCATCGTCAAGTTACCATCG |
| Ring | 26 | TACTAACCG ATAGCAGGCAAGGCAGAGCCAGCAAAATCGTCACCGATTGACG |
| Ring | 27 | CACAGGTAC GAAATTAAACCGATATGGTTTACCAGCGCTTTTGTCTATAAAA |
| Ring | 28 | ACACGACTT GAAACGCAAAATACTAAGACTCCTTATTACGGAATAAAGTTAC |
| Ring | 29 | CCACACCTA CAGAAGGAAGAAAAATGAAATAGCAATAGTAAGCCCGCGCTAA |
| Ring | 30 | AAATCGCTT TATCAGACCTGAACCAGGGAAGCGCATTAGCCTTTAAACGATT |
| Ring | 31 | CCTCGAACT TTTTGTTTATTATTCCAGAGCCTAATTTGATCTTACAGTTGCT |
| Ring | 32 | CCACTGTAC ATTTTGCAGGTTTTAACGCGAGGCGTTTTTATAGAAAGGAATC |
| Ring | 33 | CCAGTCAGG ATTACCGAAGCAAGAACGGGTATTAAACCTCGGCTGCATCCTA |
| Ring | 34 | ACCAATCTC ATTTACGAGTCCTGGCTAATGCAGAACGCAGACGACATATAAA |
| Ring | 35 | TACAATCAC GTACCGAGGCATTTGCCATATTTAACAACCTCAACAATGCGTT |
| Ring | 36 | CTACGCAAA ATACAAAACTAGAACGCCACCCAAATAAGCTCCCTCTCAAAAT |
| Square | 1 | TACCAGACTTTGCCAGAGGGGGTATACTGCGGAATCGTCA |
| Square | 2 | CTAATGCAGATACATAAACAACATTATTACAGTGCGATTT |
| Square | 3 | ACGCCAAAAGGAATTCCTCGTT |
| Square | 4 | TAAGAACTGTGAATAAGGCTTGCCGCTGACCT |
| Square | 5 | CTGACGAGAAACACCAATTGTGAATTACCTTAGTAGAAAG |
| Square | 6 | CTCATTCAGGCTCATTATACCAG |
| Square | 7 | TCATCAAGCCGGAACGAGGCGCAGGAAACAAA |
| Square | 8 | CCAAGCGCACGGTCAATCATAAGG |
| Square | 9 | GTACAACGAGAGGCAAAAGAATAC |
| Square | 10 | AAAACGAAGAGATTTGTATCATCCTCCATG |
| Square | 11 | GAGGGTAGGAAGTTTCCATTAAACCAACCT |

| | | |
|---|---|---|
| Square | 12 | TTAAAGGCCGCTTTTGCTCGGAAC |
| Square | 13 | GTTTATCAGTTGCGCCGACAATGTTCGGTCGCTGAGGCTT |
| Square | 14 | GCGAATAATAATTTTTCTAAACAACTTTCAACCCTCATAG |
| Square | 15 | TCACGTTGAAAATCTTGTATCG |
| Square | 16 | TTAGCGTATTTCAGGGATAGCAAGCGTACTCA |
| Square | 17 | CCCAATAGGAACCCATGCATTCCACAGACAGCAGTTTCAG |
| Square | 18 | ACCCTCATACGATCTAAAGTTTT |
| Square | 19 | GGAGGTTTGAGAAGGATTAGGATTAAACAGTT |
| Square | 20 | GCCCGTATAGCGGGGTTTTGCTCA |
| Square | 21 | AATGCCCCAGGAGTGTACTGGTAA |
| Square | 22 | GATGATACCTGCCTATTTCGGAAGCTGAGA |
| Square | 23 | GACGATTGTGGAAAGCGCAGTCTGGCTTTT |
| Square | 24 | CACCAGAACCACCACCACAGGTCA |
| Square | 25 | AACTATATAAAACTTTTTCAAATTTTAATGGTTTGAAATA |
| Square | 26 | ATAGTGAATTTATCAATTCCCTTAGAATCCTTTTTTAATG |
| Square | 27 | AATCATAGGTCTGAGGTTATAT |
| Square | 28 | GAAACAGTATTATTCATTTCAATTACCTTTTA |
| Square | 29 | ACCTGAGCAAAAGAAGTCATTTGAATTACCTTGAAAACAT |
| Square | 30 | AGAGGCGAACATAAATCAATATA |
| Square | 31 | CATCGGGAAGAACCTACCATATCATTCCTGAT |
| Square | 32 | TCATCATAAAATTATTTGCACGTA |
| Square | 33 | TATCAGATGTAACATTATCATTTT |
| Square | 34 | AAGTTTGAGATGGCAATTCATCAAATAATG |
| Square | 35 | TAGAGCCGCAAACAATTCGACAAATTTTAA |
| Square | 36 | AAGGAATTGAGGAAGGTAATAGAT |
| Square | 37 | ACCGCCTGAGCATCACCTTGCTGGGTCAGTTGGCAAATCA |
| Square | 38 | CATCGCCATTAAAAATCACAGACAATATTTTTCACACGAC |
| Square | 39 | ACCGAACGAACCACCTATTAAC |
| Square | 40 | CAGTAATAGCCAGCCATTGCAACAATTAGTAA |
| Square | 41 | GGAAAAACGCTCATGGTGGCAGATTCACCAGTGAATGGCT |
| Square | 42 | ATATTACCAAAGGGACATTCTGG |
| Square | 43 | TAACATCAGCCAGAATCCTGAGAATAACGTGC |
| Square | 44 | AGCACGTAGTGTTTTTATAATCAG |
| Square | 45 | TTTCCTCGCCGCCGCGCTTAATGC |
| Square | 46 | CACCACACTTAGAATCAGAGCGGAGACAGG |
| Square | 47 | AGCTTGACGAAAGGAGCGGGCGCGCGTAAC |
| Square | 48 | GGGTCGAGGTGCCGTAAGATTTAG |
| Square | 49 | CGATCCTGATGTACGAAAGTCTTACTTAGAGTAATCTTGACAAGAAAGCTG |
| Square | 50 | CGATCCTGATGTACGAAAGTCCTCCTCAAAGTACCGCCACCCTCAGCCACC |
| Square | 51 | CGATCCTGATGTACGAAAGTCGAAGGGTTGAAACAATAACGGATATCGCG C |
| Square | 52 | CGATCCTGATGTACGAAAGTCAACGGTACCTTGCCTGAGTAGAACAGAAC A |
| Square | 53 | AAACCAAAATAGTTTTTGAAAGGAAGGG |
| Square | 54 | ATTCATCAGTTGAGTTTTTTTTGGTTGCTTTGACG |

| | | |
|---|---|---|
| Square | 55 | GTACAGAGAACCGAACTGACCTTTTTTCTACAACGCCTGTAGTACCGTAAC ACTGAATATAAGT |
| Square | 56 | ACTAAAACACTCATTTTAACTAAAGGAATT |
| Square | 57 | TTCATGAGCAACGGCTACATTTTTTTTGATACCGATAGCTTGCTT |
| Square | 58 | TCGAGGTGAATTTTTTTCTAAAGACTTT |
| Square | 59 | CGGAGTGAGAATAGTTTTTTTCCCCAGCGATTATA |
| Square | 60 | GTTTCGTCTTTTAGGACAGATGGGCTTGTTTTTCCATCAC |
| Square | 61 | ATAGCCCGTACCAGGCGGATATTTTTTTACATTTAACAATTATGATGAAAC AAACAGTTTAACG |
| Square | 62 | TAAGTTTTAACGGTTTTCTGAGAAGAGTCA |
| Square | 63 | AGCCAGAAGCCTTGATATTTTTTTTTAAGAACGCGAGGTAAATGC |
| Square | 64 | TGATGCAAATCCTTTTTATCCTCATTAA |
| Square | 65 | AGCGATAGCTTAGATTTTTTTCCTTGAGTAACAGT |
| Square | 66 | TCAGATGAAACAGAAATAAAGTTTTTTTGGATTATTTACATAAATACCTAC ATTTTGCAAATTA |
| Square | 67 | GCGGAACAAAGAATTTTGATAGCCCTAAAA |
| Square | 68 | AGACTTTATCAATAGATAATTTTTTTGAAAAATCTAACAACAGTG |
| Square | 69 | CCACGCTGAGAGTTTTTTTAGAAGTATT |
| Square | 70 | ATTAGTCTTTAATGTTTTTTTAAGGAGCGGAATTA |
| Square | 71 | GACGCTCATTTTATTTTCAGTCAAGAAATTTTGAGGGTTG |
| Square | 72 | ACCGTTGTGAGGCCACCGAGTTTTTTTTTTCAACTTTAATCGAACGAGTAGT AAATTGAACGGT |
| Square | 73 | GCCGCTACAGGGCTTTTATACCACATTCAA |
| Square | 74 | AAGAAAGCGGGGAAAGCCGTTTTTTTGCAAAAGAAGTGACGATAA |
| Mini-barrel | 1 | GCCTCACCTGCATGCGGGCAAAATCTTGATAAGAGG |
| Mini-barrel | 2 | CCCACCACCGGATCCGGGCAAAGAACCGGAGAGGGT |
| Mini-barrel | 3 | GGGCACACGGTTTCGCTAGCCAGCTAGGGCGATCGG |
| Mini-barrel | 4 | CCACTCGCACCCACAAATTGTTGTGGCAATACATCA |
| Mini-barrel | 5 | GCGCGGCACTGGAAGTGTAACTATCGCTGATACCGT |
| Mini-barrel | 6 | CGTATCCTCGCAAGCCCGATACTTGGTGTAAAGCCT |
| Mini-barrel | 7 | TCATTTTTGCATACAGGCAATCTACACGTCGTTTGC |
| Mini-barrel | 8 | AGCTATTTTTGGCCTTCCTGGTTGAACGGGTCTGCT |
| Mini-barrel | 9 | TGCGGGCCTATCTGCCACTCCGCACGTTCGAAATGG |
| Mini-barrel | 10 | AACGCCGCGAAGACCCGTTAAGGACACAGCTGACTA |
| Mini-barrel | 11 | TTAGCTGAATACGGTGGAAACCTGATGTGAATGGTG |
| Mini-barrel | 12 | GGGGTGCCTGTTCCGAAATCACCAACTGGAGACCCG |
| Mini-barrel | 13 | CTGTCGCAGCAAAGGCAAAATCAAAGATTAGAGAGT |
| Mini-barrel | 14 | CCGCGGCTAGCCAGCAATAATTAAGTTCAACCGTTC |
| Mini-barrel | 15 | TGGCTGGGCCGCTACCCAACATTAACGCCATTCAGG |
| Mini-barrel | 16 | AGGTTCACCTGAAGCGCTCGATCCGAACTGCTGGAT |
| Mini-barrel | 17 | TAGCATATCTGGGACTGCTTACGCATATCTTACTGT |
| Mini-barrel | 18 | ACACGGCGGTGGCACAAATGTACAACACACAACATA |
| Mini-barrel | 19 | ACTTAGAGCATAGTAGTAGCGTCTGTCGGAGCGTTA |
| Mini-barrel | 20 | TACTACAAAAGGAACGCCATTGAGTTCTACAACCTA |
| Mini-barrel | 21 | CTTTACGCCAAATGCGCCGCGCCCCTGCATGTGGGC |
| Mini-barrel | 22 | GAAACGAGGGAAGAGTTTCTGGGCGGCCATGCCAGA |

| | | |
|---|---|---|
| Mini-barrel | 23 | TTCATTGCATGATACCGTGCGCACAGAAGTTCCGGG |
| Mini-barrel | 24 | CGAGCTAACCAGCAGGCGAATCCATCGCTGCTTGGT |
| Mini-barrel | 25 | CGAGCGGTCTACTAACTCCCCGAGAAGACCGGAAGC |
| Mini-barrel | 26 | TGGCTGAGGGATCTTTTGGCCTCAGAGACAGTCAAA |
| Mini-barrel | 27 | CTGAGCCGCCGATGAACTCGAGTAAGGTGCCGGAAA |
| Mini-barrel | 28 | CGGTTATCGACCTGCTGCAACGAAGGAATTGGTAAC |
| Mini-barrel | 29 | GTGCTGCCCATAGGGAACTACGGGGGACCGTACTCA |
| Mini-barrel | 30 | ACCGTTGCGGGTCACCAAAGATGATGTGTGAAATTG |
| Mini-barrel | 31 | AATGAATATAGCTGAAAAGGCGGAGGTCGGCCTCGG |
| Mini-barrel | 32 | TCGGTCATTTGTTAAATCAGCACCCGAGGGGCGTGG |
| Mini-barrel | 33 | CCAAAGGGGGAAGAATTACACGGGGATCGTAGTGCT |
| Mini-barrel | 34 | ACCTAACAGTGTTATCAAGCACGGACGAGGAGTGGG |
| Mini-barrel | 35 | AAATAAATGCCCCATTCTGCATTAGGCCCCTGAACC |
| Mini-barrel | 36 | TTATTGCGTGCAGCAAGCGGGTGTTCTCCTGCTAGC |
| Mini-barrel | 37 | TGACTCTCAGGATACCCTGAGTGTTCGTTTTAATTC |
| Mini-barrel | 38 | CGGCTATCCCCACTCCTTAGCTAAAAAAGATTCAAA |
| Mini-barrel | 39 | GCGCGAGACCTGGGATAATCGGATTCTCCAGCCAGC |
| Mini-barrel | 40 | TCAGCTTGGACACAGAATGTCGTTCCTGGGGATTTG |
| Mini-barrel | 41 | TCCTCTCTCAGGGATCCATCAATGGGATGCCAGAGT |
| Mini-barrel | 42 | CCCGTGGATTGGCACAGTAATATTATTCGTAATCAT |
| Mini-barrel | 43 | GAAGCTCAAGTTTAGCTATACTACTTGGGGGCGGGC |
| Mini-barrel | 44 | AGGTCTGGATATTTTGTTAATTGCTCAAGGCGCACT |
| Mini-barrel | 45 | TTGCAAGGCAGACATCATTGGAGCCGCATGGCCGAT |
| Mini-barrel | 46 | ACCTGCGTGTTGTTGTTCGCCTCGGTTCGGAGCCTG |
| Mini-barrel | 47 | CTTGAGTTAAAGGTTTATAACAACACTGGGCCCCGC |
| Mini-barrel | 48 | GGCTGCCCGCCCTTCACCGCGAGTGCTTCATCGCCC |
| Mini-barrel | 49 | GAACCGAGACACACATCGTTTGGAAGAGGAAGCCCG |
| Mini-barrel | 50 | GAACCCCATCTGCCCGCATACCAAAAAATGCAATGC |
| Mini-barrel | 51 | TCTCCGCCACCGCATCTAGGAACAACGACAGTATCG |
| Mini-barrel | 52 | GGTGGCATGGGCGATTGATCGGACTAAGCGGCAGAG |
| Mini-barrel | 53 | GGGTTCGGGAGTGACAAGATGCAGGATGCTGAATTT |
| Mini-barrel | 54 | GTTCCCGACCTCATCGCAATCCTCGGAATGGATCCC |
| Mini-barrel | 55 | AAAAATATGGATACATTTCGATCCCAGGTCCGCCGT |
| Mini-barrel | 56 | CTGAGAATCAAGCAAATATTAACCGAGCCTAGACGC |
| Mini-barrel | 57 | GCTGGGTAAAACAGTTCAGGGGTAACAACCTCAGTT |
| Mini-barrel | 58 | CAGAAACAGGAAGTCCGTGACAGAGACCCGTCGAGC |
| Mini-barrel | 59 | CGGCAAAAATATAGAGTCGGAAGTCAGCGCGCACCT |
| Mini-barrel | 60 | CGTCGGGAACACCAGTGAGACTTGGGGCGGCGTGCA |
| Mini-barrel | 61 | ATGTCTTCTCAGAATGAGCCACTATGCAAAGCGGAT |
| Mini-barrel | 62 | CCAGAAATCACGGGGCATTGACCCTAAAAATTTTTA |
| Mini-barrel | 63 | GTGGCGTTCACTTGTTAAATTGACCCCGTGCATCTG |
| Mini-barrel | 64 | GTCGTACGTTGTCCAACCGTTGCCAAGCGAAATTAA |
| Mini-barrel | 65 | CCAATTTGCGACCCCGCTCTGCATAGGTTTTGTAAA |
| Mini-barrel | 66 | GGTGCCTCAGTATCCGGTGGGGATTATGATAAATGC |
| Mini-barrel | 67 | TGGTACGGTCGAACGAGTAGGAGCAGGCCCGGACCG |
| Mini-barrel | 68 | GAGTAATCGAAAAGCCCCAAGGCACTGCCTTCGTTC |

| | | |
|---|---|---|
| Mini-barrel | 69 | CCTTTTCCCTTCGCATTCACTGTGGGGCGACGAACC |
| Mini-barrel | 70 | CTAAACTCATAAGCGTATTGTTTCCCACTTGCTGCG |
| Mini-barrel | 71 | AGGTTATCAAAGGTGTTTATCATCTGAGGGAGTGCC |
| Mini-barrel | 72 | ACTGCCAGCTATTGGGCGCCCCGAGCGCCCCTGCCC |
| Mini-barrel | 73 | CAAAAGCCTGTGATCGGGCGTGGACTCCTTTACCCT |
| Mini-barrel | 74 | CGCGCCGCTGATAGGAAGCTGGAACTTATCAGTAAA |
| Mini-barrel | 75 | GAGTTTCATTCCATATAACAATGATTAGGACGCAGT |
| Mini-barrel | 76 | CACGTGAGTATTACGAAGGTCACAGCGGCGGGATTA |
| Mini-barrel | 77 | GCGCAGGGCTCCGACCGTTTTTGCGGGA ATAGGCTG |
| Mini-barrel | 78 | CTGGGCCCGGCCGATAGGTCACGTTGGTGTAGCGTTGTAAAA TGTATCAC |
| Mini-barrel | 79 | CGATCCGGCTCACCCAGTTGACGCTGGC GTAACAGT |
| Mini-barrel | 80 | AGGTCGGATGTCTCTGAACTCGCTACGGCGGGTGAATCGGCC CTTCTTTG |
| Mini-barrel | 81 | CCAGGCGCGAAGCCTTTAGCATGTCAATCATATGTACGTACTGGGAAACC GG |
| Mini-barrel | 82 | GGAATAGG CGACGGCCATCCGGACACCTCTCGATGAGA |
| Mini-barrel | 83 | AATATACAATTCGCATCACAGATCCGGTGTCTTGTCTCGATCGCCAGTTAT G |
| Mini-barrel | 84 | TAGCAATA AACGCGCGCGCATGCCGAACCTGGGGGGCT |
| Mini-barrel | 85 | CTGTTTGATGGTGAATGAGTGAGCCGGAAGCATAAACCCTCTCAA |
| Mini-barrel | 86 | ACATCCAATAAATCGGATGGCCTTTAATTGCTCCTTCCTTATATC |
| Mini-barrel | 87 | AATAATTCGCGTCTGAGAGATGCTGATAAATTAATGTTAGCAATA |
| Mini-barrel | 88 | ACCACCAGGCTATCTTCGCTAGCGCAACTGTTGGGATTCATCAAA |
| Mini-barrel | 89 | CAGTTAATCGAACACCAGGAGACGGGAAAGAAACCAAGTGTGGGA |
| Mini-barrel | 90 | TTATTATCACGAGACGACATACTTTACATAAACATTGACATCAGG |
| Mini-barrel | 91 | TCCAACAGGTCAGAGAATAGCACGCTGGTTTGCCCTCACATTAAT |
| Mini-barrel | 92 | CATCAATATGATACAATAAAGCATCAATTCTACTATTAATTGCAC |
| Mini-barrel | 93 | GCAAAGCGCCATTATGTGAGCATTTTTTAACCAATGGCTATCAAC |
| Mini-barrel | 94 | TCGATTGTGCTGGATAGATGGCAACACAGCAATAAAGCTGGCGAG |
| Mini-barrel | 95 | TCGGGTTGAGTATTCGCTATTGCACTGGTGACCTGATATTGCGCA |
| Mini-barrel | 96 | CCGCTCACAATTCAACATATTGTGCGAGAAATGACAGGAGTTTCA |
| Mini-barrel | 97 | CCCTGAGAGAGTTTGCGCTCATCATAGCTGTTTCCTTAAACCCCT |
| Mini-barrel | 98 | CATTTGGGGCGCGAATGCTGTGCTTCAAAGCGAACCTAGGGTTGG |
| Mini-barrel | 99 | CGCATTAAATTTTGCCTGAGAGGTGAGAAAGGCCGGAGCATAATT |
| Mini-barrel | 100 | AGCATCAGAAATAGATGTGCTTCCGGCACCGCTTCTCAACCCGTT |
| Mini-barrel | 101 | CTGGGAAGACTCCTAGGGAAAGCAGACCTTTTCCATACGCCTGTC |
| Mini-barrel | 102 | AATGAAGACAAATAGTATCAAGTAGTGTCAGATGATTTGGAGGTC |
| Mini-barrel | 103 | ACTTCAAATATCGGTTCCAGGGCAACAGCTGATTGCTTTCCAGGG |
| Mini-barrel | 104 | GTAATGTGTAGGTTCGGTTGAATGGTCAATAACCTCATGTTTTAG |
| Mini-barrel | 105 | CAGGAAGATCGCACTCCGTGAATTGTAAACGTTAAGCAAACAAGA |
| Mini-barrel | 106 | CAATGCATGACGAAGGGTTGTTAATGAAAGATGGCGATTAAGTCT |
| Mini-barrel | 107 | TCGTCTTCACAGCGTTCAGGACGGAAACCAGTTTCTTGAGCTTGG |
| Mini-barrel | 108 | TACCGAGCTCGAACATAACATACAAATATTCCATGGAGTCTGACG |
| Mini-barrel | 109 | TGGTTTTTCTTTTACCTGTCGTTCCGAGTCACAGGACACTCGCAG |
| Mini-barrel | 110 | AGTTTGACCATTACAACTAAACATCAAAAAGATTAACAAGAGTGG |
| Mini-barrel | 111 | AGGAAGATTGTATGATGAACGACCCTCATATATTTTAACATTATT |
| Mini-barrel | 112 | ATGCGTATTAACCCGCCAGGGAGTTTGAGGGGACGAACGGCGGAC |

| | | |
|---|---|---|
| Mini-barrel | 113 | ACTGGAAAGCAACCAAAATCACTCAGGCACTGCGTGTGTGCAATC |
| Mini-barrel | 114 | ATGAAGGTATAGAGATTGGGCATAACGCTTGTGAAATGAGTATAA |
| Mini-barrel | 115 | ATTATAGTCAGAATAAAGAAGAGAGGCGGTTTGCGTGCATTAATT |
| Mini-barrel | 116 | TCAACGCAAGGATGTAATACTGATTCCCAATTCTGGTCTGGAACT |
| Mini-barrel | 117 | GGGCGCATCGTAAGTAATGGCCGGTTGATAATCAGTAAAACTATT |
| Mini-barrel | 118 | GAGGTTCGAAGTGGGAGGATTGCCAAGCTTTATTAAGTCACGAAT |
| Mini-barrel | 119 | GGAGAGTGAGATCTGATGTCTATCTCGGATGGGAGACGAGCAGGA |
| Mini-barrel | 120 | TTGTTTTATGGAGTATTTTACATGCAGACATCACGATGTTGTGAA |
| Mini-barrel | 121 | CGTGTAGACGGATCCGGTGGTGGGAGCAGACC |
| Mini-barrel | 122 | CGTTCAACGCGAAACCGTGTGCCCCCATTTCG |
| Mini-barrel | 123 | AACGTGCGTTGTGGGTGCGAGTGGTAGTCAGC |
| Mini-barrel | 124 | TGTGTCCTACTTCCAGTGCCGCGCCACCATTC |
| Mini-barrel | 125 | ACATCAGGGGCTTGCGAGGATACGCGGGTCTC |
| Mini-barrel | 126 | CAGTTGGTCGCATGCAGGTGAGGCGCAAACGA |
| Mini-barrel | 127 | CGACAGACTGCTGGCTAGCCGCGGTAGGTTGT |
| Mini-barrel | 128 | AGAACTCAGGTAGCGGCCCAGCCAGCCCACAT |
| Mini-barrel | 129 | GCAGGGGCCGCTTCAGGTGAACCTTCTGGCAT |
| Mini-barrel | 130 | GGCCGCCCAGTCCCAGATATGCTACCCGGAAC |
| Mini-barrel | 131 | TTCTGTGCTGTGCCACCGCCGTGTACCAAGCA |
| Mini-barrel | 132 | GCGATGGAGCCTTTGCTGCGACAGTAACGCTC |
| Mini-barrel | 133 | GACCTCCGAAAGATCCCTCAGCCACCACGCCC |
| Mini-barrel | 134 | CTCGGGTGTTCATCGGCGGCTCAGAGCACTAC |
| Mini-barrel | 135 | GATCCCCGAGCAGGTCGATAACCGCCCACTCC |
| Mini-barrel | 136 | TCGTCCGTTCCCTATGGGCAGCACGGTTCAGG |
| Mini-barrel | 137 | GGCCTAATGGTGACCCGCAACGGTGCTAGCAG |
| Mini-barrel | 138 | GAGAACACGTTAGTAGACCGCTCGCCGAGGCC |
| Mini-barrel | 139 | CCAAGTAGGGAGTGGGGATAGCCGAGTGCGCC |
| Mini-barrel | 140 | TTGAGCAAATCCCAGGTCTCGCGCATCGGCCA |
| Mini-barrel | 141 | TGCGGCTCTCTGTGTCCAAGCTGACAGGCTCC |
| Mini-barrel | 142 | GAACCGAGGATCCCTGAGAGAGGAGCGGGGCC |
| Mini-barrel | 143 | CAGTGTTGTGTGCCAATCCACGGGGGGCGATG |
| Mini-barrel | 144 | AAGCACTCGGTATCCTGAGAGTCAGCCCGCCC |
| Mini-barrel | 145 | CCTGGGATCGGGCAGATGGGGTTCGCGTCTAG |
| Mini-barrel | 146 | GCTCGGTTGATGCGGTGGCGGAGAAACTGAGG |
| Mini-barrel | 147 | TTGTTACCAATCGCCCATGCCACCGCTCGACG |
| Mini-barrel | 148 | GGTCTCTGTGTCACTCCCGAACCCAGGTGCGC |
| Mini-barrel | 149 | GCTGACTTCGATGAGGTCGGGAACTGCACGCC |
| Mini-barrel | 150 | GCCCCAAGATGTGTGTCTCGGTTCACGGCGGA |
| Mini-barrel | 151 | GCCTGCTCGCCCCGTGATTTCTGGGAACGAAG |
| Mini-barrel | 152 | GCAGTGCCAACAAGTGAACGCCACGGTTCGTC |
| Mini-barrel | 153 | GCCCCACATTGGACAACGTACGACCGCAGCAA |
| Mini-barrel | 154 | GTGGGAAACGGGGTCGCAAATTGGGGCACTCC |
| Mini-barrel | 155 | CTCAGATGCGGATACTGAGGCACCGGGCAGGG |
| Mini-barrel | 156 | GCGCTCGGCATTCTGAGAAGACATCGGTCCGG |
| Mini-barrel | 157 | CTAATCATGGTCGGAGCCCTGCGCCCGGTTTC |
| Mini-barrel | 158 | CCAGTACGCCGGGCCCAGTCTCATCGAGAGGT |

| | | |
|---|---|---|
| Mini-barrel | 159 | GTCCGGATTCCTATCAGCGGCGCGTAATCCCG |
| Mini-barrel | 160 | CCGCTGTGTGGGTGAGCCGGATCGCATAACTG |
| Mini-barrel | 161 | GCGATCGACATCCGACCTAGCCCCCCAGGTTC |
| Mini-barrel | 162 | GGCATGCGCGATCACAGGCTTTTGACTGCGTC |

**SI Table 5. Staple list for DNA origami barrel to bind DNA origami cap (replace subpool "IM H1/24 -overhang")**

| Subpool | # | Sequence |
|---|---|---|
| IM H1/24 +sockets | 1 | CCGTCTATTGTAGCAATACTTCTTTGATTCACCAG |
| IM H1/24 +sockets | 2 | TGCCATCTATTCAACCGATTGAGGGAGGTATTGAC |
| IM H1/24 +sockets | 3 | GATATAAGAGCTACAATTTTTACCAGCGCCGTTCC |
| IM H1/24 +sockets | 4 | CAACCATCTTGAAGCCTTAAATCAAGATTTCCAGA |
| IM H1/24 +sockets | 5 | AAGAACCGGCGAGGCGTTTTAGCGAACCACACTCA |
| IM H1/24 +sockets | 6 | TCCCCCTCTCAAATATATATAGAAGGCTAAAGATT |
| IM H1/24 +sockets | 7 | GTAGCATTCAAATCCAATCGCAAGACAATTGCGGA |
| IM H1/24 +sockets | 8 | GTTAATATGCTTAGGTTGGGTTATATAATCAAATC |
| IM H1/24 +sockets | 9 | GTGCCAAGTCATTTTGCGGGTCTGAGAGGACGACG |
| IM H1/24 +sockets | 10 | AAACTGCGGCCCGAACGTTATTAATTTTCAGGAGG |
| IM H1/24 +sockets | 11 | TACATAAAGACTTTACAAACAATTCGACACATCAT |
| IM H1/24 +sockets | 12 | AATCATGGCTGAGTAGAAATAATACATTCAATGTG |
| IM H1/24 +sockets | 13 | AAATTAACCGTCAAGCGGTCGTCCATCGTAAAGAAGACGC TGAGTGAGT |
| IM H1/24 +sockets | 14 | AAAAGGGCGACTTTCATAATTCTCTGAATTTACCAAAGAC CGGTTAGTA |
| IM H1/24 +sockets | 15 | ATTTTGCACCCTATAGCCCGGTTTTGTCGTCTTAGTTGCT GTACCTGTG |
| IM H1/24 +sockets | 16 | TGCGGGAGGTTGCCCACGCAGAATACACTAAATCCCGACT AAGTCGTGT |
| IM H1/24 +sockets | 17 | ATTCTAAGAACGATATTCATTATTACAGGTAGTATCCGGT TAGGTGTGG |
| IM H1/24 +sockets | 18 | AGAAAACTTTTAAATGCTTTAAGAGGTCATTTAGAACGCG AAGCGATTT |
| IM H1/24 +sockets | 19 | AAATGCTGATGAACATCCAAGGCCGGAGACAGCTATATGT AGTTCGAGG |
| IM H1/24 +sockets | 20 | TTTAACCTCCGTTTGTTAAACCAGTTTGAGGGACTACCTT GTACAGTGG |
| IM H1/24 +sockets | 21 | GAGTAACATTACTTTATTATTGTGCAAGTTGCAAAAGTTT CCTGACTGG |
| IM H1/24 +sockets | 22 | TTAAATCCTTTTGTTGAGCTTAGTAACTATCGAACTCGTA GAGATTGGT |
| IM H1/24 +sockets | 23 | TAGAAGTATTACATTGCTGAATCCCCATTCTGTGAGGATT GTGATTGTA |
| IM H1/24 +sockets | 24 | ACATCACTTGCTCATAGCTGTGGTTTTTCTTTTAGTAATA TTTGCGTAG |

### SI2.4. DNA origami folding

Nanostructure synthesis was carried out by mixing 10 nM M13 scaffold with a 10x excess of staples in 1x TE (5 mM Tris + 1 mM EDTA, pH 8) + 12 mM (DNA origami barrel) or 10 mM

$MgCl_2$. The solutions were subjected to a thermal annealing ramp on a Tetrad 2 Peltier Thermal Cycler (Bio-Rad) according to the following schedule:

DNA origami barrel
Incubate at 65°C for 15 minutes
Decrease to 50°C at 20 seconds/°C
Incubate at 50°C for 6 hours
Decrease to 40°C at 6 hours/°C
Incubate at 40°C for 6 hours
Store at 4°C

DNA origami cap
Incubate at 80°C for 15 minutes
Incubate at 60°C for 30 minutes
Decrease to 25°C at 30 minutes/°C
Incubate at 25°C for 30 minutes
Store at 4°C

**SI2.5 DNA origami purification**

To remove excess staple, DNA origami barrel was purified using solid-phase reversible immobilization (SPRI)[SI-R2], and DNA origami cap was purified using PEG precipitation[SI-R3]. The assembled tetramer of DNA origami barrels were purified via rate-zonal centrifugation[SI-R4]. Following purification, the stock concentration was determined by UV-absorbance at 260 nm on a Nanodrop spectrophotometer (Thermo Scientific). Purification was performed right before use to prevent any aggregation or denaturation of DNA origami.

SPRI
The 100-mL of SPRI solution was prepared as the following:
6.3 mL of distilled water
50 mL of 5 M NaCl
1 mL of 1 M Tris-HCl, pH 8
200 μL of 0.5 M EDTA
40 mL of 50% PEG 8000
0.5 mL of 10% Tween20
2 mL of Sera-Mag™ Magnetic SpeedBeads™

0.3x volume of SPRI solution was added to 1x volume of DNA origami barrel solution in 1.5-mL centrifuge tube. The resulting solution was incubated for 5 minutes at room temperature. The tube was placed in the rack of DynaMag™-2 Magnet (Thermo Fisher Scientific) for 10 minutes, and the supernatant containing excess staple strands was aspirated without disturbing the beads using pipette. The magnetic beads were washed twice with 200-500 μL of 70% ethanol with 1x TE (5 mM Tris-HCl + 1 mM EDTA, pH 8) + 10 mM $MgCl_2$ followed by aspiration without disturbing the beads. The beads were air-dried at room temperature for 5 minutes. The

tube was removed from the magnet, and desired volume of 1x TE + 12 mM $MgCl_2$ was added followed by pipette mix to break down the clumped beads. The tube was incubated at 37°C with 1k RPM for 10 minutes. The tube was returned to the magnet for 2 minutes, and 95% of the solution was transferred to a fresh tube. The purification step was performed twice to remove sufficient amount of excess staple strands.

PEG precipitation

The 2x PEG precipitation solution was prepared as the following:
12% PEG 8000 (w/v)
5 mM Tris-HCl, pH 8
1 mM EDTA
750 mM NaCl
10 mM $MgCl_2$

1x volume of 2x PEG precipitation solution and 1x volume of DNA origami cap were mixed in 1.5-mL centrifuge tube and incubated at room temperature for 10 minutes. The resulting solution was centrifuged at 16.9k x g for 20 min using temperature control set to 25°C. The supernatant containing excess staple strands was removed using pipette without disturbing pellet. The desired volume of 1x TE + 12 mM $MgCl_2$ was added to the tube followed by pipette mix to break down the pellet. The tube was incubated at 37°C with 1k RPM for 30 minutes.

Rate-zonal centrifucation

The crude reaction to assemble tetramer of DNA origami barrels was concentrated using a 100k MWCO Amicon Ultra centrifugal filter device (Millipore) and purified by glycerol gradient ultracentrifugation. Instead of 15-45% gradient as previously described [SI-R4], we used 35-65% gradient since the tetramer equilibrated at higher % glycerol fraction compared to monomer. Following purification, the stock solution was diluted appropriately for TEM imaging to verify quality.

**SI2.6 Assembly of DNA origami structures**

Tetramer of DNA origami barrels

2 nM of homodimer of DNA origami barrels and 4 nM of DNA origami barrel with DNA overhangs for assembly were mixed with 500 nM each of connecting strands in PCR tube. The sample was incubated for 1 hour at 37°C.

DNA origami capsule

~1 nM of purified tetramer of DNA origami barrels was incubated with 10 nM of purified DNA origami cap for 1 hour at 37°C.

**SI2.7. Agarose gel electrophoresis**

DNA nanostructures were analyzed by gel (1.5% agarose, 0.5x TBE + 10 mM MgCl2, 1x SYBR Safe) electrophoresis with Thermo Scientific Owl B2 EasyCast Mini Gel System apparatus. The samples were loaded into the agarose gel and allowed to migrate for 2-4 hours (running buffer:

0.5x TBE, 10 mM MgCl2; 4.3V/cm). The gel was imaged with Typhoon FLA 9000 (GE Healthcare Life Sciences).

### SI2.8. Negative-Stain Transmission Electron Microscopy

TEM imaging was carried out by dropping 3.5 μL of product onto a plasma-treated carbon-formvar grid (Electron Microscopy Sciences). This was incubated for 1-5 minutes depending on the concentration of DNA origami. The solution was wicked away onto the edge of folded filter paper at 45° without completely drying out the sample, and 5 μL of 2% uranyl formate (in water, w/v) was immediately added. The grid was incubated for 10-30 seconds, and the uranyl formate was wicked away completely onto the edge of folded filter paper at 90°. Imaging was carried out on a JEOL 1400 transmission electron microscope.

### SI3. Supplemental References


SI-R1. Douglas, S. M.; Chou, J. J.; Shih, W. M. DNA-Nanotube-Induced Alignment of Membrane Proteins for NMR Structure Determination. *Proceedings of the National Academy of Sciences* **2007**, *104*, 6644–6648.

SI-R 2. DeAngelis, M. M.; Wang, D. G.; Hawkins, T. L. Solid-Phase Reversible Immobilization for the Isolation of PCR Products. *Nucleic acids research* **1995**, *23*, 4742–3.

SI-R 3. Stahl, E.; Martin, T. G.; Praetorius, F.; Dietz, H. Facile and Scalable Preparation of Pure and Dense DNA Origami Solutions. *Angewandte Chemie (International ed. in English)* **2014**, *53*, 12735–40.

SI-R 4. Lin, C.; Perrault, S. D.; Kwak, M.; Graf, F.; Shih, W. M. Purification of DNA-Origami Nanostructures by Rate-Zonal Centrifugation. *Nucleic Acids Research* **2013**, *41*, e40–e40.

# Chapter 4: Extrusion of RNA From a Cytosolic Nanofactory

Jaeseung Hahn, Leo Y. T. Chou, Rasmus S. Sørensen, Richard M. Guerra, William M. Shih

## 4.1 Introduction

RNA is a programmable drug candidate for treatment of wide variety of diseases owing to its involvement in many biological processes such as protein synthesis and gene regulation.[1,2] However, RNA-based therapeutics are unstable in the biological environments due to the plethora of RNA nucleases present. The instability of RNA was addressed with moderate success by chemical modification[3] and use of nanovehicles[4] to increase the half-life of RNA molecules. Nevertheless, the current delivery systems are unable to deliver a sufficient amount of RNA-based therapeutics that would be useful for general therapeutic applications.

We propose an alternative solution for the problem of RNA delivery through integrated rolling-circle transcription and processing of therapeutic RNAs within the cell cytoplasm. Cytoplasmic viral factories (e.g. poxviridae) co-localize replication machinery for efficient RNA transcription and processing. However, synthetic mimicry of such molecular organization remains challenging to implement using current genetic and protein engineering methods. Cytoplasmic expression systems have been developed by co-delivery of bacteriophage DNA-dependent RNA polymerase (RNAP) genes[5–7] or proteins[8] with DNA templates. However, the cytoplasmic concentration of DNA templates was shown to be the limiting factor when T7 RNAP mRNA was co-delivered.[6] Therefore, an alternative approach is necessary to integrate molecular components, which improves the interaction-dependent function under limited delivery efficiency. Solving this challenge could compensate for inefficiencies in delivery (e.g. endosomal-entrapment difficulties) since the escape of even a single vector particle to the cytoplasm can lead to the production of thousands of RNA molecules, without the need for trafficking to the nucleus.

We developed a biomolecular nanofactory that is capable of producing and processing an RNA transcript (Figure 1a). Specifically, this work addressed two design challenges: (1) complex molecular integration and (2) spatially coordinated enzymatic cascade. We demonstrated co-localized RNA production and processing through modular assembly of DNA origami structures programmed with RNA production and processing units. The modular nature of the design allows functional modification through addition of components such as DNA templates that encode different RNA products and RNA processing enzymes that can perform different modifications of RNA.

## 4.2. Results and Discussion

### 4.2.1 DNA origami chassis

A DNA origami barrel structure with a diameter and a height of 58 and 24 nm, respectively, was used as a molecular chassis (Figure 1b). The inner layer of DNA helices has 48 addressable "pixels", which are nick points of staple strands that can have ssDNA "handles" at the 5'-ends that can be used as attachment points for components modified with complementary ssDNA. The pixels were arranged in a rhombic-like lattice with the shortest distance being the side of the rhombus at 7.4 nm. The barrel can be modified with orthogonal sequences of ssDNA extensions for each molecular component in the desired configuration to assemble functional units for the nanofactory. The barrels can be homodimerized or stacked on top of one another to assemble the chassis functionalized with different functional units.

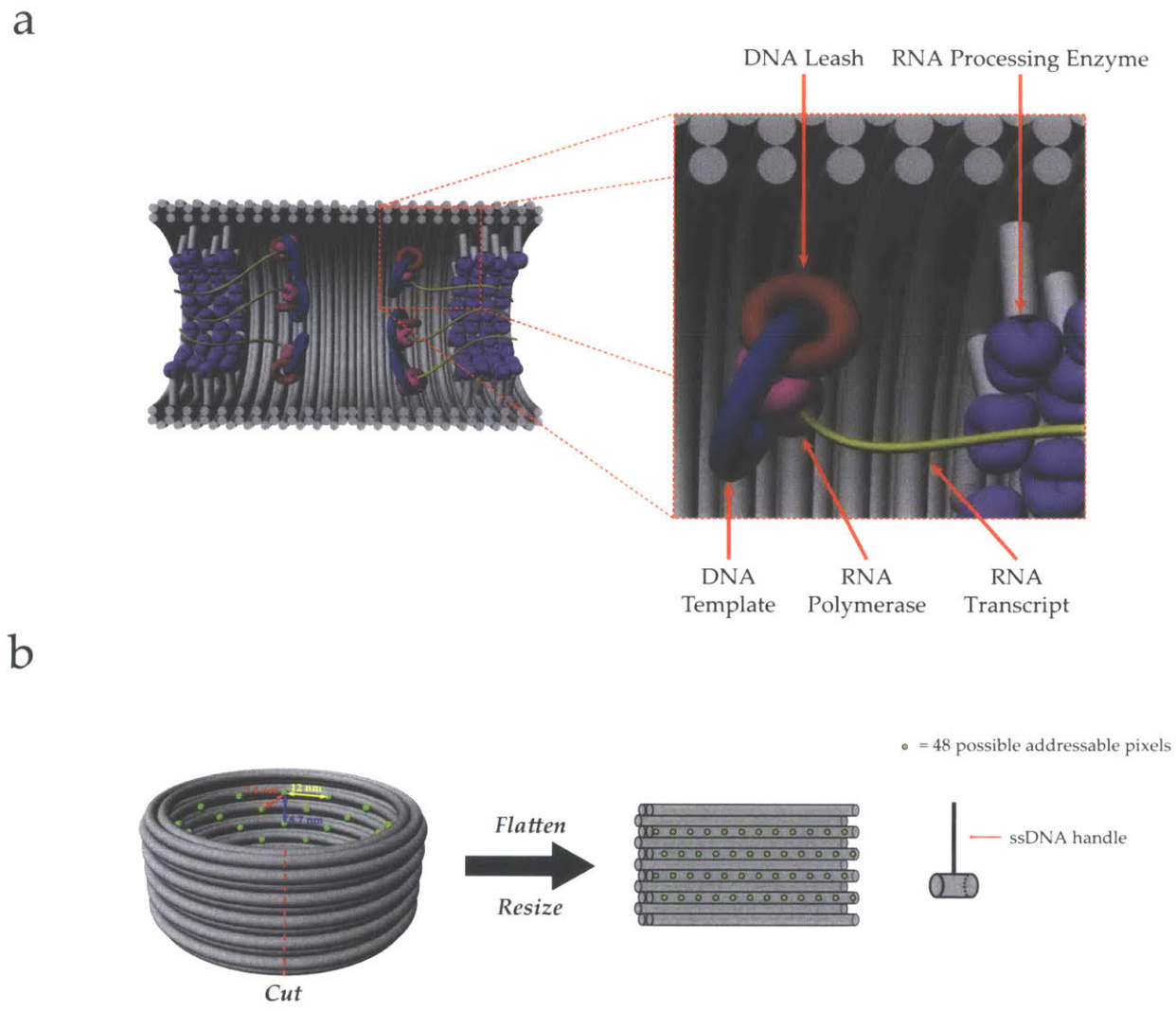


**Figure 1. Illustration of envisioned nanofactory and basic subunit of DNA origami chassis.** (a) Cross-section schematic of a cytosolic nanofactory. Each RNA polymerase is tethered to a circular DNA template via a catenated DNA leash, which is tethered to the DNA origami chassis. The co-localization of RNA polymerase and circular DNA template allow rolling-circle transcription of RNA concatemer. RNA processing enzymes are tethered towards the exit point of the DNA origami chassis for post-transcriptional modification prior to export. (b) Schematic of basic subunit of DNA origami chassis. A DNA origami barrel is a basic subunit of DNA origami chassis composed of four DNA origami barrels. The green spheres represent addressable pixels, and the distances between the pixels are labeled. To easily visualize all 48 addressable pixels inside the DNA origami barrel, the illustration of cut-opened and flattened DNA origami barrel structure is shown to the right. The addressable pixel is a ssDNA handle that can bind to any molecules that is attached to complementary DNA oligonucleotides. Each cylinder represents a DNA duplex, and each ribbon (3D illustration) or line (2D illustration) represents single-stranded nucleic acids.

### 4.2.2 RNA production unit

An RNA production unit capable of rolling-circle transcription of target RNA is composed of T7 RNA polymerase (RNAP) and a circular DNA template with T7 promoter sequence followed by a desired transcript sequence. To allow rolling-circle transcription while co-localizing T7 RNAP and circular DNA template, we mechanically locked another circular DNA strand to the circular DNA template to form a DNA catenane. This way, T7 RNAP modified with ssDNA oligonucleotide can self-assemble to the circular DNA template through DNA hybridization with the mechanically locked circular DNA to form the RNA production unit.

A catenane DNA template was constructed by ligating two linear ssDNA oligonucleotides, leash and template strands (Figure 2a). The leash and template strands were assembled by a 10-bp complementary region along with other adaptor oligonucleotides to help bring leash and template strands together in the right conformation and to splint 3'- and 5'-ends of the leash and template strands for circularization of each strand (see SI1). The leash strand has a complementary sequence to the ssDNA oligonucleotide attached to T7 RNAP so that the two components can self-assemble in solution as well as complementary sequence to one of the ssDNA handle sequences on the DNA origami barrel. In addition, we installed a 9-nt sequence for the quantification of the incorporated catenane DNA template using DNA-PAINT[9–11] to quantify its incorporation efficiency on the DNA origami chassis.

The SNAP-tag[12,13] was fused to the N-terminus of T7 RNAP known to be amenable to modification[14], and the fused SNAP-tag covalently attached T7 RNAP to the desired sequence of ssDNA oligonucleotide modified with $O^6$-benzylguanine at 3'-end (Figure 2b). To impose transcription specificity of T7 RNAP to the DNA template hybridized to the protein, T7 RNAP was complexed with a transcription inhibitor. The transcription inhibitor is a T7 promoter sequence without downstream sequence for transcription. The DNA binding pocket of T7 RNAP is therefore occupied with T7 promoter on the transcription inhibitor and cannot bind other other DNA templates. The DNA duplex formed between T7 RNAP and the transcription inhibitor is 13 bp, which leaves 8-nt ssDNA region on the oligonucleotide covalently attached to the T7 RNAP so that DNA template can hybridize to T7 RNAP and dehybridize the transcription inhibitor through toehold-mediated DNA strand displacement.

The resulting RNA production unit was programmed to transcribe Broccoli aptamer, RNA-equivalent of green fluorescent protein. Following the fluorescence signal, we were able to observe production of RNA over time (Figure 2c). T7 RNAP was able to produce observable amount of Broccoli aptamer only when complexed with the catenane DNA template. The transcription of Broccoli aptamer was effectively inhibited by the introduction of DNA oligonucleotide capable of masking the binding region on the catenane DNA template for T7 RNAP.

### 4.2.3 RNA production unit functions when anchored to the DNA origami structure

The RNA production unit was incorporated into the DNA origami barrel through programming six 5'-end ssDNA handles of DNA origami staple strand complementary to the

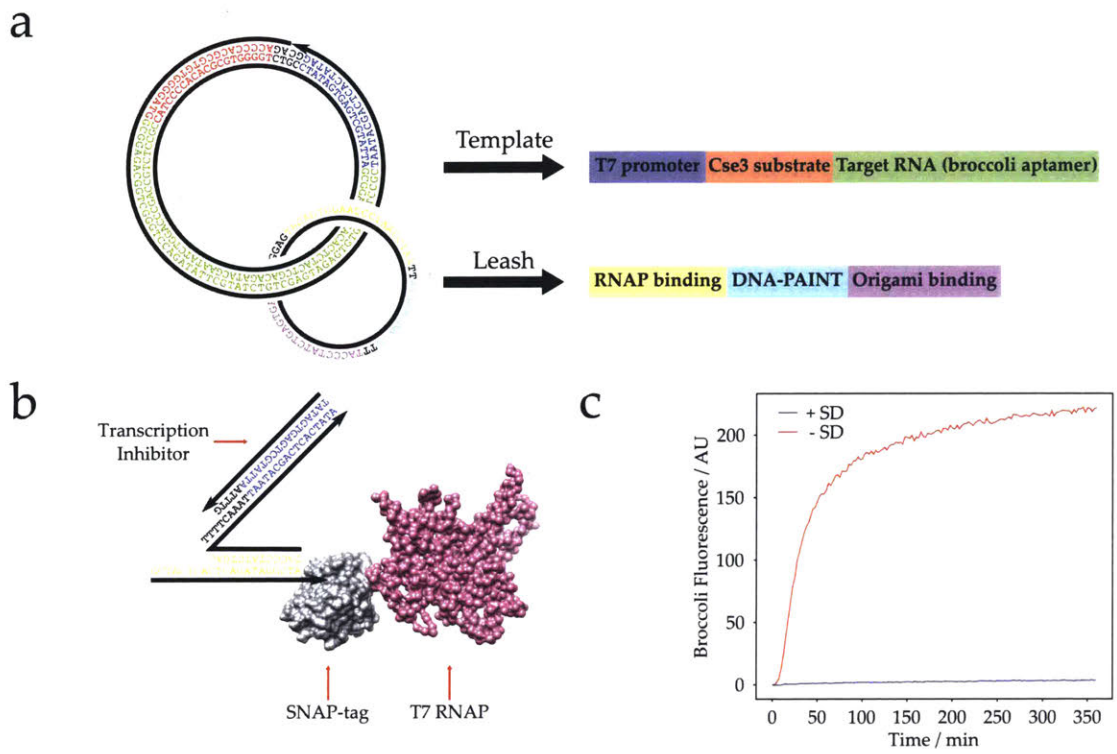


Figure 2. RNA production unit. (a) Catenane DNA template is composed of a circular DNA template and a circular DNA leash mechanically locked to one another. The different domains on the catenane DNA template are color-coded and labeled to the right. (b) T7 RNAP is attached to DNA oligonucleotide modified with $O^6$-benzylguanine via fused SNAP-tag. Transcription inhibitor is hybridized to the oligonucleotide to prevent transcription unless bound to target DNA template (i.e. catenane DNA template). (c) The assembly of the catenane DNA template and T7 RNAP polymerase results in an RNA production unit (-SD) that can produce a Broccoli aptamer in the presence of rNTP. The addition of DNA oligonucleotide (+SD) complementary to the part of the DNA leash strand that allows hybridization of T7 RNAP pre-complexed with a transcription inhibitor results in the abolition of RNA transcription in the sample because the transcription inhibitor effectively prevent transcription activity of T7 RNAP.

leash strand of the catenane DNA template (Figure 3a). The staple strands programmed with the handles also had a 3'-end DNA-PAINT docking site that is orthogonal to the sequence programmed into the leash strand of the catenane DNA template. We utilized the two orthogonal DNA-PAINT docking sites to measure the availability of the ssDNA handles on the structure and the incorporation of these sites with the catenane DNA template using the super-resolution microscopy technique (Figure 3b). The 93% availability of programmed pixels agreed with the previously reported number[15] for DNA origami. 57% of these available pixels were occupied with the catenane DNA template, which resulted in 53% final incorporation yield. The availability of programmed pixels is lower than 100% because not all staple strands are incorporated into the DNA origami assembly, some staple strands have missing or damaged nucleotides from DNA synthesis procedure, and some of the ssDNA handles may have folded

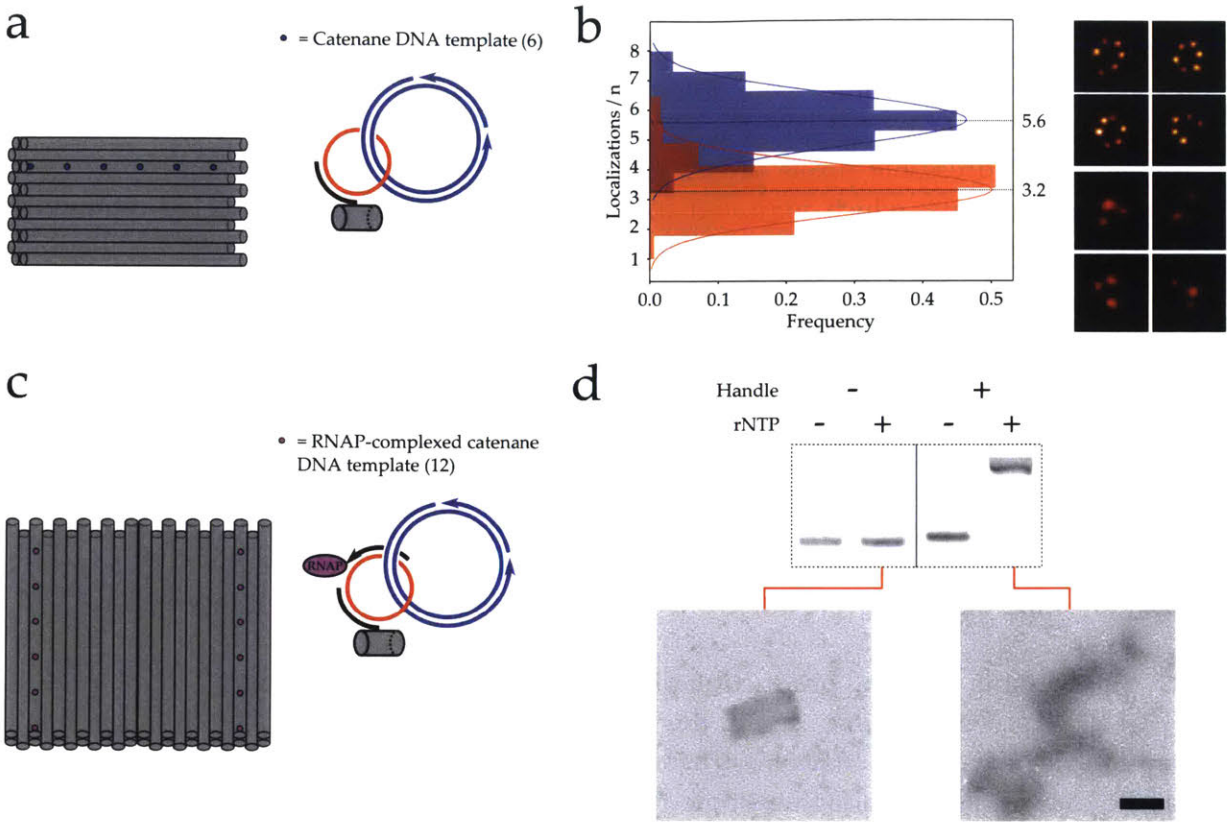


**Figure 3. Tethered RNA production unit.** (a) A DNA origami barrel is programmed to incorporate six catenane DNA templates. (b) DNA-PAINT analysis shows 93% availability of staple strands programmed with ssDNA handles and 57% of available handles occupied with catenane DNA template. Therefore, 53% of programmed sites were occupied with the catenane DNA templates. The top four images of inset show representative image of DNA-PAINT experiment for availability of staple strand with ssDNA handles, and the bottom four images show representative images of DNA-PAINT experiment for incorporated catenane DNA template. (c) A homodimer of DNA origami barrels was programmed to incorporate 12 RNA production units. (d) The data from agarose gel electrophoresis and transmission electron microscopy show production of rolling-circle transcript only from the DNA origami structure programmed (+) with ssDNA handles for RNA production units (Handle) in the presence (+) of rNTP. Scale bar = 50 nm.

into a conformation not amenable to DNA hybridization during the DNA origami folding. Moreover, the incorporation of molecular components can be hindered by damaged nucleotides as well as the spatial limitation of DNA origami structure that cannot accommodate incorporation of bulky materials densely on the surface of the structure, which may have contributed to the incorporation efficiency of the catenane DNA template.

Then, we tested the function of the RNA production unit anchored on the surface of DNA origami chassis. The barrel used to characterize incorporation efficiency was homodimerized to present 12 ssDNA handles in total (Figure 3c). The RNA production units

were assembled by introducing the engineered T7 RNAP after the incorporation and purification of the catenane DNA template on the surface of DNA origami chassis. The anchored RNA production units were able to transcribe Broccoli aptamer in the presence of rNTP. However, there was no observable fluorescence signal from the control structure that did not possess any addressable pixels programmed with ssDNA handle complementary to the catenane DNA template, which indicated that the purification step was able to remove the unincorporated catenane DNA template. The samples were further analyzed after incubation at 37°C with or without rNTP using agarose gel electrophoresis (AGE) and transmission electron microscope (TEM) (Figure 3d). There was no observable difference between the DNA origami structure without any ssDNA handles incubated in the presence or absence of rNTP. When the structure was programmed with ssDNA handles and incubated in the presence of rNTP, there was a band mobility shift closer to the well compared to the structure incubated without rNTP, implying the increase in molecular weight due to production of RNA. When observed using TEM, the sample with the band mobility shift showed amorphous structures coming out of the DNA origami barrel structures. The amorphous structures were not observed in any other samples, indicating that they were indeed RNA product from rolling-circle transcription.

### 4.2.4 RNA processing unit and production of mature RNA from nanofactory

An RNA processing unit used in this study was endoribonuclease Cse3 that can bind a specific sequence of an RNA hairpin structure and cleave at 3'-end of the hairpin leaving 5'-AUG at the cleaved RNA. Though a single-turnover enzyme in nature, the introduction of the single nucleotide mutation in its RNA substrate results in multi-turnover nuclease activity.[16] Therefore, the multi-turnover sequence was added to the flanking region between T7 promoter and RNA of interest so that the RNA product from rolling-circle transcription can be processed into target RNA monomers (Figure 2a).

To attach the ssDNA oligonucleotide, we fused SNAP-tag to the C-terminus of Cse3 (Figure 4a). Cse3 was covalently attached to ssDNA oligonucleotide with sequence orthogonal to ssDNA oligonucleotide attached to T7 RNP through $O^6$-benzylguanine-modification at 3'-end of the oligonucleotide. The DNA origami barrel for processing unit was programmed with 48 ssDNA handles complementary to the oligonucleotide attached to Cse3 (Figure 4b). The large quantity of programmed ssDNA handles and incorporated Cse3 allowed characterization with PAGE. Therefore, we analyzed the incorporation efficiency of Cse3 using PAGE-based bulk assay (Figure 4c). The bulk assay showed very little incorporation efficiency for either handle or Cse3 (<2%) when the structure is not programmed with ssDNA handles for Cse3. In fact, the result is likely due to an artifact of PAGE, since there shouldn't be any handle incorporation. The handle availability and Cse3 incorporation of the molecular chassis programmed with 96 ssDNA handles in total was estimated to be 66% and 41% respectively. The handle availability was much lower than what was measured for incorporation of RNA production unit using DNA-PAINT. There are eight times more ssDNA handles for RNA processing units than RNA production units, and the extensive introduction of ssDNA handles could affect the stability and staple strand incorporation. Moreover, the concentration of DNA origami structures may be inaccurate as A260 is used to estimate the molar concentration of DNA origami structures.

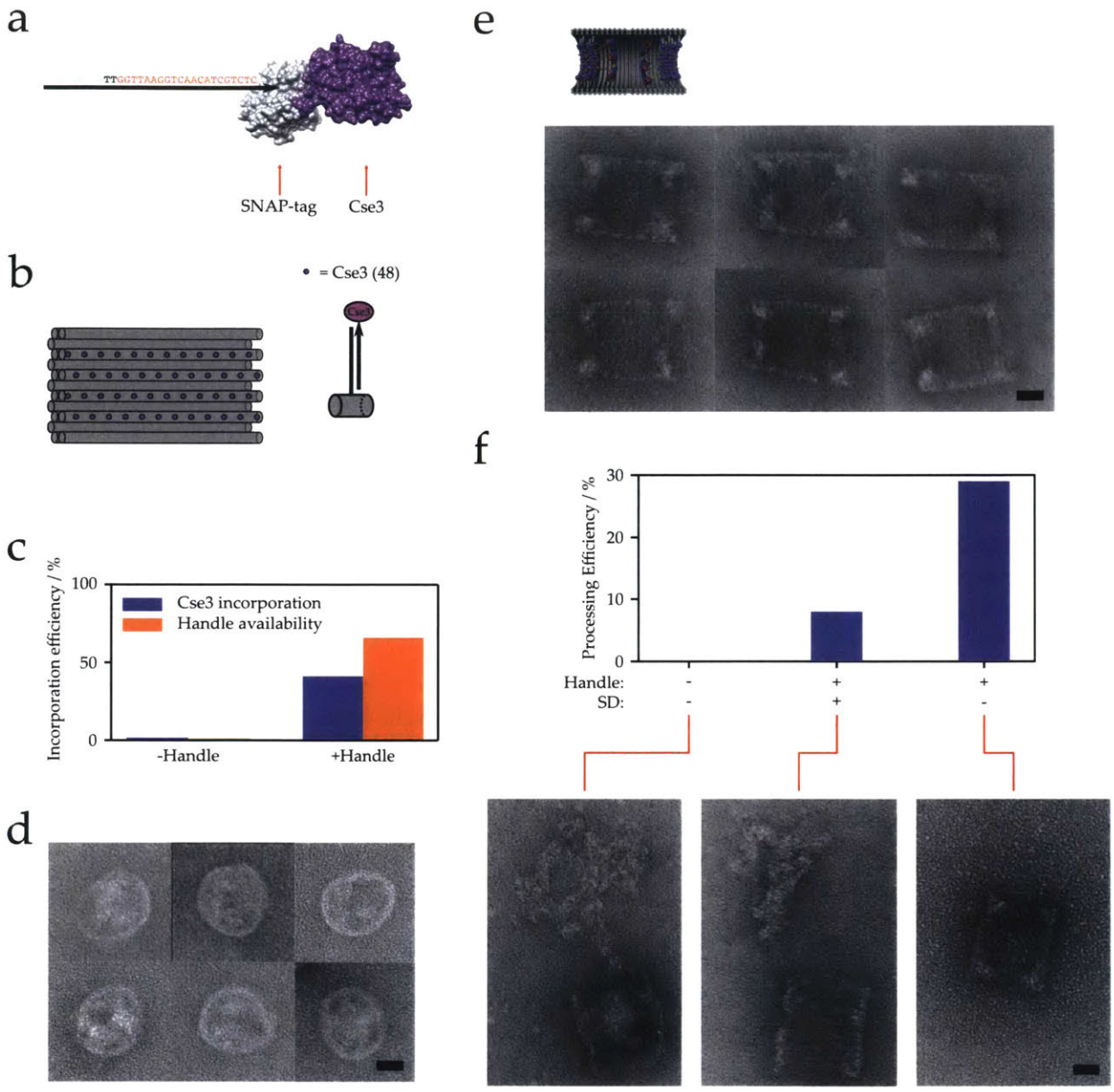


**Figure 4. Incorporation of RNA processing units.** (a) Cse3 is attached to DNA oligonucleotide modified with $O^6$-benzylguanine via fused SNAP-tag. (b) A DNA origami barrel is programmed to incorporate 48 Cse3. (c) PAGE-based assay was used to quantify bulk incorporation efficiency of handles and Cse3 (see SI2). (d) Cse3 incorporated in DNA origami barrels can be visualized using TEM. (e) The Cse3 incorporated in the tetramer of DNA origami barrels can be also visualized using TEM. (f) PAGE-based assay was used to quantify RNA processing efficiency (see SI3). The representative TEM images of corresponding samples are shown below. Scale bar = 20 nm.

However, the cargo incorporation efficiency to available ssDNA handles was comparable. Moreover, the incorporation of Cse3 on the lumen of the DNA origami barrel was visualized using TEM (Figure 4d).

Finally, we assembled the homodimer barrel with 12 production units and stacking barrels with 48 processing units each to form a nanofactory with four DNA origami barrel monomers filled with molecular cargos. TEM images verify the formation of a tetramer of DNA origami barrels with Cse3 incorporated at the terminal barrels visible (Figure 4e). The processing efficiency was measured using a PAGE-based assay that could visualize concatemers of a Broccoli aptamer (see SI2). Two control samples were prepared by either not programming any ssDNA handles for Cse3 or dehybridizing Cse3 from the prepared and purified nanofactory through toehold-mediated DNA strand displacement using ssDNA region at the 5'-end of the oligonucleotide attached to Cse3. The control sample without any handles produced RNA with no observable processing of RNA transcript (Figure 4f). The second control sample that dehybridized Cse3 from the DNA origami chassis was able to produce and process the RNA transcript since the same molar concentration of Cse3 was available in the solution after the strand displacement, though not co-localized with RNA production unit. However, the complete nanofactory that co-localized all the components on the DNA origami chassis were able to produce a more processed RNA transcript compared to the second control sample. When visualized using TEM, the nanofactory integrating RNA production and processing was the only sample that did not have any DNA origami structures spooling out amorphous RNA structures, presumably because the RNA transcript was being processed soon after being synthesized.

### 4.2.5 Verification of co-transcriptional processing using single-molecular imaging

The DNA origami chassis with integrated production and processing units was observed in a single-molecular level to verify the co-transcriptional processing. We prepared a control sample possessing only the production units to compare its behavior with the nanofactory, integrating both the production and processing units. The outer layer of the DNA origami chassis was decorated with biotin molecules for positioning each nanofactory on the glass surface covered with biotin using streptavidin and Alexa688 for visualizing each nanofactory using a fluorescence microscope. A quencher-fluorophore pair (Cy3-BHQ2) was attached to a DNA duplex with ssDNA toehold on the fluorophore-attached oligonucleotide complementary to the part of RNA transcript. The production of RNA transcript results in displacement of the quencher-attached oligonucleotide, and the RNA transcript can be visualized using Cy3 signal.

We used TIRF illumination to observe the nanofactory attached to the glass surface and RNA transcript produced (Figure 5). The control sample with only production units had a continuous increase in Cy3 signal over time implying the accumulation of RNA from rolling-circle transcription. However, the nanofactory with integrated production and processing units showed an increase and decrease of the Cy3 signal indicative of continuous production and processing of RNA. The single-molecular imaging of the nanofactory further demonstrates co-transcriptional processing of RNA product and shows that the nanofactory functions as intended through programming the molecular integration.

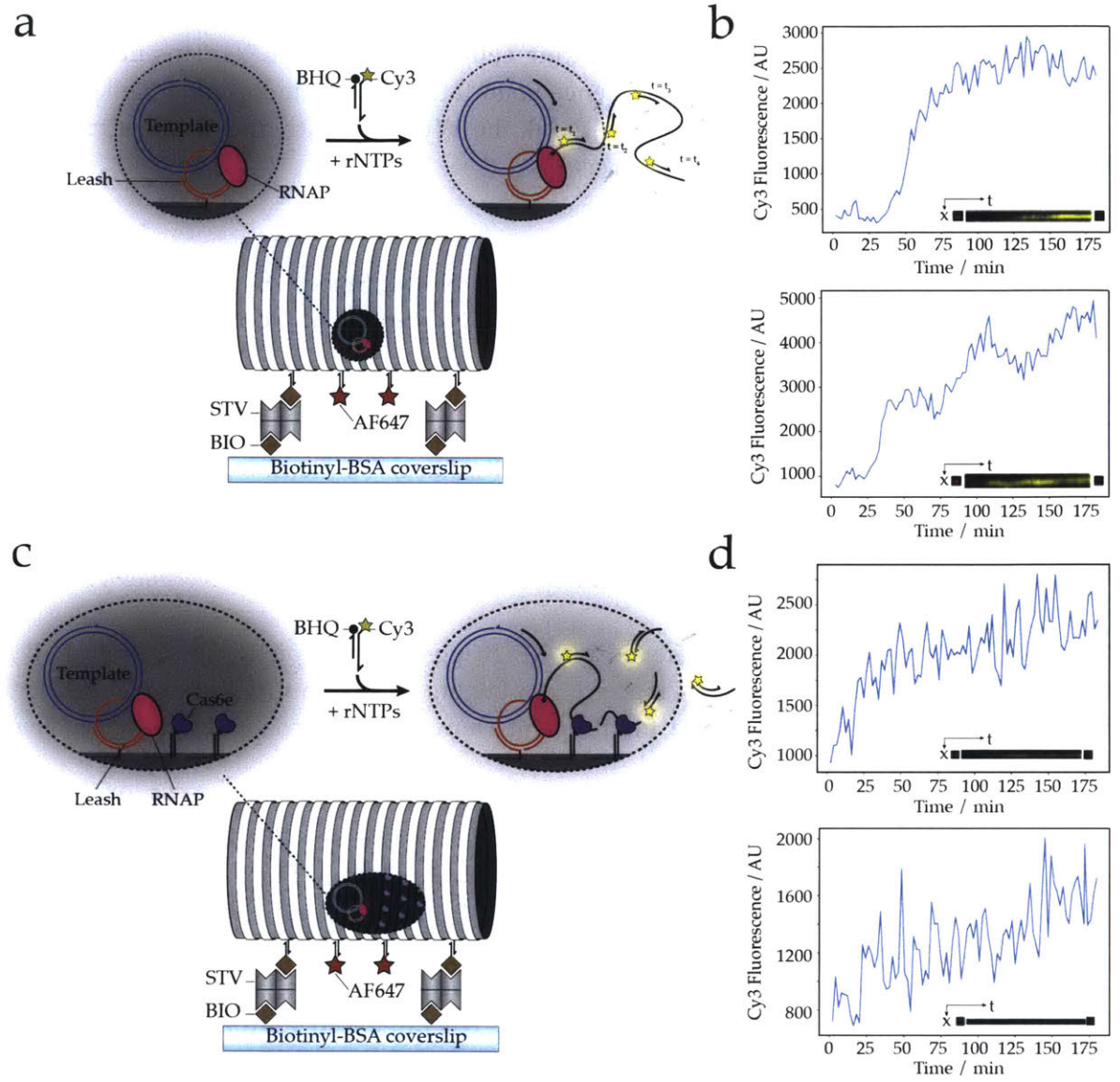


**Figure 5. Single-molecular imaging of RNA production and processing.** The cytosolic nanofactory was immobilized on a glass surface with fluorescence dye for localization. Rolling-circle transcription (a) and integrated RNA production and processing (b) were visualized over time and resulted in time-course measurement of fluorescence signal due to RNA production.

## 4.3 Conclusion

The nanofactory described here establishes a platform for RNA production *in vitro* and provides insight into the effect of molecular organization on the production and processing of RNA. We envision our nanofactory as a model system for how molecular organization can impact performance of molecular components, and the insights gleaned here could be translated into future studies of other types of nanofactories. The modular nature of DNA origami will allow augmentation such as production of different therapeutic RNA (e.g. shRNA and mRNA) and further RNA processing beyond ribonuclease digestion that could result in more sophisticated nanofactories with formidable therapeutic potential.

## 4.4 Acknowledgement

Leo Chou acknowledges support from Banting Fellowship and NSERC. This material is based upon work supported by the National Science Foundation Graduate Research Fellowship (Jaeseung Hahn) under Grant No. 1122374. We thank the Wyss Institute and the Institute for RNA Medicine (BIDMC) for support of this project.

## 4.5 References

1. Tavernier, G.; Andries, O.; Demeester, J.; Sanders, N. N.; Smedt, S. C. De; Rejman, J. MRNA as Gene Therapeutic: How to Control Protein Expression. *J. Control. Release* **2011**, *150*, 238–247.
2. Burnett, J. C.; Rossi, J. J. RNA-Based Therapeutics: Current Progress and Future Prospects. *Chem. Biol.* **2012**, *19*, 60–71.
3. Kormann, M. S. D.; Hasenpusch, G.; Aneja, M. K.; Nica, G.; Flemmer, A. W.; Herber-Jonat, S.; Huppmann, M.; Mays, L. E.; Illenyi, M.; Schams, A.; Griese, M.; Bittmann, I.; Handgretinger, R.; Hartl, D.; Rosenecker, J.; Rudolph, C. Expression of Therapeutic Proteins after Delivery of Chemically Modified MRNA in Mice. *Nature biotechnology* **2011**, *29*, 154–157.
4. Read, M. L.; Singh, S.; Ahmed, Z.; Stevenson, M.; Briggs, S. S.; Oupicky, D.; Barrett, L. B.; Spice, R.; Kendall, M.; Berry, M.; Preece, J. A.; Logan, A.; Seymour, L. W. A Versatile Reducible Polycation-Based System for Efficient Delivery of a Broad Range of Nucleic Acids. *Nucleic Acids Research* **2005**, *33*, 1–16.
5. Brisson, M.; He, Y.; Li, S.; Yang, J. P.; Huang, L. A Novel T7 RNA Polymerase Autogene for Efficient Cytoplasmic Expression of Target Genes. *Gene therapy* **1999**, *6*, 263–270.
6. Farrow, P. J.; Barrett, L. B.; Stevenson, M.; Fisher, K. D.; Finn, J.; Spice, R.; Allan, M. A.; Berry, M.; Logan, A.; Seymour, L. W.; Read, M. L. Cytoplasmic Expression Systems Triggered by MRNA Yield Increased Gene Expression in Post-Mitotic Neurons. *Nucleic Acids Research* **2006**, *34*.
7. Finn, J.; Lee, A. C. H.; MacLachlan, I.; Cullis, P. An Enhanced Autogene-Based Dual-Promoter Cytoplasmic Expression System Yields Increased Gene Expression. *Gene therapy* **2004**, *11*, 276–283.
8. Gao, X.; Huang, L. Cytoplasmic Expression of a Reporter Gene by Co-Delivery of T7 RNA Polymerase and T7 Promoter Sequence with Cationic Liposomes. *Nucleic acids research* **1993**, *21*, 2867–2872.
9. Jungmann, R.; Steinhauer, C.; Scheible, M.; Kuzyk, A.; Tinnefeld, P.; Simmel, F. C. Single-Molecule Kinetics and Super-Resolution Microscopy by Fluorescence Imaging of Transient Binding on DNA Origami. *Nano Letters* **2010**, *10*, 4756–4761.
10. Jungmann, R.; Avendaño, M. S.; Woehrstein, J. B.; Dai, M.; Shih, W. M.; Yin, P. Multiplexed 3D Cellular Super-Resolution Imaging with DNA-PAINT and Exchange-PAINT. *Nature Methods* **2014**, *11*, 313–318.
11. Dai, M.; Jungmann, R.; Yin, P. Optical Imaging of Individual Biomolecules in Densely Packed Clusters. *Nature Nanotechnology* **2016**, *11*, 798–807.
12. Juillerat, A.; Gronemeyer, T.; Keppler, A.; Gendreizig, S.; Pick, H.; Vogel, H.; Johnsson, K. Directed Evolution of O6-Alkylguanine-DNA Alkyltransferase for Efficient Labeling of

Fusion Proteins with Small Molecules In Vivo. *Chemistry & Biology* **2003**, *10*, 313–317.
13. Keppler, A.; Kindermann, M.; Gendreizig, S.; Pick, H.; Vogel, H.; Johnsson, K. Labeling of Fusion Proteins of O6-Alkylguanine-DNA Alkyltransferase with Small Molecules in Vivo and in Vitro. *Methods* **2004**, *32*, 437–444.
14. Dunn, J. J.; Krippl, B.; Bernstein, K. E.; Westphal, H.; Studier, F. W. Targeting Bacteriophage T7 RNA Polymerase to the Mammalian Cell Nucleus. *Gene* **1988**, *68*, 259–66.
15. Strauss, M. T.; Schueder, F.; Haas, D.; Nickels, P. C.; Jungmann, R. Quantifying Absolute Addressability in DNA Origami with Molecular Resolution. *Nature Communications* **2018**, *9*, 1600.
16. Sashital, D. G.; Jinek, M.; Doudna, J. A. An RNA-Induced Conformational Change Required for CRISPR RNA Cleavage by the Endoribonuclease Cse3. *Nature Structural & Molecular Biology* **2011**, *18*, 680–687.

## 4.6 Supporting information

### SI1. Materials and methods

### SI1.1 Chemicals and supplies

10x TBE buffer was purchased from National Diagnostics. PCR tubes were purchased from USA Scientific. SYBR Safe was purchased from Life Technologies Corporation. UltraPure Agarose and Ultra Low Range DNA Ladder were purchased from Thermo Fisher Scientific. 2-log DNA Ladder (0.1-10.0 kb) was purchased from New England Biolabs (NEB). Glycerol, Tirs acid (Tris-HCl), Tris base, EDTA, Tween20, β-Mercaptoethanol (BME), magnesium chloride ($MgCl_2$), and sodium chloride (NaCl) were purchased from Sigma-Aldrich. Sera-Mag Magnetic SpeedBeads (carboxylated, 1 μm, 3 EDAC/PA5) was purchased from GE Healthcare Life Sciences. Carbon formvar grids and uranyl formate were purchased from Electron Microscopy Sciences. Amicon Ultra filtration devices were purchased from Millipore. DNA gel extraction spin column was purchased from BIO-RAD.

### SI1.2 Scaffold prep

The p8634 scaffold strand was produced from M13 phage replication in E. coli, as described previously[SI-R1].

### SI1.3 Staple strand

The staple sequences were generated using the caDNAno software by applying p8634 scaffold to the DNA origami barrel design from the last chapter and appending desired sequence at 5'- or 3'-end of the generated staple sequence (see Tables below). All DNA strands were purchased from Integrated DNA Technologies (IDT) with standard desalting option. The DNA strands were shipped dry and suspended at 100 nM in Millipore purified water and stored at -20°C. For the staple strands with 5'-end extensions (oligonucleotides in SI Table 1-2) were PAGE purified to ensure that DNA origami structures folded using these strands possess the intended handles from 5'-end extensions.

**SI Table 1. Staple list of "Inside Pixel + Clip" for DNA origami barrel with handle sequence for the production unit (replace "Inside Pixel" staple strands with corresponding number)**

| Subpool | # | Sequence |
|---|---|---|
| Inside Pixel + Clip | 1 | GTTAGGGTTCCACTCTACTCGAGTACCGGTCGCGAAAGGTGTGGTTGCCG TTGCGTGTTCTTTCAATGTAT |
| Inside Pixel + Clip | 3 | GTTAGGGTTCCACTCTACTCGACCTTTCGTCCCTAGCAGTTCCGTGGCGAG CACCTTGGCTTTCAATGTAT |
| Inside Pixel + Clip | 5 | GTTAGGGTTCCACTCTACTCGGGTCTCCGCGATCGTATAGCTCTCCCGCAC GGGTTCAGCTTTCAATGTAT |
| Inside Pixel + Clip | 7 | GTTAGGGTTCCACTCTACTCGGACCTGTTCGGCGAGCTAGGCACACGTCA CCGGGTAGTGTTTCAATGTAT |
| Inside Pixel + Clip | 9 | GTTAGGGTTCCACTCTACTCGTTCCTCCTGGGTCGGGCGAGACTTGCAGTA GATGGGCCGTTTCAATGTAT |
| Inside Pixel + Clip | 11 | GTTAGGGTTCCACTCTACTCGCTACGTTTGCTCACACGCCCGAGACGGTTA GATCGCGCCTTTCAATGTAT |

**SI Table 2. Staple list of "Inside Pixel + Fili" for DNA origami barrel with handle sequence for the processing unit (replace "Inside Pixel" staple strands with corresponding number)**

| Subpool | # | Sequence |
|---|---|---|
| Inside Pixel + Fili | 1 | GAGACGATGTTGACCTTAACCAGTACCGGTCGCGAAAGGTGTGGTTGCCG TTGCGTGTTCTTTCAATGTAT |
| Inside Pixel + Fili | 2 | GAGACGATGTTGACCTTAACCACCTTTCGTCCCTAGCAGTTCCGTGGCGA GCACCTTGGCTTTCAATGTAT |
| Inside Pixel + Fili | 3 | GAGACGATGTTGACCTTAACCGGTCTCCGCGATCGTATAGCTCTCCCGCA CGGGTTCAGCTTTCAATGTAT |
| Inside Pixel + Fili | 4 | GAGACGATGTTGACCTTAACCGACCTGTTCGGCGAGCTAGGCACACGTCA CCGGGTAGTGTTTCAATGTAT |
| Inside Pixel + Fili | 5 | GAGACGATGTTGACCTTAACCTTCCTCCTGGGTCGGGCGAGACTTGCAGT AGATGGGCCGTTTCAATGTAT |
| Inside Pixel + Fili | 6 | GAGACGATGTTGACCTTAACCCTACGTTTGCTCACACGCCCGAGACGGTT AGATCGCGCCTTTCAATGTAT |
| Inside Pixel + Fili | 7 | GAGACGATGTTGACCTTAACCGGCTCCCGGCCGTACGTATGCCTGCCTTCT ACCTGCAGTTTTCAATGTAT |
| Inside Pixel + Fili | 8 | GAGACGATGTTGACCTTAACCCAGTGGCCCATTTCGCCAATTGGGTGCGC GCACTGTGAATTTCAATGTAT |
| Inside Pixel + Fili | 9 | GAGACGATGTTGACCTTAACCCGGTAGACTGGTTAGGGCCATGGGCGCCC GTCAATGAGGTTTCAATGTAT |
| Inside Pixel + Fili | 10 | GAGACGATGTTGACCTTAACCTGCCCACTCATGCACTAGCACGCTCACGC CTGGGATGGATTTCAATGTAT |
| Inside Pixel + Fili | 11 | GAGACGATGTTGACCTTAACCGCCGCGGCCGCATTTACATAGCAGCCTGG CATGTATCGTTTTCAATGTAT |
| Inside Pixel + Fili | 12 | GAGACGATGTTGACCTTAACCCTGTGAAAGGACTGCCCTCTGACTCGGGC CCGCTTCCGTTTTCAATGTAT |
| Inside Pixel + Fili | 13 | GAGACGATGTTGACCTTAACCGCGAACATCCACGTCGGAGCATCGTGCGT CCTTGACCCATTTCAATGTAT |
| Inside Pixel + Fili | 14 | GAGACGATGTTGACCTTAACCGCTGACGTGTTCGCCACCGGAGCATTGAG ACAGCCCATCTTTCAATGTAT |
| Inside Pixel + Fili | 15 | GAGACGATGTTGACCTTAACCGATGCGCCGACACGCGTGCTATCAGTCAG ACCGTTGGTGTTTCAATGTAT |
| Inside Pixel + Fili | 16 | GAGACGATGTTGACCTTAACCCGCGCATCAGCTGCCCGGGAAGCACGAG TGCATTGATTTTTTCAATGTAT |
| Inside Pixel + Fili | 17 | GAGACGATGTTGACCTTAACCCTACCGGACAGACAGCGGCGTAAAGACC CGAAAGCGGCATTTCAATGTAT |
| Inside Pixel + Fili | 18 | GAGACGATGTTGACCTTAACCCGATGAAGACCGGCCCTCGAATCGGCCCT CGGACTCATGTTTCAATGTAT |
| Inside Pixel + Fili | 19 | GAGACGATGTTGACCTTAACCGGCGGCATGAAGGCACCTCAGTGACGTCC AGTCTAGGCGTTTCAATGTAT |
| Inside Pixel + Fili | 20 | GAGACGATGTTGACCTTAACCGTCAGCGCTCGGTAACTGTTATCCGACGT GTACCGCGGCTTTCAATGTAT |
| Inside Pixel + Fili | 21 | GAGACGATGTTGACCTTAACCTGCCGGTGGTCCAACCCGTCATCCACGAC CGTTAGACGATTTCAATGTAT |

| | | |
|---|---|---|
| Inside Pixel + Fili | 22 | GAGACGATGTTGACCTTAACCGCTCAATGAAGGGCCTCTTTTCAGGGCGG GCTGCGGACATTTCAATGTAT |
| Inside Pixel + Fili | 23 | GAGACGATGTTGACCTTAACCAACTAAGCACTCATCGAGATGCGGGCCAT TGCGACGCGGTTTCAATGTAT |
| Inside Pixel + Fili | 24 | GAGACGATGTTGACCTTAACCACCGCTCGTGATCGTGAGTATTGCGTCTCC CGAGGAGCGTTTCAATGTAT |
| Inside Pixel + Fili | 25 | GAGACGATGTTGACCTTAACCCTGCTTTCCTGTCTCGGACCAGCTCGGCCG GTGGAGATGTTTCAATGTAT |
| Inside Pixel + Fili | 26 | GAGACGATGTTGACCTTAACCTGCGCCGGCGAAGTGTAGCATCGGTTTCG CTACGACAACTTTCAATGTAT |
| Inside Pixel + Fili | 27 | GAGACGATGTTGACCTTAACCGACAGCCGCGGTTGATCGTTGCGTGAGAA GCGTCTACCCTTTCAATGTAT |
| Inside Pixel + Fili | 28 | GAGACGATGTTGACCTTAACCTCGGCAATCCGACAGCCTAGTTCGAGATC CGAGCCGCGTTTTCAATGTAT |
| Inside Pixel + Fili | 29 | GAGACGATGTTGACCTTAACCCACAGGACCCGTGAGTTTCGCCAAGGCCC TGTTTGCACGTTTCAATGTAT |
| Inside Pixel + Fili | 30 | GAGACGATGTTGACCTTAACCTCGGCCACCGGTCGCATGTCTAGACGTCC ACAAGCCTTCTTTCAATGTAT |
| Inside Pixel + Fili | 31 | GAGACGATGTTGACCTTAACCTAACTTTGCCTCTGCTGTGGTGAAGCCGGC TCGCCTTGCTTTCAATGTAT |
| Inside Pixel + Fili | 32 | GAGACGATGTTGACCTTAACCAGGGCCTCAAAGCGACGATTGCACCAGC AGCCTAGTGGGTTTCAATGTAT |
| Inside Pixel + Fili | 33 | GAGACGATGTTGACCTTAACCCGTGTAGTGACATTTTACCGCGGACCTCG GCGCTGCACCTTTCAATGTAT |
| Inside Pixel + Fili | 34 | GAGACGATGTTGACCTTAACCGGCTGTGAGGCTTTGAGAGTGCGTGTGCT CAGCGTTCCGTTTCAATGTAT |
| Inside Pixel + Fili | 35 | GAGACGATGTTGACCTTAACCTTGTGTAGCAGCCCGTTAACGCGGTGCAC GGTCGGCTAATTTCAATGTAT |
| Inside Pixel + Fili | 36 | GAGACGATGTTGACCTTAACCAGCCACAGTGCAGCTATCTTGTCCCGGTA TGGGCGGCGATTTCAATGTAT |
| Inside Pixel + Fili | 37 | GAGACGATGTTGACCTTAACCGTCGAGTGTCGGCGGTCAGTGGGAGACTT GCTGCGATGTTTTCAATGTAT |
| Inside Pixel + Fili | 38 | GAGACGATGTTGACCTTAACCGCGTAACAAGTGCGCTTTCAGGAAGCTCG TAAGCGGCGGTTTCAATGTAT |
| Inside Pixel + Fili | 39 | GAGACGATGTTGACCTTAACCGGACCGGCCTTGGGAAACGCTTAAGACGT CGCAGTGCTGTTTCAATGTAT |
| Inside Pixel + Fili | 40 | GAGACGATGTTGACCTTAACCCGGCAGGTTAAAGCTCGGCCAAGGGCGT CTTGTGCTGAGTTTCAATGTAT |
| Inside Pixel + Fili | 41 | GAGACGATGTTGACCTTAACCATCGGGCCACACGTAATGGACGCGCTCCC TGGCTTCAAGTTTCAATGTAT |
| Inside Pixel + Fili | 42 | GAGACGATGTTGACCTTAACCCACTCCGAGACGACTACTCGACACGCCGC CCGAGGTGTTTTTCAATGTAT |
| Inside Pixel + Fili | 43 | GAGACGATGTTGACCTTAACCTAACGGCGTTTGAGGCCAACTGGTCACGA TCAGCGGGAGTTTCAATGTAT |
| Inside Pixel + Fili | 44 | GAGACGATGTTGACCTTAACCGGAGAGCCTCTACGATCACGAGTGCCGA GCTGAACCCGCTTTCAATGTAT |

| | | |
|---|---|---|
| Inside Pixel + Fili | 45 | GAGACGATGTTGACCTTAACCGGCGTAGCTACTCCGTATCTGGCCGCTCG CTCAAGAGCCTTTCAATGTAT |
| Inside Pixel + Fili | 46 | GAGACGATGTTGACCTTAACCGAGACTCTAGGGTAGGGCGGGCGCGAGC TGGAGAGTAGCTTTCAATGTAT |
| Inside Pixel + Fili | 47 | GAGACGATGTTGACCTTAACCCGCCAGAGATTGCTTAATGCGTGCGAGGG TAGCGGGCCATTTCAATGTAT |
| Inside Pixel + Fili | 48 | GAGACGATGTTGACCTTAACCCGTTCTATCTACCAGCGGGAGGGCAGGAC TGCGTTGGGCTTTCAATGTAT |

**SI Table 3. Staple list of "Outside Pixel for SM" for DNA origami barrel with handle sequence for the single-molecular imaging (replace "Outside Pixel" staple strands with corresponding number)**

| Subpool | # | Sequence |
|---|---|---|
| Outside Pixel for SM | 1 | ACGTCAAAGGGCGAGACGGGCTATTGGGCGCCAGGGTTTCCTGGGGCTCT GCAATCAACTTATCCC |
| Outside Pixel for SM | 2 | AGCCCCCTTATTAAAATTATTCGAGTAAAAGAGTCTACGCTGCCAGCTCTG CAATCAACTTATCCC |
| Outside Pixel for SM | 3 | AGTGCCGTCGAGATAAGCGTCGAATGGAAAGCGCAGCAAAATCATGCTCT GCAATCAACTTATCCC |
| Outside Pixel for SM | 4 | TTGCGCCGACAATTTAGTAAAGCGTAACGATCTAAAGAATAGGTAGCTCT GCAATCAACTTATCCC |
| Outside Pixel for SM | 5 | ATCAAGAGTAATCTTTGACCCACGAAAGAGGCAAAATAACCGAAGGCTCT GCAATCAACTTATCCC |
| Outside Pixel for SM | 6 | TCATAAATATTCATCAGTTGACTAACGGAACAACATTACCCAATCGCTCTG CAATCAACTTATCCC |
| Outside Pixel for SM | 7 | TCAATTCTACTAAGCTTAGAGATTGCTCCTTTTGATAAACAGTCGGCTCTGC AATCAACTTATCCC |
| Outside Pixel for SM | 8 | AATATTTAAATTGCATCAATACAAAAGGGTGAGAAATAAATCACAGCTCT GCAATCAACTTATCCC |
| Outside Pixel for SM | 9 | GTTGTAAAACGACAGTATCGGGTAACCGTGCATCTGATTCGCACAGCTCTG CAATCAACTTATCCC |
| Outside Pixel for SM | 10 | ATTGCGCTAACAGCTGGAACTCAGGGTTGTCGGACTTCGCATTACGCTCTG CAATCAACTTATCCC |
| Outside Pixel for SM | 11 | ATTATCTTACTGTCGCATCGCTCGAACAAGACCCGTTGAAACAATGCTCTG CAATCAACTTATCCC |
| Outside Pixel for SM | 12 | TACCGAGCTCGAAAGAAATGAGTCTAATGAAGACAATACCGTTGTGCTCT GCAATCAACTTATCCC |
| Outside Pixel for SM | 13 | AAGTGTTTTTATACACCACACAAGAGTCCACTATTGATTGCCCGGTTAATT AGGAT |
| Outside Pixel for SM | 14 | CAAACAAATAAATCCAGAGCTGTAGCGCGTTTTCAGGTGAATTAGTTAATT AGGAT |
| Outside Pixel for SM | 15 | GCATTCCACAGACCCGTACTTTAGCGGGGTTTTGCGCTTTTGACATTAATTA GGAT |
| Outside Pixel for SM | 16 | ATGCCACTACGAAGGTCGCTGGTGAATTTCTTAAATCTGTATGTATTAATTA GGAT |

| | | |
|---|---|---|
| Outside Pixel for SM | 17 | AAGAAAAATCTACTAACAAATACAGACCAGGCGCATTATACCATATTAAT TAGGAT |
| Outside Pixel for SM | 18 | ACAGGTCAGGATTACGAGAATAGACTGGATAGCGTGAATACCAGGTTAAT TAGGAT |
| Outside Pixel for SM | 19 | TGCCTGAGTAATGAAGGCAATTTCATTTGGGGCGCGCTGAATACATTAATT AGGAT |
| Outside Pixel for SM | 20 | GGTCACGTTGGTGTTTGTTAAAAGCCCCAAAAACACAACCGTTAATTAATT AGGAT |
| Outside Pixel for SM | 21 | ATAGATGAACGAAATGCGTATTGGGTAACGCCAGGAAGATCGCTATTAAT TAGGAT |
| Outside Pixel for SM | 22 | ACCTGGAAGAGTTCAAAACTACATCAAACGCCGCGAAACAGAGCGTTAAT TAGGAT |
| Outside Pixel for SM | 23 | ATACAAATATTCCAACGACAGATGATGACCGTACTGGGTTGGATGTTAATT AGGAT |
| Outside Pixel for SM | 24 | CCAACGCGCGGGGTTGTTATACTTCCGAGTCACAGCGTGCAAAGCTTAATT AGGAT |
| Outside Pixel for SM | 25 | TAGGGTTGAGTGTCCTGGCCCACCTGTCGTGCCAGCCAATTCCCGTTAATT AGGAT |
| Outside Pixel for SM | 26 | AGAATCAAGTTTGTCACCGACTTAGACAGGAACGGTCGCTTAAGATTAATT AGGAT |
| Outside Pixel for SM | 27 | CTGAGACTCCTCAGGAGTGTAAGGCAGGTCAGACGAGGAACCGACTTAAT TAGGAT |
| Outside Pixel for SM | 28 | TTGTATCGGTTTAGCTAAACATTCGTCACCAGTACATTTAGTAGGTTAATTA GGAT |
| Outside Pixel for SM | 29 | AACTTTGAAAGAGAACAAAGTGGAAGTTTCCATTAAGCAGGGAAATTAAT TAGGAT |
| Outside Pixel for SM | 30 | TTGCCAGAGGGGGCTAATGCAACTGGCTCATTATACATTCAGTCCTTAATT AGGAT |
| Outside Pixel for SM | 31 | AAATGGTCAATAAGTAGCTCATCAAAGCGAACCAGAAAATCAATTTTAAT TAGGAT |
| Outside Pixel for SM | 32 | ATCATATGTACCCATAAATTATTTTTAGAACCCTCAGCAAAATGCTTAATT AGGAT |
| Outside Pixel for SM | 33 | AAGGGGGATGTGCCCAGCTTTGAACAAACGGCGGATTCATTTTCATTAATT AGGAT |
| Outside Pixel for SM | 34 | CTGGATGAACGGGAAGTGAGCTGCCACTCATTGTTGACAGTTCGATTAATT AGGAT |
| Outside Pixel for SM | 35 | CACAGCGATGCCAGGGTTCAGAAGACTCCTGTTATCCAGCGTGTGTTAATT AGGAT |
| Outside Pixel for SM | 36 | GGTTTTGTTTTATTCACGAGTATGTAGATGAAGGTACAAGGAGTTTTAATTA GGAT |
| Outside Pixel for SM | 37 | CTAAACAGGAGGCCTACAGGAATCCCTTATAAATCGTTGCAGCGCTTAATT AGGAT |
| Outside Pixel for SM | 38 | GCCGCCGCCAGCACAGAGCCCCATCGATAGCAGCAATTTGGGAAGTTAAT TAGGAT |
| Outside Pixel for SM | 39 | AGGAACCCATGTACCTCAGACTATTATTCTGAAACTAAGTTTTGATTAATT AGGAT |

| | | |
|---|---|---|
| Outside Pixel for SM | 40 | CTTTGAGGACTAAGCCGCTTTCCAAAAAAAAGGCTACAGTTTCATTTAATT AGGAT |
| Outside Pixel for SM | 41 | TGTGAATTACCTTGCTTGCCAGACGGTCAATCATAAGATTTGTGGTTAATTA GGAT |
| Outside Pixel for SM | 42 | TTCAAATATCGCGGTCTTTACAAAATAGCGAGAGGAACGCCAAATTTAATT AGGAT |
| Outside Pixel for SM | 43 | GCCTTTATTTCAATAAAGCCTAGATTTAGTTTGACTTAAATATACTTAATTA GGAT |
| Outside Pixel for SM | 44 | AGTAACAACCCGTATAGGAACGATGAACGGTAATCAGAGGGTAAATTAAT TAGGAT |
| Outside Pixel for SM | 45 | GCGCCGCCTGAACAATGAAAGCGGGCCTCTTCGCTCGCTTCTGCGTTAATT AGGAT |
| Outside Pixel for SM | 46 | CAGTTTCTTGTTGCGAAGGTAATTGGTAACACCATACTCTCAGATTTAATTA GGAT |
| Outside Pixel for SM | 47 | CTCCATGCAGACAATGAGTAGCTTGTGAAAATGCTGTGAGTATACTTAATT AGGAT |
| Outside Pixel for SM | 48 | GCTCACTGCCCGCATACGAGGGGGATTTATTTTATAAACGATAGTTTAATT AGGAT |
| Outside Pixel for SM | 49 | TGTTTGATGGTGGCCACGCTGTGAGTGAGCTAACTCCATAAAGCC |
| Outside Pixel for SM | 50 | AGCAAGGCCGGAACCAGCAAACGTGCTTTCCTCGTTCTATGGTCC |
| Outside Pixel for SM | 51 | AGTTAATGCCCCCTCAGTGCCCCTCAGAGCCGCCACTCAGAACTT |
| Outside Pixel for SM | 52 | GAATAATAATTTTTGAGAATACACCCTCATTTTCAGCCCTCAGAC |
| Outside Pixel for SM | 53 | TCCATGTTACTTACCTGATAAATCGGAACGAGGGTAATCGTCAGC |
| Outside Pixel for SM | 54 | CCCTCGTTTACCATACGAGGCCTTGAGATGGTTTAAGAAACACGC |
| Outside Pixel for SM | 55 | ACAGTTGATTCCCAAGTACGGATCAAAAAGATTAAGTATTATAAA |
| Outside Pixel for SM | 56 | CCTGAGAGTCTGGTTGAGAGAATTATGACCCTGTAAATAAAGCTA |
| Outside Pixel for SM | 57 | TGCGCAACTGTTGAAACCAGGAGCCAGCTTTCATCAAAAAATATG |
| Outside Pixel for SM | 58 | TGGGGATTTGACGGTGAAGCGAAGAATTACAGCGCAGACATCAGC |
| Outside Pixel for SM | 59 | GAGTGAGATCGGTTGATGTCTGGAAAGCAACGAAGTCGGATGGAC |
| Outside Pixel for SM | 60 | AATATTACATAACTCTCTGTATTATCAATGTTGTGCGTTAGAGGA |

**SI1.4 DNA origami folding**

Nanostructure synthesis was carried out by mixing 10 nM M13 scaffold with a 10x excess of staples in 1x TE (5 mM Tris-HCl, 1 mM EDTA, pH 8) with 12 mM $MgCl_2$. The solution

was subjected to a thermal annealing ramp on a Tetrad 2 Peltier Thermal Cycler (Bio-Rad) according to the following schedule:

Incubate at 65°C for 15 minutes
Decrease to 50°C at 20 seconds/°C
Incubate at 50°C for 6 hours
Decrease to 40°C at 6 hours/°C
Incubate at 40°C for 6 hours
Store at 4°C

### SI1.5 DNA origami purification

To remove excess staple, DNA origami barrel was purified using solid-phase reversible immobilization (SPRI)[SI-R2]. The homodimer of DNA origami barrels functionalized with the RNA production units was purified using agarose gel electrophoresis (AGE) purification. The assembled tetramer of DNA origami barrels functionalized with the RNA production units and/or processing units were purified via rate-zonal centrifugation[SI-R3]. Following purification, the stock concentration was determined by UV-absorbance at 260 nm on a Nanodrop spectrophotometer (Thermo Scientific). Purification was performed right before use to prevent any aggregation or denaturation of DNA origami.

#### SPRI

SPRI was performed as described in the previous chapter to remove excess staple strands from the crude DNA origami sample.

#### AGE purification

DNA nanostructures were purified by gel (0.75-1% agarose, 0.5x TBE, 10 mM MgCl2, 1x SYBR Safe) electrophoresis with Thermo Scientific Owl B2 EasyCast Mini Gel System apparatus. The samples were loaded into the agarose gel and allowed to migrate for 1-2 hours (running buffer: 0.5x TBE, 10 mM MgCl2; 4.3V/cm). The gel was visualized with Safe Imager™ 2.0 Blue Light Transilluminator (Thermo Fisher Scientific), and the desired band of DNA origami structure was extracted. The extracted gel band was crushed in a 1.5-mL centrifuge tube, and the tube was spun at 4k x g for 1 minute. The tip of the tube containing the crushed gel band was cut and place upside down in Freeze 'N Squeeze™ DNA Gel Extraction Spin Column. The spin column was spun at 4k x g for 3 minutes to recover the purified DNA origami structure.

#### Rate-zonal centrifucation

The crude reaction to assemble tetramer of DNA origami barrels with the RNA production and/or processing units was purified by rate-zonal centrifugation with 35-65% glycerol gradient as described in the previous chapter. Following purification, the stock solution was diluted appropriately for TEM imaging to verify quality.

### SI1.6 Synthesis of catenane DNA template

The catenane DNA template was synthesized by forming DNA nanostructure that weaves leash and template strands to form catenane with linking number of 1 (Figure S1a). The oligonucleotide sequences were generated using NUPACK[SI-R4] (SI Table 4). All DNA strands were purchased from IDT with standard desalting option. The DNA strands were shipped dry and suspended at 0.5-2.5 mM in Millipore purified water and stored at -20°C. The mixture of DNA oligonucleotides (ratio indicated in SI Table 4 multiplied by 0.5 μM) in 1x TE + 10 mM $MgCl_2$ was subjected to a thermal annealing ramp on a Tetrad 2 Peltier Thermal Cycler (Bio-Rad) according to the following schedule:

Incubate at 80°C for 1 minute
Decrease to 5°C at 2 seconds/°C
Store at 5°C

1/10x volume of 10x T4 ligase buffer (NEB) and T4 ligase (NEB) at the final concentration of 0.4 unit/μL were added to the solution, and the resulting sample was ligated at room temperature overnight. The resulting product was purified via PAGE purification to obtain the catenane DNA template (Figure S1b).

**SI Table 4. List of DNA oligonucleotides for synthesis of catenane DNA template**

| Name | Sequence | Molar Ratio |
|---|---|---|
| DNA leash | /5Phos/GGTTTACCCTATCTGAGTGAGTAGCGGAGTAGAGT GGAACCCTAACCTAATTATAGAGAA | 4 |
| DNA template | /5Phos/GCGGAGCCCACACTCTACTCGACAGATACGAATAT CTGGACCCGACCGTCTCCGCCATCCCCACACGCGTGGGGT CTGCCTATAGTGAGTCGTATTA | 1 |
| DNA template splint | TTAGGCAGACCCCACGCGTGTGGGGATGTGGGCTCCGCTA ATACGACTCACTATTT | 2 |
| Catenane adaptor1 | TCGTATCTGT | 5 |
| Catenane adaptor2 | GCTACTCACT | 5 |
| Catenane adaptor3 | GTTAGGGTTC | 5 |
| DNA leash splint | AGGGTAAACCTTCTC | 5 |

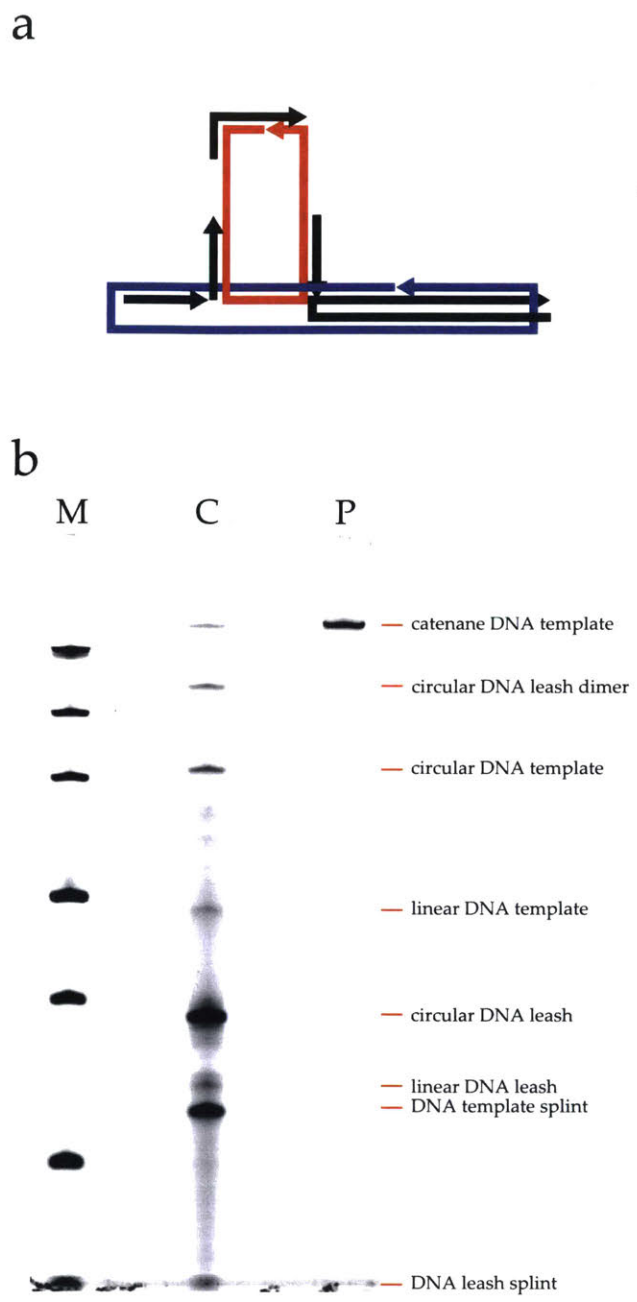


**Figure S1. Synthesis of catenane DNA template.** (a) Illustration of nanostructure architecture for synthesis of catenane DNA template. DNA leash (red), template (blue), and splint/adaptor (black) strands assemble together through hybridization, and DNA leash and template strands are mechanically locked to one another following the ligation reaction that circularizes each strand. Line and arrowhead represent ssDNA and 3'-end, respectively. (b) PAGE analysis of catenane DNA template. M = Ultra Low Range DNA Ladder, C = crude ligation reaction for synthesis of catenane DNA template, P = PAGE-purified catenane DNA template

### SI1.7 Preparation of protein-DNA conjugate

T7 RNA polymerase (RNAP) and Cse3 were fused to SNAP-tag at N- and C-terminus, respectively, to allow covalent attachment with DNA oligonucleotide modified at 3'-end with $O^6$-benzylguanine.

### Preparation of plasmids

Plasmids for SNAP-tag-fused proteins were prepared by Gibson assembly[SI-R5] of SNAP-tag gene from pSNAP-tag® (T7)-2 Vector (NEB) with linearized plasmid of either T7 RNAP (pT7-911Q) or Cse3 (pET30a-Cse3)[SI-R6] using polymerase chain reaction (PCR) that introduces overlapping sequence with SNAP-tag gene using 5'-end extensions of the primers (SI Table 5). The assembled products were transformed into XL10-Gold Ultracompetent Cells (Agilent), and the resulting plasmid products were obtained using Plasmid Miniprep Kit (Qiagen). The plasmids were sequenced by Genewiz, Inc (South Plainfield, NJ, USA) and verified that the SNAP-tag gene was introduced correctly.

**SI Table 5. List of primer sequence for PCR of T7 RNAP and Cse3 plasmids**

| Name | Seqeunce |
|---|---|
| pT7-911Q forward primer | TGGGTAAACCGGGTCTGGGAGGATCCATGAACACGATTAA |
| pT7-911Q reverse primer | TTCATTTCGCAATCTTTGTCGTGATGGTGATGGTGATGCG |
| pET30a-Cse3 forward primer | CTGGGCAAGCCTGGGCTGGGTTAGTAATGAGAATTCGAGCTC |
| pET30a-Cse3 reverse primer | CATTTCGCAGTCTTTGTCCATGGGGGCCACGGAAAGGAG |

### Expression and purification of SNAP-tag-fused proteins

The SNAP-tag-fused proteins were transformed into BL21 Competent *E. coli* (NEB). The transformed BL21 cells were grown to OD600 around 0.5 and induced with IPTG at 0.4 mM for 3 hours. The bacterial cells were spun to pellet and redissolved in lysis buffer (50 mM Tris-HCl, pH 8, 300 mM NaCl, 5% Glycerol, 5 mM BME), and the redissolved pellet was sonicated to lyse the cells. The lysate was spun once again to collect supernatant, and the proteins were purified using Pierce HisPur Ni-NTA Spin Columns (Thermo Scientific) by binding His-tag on each protein to the resin and eluting with buffer containing 200 mM imidazole to collect the purified products. The eluted proteins were buffer exchanged using Amicon Ultra filtration columns with 2x storage buffer (T7 RNAP: 100 mM Tris-HCl (pH 8), 200 mM NaCl, 40 mM BME, 2 mM EDTA, 0.2% Triton X-100; Cse3: 100 mM HEPES, 200 mM NaCl, 4 mM DTT). The SNAP-tag-fused proteins were mixed 1:1 with glycerol and stored at -20°C.

### Preparation of $O^6$-benzylguanine-modified DNA oligonucleotides

The DNA oligonucleotides with 3'-end modified with amine group was purchased from IDT (SI Table 6). The oligonucleotides were mixed with BG-GLA-NHS (NEB), an amine-reactive substrate for SNAP-tag, to prepare $O^6$-benzylguanine-modified DNA oligonucleotides. BG-GLA-NHS was added in excess to the oligonucleotides and kept above 1 mM to ensure efficient conjugation. The excess BG-GLA-NHS was removed from modified oligonucleotides by Oligo Clean & Concentrator (Zymo Research). The concentrations of the resulting DNA oligonucleotides were measured using A260, and the oligonucleotides were stored at -20°C.

**SI Table 6. List of DNA oligonucleotides modified with amine group at 3'-end**

| Name | Sequence |
|---|---|
| Dwalin | /5Phos/GCTACTCACTCAGATAGGGTA/3AmMO/ |
| aFili | ATACATCTATTGGTTAAGGTCAACATCGTCTC /3AmMO/ |

**Preparation and purification of protein-DNA conjugates**

$O^6$-benzylguanine-modified DNA oligonucleotides, Dwalin and aFili, were incubated with SNAP-tag-fused proteins, T7 RNAP and Cse3, respectively, to form protein-DNA conjugates by enzymatic activity of SNAP-tag that self-labels any substrate with $O^6$-benzylguanine. $O^6$-benzylguanine-modified DNA oligonucleotides were added at 1.5-2x the molar concentration of SNAP-tag-fused proteins to ensure complete conjugation. Excess $O^6$-benzylguanine-modified DNA oligonucleotide was removed from each reaction using Pierce Strong Cation Exchange Spin Column (Thermo Scientific). The protein-DNA conjugates were eluted from the column with buffer containing 0.5 M NaCl. The eluted protein-DNA conjugates were buffer exchanged using Amicon Ultrafiltration device with 2x storage buffer (T7 RNAP: 100 mM Tris-HCl (pH 8), 200 mM NaCl, 40 mM BME, 2 mM EDTA, 0.2% Triton X-100; Cse3: 100 mM HEPES, 200 mM NaCl, 4 mM DTT). The conjugates were mixed 1:1 with glycerol and stored at -20°C.

**SI1.8 Assembly of DNA origami structures with functional units**

**Preparation of catenane DNA template with double-stranded circular DNA template**

The catenane DNA template was assembled with non-template strands (SI Table 7) that are complementary to the circular DNA template by heating the mixture of the catenane DNA template at 3 μM and non-template strands at 3.6 μM each in a folding buffer (1x TE, 10 mM $MgCl_2$) to 80°C for 2 minutes and quickly cooling to 25°C on a Tetrad 2 Peltier Thermal Cycler.

**SI Table 7. List of non-template strands**

| Name | Sequence |
|---|---|
| NT1 | /5Phos/AGACCCCACGCGTGTGGGGATGGCGGAGACGGTCGGGTCCAGATATTCGTAT CTGTCGAGTAGAGTGTGGGC |
| NT2 | TCCGCTAATACGACTCACTATAGGC |

**Preparation of DNA origami structures loaded with molecular cargos**

The catenane DNA template or the processing unit was added at three times the molar concentration of the programmed handles on DNA origami barrel with excess staple removed using SPRI. The solution was incubated at 37°C for 1 hour before further assembly or purification step.

**Preparation of RNA production unit**

Transcription inhibitor was first prepared by annealing the strands at equimolar concentration (SI Table 8) in a folding buffer (1x TE, 10 mM $MgCl_2$) by heating the solution to 80°C for 2 minutes and quickly cooling to 25°C on a Tetrad 2 Peltier Thermal Cycler. DNA-conjugated T7 RNAP was mixed with the 5 times the molar concentration of prepared

transcription inhibitor to form inhibited T7 RNAP. The production unit was prepared by adding excess of inhibited T7 RNAP to the sample with catenane DNA template.

**SI Table 8. List of transcription inhibitor strands**

| Name | Sequence |
|---|---|
| AI sense | TACCCTATCTGAGTTTTCAAATTAATACGACTCACTATA |
| AI antisense | TATAGTGAGTCGTATTAATTTG |

**Assembly of loaded DNA origami structure**

DNA origami tetramer was assembled as described in the previous chapter. However, the presence of loaded molecular cargos on the lumen of the barrel structures decreased the kinetic of DNA origami assembly. Therefore, the incubation time for the assembly took 2 hours instead of 1 hr. The assembled origami was purified using rate-zonal centrifugation.

**SI1.9 Agarose gel electrophoresis**

DNA nanostructures were analyzed by gel (1.5% agarose, 0.5x TBE + 10 mM MgCl2, 1x SYBR Safe) electrophoresis with Thermo Scientific Owl B2 EasyCast Mini Gel System apparatus. The samples were loaded into the agarose gel and allowed to migrate for 2-4 hours (running buffer: 0.5x TBE, 10 mM MgCl2; 4.3V/cm). The gel was imaged with Typhoon FLA 9000 (GE Healthcare Life Sciences).

**SI1.10 Polyacrylamide gel electrophoresis**

**Denaturing PAGE**

Catenane DNA template synthesis and RNA processing efficiency of transcript were analyzed by gel (TBE-Urea; 8-12% polyacrylamide) electrophoresis with Invitrogen XCell SureLock Mini-Cell Electrophoresis System apparatus. The samples were loaded into the gel and allowed to migrate for 20-60 minutes (running buffer: 0.5x TBE; 25-37.5V/cm). The gel was stained with SYBR Gold for nucleic acids or DFHBI-1T for Broccoli aptamer and imaged with Typhoon FLA 9000.

**SDS-PAGE**

Incorporation efficiency of handles and Cse3 in DNA origami barrel was analyzed by gel electrophoresis using Invitrogen NuPAGE Bis-Tris Gels (Bis-tris; 4-12% polyacrylamide) with Invitrogen XCell SureLock Mini-Cell Electrophoresis System apparatus. The samples were loaded into the gel and allowed to migrate for 30 minutes (running buffer: 1x NuPAGE MES SDS Running Buffer (Invitrogen); 25V/cm). The gel was washed and stained with SYBR Gold for nucleic acids and SimplyBlue SafeStain for protein and imaged with Typhoon FLA 9000 and FluorChem M system (ProteinSimple), respectively.

**SI1.11 Negative-Stain Transmission Electron Microscopy**

TEM imaging was carried out by dropping 3.5 μL of product onto a plasma-treated carbon-formvar grid (Electron Microscopy Sciences). This was incubated for 1-5 minutes

depending on the concentration of DNA origami. The solution was wicked away onto the edge of folded filter paper at 45° without completely drying out the sample. The sample was washed three times by adding 5 μL of folding buffer (5 mM Tris-HCl (pH 8) + 1 mM EDTA + 12 mM $MgCl_2$) and wicking away the solution onto the edge of folded filter paper at 45° without completely drying out the sample. Finally, 5 μL of 2% uranyl formate (in water, w/v) was added before the grid was dry. The grid was incubated for 10-30 seconds, and the uranyl formate was wicked away completely onto the edge of folded filter paper at 90°. Imaging was carried out on a JEOL 1400 transmission electron microscope.

### SI1.12 DNA-PAINT

**Reagents**

Stored at room temperature:
Buffer A (10 mM Tris-HCl, 100 mM NaCl, 0.05% Tween 20, pH 7.5)
Buffer B (10 mM Tris-HCl, 10 mM MgCl2, 1 mM EDTA, 0.05% Tween 20, pH 8)

Stored at -20C:
20× Streptavidin (10 mg/mL in 1× Buffer A)
20× Biotin-BSA (20 mg/mL in 1× Buffer A)
1 μM P5 imager strand stock in water (ATACATTGA/Cy3b/)
1 μM P9 imager strand stock in water (CATCCTAATT/Cy3b/)
40× PCD (9.3 mg PCD in 13.3 mL buffer containing 50% glycerol in 50 mM KCl, 1 mM EDTA, 100 mM Tris-HCl, pH8)
100× PCA (154 mg PCA in 10 mL water, pH adjusted to 9.0 with NaOH)
100× Trolox (100 mg Trolox, 430 ul 100% MeOH, 3.2 mL water, 345 uL of 1N NaOH)

**Procedure**

DNA origami for DNA-PAINT was prepared as follows: 2× PEG precipitated DNA origami (15 nM) were incubated with "anti-handle" oligonucleotides labeled with Alexa Fluor 647 (1.8 μM) and "anti-handle" oligonucleotides labeled with biotin (1.8 μM) in 1× buffer of 5 mM Tris, 1 mM EDTA, 10 mM MgCl2 at 25°C for 1 hour. Excess anti-handles were purified away from labeled DNA origami by gel electrophoresis using a 1× SYBR Safe pre-stained 0.7% agarose gel running at 60V for 120 minutes. Band containing the functionalized DNA origami was extracted from the gel using razor blades and eluted using a BioRad Freeze 'N Squeeze DNA Gel Extraction Column following manufacturer's instructions.

A flow chamber was fabricated by attaching a coverslip to a microscope slide using double-sided tape. The chamber was first incubated with 20 μl of freshly prepared 1× biotin-BSA in Buffer A for 2 min, followed by 2× 20μl washing with Buffer A. The chamber was next incubated with 20 μl of freshly prepared 1× streptavidin in Buffer A for 2 min, followed by 1× 20μl washing with Buffer A and 2× 20μl washing with Buffer B. The chamber was next incubated with 20 μl of gel extracted DNA origami sample diluted to 200~400 pM in Buffer B and incubated for 2 min, followed by 2× 20 μl washing with Buffer B. Finally, the chamber was sealed with 2× 20 μl of freshly prepared imager buffer (1× Trolox, 1× PCA, 1x PCD in Buffer B) containing optimal concentration of the imager strand (i.e., 2 nM P5 and 10 nM P9). Flow

chamber was sealed with epoxy prior to imaging. Images were acquired on the ONI Desktop Nanoimager with a 100× oil objective, 561 nm laser operating at a power of 30 mW, acquisition speed of 5 Hz for 30,000 to 50,000 frames. Images were analyzed and rendered using the Picasso software.

**SI1.13 Single-molecule imaging**

**Reagents**

Stored at room temperature:
Buffer A (10 mM Tris-HCl, 100 mM NaCl, 0.05% Tween 20, pH 7.5)
Buffer B (10 mM Tris-HCl, 10 mM MgCl2, 1 mM EDTA, 0.05% Tween 20, pH 8)

Stored at -20C:
100 μM Quencher strand (ACTCACTATAGGC/3BHQ_2/)
100 μM Imager strand (/5Cy3/GCCTATAGTGAGTCGTATTA)
20× Streptavidin (10 mg/mL in 1× Buffer A)
20× Biotin-BSA (20 mg/mL in 1× Buffer A)
40× PCD: (9.3 mg PCD in 13.3 mL buffer containing 50% glycerol in 50 mM KCl, 1 mM EDTA, 100 mM Tris-HCl, pH8)
100× PCA (154 mg PCA in 10 mL water, pH adjusted to 9.0 with NaOH)
10× Transcription buffer (400 mM Tris-HCl, 60 mM MgCl2, 10 mM DTT, 20 mM spermidine pH 7.9 @ 25°C)
1× PBS (Invitrogen)
25 mM rNTP mix (NEB)
40 U/μl RiboLock RNase inhibitor (Invitrogen)

**Procedure**

DNA origami functionalized with anti-biotin and Alexa Fluor 647 were purified by rate-zonal centrifugation using a 10% to 45% glycerol gradient buffer (5 mM Tris, 1 mM EDTA, 10 mM MgCl2). Purified DNA origami was diluted to 75 pM in 1× PBS supplemented with 5 mM Tris, 1 mM EDTA, and 10 mM MgCl2. A 10× solution of quencher (20 μM ) and imager strands (1 μM) were annealed in buffer (5 mM Tris, 1 mM EDTA, and 5 mM MgCl2) from 60°C to 25°C over 10 minutes. 1× imaging buffer was prepared fresh by combining PCA (1×), PCD (1×), quencher-imager complex (1×), transcription inhibitor (50 nM), transcription buffer (1×), PBS (1×), rNTPs (1 mM), and RiboLock RNase inhibitor (8 U/μl).

A flow chamber was fabricated by attaching a coverslip to a microscope slide using double-sided tape. The chamber was first incubated with 20 μl of freshly prepared 1× biotin-BSA in Buffer A for 2 min, followed by 2× 20μl washing with Buffer A. The chamber was next incubated with 20 μl of freshly prepared 1× streptavidin in Buffer A for 2 min, followed by 1× 20μl washing with Buffer A and 2× 20μl washing with Buffer B. The chamber was next incubated with 20 μl of purified DNA origami sample and incubated for 2 min, followed by 2× 20 μl washing with Buffer B. Finally, the chamber was sealed with 2× 20 μl of freshly prepared imaging buffer and sealed with epoxy. Sample was imaged on a Zeiss LSM710 TIRF microscope with a 100× oil objective equipped with a temperature-controlled incubation chamber pre-

heated to 37°C. Time-lapse images of the Cy3 channel was captured using a 514 nm laser operating at 15 % power level and 500 ms exposure taken over 180 minutes at 2 minute intervals. Alexa Fluor channel was captured once at the beginning and end of the experiment using the 647 nm laser operating at 20 % power level and 500 ms exposure.

**SI2. Quantification of Cse3 handle and cargo incorporation**

The availability of ssDNA handle for Cse3 and incorporation efficiency of Cse3 were quantified using SDS-PAGE analysis after incorporation and purification. The concentration of staple strands with ssDNA handle was estimated by using Cse3 and staple strands with ssDNA handles of known concentration as standards (Figure S2). The estimated concentration of each molecule was divided by the estimated concentration of the DNA origami barrel from A260 to quantify the availability of ssDNA handle and incorporation efficiency of Cse3.

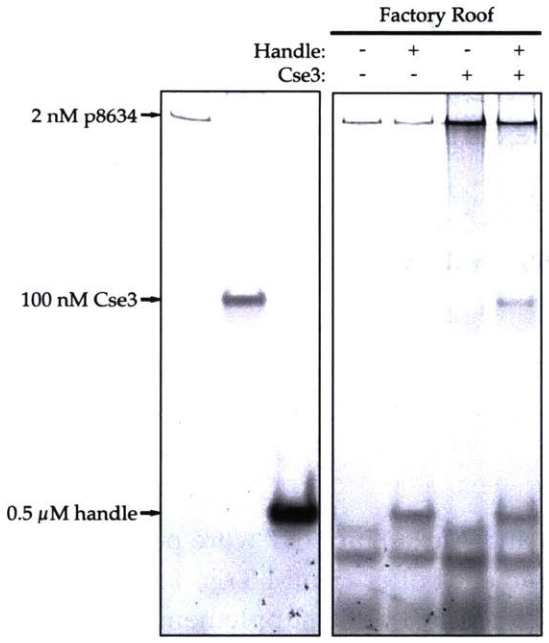


**Figure S2. SDS-PAGE of DNA origami barrel with Cse3 for bulk quantification of incorporation efficiency.** DNA origami barrel structures with (+) or without (-) ssDNA handles for Cse3 (Handle) was incubated with (+) or without (-) Cse3. Samples were purified before loading into the gel. Using standards of known concentrations, the availability of ssDNA handle and incorporation efficiency of Cse3 were quantified.

**SI3. Quantification of RNA processing efficiency**

The RNA processing efficiency was quantified using denaturing PAGE analysis after samples were incubated at 37°C for transcription and ribonuclease activity. The band intensity from fluorescence signal was measured for RNA transcript with Broccoli aptamer (Figure S3). The processing efficiency was calculated by dividing the band intensity of completely processed transcript monomer (97 nt) and partially processed concatemers (dimer-hexamer) with sum of all Broccoli aptamer signal in the lane.

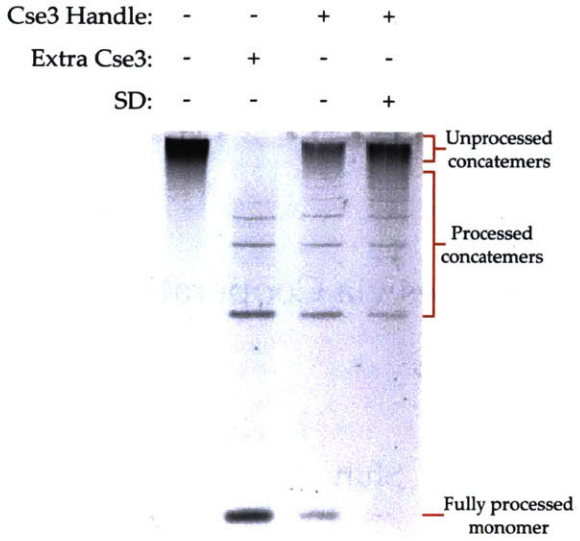


**Figure S3. Denaturing PAGE of nanofactory for RNA production and processing stained for Broccoli aptamer.** Tetramer of DNA origami barrel was programmed with handles for 12 production units and either with (+) or without (-) handles for 96 processing units (Cse3 Handle). As a positive control for RNA processing, excess processing units (Extra Cse3) were added (+) to a sample without handles for processing units. As another control to characterize the effect of co-localization between production and processing units, handles hybridized to oligonucleotides attached to Cse3 were displaced (+) using DSD oligonucleotides (SD) added to a sample with handles for processing units.

**SI4. Supplemental references**

SI-R1. Douglas, S. M.; Chou, J. J.; Shih, W. M. DNA-Nanotube-Induced Alignment of Membrane Proteins for NMR Structure Determination. *Proceedings of the National Academy of Sciences* **2007**, *104*, 6644–6648.

SI-R 2. DeAngelis, M. M.; Wang, D. G.; Hawkins, T. L. Solid-Phase Reversible Immobilization for the Isolation of PCR Products. *Nucleic acids research* **1995**, *23*, 4742–3.

SI-R 3. Lin, C.; Perrault, S. D.; Kwak, M.; Graf, F.; Shih, W. M. Purification of DNA-Origami Nanostructures by Rate-Zonal Centrifugation. *Nucleic Acids Research* **2013**, *41*, e40–e40.

SI-R 4. Zadeh, J. N.; Steenberg, C. D.; Bois, J. S.; Wolfe, B. R.; Pierce, M. B.; Khan, A. R.; Dirks, R. M.; Pierce, N. A. NUPACK: Analysis and Design of Nucleic Acid Systems. *Journal of Computational Chemistry* **2011**, *32*, 170–173.

SI-R 5. Gibson, D. G.; Young, L.; Chuang, R.-Y.; Venter, J. C.; Hutchison, C. a; Smith, H. O. Enzymatic Assembly of DNA Molecules up to Several Hundred Kilobases. *Nature methods* **2009**, *6*, 343–5.

SI-R 6. Gesner, E. M.; Schellenberg, M. J.; Garside, E. L.; George, M. M.; MacMillan, A. M. Recognition and Maturation of Effector RNAs in a CRISPR Interference Pathway. *Nature Structural & Molecular Biology* **2011**, *18*, 688–692.

# Chapter 5: Thermal Cycling of DNA Devices via Cooperative Strand Displacement

Jaeseung Hahn, William M. Shih

## 5.1 Abstract

DNA-based devices often are powered by mixing-driven cycles of hybridization with "fuel" strands and toehold-mediated displacement by "recovery" strands. However, mixing can be cumbersome, non-robust, and wasteful of materials. Here we demonstrate mixing-free thermal cycling of DNA devices that is actuated through cooperative strand displacement. Using a simple DNA reaction based on an associative strand displacement process, we developed a mechanism that can induce DNA strand displacement by lowering the temperature and experimentally demonstrated simple digital logic circuits operated and reset, respectively, by lowering and increasing the temperature. We investigated the engineering parameters based on design and experimental considerations, and the resulting behavior was determined by the displacement efficiency at varying temperature. Remarkably, the degradation of function was not observable even after 500 cycles of temperature change resulting in 1000 consecutive DNA strand displacement operations. In essence, the mechanism provides a means to operate DNA-based systems for repeated and extended operation in a closed system.

## 5.2 Introduction

Toehold-mediated DNA strand displacement (DSD) has enabled construction of sophisticated molecular devices fueled by DNA.[1–3] The well-characterized thermodynamics of DNA hybridization[4] allows quantitative design of structures and dynamics of the enzyme-free molecular devices. While expanding the capability and robustness of the DSD-based systems,[5,6] the DNA nanotechnologists have also begun to develop applications of DSD such as label-free single-nucleotide polymorphism genotyping[7], microRNA detection[8], and directed chemical synthesis[9]. However, the molecular devices fueled by DNA lack reliable and facile means to refuel for repeated operations without specialized equipment unavailable in a typical lab setting[10]. In this work, we present a mechanism that utilizes thermal energy to fuel DSD for DNA devices capable of repeated operation.

Toehold-mediated DSD is the process through which two strands with complementarity hybridize and displace one or more pre-hybridized strands via branch migration catalyzed by toehold binding at the single-stranded region.[11] The free energy for this reaction is therefore provided by reactants, and the system cannot be easily recharged once reaching equilibrium unlike circuits and machines powered by standardized energy (e.g. electricity, heat). Addition of reactant DNA strands can provide supplementary free energy that refuels the systems for repeated operation.[1] However, the resulting accumulation of double-stranded DNA (dsDNA) waste products and further dilution of components leads to deterioration of performance.

To circumvent the drawbacks of adding extra reactant species, DNA devices can be replenished by continuous exchange of buffer to refill fuel strands and remove waste products.[10] However, the system requires immobilization of DNA devices on a surface for the exchange and also requires a fluidic system for automation. Alternatively, other mechanisms with orthogonal energy sources have been developed to manipulate the system more easily. Chemical modification of DNA with azobenzene allows the use of photons to direct hybridization and dehybridization, fueling the reaction for the operation of DNA systems.[12] However, chemical modification of DNA strands is required, and a high-power laser system is

required for operation. Ions have been used to fuel DNA devices that contain i-motif,[13] G-quadruplex,[14] and triplex.[15] However, the DNA sequence is constrained for these devices, and a similar fluidic system required for exchanging DNA strands is necessary for automation of adding energy source (i.e. ions) and removing waste products that will eventually dampen the reaction. Therefore, the currently available approaches for repeated operation of DNA devices require specialized equipment, physical/chemical modification of DNA, and/or stringent constraint on DNA sequence, which collectively limit the scale of the system and make it difficult to accommodate in a typical lab setting.

Due to our understanding of the thermodynamics of DNA duplex, thermal energy can be used to drive DNA-based systems through controlling hybridization and dehybridization. For instance, polymerase chain reaction (PCR) amplifies target DNA duplex by cycling the process to dehybridize DNA template duplex at melting temperature, hybridize DNA primers to complementary regions in DNA template at annealing temperature, and extend DNA primer via DNA polymerase.[16,17] Moreover, Gareau and colleagues used the programmable melting and annealing behavior of DNA to construct nanothermometers capable of measuring range of temperature via fluorescence signal.[18] The simple melting and annealing behavior of DNA duplex have already been exploited successfully to yield useful applications, and most molecular biology labs now have access to thermal cycler for PCR. Therefore, DSD driven by thermal energy would be easy to implement in a typical molecular biology lab setting and advance our capability to construct DNA devices with programmable behavior.

Beyond the simple melting and annealing property of DNA, Rogers and Manoharan demonstrated thermally driven phase transition of DNA-grafted microparticles programmed by carefully tuning enthalpic and entropic changes due to DSD reaction to design free energy landscape over a range of temperatures.[19] Utilizing a similar scheme, re-entrant DNA hydrogel was demonstrated as well.[20] However, some design constraints pose challenges to adapt this mechanism for DNA devices driven by DSD because the system was originally designed for microparticle assembly. First, the design is implemented with formation of relatively short DNA duplex of eight base pairs (bp). Many DNA devices require more stable duplex, typically longer than 15 bp at room temperature, to ensure that the duplex does not spontaneously dissociate during the operation, which would be detrimental to the function of the devices. Moreover, the design requires displacing strands to bind both strands of target DNA duplex that facilitates the formation of assembly, and this scheme can be problematic for some DNA circuit designs that rely on displacement reaction to free single-stranded DNA, which can further act as reactant for the next operation. Therefore, many DNA devices found in literature[11] are incompatible with these design constraints.

We developed temperature-dependent associative DSD (TAD) to reversibly actuate strand displacement by changing temperature. TAD uses association of multi-domain system to program enthalpy and entropy changes. The design presented here is a generalization of Rogers and Manoharan's approach to drive diverse DNA devices available in the literature. We explored design parameters and their effect on the system's function. Then, we demonstrated the use of TAD in a simple DNA circuit. TAD does not require any special modification of DNA, sequence constraint other than orthogonal complementarity based on the Watson-Crick base pairing, or specialized equipment except widely available PCR thermal cycler. Therefore,

TAD can be easily implemented in a typical molecular biology lab setting and potentially scale up the complexity of DSD-based system for sophisticated behavior.

## 5.3 Results and Discussion

### 5.3.1 Design and working principles of TAD

The design of TAD is inspired by the principle of remote toehold[21] and associative toehold activation.[22,23] Respective activation and deactivation, or vice versa, of two toehold domains—TAD toehold binding domain ($S_A$) and incumbent toehold binding domain ($S_I$)—flanking branch migration domain ($S_D$) on the substrate strand (S) drives the system (Figure 1a). Association of TAD toehold activator domain ($TAD_A$), TAD displacing domain ($TAD_D$), and incumbent toehold deactivator domain ($TAD_I$) allows the toehold-mediated DSD. The complex operates via initial binding to $S_A$, subsequent branch migration into $S_D$ while kicking off incumbent displacing domain ($I_D$), and lastly continued branch migration into $S_I$ for displacement of incumbent toehold domain ($I_I$) and inhibition of incumbent strand (I) from rebinding. Conversely, dissociation of TAD domains does the opposite and let I to bind $S_I$ and displace $TAD_D$ following dissociation of $TAD_A$ and $TAD_I$ from S. $TAD_A$, $TAD_D$, and $TAD_I$ can associate by stem-loop domains ($TAD_S$) or complementary TAD linker domains ($TAD_L$). $TAD_S$ and $TAD_L$ bring together multiple domains by forming a DNA junction between domains (Figure 1b).

Consequently, the design parameters change how TAD strands associate. The two design parameters are the number of base pairs between TAD strands ($l$) and the number of TAD strands ($n$). These parameters collectively determine the thermodynamic properties of each design and therefore TAD activity. To quantify TAD activity, we define displacing temperature ($T_d$) as the temperature at which 50% of I is displaced from S and displacing range ($\Delta T$) as the temperature interval spanning 1 to 99% displacement of I from S.

For DNA hybridization, the temperature dependence of duplex formation comes from free energy change that is monotonic with a steepness set by enthalpy change, which is largely independent of temperature along with entropy change.[19] Therefore, enthalpy change determines $\Delta T$ while both enthalpy change and entropy change collectively determine $T_d$. The increase in number of bp between duplex increases both enthalpy change and entropy change with net free energy change that favors hybridization in general. Thus, larger $l$ is expected to decrease $\Delta T$ while increasing $T_d$. Given the same concentration of each TAD strand ($c$) as well as the same $l$, larger $n$ results in more concentration-adjusted entropic penalty from having more components for the complex formation in addition to entropy change and enthalpy change associated with having more duplex formation from association of TAD strands. Therefore, the increase in $n$ is expected to decrease both $T_d$ and $\Delta T$ in general.

### 5.3.2 Characterization of TAD designs

By utilizing I and S conjugated with quencher and fluorophore, the activity of TAD was measured from fluorescence signal that is directly proportional to displacement of quencher and fluorophore strands (see methods in SI1). To verify the wide applicability of TAD, we used two sets of I-S pairs with different lengths, sequence, placement of modification, and fluorophore-quencher pair used (Figure 1c). The fluorescence signal from dissociation of I-S pair

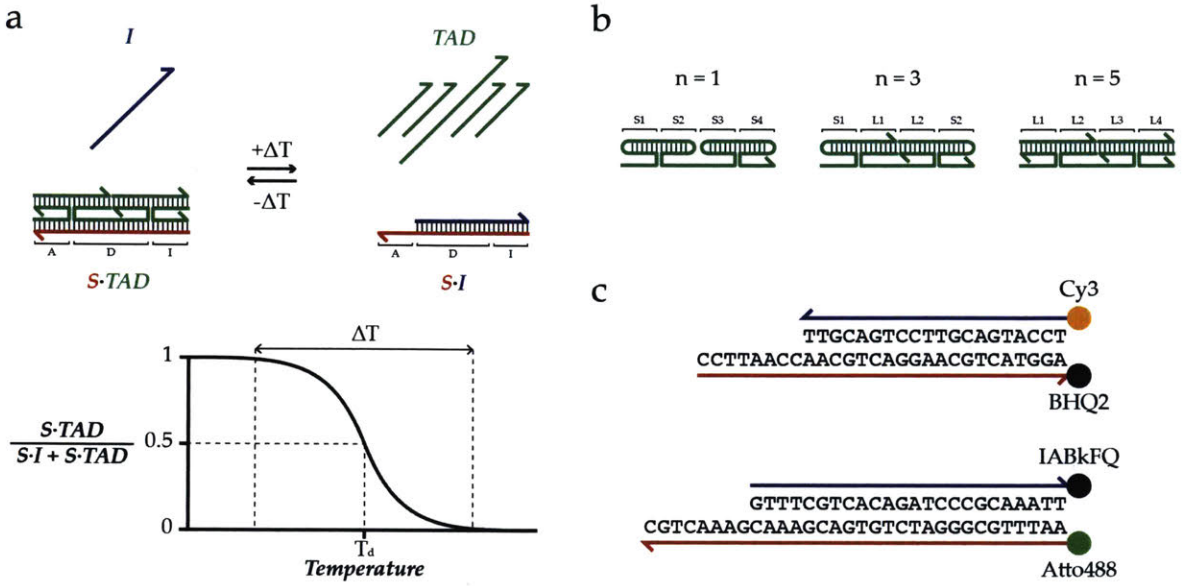


**Figure 1. Schematics showing the principle of TAD and different TAD designs.** (a) A schematic showing the working principle of TAD. Change of temperature drives association and dissociation of TAD strands that lead to displacement and rebinding of I-S pair, respectively. Colored lines represent DNA strands with arrowheads indicating 3′-end and colors indicating identities. The formation of appropriate duplex is indicated with black lines between DNA strands that represent hydrogen bonds formed between complementary bases. (b) Three different TAD designs can be constructed when the number of junctions is fixed at two, the number of junction branches is fixed at four, and the assembly is set to be symmetric. (c) Two sets of sequentially and spectrally orthogonal I-S pairs are used to verify and quantify TAD operation.

was normalized using the controls to yield quantified TAD activity (see data processing in SI1). The behaviors of different designs were in qualitative agreement with our model (see SI Table 2). The larger $l$ increased $T_d$ and decreased $\Delta T$ (Figure 2a) when $n$ and $c$ were constant. With the same $l$ and $c$, the larger $n$ decreased $T_d$ and $\Delta T$ (Figure 2b) although we observed some exceptions, which might be ascribed to unfavorable enthalpy change with decreasing temperature from DNA four-way junction[24] (see SI2). It was somewhat surprising to find that a TAD design (n = 1) could be outcompeted by I with the observed $T_d$ (63.8°C) since it is predicted to make more base pairs (Unafold not shown) and the number of strands exchanged is the same (i.e. 1). Possible explanations are that the hairpins are less stable than predicted by Unafold at the $T_d$ and/or junctions are highly unstable at higher temperatures. In addition, increasing $c$ of the same design resulted in higher $T_d$ with similar $\Delta T$. By changing the design parameters, $l$ and $n$, as well as experimental parameter, $c$, it would be possible to fine-tune the TAD properties, $T_d$ and $\Delta T$, for the operation of DNA-based devices.

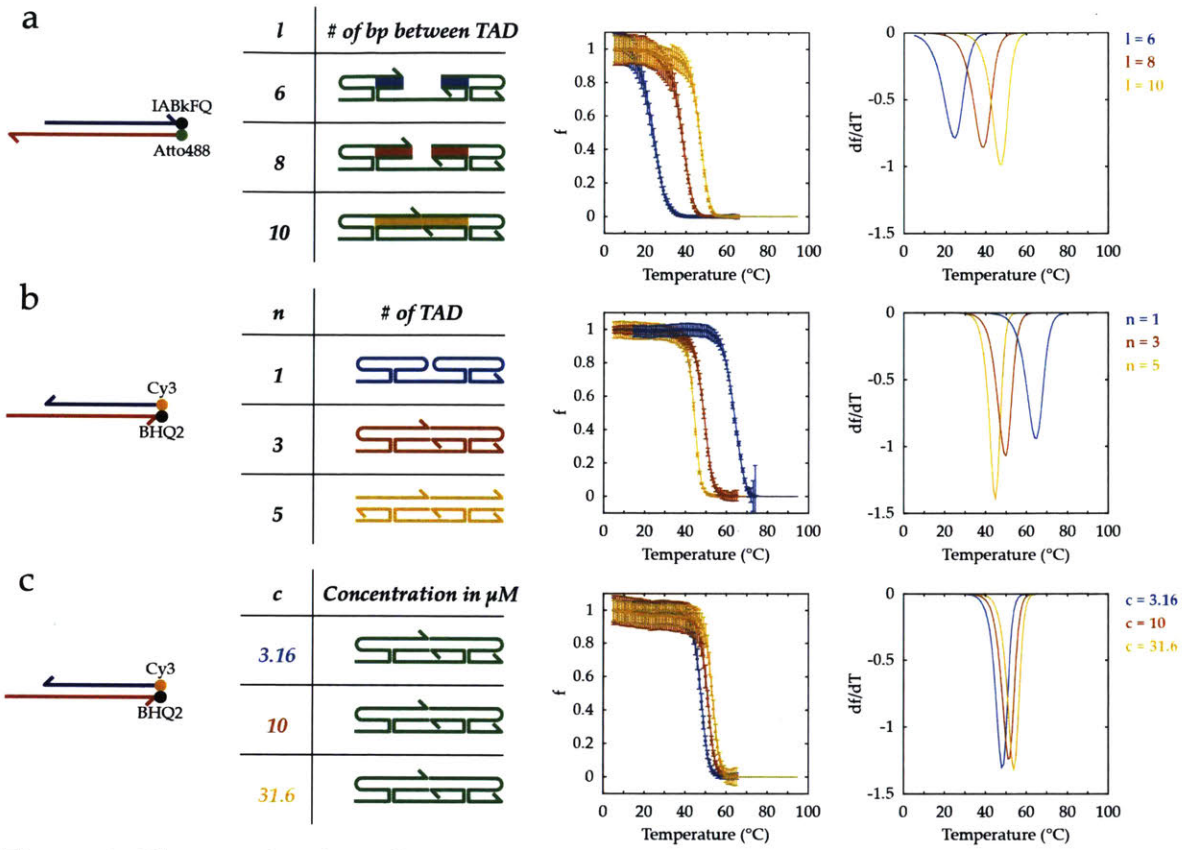


**Figure 2. Characterization of TAD.** Fluorescence signal is measured as a surrogate for fraction of I-S pair displaced to determine the effect of varying (a) *l*, (b) *n*, and (c) *c* on TAD. The experimental data (dot) of displacement fraction, f, are fitted to derive melting curve (line), and its first derivative with respect to temperature, df/dT, is plotted to visualize the sharpness of transition. Error bars here represent standard deviation.

### 5.3.3 Repeated operation of TAD

The repeated operation of TAD should maintain the activity because there is no accumulation of waste product or dilution of the sample associated with other mechanisms that require exchange of mass. First, the kinetics of TAD activation and deactivation of a TAD design ($n$ = 1; Cy3-BHQ2 pair) at ON (49°C) and OFF (74°C) temperatures corresponding to 99% and 1% displacement, respectively, were measured to determine the cycling time (Figure 3a). Both reactions took less than 30 seconds for this particular design. Nearly identical TAD activity was observed when cycling between ON and OFF temperatures while measuring fluorescence for 500 cycles, equivalent to 1000 DSD operations (Figure 3b). As a comparison, a microfluidics-based method to refuel a DNA bipedal walker was able to achieve 32 steps, equivalent to 64 consecutive DSD operations, though it should be noted that the system cycled through eight possible states (four stepping states and four intermediate states) requiring eight distinct DSD operations, compared to two here, and therefore was more complex in nature.[10] It may be possible that the activity would eventually deteriorate as degradation of DNA progresses from cycling through the range of temperature. Nonetheless, the durability and ease of operation

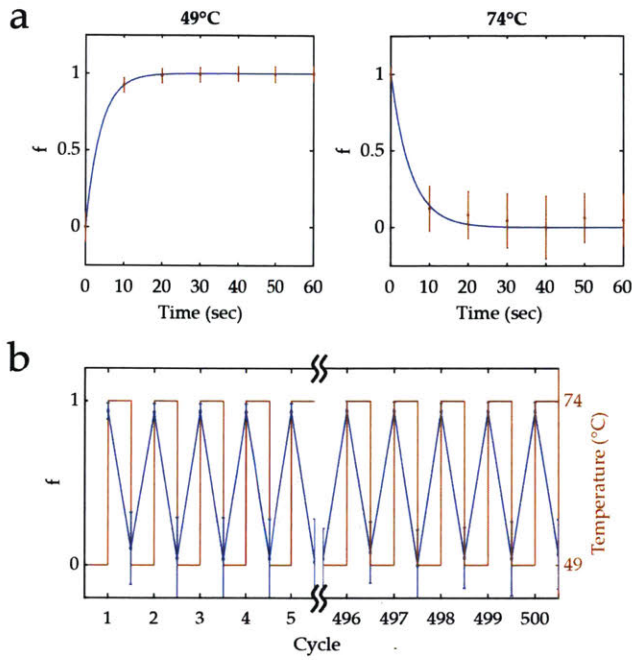


**Figure 3. Kinetics and repeated operation of TAD.** (a) Experimental data (dot) and fitted curve (line) of displacement fraction, f, showing activation (left) and deactivation (right) kinetics of TAD design with $n = 1$ for I-S pair conjugated with Cy3-BHQ2 pair. (b) Repeated operation of the same sample from panel (a) showing first and last five cycles of a 500-cycle experiment. Error bars here represent standard deviation.

compared to other existing technologies makes TAD an attractive mode of controlling DSD-based devices.

### 5.3.4 Operation of two orthogonal TADs

In principle, multiple TAD operations could be performed in the same reaction by careful sequence design of DNA. We tested orthogonal sequences of TAD strands acting independently on different I-S pairs in the same solution. As a proof-of-principle, two sets of TAD strands with different $T_d$ were chosen so that there can be three distinct states in the system: both fluorophores off, one fluorophore on, and both fluorophores on (Figure 4a). The melting curve confirmed the TAD activity on two spectrally and sequentially orthogonal I-S pairs and determined the corresponding temperature for each state (Figure 4b). Programmed temperature changes could switch among each state freely (Figure 4c). As it would be expected, TAD operation at a lower temperature resulted in slower kinetics. Though not explored in this work, it should be possible to make more accessible states as long as sequence design is stringent, and TAD designs possess narrow $\Delta T$.

### 5.3.5 TAD-based circuit

The reversible nature of TAD allows refueling of the system via temperature change to build DNA circuits and devices for repeated operations. As a proof-of-principle, a reusable

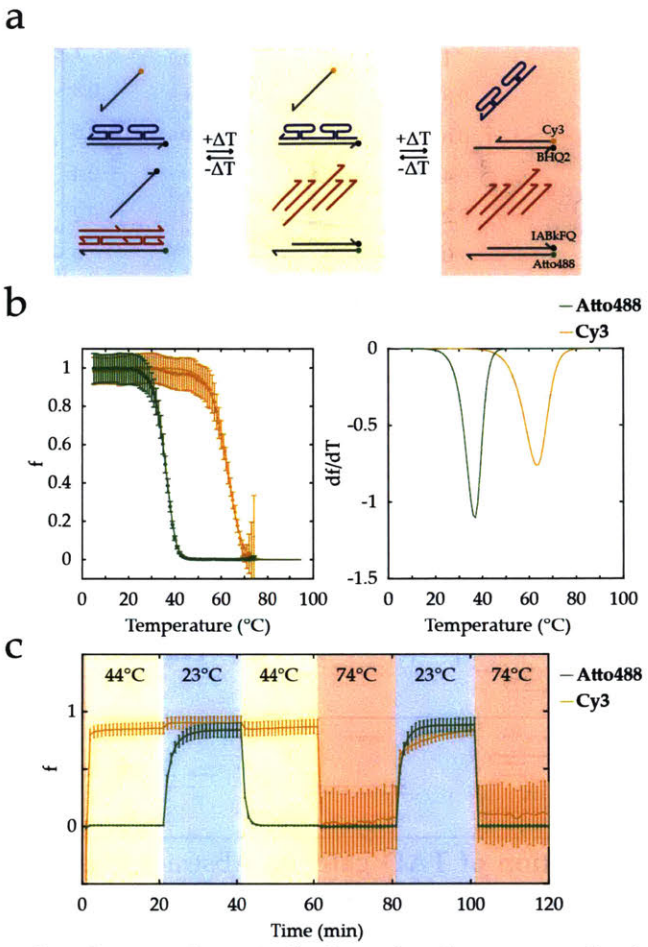


**Figure 4: Operation of orthogonal TAD designs in the same solution.** (a) Programmed states of TAD designs at low (blue), medium (yellow), and high (red) temperature. (b) Melting curve and its first derivative verifying the orthogonal operation of two TAD designs in the same solution and showing three accessible states in the system. The experimental data (dot) of displacement fraction, f, are fitted to derive melting curve (line), and its first derivative with respect to temperature, df/dT, is plotted to visualize the sharpness of transition. (c) Time course trace of f depending on the temperature. Error bars here represent standard deviation.

circuit inspired by the DNA seesaw circuit[6] was designed to be compatible with the TAD mechanism and powered by temperature as universal fuel (Figure 5a). This TAD-based circuit does not "seesaw" like the DNA seesaw gate that exchanges activity of DNA signals through the toehold exchange-based reversible reaction. Instead, a TAD reaction acts as an initiation stepin the presence of input strand, and another TAD reaction acts as a catalytic cycle that allows signal amplification much like the DNA seesaw circuit (Figure 5b). The circuit was designed to preserve the threshold capability of DNA seesaw circuit by adding extra gate base strand to quench the specified amount of input strand. Therefore, the TAD circuit can be reconfigured to perform an OR logic function as well as an AND logic function through

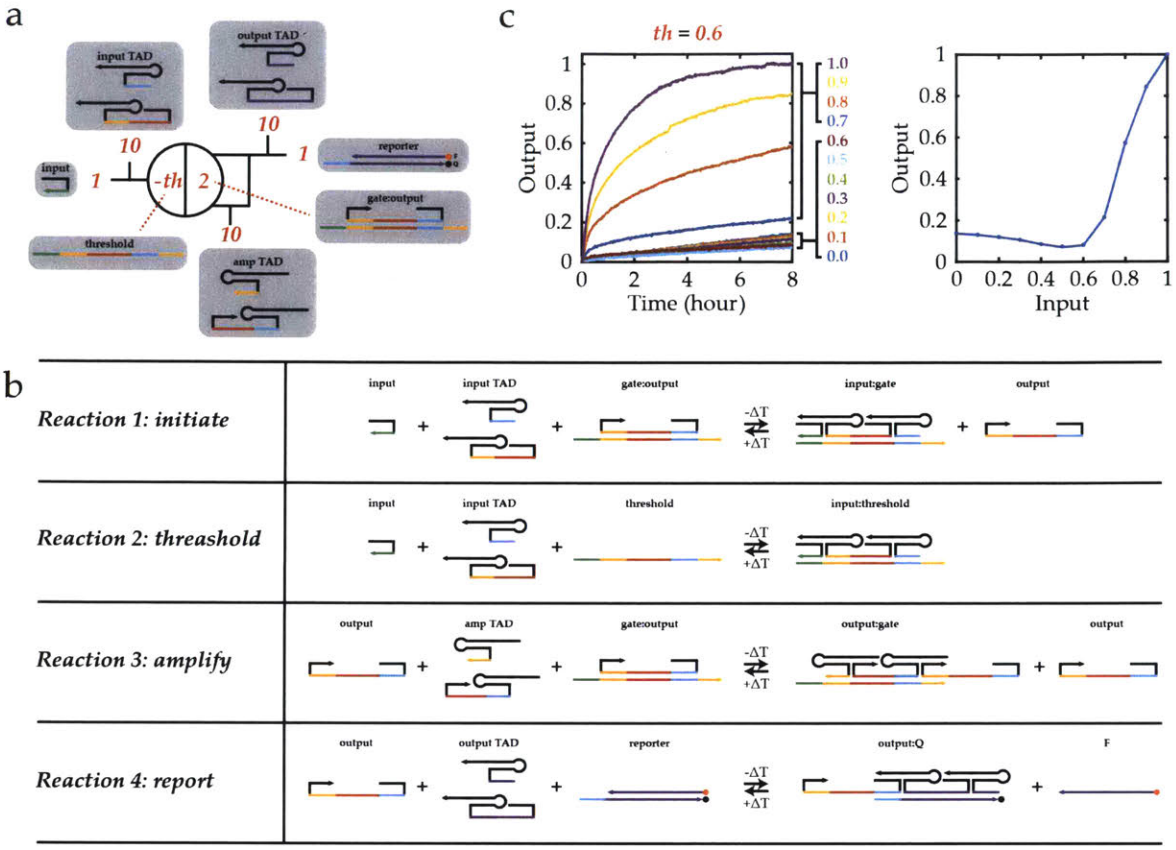


**Figure 5. Design and implementation of TAD gate.** (a) Abstract schematic of the gate. Red numbers indicate relative concentrations of initial DNA species shown in gray boxes. Colored lines here indicate DNA strands at the domain level with distinct DNA sequence for each color except $TAD_L$ and TADs, which are simply depicted in black even when sequences are different. (b) Four basic reactions involved in TAD gate: initiation, thresholding, amplification, and reporting. (c) Kinetics experiment of TAD gate at varying input strand concentration (left). Input-versus-output relationship is determined by plotting output at 8 hours against initial input strand concentration.

concentration adjustment for thresholding that allow universal Boolean function evaluation using dual-rail logic[6]. The reporter gate is used to transform the output into a fluorescence signal through another TAD reaction. Finally, all reactions are based on TAD so the circuit can operate and reset by changing temperature. The resulting DNA circuit demonstrated input concentration-dependent fluorescence kinetics, and the input-versus-output relationship showed the performance of threshold (Figure 5c). With the input concentration at or below the threshold concentration, the fluorescence signal was suppressed at or below the circuit leak. Above the threshold concentration, the additional input increased fluorescence kinetics with moderately sharp transition. The input-versus-output relationship may be improved further by purification of the oligonucleotide components that have damages during the chemical synthesis (e.g. 5′-end truncation). The damaged oligonucleotide components could dampen the reaction kinetics by preventing the formation of the complex with full nucleotide sequence for

stable and robust DSD. The increased kinetics would allow addition of less TAD strands, which could decrease the leak further.

Adjusting the threshold concentration enabled the OR and AND operations, and renewed operation was possible by simply resetting the circuit at 65°C and re-operating at 35°C (Figure 6). 0.6x and 1.2x concentration of threshold was used for OR and AND gate, respectively, and 1x and 2x concentration of input strand was added to the circuit to simulate the two-input OR and AND signals, respectively. If the gate were to receive two or more input strands coming from other upstream reactions, the input signals would include the input sequence used in this experiment appended to different sequences. The fluorescence kinetics demonstrated OR and AND computations with the same set of molecules except the different concentrations of input and threshold. In general, the bigger difference between input and threshold concentrations resulted in faster kinetics due to the linear nature of amplification step (i.e. faster amplification in the presence of higher concentration of input).

## 5.4 Conclusion

We have developed a mechanism to drive DSD by changing temperature, characterized the engineering parameters of the mechanism, and successfully demonstrated the operation of circuit that is based on the mechanism. Importantly, TAD provides a facile means to design, produce, and operate DNA-based devices that require repeated and extended operation because it can operate using readily available PCR thermal cycler without any special modification of DNA molecules. Moreover, the ability to drive multiple DSD at specific temperature can allow development of devices with more complex behavior than a reaction that

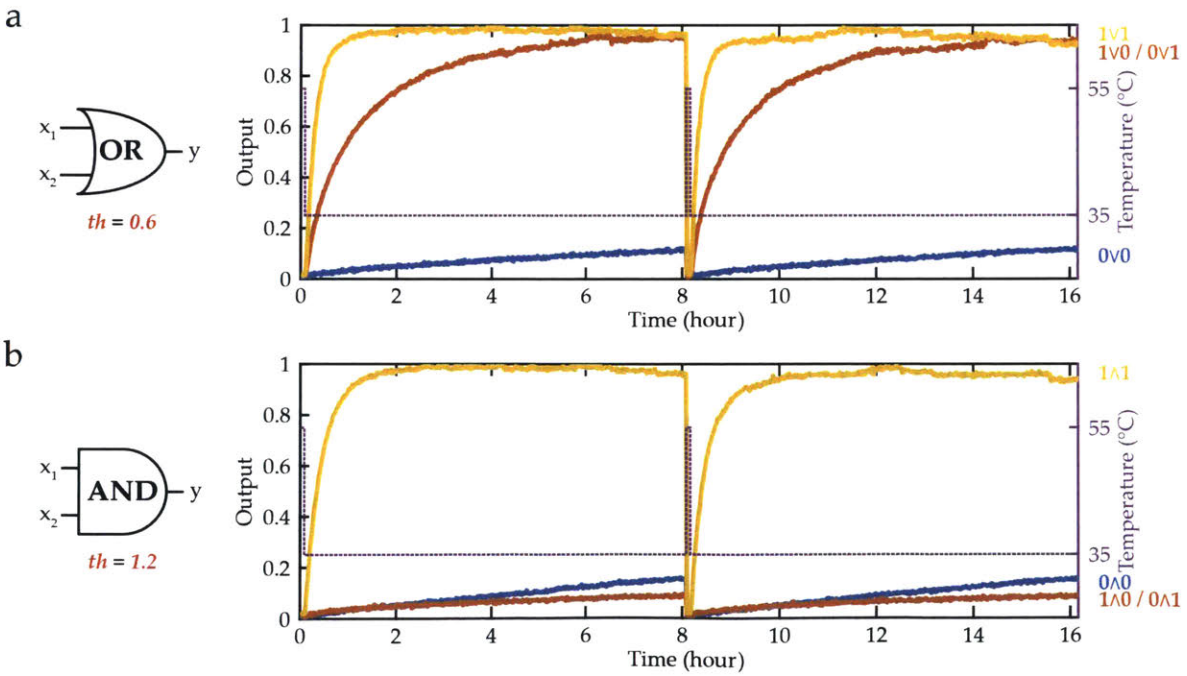


**Figure 6. TAD logic gates.** Kinetic experiments showing TAD gate operating two-input (a) OR and (b) AND computation depending on the initial thresholding strand concentration.

goes to completion upon activation. When used with other mechanisms, such as photon- and proton-mediated DSD, TAD would expand our ability to control DNA-based systems even further.

In order to use DNA devices much like everyday electronics such as cell phones and computers, a reliable energy source for actuation is necessary to easily program and operate the system. Though the first generation of TAD described here is a promising progress towards this direction, further improvement to fine-tune TAD properties with faster kinetics especially at lower temperature would be required. Furthermore, the quantitative design of TAD strands would require an advanced understanding of the thermodynamic properties of DNA junctions that we currently lack. Nonetheless, virtually any kind of energy can power heat source, and thus the thermally driven actuation via TAD is versatile and widely applicable to develop DNA devices with extended lifetime and operation.

## 5.5 Acknowledgement

This material is based upon work supported by the National Science Foundation Graduate Research Fellowship (Jaeseung Hahn) under Grant No. 1122374. The authors thank Bhavik Nathwani and Toma Tomov for insightful conversations. We thank the Wyss Institute for support of this project.

## 5.6 References

1. Yurke, B.; Turberfield, A. J.; Mills, A. P.; Simmel, F. C.; Neumann, J. L. A DNA-Fuelled Molecular Machine Made of DNA. *Nature* **2000**, *406*, 605–608.
2. Seelig, G.; Soloveichik, D.; Zhang, D. Y.; Winfree, E. Enzyme-Free Nucleic Acid Logic Circuits. *Science (New York, N.Y.)* **2006**, *314*, 1585–8.
3. Zhang, D. Y.; Turberfield, A. J.; Yurke, B.; Winfree, E. Engineering Entropy-Driven Reactions and Networks Catalyzed by DNA. *Science (New York, N.Y.)* **2007**, *318*, 1121–5.
4. SantaLucia, J.; Hicks, D. The Thermodynamics of DNA Structural Motifs. *Annual Review of Biophysics and Biomolecular Structure* **2004**, *33*, 415–440.
5. Yin, P.; Choi, H. M. T.; Calvert, C. R.; Pierce, N. A. Programming Biomolecular Self-Assembly Pathways. *Nature* **2008**, *451*, 318–22.
6. Qian, L.; Winfree, E. Scaling Up Digital Circuit Computation with DNA Strand Displacement Cascades. *Science* **2011**, *332*, 1196–1201.
7. Zhang, Z.; Zeng, D.; Ma, H.; Feng, G.; Hu, J.; He, L.; Li, C.; Fan, C. A DNA-Origami Chip Platform for Label-Free SNP Genotyping Using Toehold-Mediated Strand Displacement. *Small* **2010**, *6*, 1854–1858.
8. Miao, P.; Wang, B.; Chen, X.; Li, X.; Tang, Y. Tetrahedral DNA Nanostructure-Based MicroRNA Biosensor Coupled with Catalytic Recycling of the Analyte. *ACS Applied Materials & Interfaces* **2015**, *7*, 6238–6243.
9. He, Y.; Liu, D. R. A Sequential Strand-Displacement Strategy Enables Efficient Six-Step DNA-Templated Synthesis. *Journal of the American Chemical Society* **2011**, *133*, 9972–9975.
10. Tomov, T. E.; Tsukanov, R.; Glick, Y.; Berger, Y.; Liber, M.; Avrahami, D.; Gerber, D.; Nir, E. DNA Bipedal Motor Achieves a Large Number of Steps Due to Operation Using Microfluidics-Based Interface. *ACS Nano* **2017**, *11*, 4002–4008.

11. Zhang, D. Y. Dynamic DNA Nanotechnology Using Strand-Displacement Reactions. *Nature Chem.* **2011**, *3*.
12. Liang, X.; Nishioka, H.; Takenaka, N.; Asanuma, H. A DNA Nanomachine Powered by Light Irradiation. *ChemBioChem* **2008**, *9*, 702–705.
13. Liu, D.; Balasubramanian, S. A Proton-Fuelled DNA Nanomachine. *Angewandte Chemie International Edition* **2003**, *42*, 5734–5736.
14. Hou, X.; Guo, W.; Xia, F.; Nie, F.-Q.; Dong, H.; Tian, Y.; Wen, L.; Wang, L.; Cao, L.; Yang, Y.; Xue, J.; Song, Y.; Wang, Y.; Liu, D.; Jiang, L. A Biomimetic Potassium Responsive Nanochannel: G-Quadruplex DNA Conformational Switching in a Synthetic Nanopore. *Journal of the American Chemical Society* **2009**, *131*, 7800–7805.
15. Chen, Y.; Lee, S.-H.; Mao, C. A DNA Nanomachine Based on a Duplex–Triplex Transition. *Angewandte Chemie International Edition* **2004**, *43*, 5335–5338.
16. Saiki, R. K.; Scharf, S.; Faloona, F.; Mullis, K. B.; Horn, G. T.; Erlich, H. A.; Arnheim, N. Enzymatic Amplification of Beta-Globin Genomic Sequences and Restriction Site Analysis for Diagnosis of Sickle Cell Anemia. *Science (New York, N.Y.)* **1985**, *230*, 1350–4.
17. Mullis, K.; Faloona, F.; Scharf, S.; Saiki, R.; Horn, G.; Erlich, H. Specific Enzymatic Amplification of DNA in Vitro: The Polymerase Chain Reaction. *Cold Spring Harbor symposia on quantitative biology* **1986**, *51 Pt 1*, 263–73.
18. Gareau, D.; Desrosiers, A.; Vallée-Bélisle, A. Programmable Quantitative DNA Nanothermometers. *Nano Letters* **2016**, *16*, 3976–3981.
19. Rogers, W. B.; Manoharan, V. N. Programming Colloidal Phase Transitions with DNA Strand Displacement. *Science* **2015**, *347*, 639–642.
20. Bomboi, F.; Romano, F.; Leo, M.; Fernandez-Castanon, J.; Cerbino, R.; Bellini, T.; Bordi, F.; Filetici, P.; Sciortino, F. Re-Entrant DNA Gels. *Nature Communications* **2016**, *7*, 13191.
21. Genot, A. J.; Zhang, D. Y.; Bath, J.; Turberfield, A. J. Remote Toehold: A Mechanism for Flexible Control of DNA Hybridization Kinetics. *Journal of the American Chemical Society* **2011**, *133*, 2177–2182.
22. Chen, X. Expanding the Rule Set of DNA Circuitry with Associative Toehold Activation. *Journal of the American Chemical Society* **2012**, *134*, 263–271.
23. Zhu, J.; Zhang, L.; Dong, S.; Wang, E. Four-Way Junction-Driven DNA Strand Displacement and Its Application in Building Majority Logic Circuit. *ACS Nano* **2013**, *7*, 10211–10217.
24. Lu, M.; Guo, Q.; Marky, L. A.; Seeman, N. C.; Kallenbach, N. R. Thermodynamics of DNA Branching. *Journal of Molecular Biology* **1992**, *223*, 781–789.

## 5.7 Supporting information

### SI1. Sequences, Methods, and Data Processing

#### SI1.1 Sequences

The sequences were designed and analyzed using NUPACK[SI-R1]. Sequences of all the strands used in this study are listed in SI Table 1. Temperature-dependent Associative DNA Strand Displacement (TAD) strands nomenclature ($TAD_{\#,x,n,l}$) is as the following:

\# = target fluorophore-quencher pair (1 = Cy3-Black Hole quencher 2 (BHQ2); 2 = Atto488-Iowa Black FQ (IABkFQ))

x = identity of strand (A = toehold activator strand, D = displacing strand, I = incumbent toehold deactivator strand, L = linker strand, S = single strand with all the domains in A, D, and L)

*n* = number of TAD strands in the design

*l* = number of base pair between TAD strands in the design

**SI Table 1. Sequence Data**

| Strand | Sequence | IDT Purification |
|---|---|---|
| Substrate$_1$ ($S_1$) | CCTTAACCAACGTCAGGAACGTCATGGA/3BHQ_2/ | HPLC |
| Incumbent$_1$ ($I_1$) | /5Cy3/TCCATGACGTTCCTGACGTT | HPLC |
| $S_1$ Full Complement ($S_{1,FC}$) | TCCATGACGTTCCTGACGTTGGTTAAGGTCAACATCG TCTC | SD |
| $TAD_{1,S,1,n/a}$ | TCCATGACCGCACGTTTACGTGCGCGTCGCCCTCGCG ACGGTTCCTGACGTTCGCACCAGATGGTGCGCGTGG CTGTAGCCACGGGTTAAGG | SD |
| $TAD_{1,A,3,6}$ | GATGGGCGTGGCGAGTGCCACGGGTTAAGG | SD |
| $TAD_{1,D,3,6}$ | GCACCTGTTCCTGACGTTCCCATC | SD |
| $TAD_{1,I,3,6}$ | TCCATGACCGTCGCACAAGCGACGAGGTGC | SD |
| $TAD_{1,A,3,8}$ | GGGATTGGCGTGCTCTTGAGCACGGGTTAAGG | SD |
| $TAD_{1,D,3,8}$ | AGTGCTTAGTTCCTGACGTTCCAATCCC | SD |
| $TAD_{1,I,3,8}$ | TCCATGACCGTGCGGATACGCACGTAAGCACT | SD |
| $TAD_{1,A,3,10}$ | AGGTATTGGTAGCCTGGATACAGGCTGGTTAAGG | SD |
| $TAD_{1,D,3,10}$ | CCGAGATCTTGTTCCTGACGTTACCAATACCT | SD |
| $TAD_{1,I,3,10}$ | TCCATGACCGACGCGAGTGCGTCGAAGATCTCGG | SD |
| $TAD_{1,A,5,8}$ | GTTAGGCAGGTTAAGG | SD |
| $TAD_{1,L1,5,8}$ | CGAAATGGTGCCTAAC | SD |
| $TAD_{1,D,5,8}$ | CTTGTTCGGTTCCTGACGTTCCATTTCG | SD |
| $TAD_{1,L2,5,8}$ | GCTACTCTCGAACAAG | SD |
| $TAD_{1,I,5,8}$ | TCCATGACAGAGTAGC | SD |
| $TAD_{1,A,7,10}$ | CGTGCTACTAGCGAGCCCTAGCTCGCGGTTAAGG | SD |
| $TAD_{1,L1,7,10}$ | AGATTCAAGGTAGTAGCACG | SD |
| $TAD_{1,L2,7,10}$ | GTTGTATGGTCCTTGAATCT | SD |
| $TAD_{1,D,7,10}$ | CGATTTGACTGTTCCTGACGTTACCATACAAC | SD |
| $TAD_{1,L3,7,10}$ | CTCATCTCCAAGTCAAATCG | SD |
| $TAD_{1,L4,7,10}$ | CGTGAAGTAGTGGAGATGAG | SD |
| $TAD_{1,I,7,10}$ | TCCATGACCCGGTGGATACACCGGCTACTTCACG | SD |
| Substrate$_2$ ($S_2$) | /5ATTO488N/AATTTGCGGGATCTGTGACGAAACGAA ACTGC | HPLC |

| | | |
|---|---|---|
| Incumbent$_2$ ($I_2$) | GTTTCGTCACAGATCCCGCAAATT/3IABkFQ/ | HPLC |
| $S_2$ Full Complement ($S_{2,FC}$) | GCAGTTTCGTTTCGTCACAGATCCCGCAAATT | SD |
| $TAD_{2,S,1,n/a}$ | GCAGTTTCCGTGCCAGTTGGCACGCGAGCGCGATCG CTCGGTTTCGTCACAGATCCGCACCGAACTCGGTGCC GTGCGGTAACGCACGCGCAAATT | SD |
| $TAD_{2,A,3,6}$ | GCAGTTTCCGCAAGGACTCTTGCGTGGGAG | SD |
| $TAD_{2,D,3,6}$ | CTCCCAGTTTCGTCACAGATCCAGTCCA | SD |
| $TAD_{2,I,3,6}$ | TGGACTAGGCAGCCTACTGCCTCGCAAATT | SD |
| $TAD_{2,A,3,8}$ | GCAGTTTCCGGTCACTTGTGACCGTATGGACG | SD |
| $TAD_{2,D,3,8}$ | CGTCCATAGTTTCGTCACAGATCCACCTCCAT | SD |
| $TAD_{2,I,3,8}$ | ATGGAGGTCGTGGCTGCTGCCACGCGCAAATT | SD |
| $TAD_{2,A,3,10}$ | GCAGTTTCCGCACGGAAGCGTGCGTGGCCTAAAG | SD |
| $TAD_{2,D,3,10}$ | CTTTAGGCCAGTTTCGTCACAGATCCACCTCACTTA | SD |
| $TAD_{2,I,3,10}$ | TAAGTGAGGTCGTGCCGTCTGGCACGCGCAAATT | SD |
| $TAD_{2,A,5,8}$ | GCAGTTTCACAAGGAC | SD |
| $TAD_{2,L1,5,8}$ | GTCCTTGTTATGCTCA | SD |
| $TAD_{2,D,5,8}$ | TGAGCATAGTTTCGTCACAGATCCATTTCACC | SD |
| $TAD_{2,L2,5,8}$ | GGTGAAATAGTAGAGG | SD |
| $TAD_{2,I,5,8}$ | CCTCTACTCGCAAATT | SD |
| $TAD_{2,A,5,10}$ | GCAGTTTCGAGTCTTAGC | SD |
| $TAD_{2,L1,5,10}$ | GCTAAGACTCTAATGACAAC | SD |
| $TAD_{2,D,5,10}$ | GTTGTCATTAGTTTCGTCACAGATCCACAGCTTAAC | SD |
| $TAD_{2,L2,5,10}$ | GTTAAGCTGTATGAGTAAGG | SD |
| $TAD_{2,I,5,10}$ | CCTTACTCATCGCAAATT | SD |
| input | TTCAGGCTTTAGGGACGG | SD |
| input TAD strand 1 | TGTGGACTGGTGCGATGACCGACCTTATGGTCGGAG CCTGAA | SD |
| input TAD strand 2 | TTGGTTAACGACGCGCAAGCGTCGAGTCCACA | SD |
| output | AGGATGGATTGGTTAAGGTGCGATGATTCAGAGTGG | SD |
| amp TAD strand 1 | CCACTCTGAGACCGCGTACGGTCTGGTTAAGGTGATT CAGGC | SD |
| amp TAD strand 2 | GCCTGAATGCAGCGTAGTCGCTGCCGATGATT | SD |
| output TAD strand 1 | TGTAGCTTGTTCCTGACGGGTCGGTTCGCCGACCTCC ATCCT | SD |
| output TAD strand 2 | TCCATGACAAGTTGATGCCAACTTAAGCTACA | SD |
| gate/threshold | CCGTCCCTAATCATCGCACCTTAACCAATCATCGCA | SD |

**SI1.2: Experimental Methods**

All DNA strands were purchased from Integrated DNA Technologies (IDT) with the purification options (SD = standard desalting, HPLC = high performance liquid chromatography) listed in SI Table 1. The DNA strands were suspended at around 200-1000 mM in Millipore purified water and stored at -20°C. The stock concentrations were determined by measuring the absorbance of light at a wavelength of 260 nm (A260) with the extinction

coefficient (Ext) for each strand provided by IDT using the Beer-Lambert law ([DNA] = A260/Ext).

We prepared samples in 5 mM Tris/1 mM EDTA buffer (1x TE) with 10 mM $MgCl_2$. All samples included incumbent (I) and substrate (S) pair (I-S). $I_1$ and $S_1$ pair ($I_1$-$S_1$) conjugated with Cy3 at 5'-end and BHQ2 at 3'-end, respectively, was added at final concentrations of 1 μM for both. $I_2$ and $S_2$ pair ($I_2$-$S_2$) conjugated with IABkFQ at 3'-end and Atto488 at 5'-end, respectively, was added at final concentrations of 10 μM for $I_2$ and 1 μM for $S_2$. Except for the experiment to determine the effect of concentration of TAD strands (*c*), TAD strands were added at 10 μM each. To subtract background and normalize the data, we included negative control ($I_1$-$S_1$ or $I_2$-$S_2$ only) and positive control ($I_1$-$S_1$ with 10 μM of $S_{1,FC}$ or $I_2$-$S_2$ with 10 μM of $S_{2,FC}$) corresponding to 0% and 100% displacement, respectively, for each experiment. Reactions were prepared in black 96-well plates (HSP9666; BioRad) at 20 μL/well volume to ensure rapid temperature change. In a typical experiment, we first added 10 μL of I-S at 2x concentration in 2x TE buffer with 20 mM $MgCl_2$ per well. Then, 10 μL of TAD strand(s) at 2x concentration in water was added to appropriate well. Finally, fluorescence signal at specific temperature was measured using quantitative PCR (qPCR) machines (BioRad CFX96 C1000 series).

For characterization of TAD, five replicates were prepared for each sample condition to account for random variation in fluorescence signal including the controls. Melting curves were typically obtained by measuring fluorescence signal from 5°C to 65°C at 1°C resolution with specified incubation time before each measurement. If the operation range was at higher temperature, the protocol was adjusted to measure signal at higher temperature range. The same protocol with decreasing temperature was applied before the measurement of melting curve to anneal the sample and also confirm that the fluorescence signal was measured in equilibrium at each temperature point. If the annealing and melting curves showed hysteresis-like behavior, the melting curve was measured using longer incubation time. Upon derivation of displacing temperature ($T_d$) and displacing range ($\Delta T$) from the melting curve, the kinetics and repeated operation were measured at the determined temperatures. The same procedure was used to test two orthogonal TAD operations with both $I_1$-$S_1$ and $I_2$-$S_2$ in the same solution.

For TAD circuits, we prepared reporter ($I_1$-$S_1$) strands at 1 μM each, gate and output strands at 2 μM each, all TAD strands at 10 μM each, and threshold strand (same as gate strand) at the specified concentration (0.6 or 1.2 μM) in the final sample solution to be measured. The circuit was reset at 65°C and operated at 35°C. First, the circuit response to varying concentration of input strand was measured by adding 0 to 1 μM of input strand at the 0.1 μM increment in the presence of 0.6 μM of threshold strand. The fluorescence signal was measured every minute. The fluorescence signal from each sample after 8-hour operation at 35°C was used to produce input-output relation plot. The circuit was used to operate OR and AND function by using 0.6 and 1.2 μM of threshold strand, respectively. The qPCR machine was programmed to incubate samples at 65°C for 5 minutes and 35°C for 8 hours for two cycles while measuring fluorescence signal every minute. The input strand was added at 1 and 2 μM to simulate the two-input OR and AND signals, respectively.

**SI1.3: Data processing**

All the data processing was performed using MATLAB. The fluorescence signals from both Cy3 and Atto488 were dependent on temperature, which necessitated the background subtraction and normalization of signal to obtain melting curves (Figure S1). The signals from all the samples were subtracted by the signal from negative control to account for the background signal. Then, the data were normalized by dividing the value with positive control. For the samples with replicates (i.e. TAD characterization samples), we used an average value of five replicates for each control. Further normalization by subtracting with minimum signal and dividing the resulting values with the maximum value within the dataset was applied to the melting curves that have clearly reached the steady state (i.e. no further change in signal at varying temperature), which could be due to experimental errors (e.g. plate reader, contaminated plate, pipetting error). The melting curve was fitted using explicit equation for bimolecular reaction of DNA hybridization[SI-R2] with assumptions that TAD roughly follows two-state transition, and concentrations of TAD strands in large excess to S will not change much during the reaction. The fitted curve was used to obtain $T_d$ and $\Delta T$ (SI Table 2). The fitted melting curve was used to obtain the first derivative curve as well as $T_d$ and $\Delta T$. For the kinetic experiment, the curve was fitted using exponential equation with an assumption that it follows pseudo-first order kinetic.

**SI2. Further discussion on design parameters and their effects on TAD activity**

In our qualitative TAD model, we assumed temperature-independent enthalpy and entropy changes of DNA complex formation via assembly of TAD strands on S that displaces I. This assumption was based on the fact that these thermodynamic parameters can be regarded as largely independent of temperature for regular DNA duplex formation[SI-R3]. Though detailed thermodynamic properties of DNA junctions are not fully elucidated, decrease in temperature results in an unfavorable enthalpy change opposed by a favorable entropic change in DNA four-way junction compared to regular DNA duplex.[SI-R4] We use DNA junctions to connect different TAD domains in our designs, and therefore the decrease in enthalpy change is associated with lower $T_d$. As a consequence, a TAD design with larger $n$ ($c$ = 10 μM, $l$ = 8, $n$ = 5)

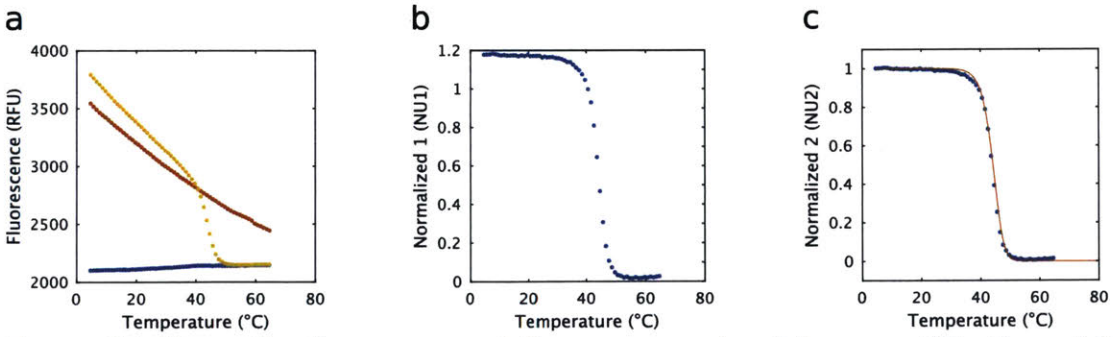


**Figure S1. Normalization process of fluorescence signal for quantification of TAD activity.** (a) Raw data from TAD characterization experiment (blue = negative control, red = positive control, yellow = experimental sample). (b) Background subtraction and normalization using negative and positive controls. (c) Further background subtraction and normalization using minimum and maximum value within the dataset (blue dot) followed by melting curve fitting (red line).

**SI Table 2. Summary of observed $T_d$ and $\Delta T$**

| Fluorophore-Quencher pair | $l$ | $m$ | $n$ | $c$ (μM) | $T_d$ | T01* | T99** | $\Delta T$ |
|---|---|---|---|---|---|---|---|---|
| Atto488-IABkFQ | 6 | 2 | 3 | 10 | 23.8 | 14.2 | 34.1 | 19.9 |
| Atto488-IABkFQ | 8 | 2 | 3 | 10 | 37.8 | 28.9 | 47.2 | 18.2 |
| Atto488-IABkFQ | 10 | 2 | 3 | 10 | 46.6 | 38.9 | 54.7 | 15.8 |
| Atto488-IABkFQ | 8 | 2 | 5 | 10 | 27.2 | 17.9 | 37.1 | 19.2 |
| Atto488-IABkFQ | 10 | 2 | 5 | 10 | 39.9 | 32.5 | 47.7 | 15.2 |
| Cy3-BHQ3 | n/a | 2 | 1 | 10 | 63.8 | 49.1 | 73.6 | 24.5 |
| Cy3-BHQ3 | 6 | 2 | 3 | 10 | 43.7 | 30.6 | 52.4 | 21.7 |
| Cy3-BHQ4 | 8 | 2 | 3 | 10 | 49.0 | 36.0 | 57.6 | 21.6 |
| Cy3-BHQ5 | 10 | 2 | 3 | 10 | 52.1 | 40.1 | 60.1 | 19.9 |
| Cy3-BHQ2 | 8 | 2 | 5 | 10 | 44.3 | 34.2 | 50.8 | 16.6 |
| Cy3-BHQ6 | 10 | 4 | 7 | 10 | 32.2 | 14.9 | 44.0 | 29.1 |

*T01 = temperature at which temperature at which 1% of I is displaced from S

**T99 = temperature at which 99% of I is displaced from S

resulted in larger $\Delta T$ compared to a TAD design with smaller $n$ ($c$ = 10 μM, $l$ = 8, $n$ = 3) using $I_2$-$S_2$, which operated at lower temperature compared to $I_1$-$S_1$ because of higher concentration of $I_2$ at 10 μM compared to $I_1$ at 1 μM (Figure S2).

In addition, the number of junction branches ($m$) is an associated parameter $n$. In the current TAD design, the number of DNA junctions is fixed at two, one between $TAD_A$ and $TAD_D$ and another between $TAD_D$ and $TAD_I$. In order to increase $n$, $m$ must increase to accommodate the assembly of more strands. For instance, $m$ is 4 for four-way junctions used in all TAD designs in the main text. However, $m$ cannot be 4 for TAD design with $n$ = 7 because 5-strand system is maximum for TAD design that has two junction points (Figure S3a). To make sure that all branches pair up to form base stacking, $m$ must be even. Therefore, $m$ has to increase to 6 in order to increase $n$ to 7 in our current design. We have characterized 7-strand system ($c$ = 10 μM, $l$ = 10, $m$ = 6, $n$ = 7) using $I_1$-$S_1$ (Figure S3b). Lower $T_d$ was observed compared to the system with the same design and experimental parameters except for lower $n$ at 3. This

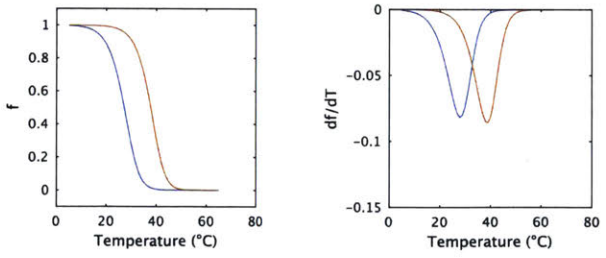


**Figure S2. Effect of temperature-dependent thermodynamic parameters of four-way junction on TAD.** Fitted melting curve (left) and its first derivative (right) of TAD designs. A TAD design with $n$ = 5 (blue) has larger $\Delta T$ compared to a TAD design with $n$ = 3 (red), presumably due to decrease in enthalpy change that determines steepness of transition at lower $T_d$. f = fraction displaced.

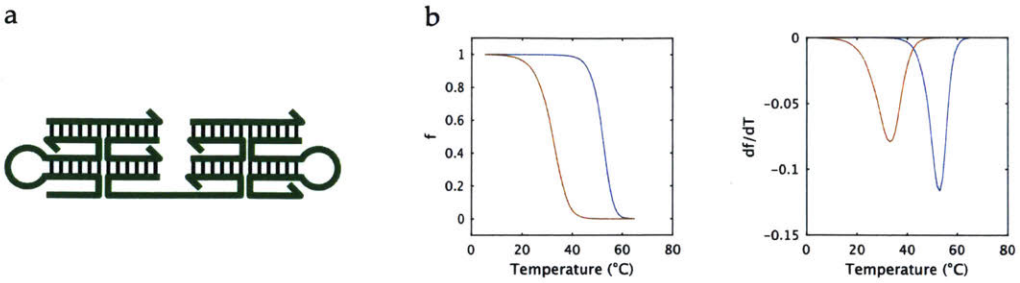


**Figure S3. Characterization and comparison of 7-strand TAD with 3-strand TAD.** (a) A schematic of TAD system with $n = 7$. (b) Fitted melting curve (left) and its first derivative (right) of TAD designs. A TAD design with $n = 3$ (blue) has smaller $\Delta T$ compared to a TAD design with $n = 7$ (red). f = fraction displaced.

result was as expected due to increased concentration-adjusted entropic penalty. However, the design resulted in much wider $\Delta T$. In addition to the fact that enthalpy change of four-way junction is strongly dependent on temperature, it is possible that DNA junctions with more branches result in even stronger dependence of enthalpy change on temperature. Further study is necessary to determine whether or not $m$ affects the behavior of TAD.

Though our first-generation TAD has demonstrated feasibility of operating DNA devices and circuit by changing temperature, it will be necessary to improve our ability to quantitatively predict the behavior of TAD with given design and experimental parameters. Moreover, it will be necessary to achieve sharper $\Delta T$ and faster kinetics at low temperature (< 35°C) to imbue more complex behavior and being useful for applications that require faster response time at low temperature. As demonstrated in this section, it is pertinent that we first understand the thermodynamic parameters of DNA junctions better, and the knowledge gained will lead to next generation of designs with improved characteristics.

**SI3: Supplemental References**

SI-R1. Zadeh, J. N.; Steenberg, C. D.; Bois, J. S.; Wolfe, B. R.; Pierce, M. B.; Khan, A. R.; Dirks, R. M.; Pierce, N. A. NUPACK: Analysis and Design of Nucleic Acid Systems. *Journal of Computational Chemistry* **2011**, *32*, 170–173.

SI-R 2. Böttcher, A.; Kowerko, D.; Sigel, R. K. O. Explicit Analytic Equations for Multimolecular Thermal Melting Curves. *Biophysical Chemistry* **2015**, *202*, 32–39.

SI-R 3. Rogers, W. B.; Manoharan, V. N. Programming Colloidal Phase Transitions with DNA Strand Displacement. *Science* **2015**, *347*, 639–642.

SI-R 4. Lu, M.; Guo, Q.; Marky, L. A.; Seeman, N. C.; Kallenbach, N. R. Thermodynamics of DNA Branching. *Journal of Molecular Biology* **1992**, *223*, 781–789.

# Chapter 6: Perspectives and Outlook

## 6.1 Implications of thesis work

Development of biomedical nano-devices is a challenging task. The advances in DNA nanotechnology have enabled precise spatial organization of molecules and programmable dynamic behaviors that are difficult to achieve using the traditional "top-down" or "bottom-up" approaches with different engineering materials such as metal nanoparticles or block co-polymer. Despite the unprecedented capability of DNA as an engineering material, some challenges remain to be overcome for viable biomedical applications of the technology. In this thesis, we focused on three main challenges to accelerate translations of DNA-based biomedical nano-devices: (1) stability of DNA nanostructures in biological environments, (2) robust 3D biomolecular integration, and (3) prolonged dynamic behavior of DNA-based devices.

### 6.1.1 Protective strategies for DNA nanostructures in biological environments

Since our initial reporting of instability of DNA nanostructures in biological environments, the members of Shih lab as well as other groups have focused their efforts to develop protective strategies to improve the stability of DNA-based systems for biomedical applications. Shih lab has already developed two orthogonal approaches that involve lipid membrane coating inspired by viral envelope[1] and oligolysine-based coating driven by electrostatic interaction.[2] The lipid membrane coating was able to protect the enveloped DNA nanostructure from cation-depletion-driven denaturation and nuclease digestion. Remarkably, the enveloped DNA nanostructure exhibited enhanced *in vivo* circulation time. The oligolysine-based coating was also able to protect the coated DNA nanostructure from the denaturation and digestion in biological environments. The advantage of the oligolysine-based strategy is that the coating is agnostic to shape and size of DNA nanostructures. Therefore, it provides a scalable method to protect DNA-based biomedical nano-devices. As denaturation and degradation of DNA nanostructures affect the function of biomedical nano-devices, it is important to make sure that the programmed molecular organization is not deteriorated in biological environments.

### 6.1.2 Platform for 3D molecular integration

DNA origami capsule possesses features attributing to the success of 2D DNA origami as well as advantageous features relevant to the molecular integration only possible through 3D DNA origami. We found that the platform was easily modified to program desired molecular integration in 3D space for development of a nanofactory capable of integrated RNA production and processing. Further analysis of the system revealed that the co-localization of RNA production and processing units resulted in more effective production of mature RNA that was fully processed as intended. The platform is expected to be easily adapted for other applications that require 3D molecular integration.

### 6.1.3 A mechanism to drive DNA-based devices

We have developed a mechanism to operate DNA-based devices by changing temperature. The mechanism enables prolonged, reversible operation of DNA-based devices using PCR thermal cyclers readily available in a typical molecular biology lab. Many DNA-based devices available in the literature can be easily adapted using the strategy developed in

this work to achieve extended operation. Therefore, further advances of the technology may allow operation of DNA-based devices much like modern electronics such as cell phones and computers for biomedical applications.

## 6.2 Future directions

In this work, we identified and addressed three challenges that are hindering translations of DNA-based biomedical nano-devices. However, there remain unsolved challenges that require further advancement of the field.

### 6.2.1 General mechanism to prolong function of DNA-based biomedical nano-devices

Our ongoing work is focused on a generalizable strategy to protect the function of DNA-based nano-devices in biological environments. Though we have focused on the stability of DNA nanostructures, different molecular cargos and mechanisms to drive the device could deteriorate even if the structural scaffold remain stable. We suspect that the robust compartmentalization of molecular cargos using DNA "membrane" nanostructure (e.g. DNA origami capsule) and the protection of this DNA nanostructure will be able to accomplish the task much like the cellular lipid membrane. In addition, the compartmentalization strategy would require the development of mechanisms to link inside and outside comparable to transmembrane proteins that allow actuation based on the environmental triggers. Such advancements would improve our ability to develop biomedical nano-devices for drug delivery and diagnostic applications.

### 6.2.2 Effect of DNA-based compartmentalization on enzymatic cascade

The effect of compartmentalization achieved by the construction of DNA origami capsule remains to be verified and characterized. We are testing the size-selective capability of a DNA origami capsule for molecular transport in and out of the structure. Moreover, we will be able to characterize the integrated RNA production and processing inside the compartment using a DNA origami capsule. We expect that the compartmentalization would improve the processing efficiency by trapping unprocessed large concatemer inside the compartment until further processing allow small enough RNA transcript to leave the compartment through the pore.

### 6.2.3 Thermodynamic parameters of DNA junctions

Currently, our knowledge of thermodynamic parameters of DNA junctions is limited. Consequently, it is difficult to quantitatively design the DNA-based systems that utilize these junction motifs as a basis for self-assembly of structure and dynamic behavior. The temperature-dependent DNA strand displacement (TAD) developed in this thesis utilizes such motifs and is therefore limited for quantitative design of its dynamic behavior. However, it should be possible to study the thermodynamics of DNA junctions using TAD by characterizing the behavior of different designs. In return, the knowledge gained should increase our ability to program more robust and reliable behavior of TAD-based nano-devices for biomedical applications.

## 6.3 References


1. Perrault, S. D. & Shih, W. M. Virus-Inspired Membrane Encapsulation of DNA Nanostructures to Achieve In Vivo Stability. *ACS Nano* (2014). doi:10.1021/nn5011914
2. Ponnuswamy, N. *et al.* Oligolysine-based coating protects DNA nanostructures from low-salt denaturation and nuclease degradation. *Nat. Commun.* **8,** 15654 (2017).